Exploring the Use of Recycled Rubber Aggregate in Seismically Resilient Concrete Structures

Adam Muscat Pitre'

A dissertation submitted to the Department of Civil and Structural Engineering of the Faculty for the Built Environment, at the University of Malta, in partial fulfilment of the requirements of the degree of Master of Engineering (Structural Engineering)

December 2025

L-Università ta' Malta

FACULTY/INSTITUTE/CENTRE/SCHOOL For the Built Environment

DECLARATIONS BY POSTGRADUATE STUDENTS

(a) Authenticity of Dissertation

I hereby declare that I am the legitimate author of this Dissertation and that it is my original work.

No portion of this work has been submitted in support of an application for another degree or qualification of this or any other university or institution of higher education.

I hold the University of Malta harmless against any third party claims with regard to copyright violation, breach of confidentiality, defamation and any other third party right infringement.

(b) Research Code of Practice and Ethics Review Procedures

I declare that I have abided by the University's Research Ethics Review Procedures. Research Ethics & Data Protection form code BEN-2024-00136.

As a Master's student, as per Regulation 77 of the General Regulations for University Postgraduate Awards 2021, I accept that should my dissertation be awarded a Grade A, it will be made publicly available on the University of Malta Institutional Repository.

Acknowledgements

I would like to thank my tutor Prof. Marc Bonello B.E.&A. (Hons) (Melit.), M.Sc.(Lond.), Ph.D.(Lond.), D.I.C., M.A.S.C.E., M.S.E.I., Eur.Ing.(FEANI), Perit for all his expertise, advice, and constant guidance throughout the entire duration of writing this dissertation and the six years I spent at the Faculty for the Built Environment.

I would like to further extend my gratitude to Nicholas Azzopardi and Alex Falzon for their constant aid and guidance throughout the entire testing process at the Faculty laboratory, as well as the entire staff at the Faculty for the Built Environment, for their constant dedication to improving our trade. Furthermore, I would like to express my sincere gratitude to Mr Reuben Vella and Ballut Blocks Ltd. for sponsoring this research through the provision of materials and for their assistance in the preparation and workmanship involved in the fabrication of all specimens.

I could not have done any of this without the constant support of my family, girlfriend, friends, and colleagues, as they encouraged me throughout this entire process.

I take full responsibility for any shortcomings in this dissertation.

Abstract

Adam Muscat Pitre'

Exploring the Use of Recycled Rubber Aggregate in Seismically Resilient Concrete Structures

This dissertation investigates the structural performance of rubberised concrete with a focus on its behaviour under static and cyclic loading. Building upon previous research conducted at the Faculty for the Built Environment at the University of Malta, an experimental programme was undertaken to compare a conventional control concrete mix with a rubberised concrete mix incorporating 25% crumb rubber replacement of fine aggregate (CR25). The experimental investigation comprised concrete cube compressive strength tests, static and cyclic reinforced concrete short column compressive strength tests, and static and cyclic reinforced concrete beam flexural tests. The experimental results confirmed that the inclusion of crumb rubber as partial fine aggregate replacement in reinforced concrete structural members leads to 56.39% and 16.16% reductions in compressive and flexural strength respectively when compared to conventional reinforced concrete structural members. However, under cyclic loading, rubberised reinforced concrete specimens exhibited enhanced deformation capacity, improved crack closure during unloading, and more ductile modes of failure. In contrast, conventional reinforced concrete specimens exhibited stiffer responses at the cost of brittle failure with reduced energy dissipation. Cyclic testing highlighted that rubberised concrete experiences accelerated stiffness degradation at higher stress levels relative to lower and moderate stress levels, where they retain superior shape recovery and damage tolerance.

Overall, the experimental results obtained indicate that rubberised concrete may not be suitable for strength-critical structural elements, rather excelling in applications where characteristics such as ductility, energy dissipation, and seismic resilience are preferred. This research study demonstrates that rubberised concrete has potential as a specialised structural material in tailored cyclic and seismic environments, provided its use is appropriately supported by further research work.

Keywords

Recycled Rubber Aggregate, Rubberised Concrete, Cyclic Loading, Seismic Resilience, Flexural Behaviour, Compressive behaviour, Ductility

Table of Contents

List of Figures

List of Tables

1. Introduction

1.1 Overview and Objectives

The construction industry is one of the largest global consumers of natural finite resources, with conventional concrete relying heavily on natural aggregates extracted through various environmentally challenging processes (Neville, 2011). Developing concerns over sustainability, material deficits, and waste management has driven research into alternative materials capable of reducing the environmental burdens caused by concrete without neglecting overall structural demands in construction. One such alternative is the use of recycled rubber aggregate, typically sourced from end-of-life tyres (ELT), as a partial replacement for conventional natural aggregates in concrete (Mehta and Monteiro, 2014).

Throughout the course of its studies, rubberised concrete has been shown to offer certain advantages, including improved ductility, energy absorption capacity, and crack resistance. However, these benefits typically come at the cost reductions in concrete's compressive and flexural performances, raising questions regarding its suitability within various structural applications. While numerous past studies have examined rubberised concrete's static mechanical responses, limited research has been conducted regarding the cyclic performance and behaviours surrounding the material, which are important characteristics for structures subjected to repeated or dynamic actions such as traffic loading, seismic effects, or fatigue-type stresses (Thomas et al., 2016).

The primary aim of this research is to further investigate the findings of Scicluna (2010), Magro (2011), and Abdilla (2012), who have delved into the static mechanical performance of rubberised concrete, particularly in relation to compressive strength, flexural strength and performance, and shear strength and performance. This research study compares the performance of regular aggregate concrete with that of rubber aggregate concrete mixes under both static and cyclic loading conditions.

The specific objectives of this dissertation are to:

- Evaluate the effects of rubber aggregate replacement within conventional reinforced concrete by means of a series of static and cyclic tests.
- Evaluate the effect on structural performance of static vs cyclic loading.
- To evaluate how loading cycles affect both conventional reinforced concrete and rubberised reinforced concrete structural members.
- To assess the potential structural application of rubberised reinforced concrete in scenarios where cyclic loading is significant, such as during seismic events.

1.2 Research Questions

The following research questions require clarification:

- What is the effect of rubber aggregate replacement on the flexural and compressive behaviour of reinforced concrete structural members?
- What is the effect of cyclic loading on conventional reinforced concrete and rubberised reinforced concrete structural members?

1.3 Research Methodology

The proposed research study will be conducted using an experimental research methodology, during which concrete specimens will be produced using natural aggregates and varying replacement percentages of crumb rubber aggregate. Standard laboratory testing procedures will be adopted in order to determine static and cyclic compressive and flexural performances of a variety of reinforced concrete structural members, including beams and short columns. The experimental results obtained should provide a clearer understanding of the structural performance of rubberised concrete in cyclic scenarios and whether it could be a suitable structural material in construction practices for buildings within seismically-active regions.

1.4 Dissertation Structure

This dissertation is structured as follows:

Chapter 1 – Introduction

This chapter gives an initial understanding of the scope of this dissertation and its research objectives.

Chapter 2 – Literature Review

This chapter gives a theoretical basis to the dissertation, reviewing the relevant literature read to provide a solid background and context for the research being conducted. It introduces the material and research studied, and its importance on this dissertation. It also outlines the research gaps present as well as what potential future research work can be done in this dissertation and/or other research.

Chapter 3 – Performance of Concrete with Different Replacement Aggregates

This chapter delves further into past research, namely that of Scicluna (2010), Magro (2011), and Abdilla (2012). Since this dissertation builds upon their research work, it is important to highlight their findings and observations in further detail.

Chapter 4 – Research Methodology

This chapter describes the research process, including the testing procedures, as well as the limitations and difficulties encountered during sample preparation and testing. This includes the specification of the experimental rig setup, materials, and specimens.

Chapter 5 – Results and Discussion

This chapter presents and tabulates the experimental results obtained, as well as an interpretation of these results, accompanied by graphs and tables for a better understanding of the structural behaviour being investigated. Alongside these results, a discussion is presented regarding past experimental results obtained by Scicluna

(2010), Magro (2011), and Abdilla (2012). Generally, these experimental results compare the strength of conventional concrete and rubberised concrete under the different loading conditions.

Chapter 6 – Conclusions and Suggestions for Future Research Work

The final chapter concludes the dissertation with closing remarks, as well as a description of the limitations within the research process and potential improvements made, along with suggestions for future research work.

2. Literature Review

2.1 Introduction to Rubberised Concrete

2.1.1 Overview

Rubberised concrete refers to an altered form of concrete, where natural aggregates such as crushed stone, sand or gravel are partially replaced with rubber aggregates of varying grades, shapes and/or sizes. Rubber aggregate materials are typically sourced from end-of-life tyres (ELT). This alternative aggregate counteracts against the environmental burdens associated with tyre disposal in landfills and the extraction of natural aggregates from quarries. In other words, rubber materials sourced from ELT counteract against the burdens imposed on the environment by unwanted, unused tyres (Zongping et al., 2016).

Figure 2.1: Example of unwanted, stockpiled end-of-life tyres (ELT) (Scott, 2022)

Rubberised concrete is a relatively recent topic of research within the construction industry, having been studied for around three decades since its inception. Past studies have concluded that it can be a suitable alternative to natural aggregate concrete under given circumstances, implying that its effectiveness and efficiency may be considered situational. Such applications in construction include scenarios where ductility is prioritised over compressive strength in the required structural member. This is because rubberised concrete can undergo considerable deformation while

maintaining its structural integrity. Moreover, its ability to absorb energy along with its post-cracking strength make it particularly valuable in such scenarios (Abdilla, 2012).

Zongping et al. (2016) explored the cyclic behaviour of short steel tubes filled with rubberised concrete. They concluded that a concrete mix with a low natural aggregate percentage replacement (percentage replacement) to tyre rubber (5% - RuC5) resulted in the smallest reduction in maximum lateral load while significantly improving the ductility of CFST columns. Therefore, they deduced that these columns were well-suited members for seismic applications, where both ductility and energy absorption are critical design considerations (Zongping et al., 2016).

2.1.2 Tyre Rubber as Waste

Waste disposal is an ongoing worldwide issue, with rubber tyre disposal having been a major concern for past decades. In fact, the situation had developed so drastically that legislations and directives were adopted to eliminate unsustainable tyre waste management in search for alternative, sustainable routes of waste disposal (Abdilla, 2012). In 1999, the European Union introduced Council Directive 1999/31/EC regarding the landfilling of waste, which banned the disposal of whole waste tyres starting in 2001 and shredded tyres in 2006. As a result, European countries were compelled to seek alternative methods for managing waste tyres (Magro, 2011). By 2019, Europe had achieved an average recovery rate of 95% for ELT, surpassing the recovery rates of the United States (89%) and Japan (91%).

The ongoing accumulation of ELT implies an increasing amount of tyre voids which are susceptible to collecting and trapping rainwater. In turn, this trapped rainwater becomes habitual to mosquitoes and other pests. Furthermore, the hoarding of ELT could result in slow burning fires under the provided circumstances, which could lead to the secretion of hazardous fumes, and subsequently air and soil pollution. As mentioned previously, the disposal of whole or shredded tyres has become illegal in European states. Moreover, tyres should be made use of up until their maximum service life (Abdilla, 2012).

Some developing countries reuse ELT once they are rethreaded. As of 2022, this process has been under intense development, as ELT have the potential to be

rethreaded several times. However, this process burdens developing countries with regards to managing the disposal of used and reused tyres (Seifali Abbas-Abadi et al., 2022).

Press release

EUROPEAN TYRE & RUBBER manufacturers' association

Annex: End of Life Tyres Management – Europe – 2019

National figures (tonnes)	ELT Arising (A)	ELT recovery				Unknown/Stocks (F)	ELT treated (H)=(G)/(A)
		Material			Energy		
		Civil engineering, public works & backfilling (B)	Recycling* (C)	Total Material recovery (D)=(B+C)	Energy recovery (E)**		
Austria	74.000		46.000	46.000	28.000		100%
Belgium	81.325		75.163	75.163	2.153	3.600	95%
Bulgaria	40.800		26.000	26.000	1.500	13.300	67%
Croatia	26.307		19.909	19.909	1.374		81%
Cyprus	6.900		2.500	2.500	7.500		145%
Czech Rep.	93.037		34.194	34.194	32.849	2.802	72%
Denmark	49.900		47.800	47.800	0		96%
Estonia	13.107	1.485	9.106	10.591	3.216		105%
Finland	61.060	56.802	10.733	67.535	5.958		120%
France	422.579	38.354	184.003	222.357	223.054		105%
Germany	434.000		295.000	295.000	137.250		100%
Greece	45.200		29.988	29.988	13.851	1.861	97%
Hungary (est.)	44.000		30.000	30.000	9.500	4.500	90%
Ireland	32.601		31.573	31.573	1.028		100%
Italy	384.000	842	170.000	170.842	170.000	32.000	89%
Latvia	12.500		8.000	8.000	3.500	1.000	92%
Lithuania	21.533		14.413	14.413	3.752	2.426	84%
Luxembourg	0	-	-	-	-		-
Malta	2.300		2.300	2.300			100%
Netherlands ***	87.746		79.933	79.933	7.813		100%
Poland (est.)	268.500		127.000	127.000	84.000	57.500	79%
Portugal	72.421	744	46.499	47.243	30.915		108%
Romania	51.413		544	544	50.869		100%
Slovak Rep. ELTMA only	27.475		22.675	22.675	632	363	85%
Slovenia	27.307		7.496	7.496	13.150	1.258	76%
Spain	238.080	202	158.125	158.327	79.753		100%
Sweden	93.532	3.013	24.623	27.636	65.896		100%
UK (estimated by UTWG)	452.659	11.065	148.643	159.708	277.283	15.669	97%
EU27+UK	3.164.282	112.507	1.652.219	1.764.725	1.254.796	136.279	95%
Norway	66.620	447	19.763	20.210	47.410		102%
Serbia (est.)	50.000		39.000	39.000	11.000		100%
Switzerland	47.200		600	600	46.600		100%
Turkey	227.509		129.619	129.619	69.009	28.881	87%
EU27+NO+CH+RS+TR+UK	3.555.611	112.954	1.841.201	1.954.154	1.428.815	165.160	95%
2018	3.573.900	96.120	1.920.100	2.016.220	1.248.880	318.800	91%
2018 vs 2019	-1%	18%	-4%	-3%	14%	-48%	4%

Figure 2.2: ELT Management in Europe, 2019 (European Tyre and Rubber Manufacturers' Association)

Other reuse and recycling methods of ELT involve applications such as controlled fuel replacement in factory furnaces, the substitution of buoys, and the fragmentation of rubber in conjunction with sand to form soft, grippy surfaces in equestrian sports tracks (Abdilla, 2012).

Over the years, several recycled tyre rubber applications have been investigated and developed in relation to concrete, a widely used construction material in modern-day architecture. Various studies have been conducted worldwide to utilise waste materials as aggregate in concrete as alternatives to natural aggregate, which is nowadays a depleting, finite resource. Some waste materials which have been studied for the given task include glass, construction and demolition waste (CDW) in the form of brick and ceramic tiles, plastic waste, and tyre rubber in its various forms. This global research may be considered imperative to the sustainable development of modern-day construction, as utilising waste materials implies both the contributions towards

the reduction of unwanted waste materials as well as the reduction of the use of natural rock, which is a depleting resource (Magro, 2011). The main issues that come along with this solution include the following:

- Feasibility regarding the production of rubberised concrete?
- Would the final product be a viable candidate for construction?
- Would the final product achieve the desired mechanical properties whilst using the maximum allowable percentage of waste material?

2.2 Effect of Rubber Aggregate Type on Concrete Behaviour

2.2.1 Shredding Method, Shape, and Texture

Tyre shredding is a process typical of ELT disposal. This is done to facilitate the reduction in overall volume and size of unwanted rubber tyres, making them easier to stockpile, handle and transport. This is done to engage in seamless waste disposal, whether it comes in the form of recycling or the burning of tyre rubber as a fuel source in industrial applications. Whole tyres take up a lot of storage space and are heavier in comparison to their shredded counterparts. Furthermore, the shredding process facilitates the removal of steel and fibres embedded in scrap tyres. The required size, shape and texture of shredded rubber depend on the opted size-reducing method. These methods are often considered difficult and costly, as tyres are manufactured to have tough and durable characteristics in order to maintain a long service life, while providing its intended product service at an optimal level. The two most common tyre shredding practices are referred to as ‘ambient-scrap tyre processing’ and ‘cryogenic tyre recycling’ (Abdilla, 2012).

Ambient-scrap tyre processing is a method specifically used to process scrap tyres near room temperature, otherwise referred to as ambient conditions. This process entails the shredding of ELT, and then further reducing the shredded product further in size by means of a granulator or cracker mill. This in turn produces rubber chips or crumb rubber as a final result. Unlike other processes, ELT are not subjected to either heating or cooling and are instead processed at room temperature in their natural state. The final product comes in the form of rubber chips, which are typically suitable in applications such as playground surfaces and athletic tracks (Abdilla, 2012).

Cryogenic tyre recycling is accomplished by freezing the scrap tyres using liquid nitrogen and lowering tyre temperatures to below glass transition temperature (-80°C). This state causes rubber to adopt brittle properties, which in turn are fed in a cooled, closed loop hammermill or multi-state screener to be crushed into smaller particles, having the fibre and steel removed by means of magnets (Magro, 2011). In this case, the end product tends to have a smoother shape when compared to the rough, angular chips produced by ambient-scrap tyre processing. These physical properties directly impact the bonding characteristics between rubber aggregate and concrete (Abdilla, 2012).

2.2.2 Size and Grading

As mentioned previously, ELT can be shredded down to various sizes by means of different shredding methods. For experimental purposes, rubber particles of comparable size and grading to natural aggregate must be considered. These are classified as follows (Magro, 2011):

- Rubber chips (76mm - 13mm)
- Ground rubber (19mm - 0.15mm)
- Crumb Rubber (9mm/5mm - 0.5mm)
- Finer Crumb Rubber (0.474mm - 0.075mm)

Ground and crumb rubber were used extensively during past investigations in relation to mineral aggregate replacement in concrete. Aside from their individual research, Magro (2011) and Abdilla (2012) documented several studies by past researchers who had opted for various sizes of rubber particles for experimentation. Scicluna (2010) used rubber chip aggregate ranging from 14mm - 10mm serving as a coarse aggregate replacement, while using 10mm - 5mm crumb rubber as a fine aggregate option for comparison. Masvroulidou and Figueiredo (2007) also opted for coarse and fine rubber aggregate comparison, having a coarse rubber aggregate range of 19mm - 10mm and a fine aggregate range of 10mm - 4.75mm. Both aggregates were sieved and split from a 20mm - 1mm collection of rubber particles (Magro, 2011).

The results from the majority of the mentioned investigations concluded that rubberised concrete having rubber chips or ground rubber as an alternative to natural

coarse aggregate had a lower compressive strength than that containing crumb rubber as the replacement of natural fine aggregate, as confirmed and reported by Masvroulidou and Figueiredo (2007), adding that the density of concrete containing coarse rubber aggregate was higher than concrete containing fine rubber aggregate (Magro, 2011).

2.2.3 Percentage (%) Replacement

As mentioned previously, multiple researchers have reported that as percentages of both coarse and fine rubber aggregate increased, the compressive strength, flexural strength and tensile splitting strength consequently decreased considerably. This was concluded after a series of percentage replacements were tested by the researchers in question, who gradually increased the volume and mass % of natural aggregate to be replaced by rubber aggregate in the concrete mixtures prior to testing. These variations were controlled from nil to extreme, bringing out any clear trends throughout the process. Abdilla (2012) and Magro (2011) alongside others, proposed limits on the percentage replacement of aggregate based on the structural viability of the concrete mixes. However, a number of researchers including Khorami et al. (2007) suggested that the percentage replacement of aggregate does not cause significant changes in material properties, nullifying the idea that the structural viability of the concrete mix will be affected at all (Abdilla, 2012). Finally, Masvroulidou and Figueiredo (2007) limited the percentage replacement to 50% for coarse rubber aggregate and 40% for fine rubber aggregate.

2.3 Physical Properties of Rubberised Concrete

2.3.1 Slump and Workability

Mohamed Amin et al. (2022) studied the mechanical behaviour of rubberised concrete containing crumb rubber aggregate as partial fine aggregate replacement in its respective concrete mix. Ease of handling, placing and finishing of concrete was generally documented to be satisfactory for a moderate percentage replacement of aggregate. The slump test results showed a decrease in slump values as the percentage of crumb rubber increased. The control concrete mix exhibited a slump of

47mm, while mixes with crumb rubber percentage replacements of 5%, 10%, and 15% exhibited slumps of 45mm, 42mm, and 39mm respectively. These results showed an overall reduction in slump as crumb rubber content in the concrete mix increased, hence concluding with a steady decrease in workability. They concluded that 10% fine aggregate replacement was the optimal percentage in concrete based on their results (Mohamed Amin et al., 2022).

Table 2.1: Slump test results (Mohamed Amin et al., 2022)

Rubber crumb mix (%)	Slump (mm)
Control	47
CRC5	45
CRC10	42
CRC15	39

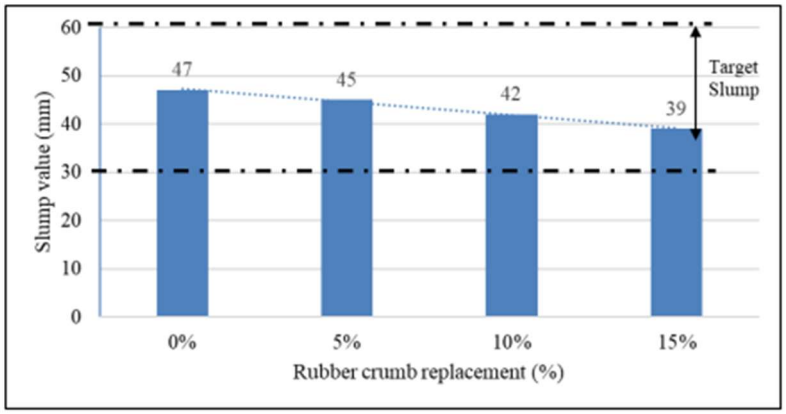

This behaviour comes as a result of the interaction between rubber aggregate and natural aggregate. On the other hand, when documenting slump results for rubber chips replacing coarse aggregate, slump reduction was significantly less than that for the coarse aggregate concrete control mix (Abdilla, 2012). Magro (2011) reported a zero-slump value when replacing 50% of the natural coarse aggregate. Moreover, cement coated rubber aggregate concluded similar results to those of plain rubber aggregate.

On the other hand, other researchers came to different results and conclusions. Eldin et al. (1994) compared slump results for rubber chips obtained by mechanical grinding (Edger) and cryogenic grinding (Preston), and crumb rubber. Their research concluded that the size and shape of the rubber particles directly affect slump of a rubberised concrete mix:

- *Edger Chips* - These rubber chips are long and angular and contain protruding steel wires. Eldin et al. (1994) stated that Edger chips resist the normal flow of concrete under self-weight.
- *Preston Chips* - These rubber chips allow for a smoother flow, having been described as “fluid” by Eldin et al. (1994).

A significant difference in slump was observed between rubber aggregate obtained from cryogenic grinding (Preston: 0.25 inches) and mechanical grinding (Edger: 0.75 - 1.5 inches), as indicated in Figure 2.3:

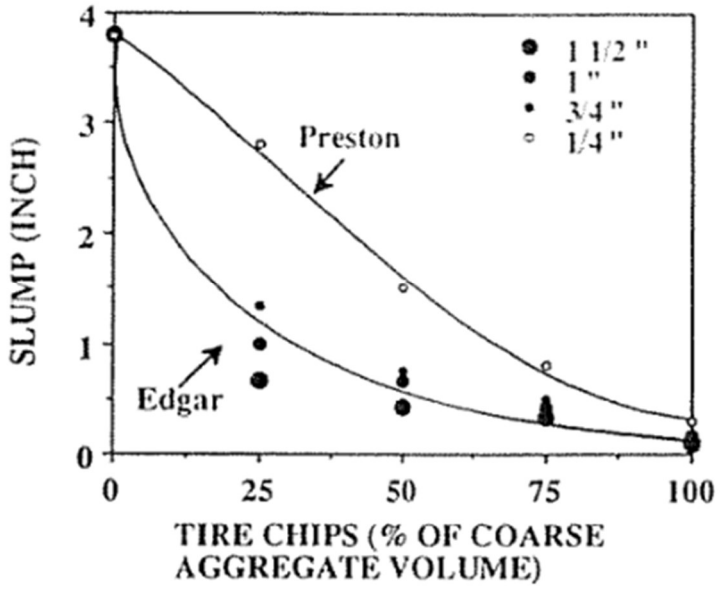

Figure 2.3: Slump values for Edger Chips and Preston Chips (Eldin et al., 1994)

Magro (2011) recorded the findings of Wong and Ting (2009), who found that high-strength concrete (water-cement ratio = 0.27) had a smaller slump than normal-strength concrete (water-cement ratio = 0.6). Furthermore, they indicated that larger rubber particles in the form of chips (i.e. Preston and Edger chips) exhibited a smaller slump than crumb rubber, due to the physical properties of the latter not containing presences of steel fibres, allowing for more fluidity in the final concrete mix. Finally, rubberised concrete with mineral admixtures (ground granulated blast-furnace slag and silica fumes) resulted in smaller slump than rubberised concrete containing 0% mineral admixtures (Magro, 2011).

2.3.2 Air Content

Siddique and Naik (2004), cited by Magro (2011), concluded that rubberised concrete contained higher volumes of air when compared to regular concrete. Nehdi et al. (2001) and Reda Taha et al. (2008), who were cited by Abdilla (2012), stated that the specific gravity of rubber was to be 1.14 and 1.1. This was concluded after observing rubber aggregate floating on water, which would imply a minimum specific gravity of 1. It was concluded that rubber particles are hydrophobic and their rough surfaces trap air (Abdilla, 2012). Furthermore, due to rubber's water-repelling capabilities, it attracted air particles when added to the concrete mixture (Magro, 2011).

Larger rubber aggregate traps more in its surrounding pores than smaller rubber aggregate, as smaller aggregate is deemed to have a higher packing factor. Moreover, pores form because of interference between the rubber particles and the cementitious paste. Figueiredo et al. (2007) stated that rubber aggregate containing protruding steel fibres had decreased overall air contents (Abdilla, 2012).

2.3.3 Unit Weight and Density

Generally speaking, the percentage replacement of natural aggregate with rubber aggregate in concrete affects concrete's unit weight and hence, density of the material. This comes as a result of rubber's specific gravity, which is significantly lower than that of natural aggregate. Therefore, higher percentage replacement mixes produce less dense concrete when hardened. Furthermore, replacing coarse aggregate produces concrete which is less dense than fine aggregate replacement concrete (Abdilla, 2012).

Various researchers have found that density is a function of the interaction of percentage replacement, rubber aggregate size, and water-cement ratio. Rubber aggregate size and water-cement ratio are attributed by the interaction between rubber's packing factor and water content. In other words, smaller rubber particles contain less pores which in turn, reduce water content (Abdilla, 2012).

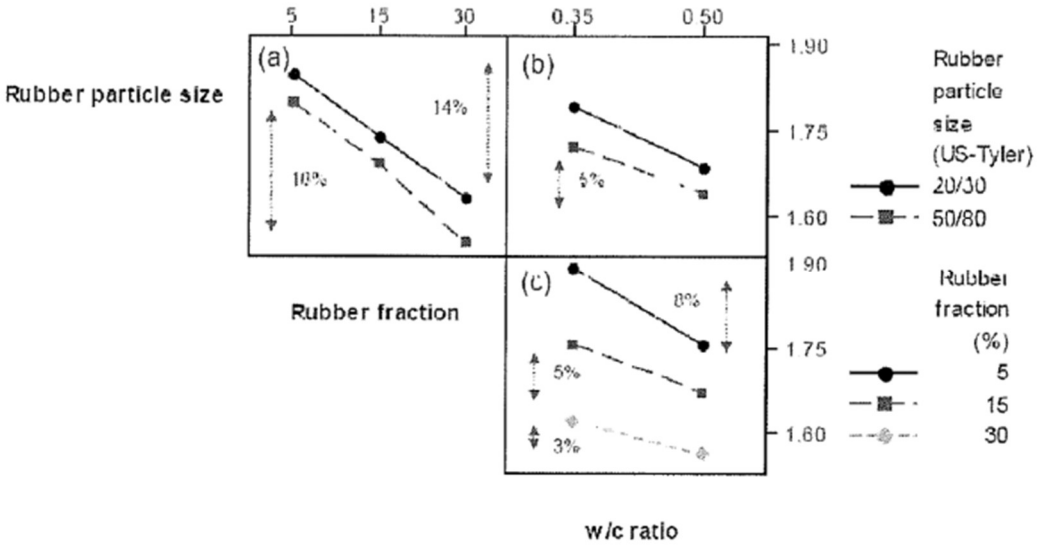

Figure 2.4: Interaction of particle size, percentage replacement, and water-cement ratio on apparent density (Abdilla, 2012)

Magro (2011) cited Caines et al. (2004), who reported a 10% reduction in the unit weight of rubberised concrete when natural coarse aggregate was replaced by 50% cement-coated rubber aggregate. This reduction in unit weight from plain rubber aggregate concrete stemmed from the low specific gravity of rubber chips. Scicluna (2010) reported a 21% reduction in unit weight when natural fine aggregate was fully replaced by crumb rubber aggregate. Furthermore, shredded rubber chip (SRC) concrete mixes had slightly higher densities than crumb rubber (CR) concrete mixes.

Table 2.2: Unit weights of control concrete and rubberised concrete (Magro, 2011)

Samples	Unit weight (kg/m^3)	% reduction
D	2500	0
DC10	2475	1
DC25	2425	3
DC50	2350	6
DP10	2450	2
DP25	2375	5
DP50	2250	10

This was concluded after a series of comparative tests were carried out, with

percentage replacement being an identical factor between the two subjects (Magro, 2011).

Table 2.3: Density of mixes (Magro, 2011)

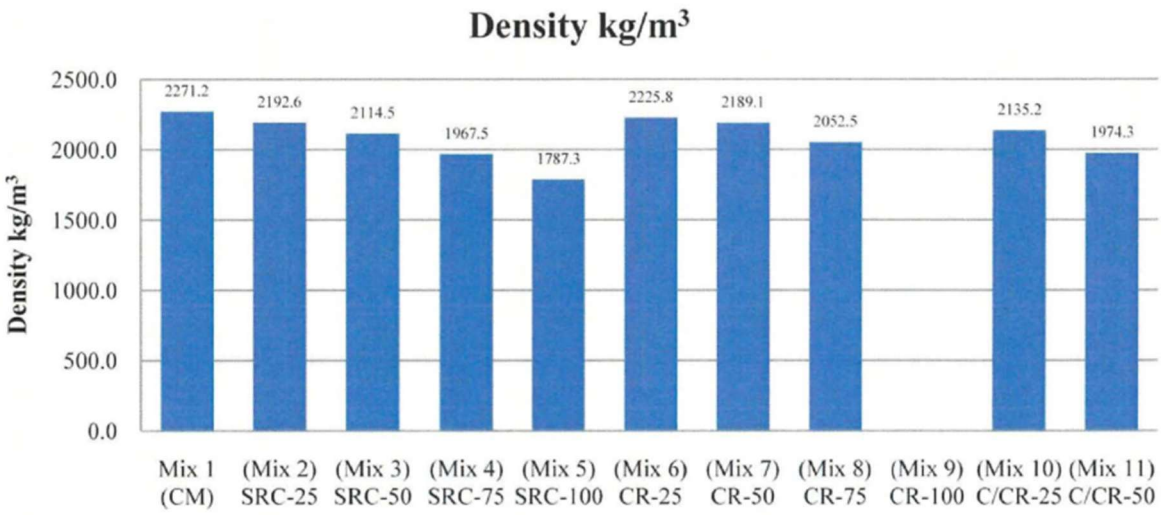

2.4 Mechanical Properties of Rubberised Concrete

2.4.1 Compressive Strength

Past investigations have proven that rubberised concrete exhibits an overall reduction in compressive strength when compared to normal aggregate concrete. The relationship between rubber aggregate percentage replacement and reduction in compressive strength is non-linear, as the compressible properties of rubber create weak inclusions within concrete when hardened. Simply put, as rubber aggregate percentage in concrete increases, compressive strength decreases (Abdilla, 2012).

Magro (2011) cited multiple researchers, discussing their experimental methods and results. Firstly, El-Gammal et al. (2010) used both chipped and crumb rubber in their compressive strength analysis of rubberised concrete. They observed a 90% decrease in compressive strength of the material when fully replacing coarse aggregate with rubber chips, whilst observing an 80% decrease in compressive strength when using crumb rubber as a full replacement. Furthermore, they reported a small difference in compressive strength when replacing 50% of the sand with crumb rubber from that full replacement (Magro, 2011).

Scicluna (2010) noted a reduction in the cube compressive strength when replacing coarse natural aggregate and fine natural aggregate with chipped rubber and crumb rubber respectively. In this case, Scicluna (2010) replaced natural aggregate in increments of 25%, concluding that rubberised concrete with crumb rubber had higher compressive strength capabilities than that with chipped rubber, when experimenting with percentage replacements of 25% and 50%. On the other hand, when replacing 75%, the chipped rubber concrete exhibited a higher compressive strength than that with crumb rubber (Scicluna, 2010).

Kew and Kenny (2009) reported a significant reduction in compressive strength when coarse aggregate was replaced by 20mm rubber chip aggregate. They indicated from their studies that the mix with the lowest water-cement ratio (0.48) performed the best from a series of varied mixes. This particular mix had a lower voids content as it contained 10mm coarse natural aggregate rather than 20mm (Magro, 2011).

Mohamed Amin, M.A. et al. (2022) documented the compressive strength of a mix over 7 and 28 days (Table 2.4). Their results proved that compressive strength over 7 and 28 days decreases as percentage replacement increases:

- 7 days - 12.73% to 27.4% reduction
- 28 days - 4.81% to 23% reduction

Table 2.4: Compressive strength test results (Mohamed Amin et al., 2022)

Rubber crumb mix (%)	7 days (MPa)	28 days (MPa)
Control	21.2	39.5
CRC5	18.5	37.6
CRC10	17.1	36.9
CRC15	15.4	30.4

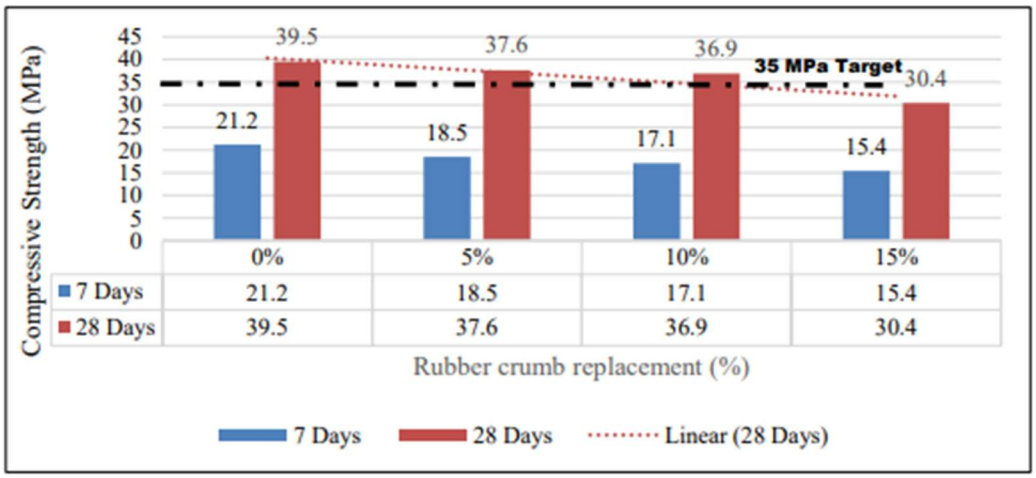

The reduction in strength for crumb rubber concrete comes down to two main reasons, namely air content and stiffness. Crumb rubber has high air content compared to fine natural aggregate, leading to low adhesion between crumb rubber and other binding materials within hardened concrete. Furthermore, crumb rubber possesses lower stiffness levels as percentage replacements increase, resulting in lower mass stiffness in concrete, reducing the overall bearing capacity of the material. However, whilst the reduction in value is evident, CRC5 and CRC10 are still capable of reaching the target strength of 35 MPa, whilst CRC15 is unable to do so (Mohamed Amin et al., 2022).

Each of these cases exhibit a common characteristic as compressive strength is reduced. This refers to the ductility each specimen undergoes before failing. Furthermore, compressive failure seems to progress in an unusual manner when compared to regular cases, as rubber aggregate binds specimen fragments together at failure. This trend becomes more noticeable as rubber content increases in the mixture (Magro, 2011).

The reduction in compressive strength in rubber aggregates comes down to the bonding characteristics between rubber aggregate materials and the concrete matrix. Abdilla (2012) cited Emiroglu et al. (2007), who described concrete to be a three-phase material consisting of the aggregate particles, cementitious paste binding aggregate particles together, and the interfacial transition zone (ITZ) between aggregate and paste. Weak bonding strength is evident for two main reasons. Firstly, the strength of rubber aggregate is inferior to that of natural aggregates. Secondly, stress transfer between rubber and paste occurs due to mechanical interlocking, and tearing of the rubber is not observed on the fracture surface. Furthermore, voids are formed in the ITZ, specifically around the rubber aggregate. These act as a starting point for crack formation (Abdilla, 2012).

Various methods to improve compressive resistance have been studied and experimented upon. Besides rubber percentage replacement, natural aggregate variation also plays a role in the ultimate compressive strength of concrete. Wong and Ting (2009) found that the inclusion of 65% ground granulated blast furnace slag (GGBS) led to a rise in compressive strength in rubberised concrete. Finally, coating

rubber aggregate with cement enhances bonding between rubber aggregate and concrete (Abdilla, 2012).

2.4.2 Splitting Tensile Strength

Just like compressive strength, an increase in percentage replacement of natural aggregate in rubberised concrete results in an overall reduction in tensile strength of the material, albeit at a lesser rate. Moreover, maturing of concrete has a more significant effect on tensile strength (Eldin et al., 1994).

Mohamed Amin et al. (2022) indicated similar results, expressing that the achieved tensile strength test results shown in Table 2.5 had shown a decreasing pattern for 28 days when percentage replacements with crumb rubber increased. They concluded that this reduction in tensile strength happened due to the smooth texture of crumb rubber. As they increased the load on the specimen, cracks had begun to form within the concrete cylinder. The smooth texture of the crumb rubber accelerates cracking as loading increases, just as Mohamed Amin et al. (2022) experienced during their tests.

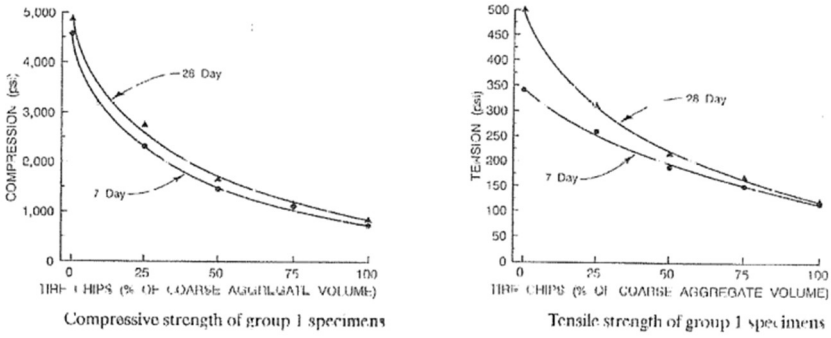

Figure 2.5: Maturing, compressive and tensile strength for chipped rubber concrete (Abdilla, 2012)

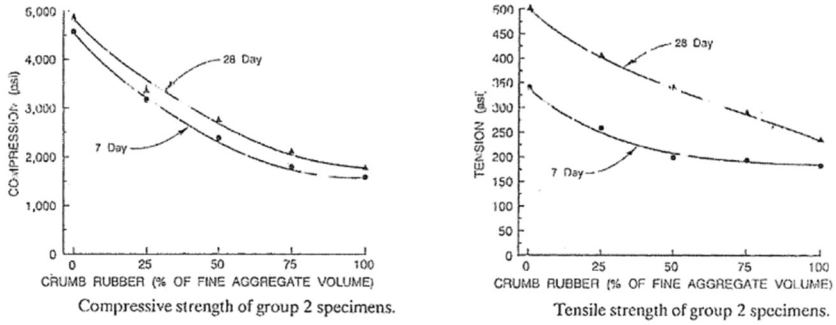

Figure 2.6: Maturing, compressive and tensile strength for crumb rubber concrete (Abdilla, 2012)

Table 2.5: Splitting tensile test results (Mohamed Amin et al., 2022)

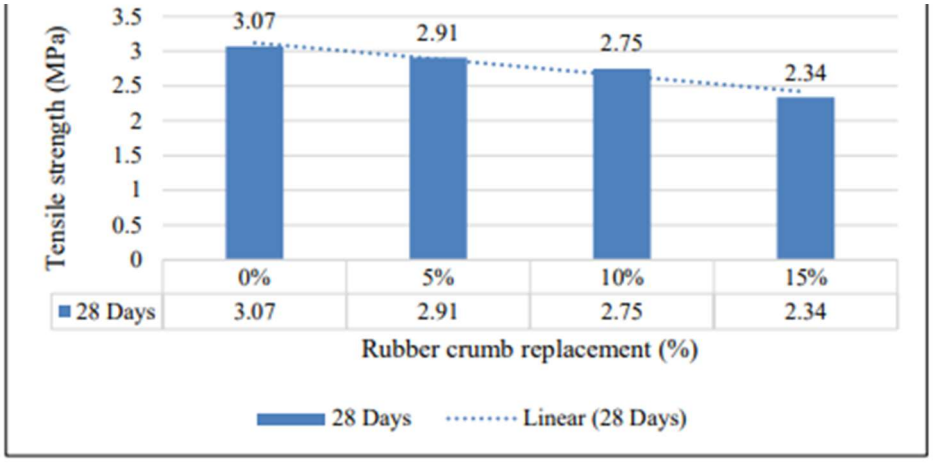

2.4.3 Flexural Strength

Scicluna (2010) noted a reduction in flexural strength of the rubberised concrete beams tested. He noted a lower reduction in flexural strength when using chipped rubber aggregate as a replacement to coarse natural aggregate in concrete, observing better overall flexural strength than the specimen containing crumb rubber as an alternative to fine natural aggregate. When testing with a 25% aggregate replacement in concrete, he achieved flexural strength reductions of 4.4% and 12.6% for mixes including crumb rubber and rubber chips respectively. As percentage replacement of natural aggregate increased, chipped rubber concrete was said to perform better under the given loading conditions than crumb rubber concrete. Finally, when both crumb rubber and rubber chips were included in the concrete mix replacing 25% of both fine and coarse mineral aggregate, a flexural strength reduction of 20% was noted (Magro, 2011).

Since flexural strength is a function of compressive and tensile stresses, a loaded beam specimen would fail under lower tensile stresses. Therefore, like tensile strength, flexural strength depends on the bonding of rubber to cementitious paste. Fine crumb rubber's smoothness makes bonding to cement paste more difficult than bonding between rubber chips and cementitious paste (Abdilla, 2012).

2.4.4 Shear Strength

Abdilla (2012) used crumb rubber as an aggregate replacement to fine coarse aggregate during experimentation on rubberised concrete (CR) unreinforced and reinforced beams. He noted an abrupt failure in both beams. Failure for the shear reinforced beam was said to be slightly more brittle due to its original stiffness when compared to the unreinforced specimen. However, Abdilla (2012) concluded that the inclusion of 25% fine aggregate replacement by crumb rubber did not hinder the general load-strain/deflection behaviour. It could be observed that the tensile reinforcement unloading path of the specimens was almost parallel to the loading path, indicating elasto-plastic behaviour of the tensile steel reinforcement in the material. Furthermore, he pointed out that adding stirrups only improved shear resistance by 5%. When experimenting on 25% crumb rubber cubes (CR25), Abdilla (2012) described failure to be abrupt and brittle. Each cube split into two separate blocks upon failure, emphasising on the lack of bonding between crumb rubber and cementitious paste (Abdilla, 2012).

When using shredded rubber chips as an aggregate replacement in the rubberised concrete mix (SRC25), shear failure occurred at a lower load, as SRC25 was considerably weaker. In this case, the tensile reinforcement unloading path started by elastically retracing the loading path, but suddenly deviating beneath the loading path at a certain point, indicating some permanent deformation present in the tensile steel reinforcement within the specimen. Failure in the beam specimens was ductile, having significant plastic deformation. Thin cracks started to develop and open erratically to form a thick vertical crack in the beams upon failure. Furthermore, vertical cracks at the end of the beam along with secondary inclined cracks began to form, and a few hairline flexural cracks were documented towards the middle regions of both beams. Failure loads for SRC25 beams were documented at 125kN and 139kN, indicating a steep decline from the CR25 beams. In this case, the addition of stirrups was calculated to improve shear resistance by 11%. When experimenting on SRC25 cubes, deformation was observed along the cubes' area before failure, when the split fragments were still held together by the interconnecting rubber chips. This research proved that rubber chips exhibit better bonding characteristics than crumb rubber (Abdilla, 2012).

2.4.5 Toughness

Abdilla (2012) stated that the inclusion of rubber in concrete provides sufficient fracture toughness. Most of the fracture energy generated within a tough material occurs in the plastic region of the stress-strain curve, which in turn identifies the toughness of a material by means of computation. Abdilla (2012) cited Eldin et al. (1994), who determined the toughness for 100percentage replacement of various sizes of rubber chips and crumb rubber, loaded in compression. Toutanji (1996) investigated the toughness of rubberised concrete beams under flexural loading based on the load-deflection curve at a flexural load of 85% of the maximum load (P_{max}). He calculated the toughness value as a ratio of the area under the load deflection up to 85% of P_{max} and the area under the load deflection corresponding to an approximation of the limit elastic behaviour. It may be concluded that rubberised concrete has ductile properties as Toutanji (1996) found no significant difference in the toughness of rubberised concrete containing 50% and 100% rubber chips, being equivalent to 1.21. On the other hand, the toughness of regular concrete is 1 (Toutanji, 1996).

Abdilla (2012) cited Nehdi et al. (2001), who observed gradual splitting failure of concrete specimens for mixes involving coarse rubber aggregate as natural aggregate replacement, as well as a shear mode for mixes involving crumb rubber aggregate as natural aggregate replacement. The observed gradual failure indicated that rubberised concrete exhibits high levels of toughness, since most of the total energy generated is plastic. Nehdi et al. (2001) cited Eldin et al. (1994), who documented their findings on the matter, stating that rubberised concrete was able to resist a fraction of the ultimate load after failure before undergoing excessive deflections, yet remaining partially intact. This is due to rubber aggregate’s mechanical properties, which allowed it to act as springs until stresses overcame the bond between the cementitious paste and the rubber particles (Abdilla, 2012).

2.5 Cracking Behaviour and Durability

2.5.1 Crack Distribution and Width

Wang et al. (2020) stated that the fracture properties of rubberised concrete may be attributed to the low adhesive properties between the rubber particles and

cementitious paste. They studied the effects of temperature and humidity on the cracking behaviour of rubberised concrete by means of a three-point bending test. The digital image correlation technique was used to observe cracking and fracture behaviour of rubberised concrete specimens under different temperature and humidity conditions. Their results indicated that the main method of fracture of the specimens consisted of an opening mode (Mode I). They documented the maximum width of the fracture process zone (FPZ) and crack width of the rubberised concrete beam specimen to be like those in regular concrete, noting an FPZ width of approximately half of the maximum aggregate diameter. Meanwhile, the crack width of the beam specimen linearly decreased with height (Wang et al., 2020).

As mentioned in chapter 2.4.5, rubberised concrete exhibits more distributed cracking patterns when compared to regular concrete. Rather than forming large, concentrated cracks, smaller and more evenly spread cracks are observed. The incorporation of rubber aggregates such as crumb rubber reduces concrete's crack width due to the material's elastic properties. This characteristic of rubberised concrete may be beneficial in applications requiring enhanced toughness and energy absorption, such as seismic zones. As discussed in chapter 2.2, rubber particle type, size, and percentage replacement also affect crack control, with larger and irregular rubber particles often aiding in crack width reduction (Wang et al., 2020).

2.5.2 Long-term Durability

Abdelaleem et al. (2024) focused their research on examining the drying shrinkage, impact and post-impact, and creep behaviour of rubberised concrete. They did this by experimenting on four groups of cylindrical samples, each containing rubberised concrete spanning 300mm in length and 150mm in diameter. In this case, Abdelaleem et al. (2024) developed concrete mixes containing crumb rubber aggregate as a replacement to fine natural aggregate, in increments of 0%, 10%, 20%, and 30%. These samples were subjected to a consistent loading corresponding to 25% of the bearing capacity determined by means of compression tests on other trial mixes. The timeframe for testing spanned throughout the course of a year, during which measurements for total strain, dependent strain, creep, and shrinkage were recorded at regular intervals. Tests on different crumb rubber aggregate mixtures were carried

out at intervals of 28 days, three months, six months, and one year. This was done to emphasise distinctions in results relating to proportions, compression tests, indirect tensile tests, flexural strength tests, and impact resistance. The achieved results demonstrated notable effects regarding concrete creep and impact energy due to the addition of rubber aggregate. Despite these outcomes, shrinkage results determined minimal influence over the given timeframe. However, there was a general decrease in the specimens' compressive strength, with regressions of 25-35%, 45-50%, and 55-65% for percentage replacements of 10%, 20%, and 30% crumb rubber respectively. Moreover, they concluded that creep negatively affects the impact resistance of regular concrete. The inclusion of rubber aggregate helped mitigate creep effects on impact resistance, resulting in reductions ranging from 6-12% across percentage replacements between 10-30% (Abdelaleem et al., 2024).

2.6 Effect of Cyclic Loading including Seismic Loading

2.6.1 Introduction to Cyclic Loading and its Relevance

Cyclic loading refers to the repeated application of stress on strain on a material over time. This is often encountered in structures subjected to various modes of dynamic loading including wind loads, traffic, or earthquakes. In other words, cyclic loads correspond to variable loads (accidental loads) such as sudden vibrations. This in turn creates stress reversals, causing fatigue and progressive degradation in regular concrete. Cyclic loads tend to vary throughout a structure's lifespan until its end-of-life, although these variations tend to happen systematically. They may arise depending on the actions imposed on the structure. For example, ships exposed to wind and waves experience cyclic loading as a result of the filling and emptying cycles during fuelling, as well as wind and wave loading from the sea (Moore and Booth, 2015).

Seismic loading is a critical type of cyclic loading, where ground movement induces repeated stresses, potentially leading to a compromise in a structure's integrity and stability. Regular concrete exhibits brittle characteristics, making it prone to cracking under such conditions. On the other hand, rubberised concrete exhibits flexible and energy-absorbing properties, making it a potential candidate for improving seismic

resilience and enabling structures the ability to withstand and recover from dynamic loads (Xu et al., 2020). The objectives of studying cyclic loading are as follows:

- To understand how rubber aggregate as a replacement to natural aggregate affects fatigue resistance in concrete.
- To assess how ductility and energy dissipation contribute to the structural integrity of a concrete structure under repeated loading.
- To optimise mix designs for seismic applications by balancing material strength and flexibility.

2.6.2 Behaviour of Rubberised Concrete under Cyclic Loading

Xu et al. (2020) investigated rubberised concrete's response to static and cyclic compression, accounting the stress-strain response of rubberised concrete materials as well as their reference to high-strength regular concrete. Their experiments involved varied percentage replacements of both fine and coarse natural aggregates in increments between 0% and 40%, comprising 90 cylindrical specimen samples. Three strain rate levels, simulating static, moderate and severe seismic action were examined under both static and cyclic loading. Their results confirmed that increases in rubber content have detrimental effects on concrete's stiffness and strength. However, the same increase in rubber content improved concrete's compressive recovery under cyclic loading, as well as improving its energy accumulation rate and inter-cycle stability. Moreover, concrete's inter-cycle degradation rates were lowered considerably. Furthermore, their results showed that an increase in strain rate from static to severe seismic lead to a notable increase in concrete's stiffness and strength, with these enhancements becoming less significant as % rubber content increased (Xu et al., 2020).

Elghazouli et al. (2022) examined the behaviour of circular steel tubes infilled with rubberised concrete under lateral cyclic deformations with and without coexisting axial loading. In this case, the percentage replacement of natural aggregate to rubber aggregate in concrete varied up to 60% under axial loads reaching up to 30% of the nominal capacity. Elghazouli et al. (2022) also tested hollow steel tubes for comparative purposes, focusing on both samples' stiffness, capacity, ductility, energy dissipation, and failure mechanisms. They concluded that although high rubber

percentage replacements lead to a noticeable loss in concrete strength, the corresponding reduction in member capacity was much less noticeable due to the addition of the steel tube, which confined the rubberised concrete within it. Furthermore, the rubberised concrete tube samples exhibited up to a 10% increase in ductility, and a 17% increase in energy dissipation when compared to the regular concrete tube samples (% depend on rubber content used). Elghazouli et al. (2022) concluded that the steel tube samples infilled with rubberised concrete were more favourable when it came to inelastic cyclic performance (Elghazouli et al., 2022).

2.6.3 Energy Dissipation and Damping Capacity

Xue and Shinozuka (2013) studied the energy dissipation and damping capabilities of rubberised concrete, thus determining the seismic performance of crumb rubber aggregate concrete. This was done to determine how rubberised concrete would perform in potential seismic applications within the construction industry. Their experimental research consisted of small-scale column models, which were fabricated using rubberised concrete with different percentage replacements of crumb rubber as an alternative to fine natural aggregate. These column models were evaluated in terms of dynamic performance, including free vibration tests to identify damping ratios, and seismic shake table tests to determine rubberised concrete's structural responses to earthquake ground motion. Furthermore, Xue and Shinozuka (2013) tested cylindrical rubberised concrete samples to determine their compressive strength and modulus of elasticity. They achieved a 62% increase in the damping coefficient of the specimens when compared to regular concrete trial mixes, hence having a 27% decrease in the seismic response acceleration of the structure. As mentioned in most other case studies, compressive strength in concrete decreases as % rubber aggregate increases, which was also the case here. However, they found that adding silica fume to the mix improved the bonding capabilities between the rubber particles and cement, increasing concrete strength in the process. They concluded that rubberised concrete as a structural material helps enhance dynamic performances and reduces seismic responses within concrete structures (Xue and Shinozuka, 2013).

2.7 Potential for Seismic Engineering Applications

As discussed previously in past research, rubberised concrete may be used in structural situations where high compressive strengths are not required. Rubberised concrete becomes beneficial when relating to its enhanced ability to undergo deformation without sudden failure (ductility), making it an ideal candidate for absorbing seismic energy (Abdilla, 2012). It also excels with regards to energy dissipation and crack resistance. The elastic behaviour of rubber particles has the ability to reduce stress concentration on structural members during seismic events, as rubber exhibits efficient energy absorbing and dissipating properties. Rubber aggregate also enhances crack distribution and width control, helping resist catastrophic failure scenarios under cyclic loading.

With that being said, rubberised concrete has potential seismic engineering applications in construction. Structural members such as columns, beams, shear walls, and various foundation systems may make use of rubberised concrete as an alternative to regular concrete in scenarios where energy dissipation and deformation capacity are critical. Furthermore, existing structures could benefit from rubberised concrete overlays or infills to improve seismic resilience and flexibility, especially in known seismic zones (seismic retrofitting). Finally, rubberised concrete could act as a suitable concrete replacement in bridge applications. In such scenarios, rubberised concrete can help reduce vibration and fatigue damage in bridges from lateral and cyclic loading.

3. Performance of Concretes with Different Percentage Replacement of Aggregates

3.1 Mix Proportions and Aggregate Characteristics in Previous Studies

This section outlines the control concrete design mixes and aggregate percentage replacement proportions corresponding to the afore-mentioned research studies carried out by Scicluna (2010), Magro (2011), and Abdilla (2012). Furthermore, this chapter focuses on the comparative performance of concretes, specifically concretes under compressive and flexural loading. Therefore, it is essential to establish the base constituents within the mix designs used for these studies, along with the different % rubber replacement mixes tested. As shown in Tables 3.1 to 3.6, each study adopted a similar water-cement ratio of 0.55, although utilising distinct ranges of rubber percentage replacements, resulting in differing mechanical responses and results.

Scicluna's (2010) research revolved around the extensive investigation of rubber percentage replacements within concrete mixes and how these various replacements would impact concrete performance, particularly when subject to compressive and flexural loads. Scicluna's (2010) objective was to understand which mixes would achieve results close to those of the control mix, hence the variety in final mixes.

Magro's (2011) followed that of Scicluna (2010), where the mixes with the highest compressive strengths achieved by Scicluna (2010) were chosen to study their flexural strengths. Abdilla (2012) opted to continue both these studies by assessing the performance of rubberised concrete from a shear point of view. In his case, he opted for identical percentage replacement mixes to Magro (2011).

Tables 3.1 and 3.2: Control mix contents / Table of concrete mixes – Scicluna (2010)

Material	Quantities (per m^3)
Cement (kg)	360
Water(kg/ltr)	200
Fine Aggregate (kg)	605
Coarse Aggregate 5-10mm (kg)	410
Coarse Aggregate 10-20mm (kg)	820

Water-Cement Ratio	0.55

3. Performance of Concretes with Different Percentage Replacement of Aggregates

Mix no.	Mix Type	Fine Aggregate (63µ to 4mm)	Coarse Aggregate (5mm to 10mm)	Coarse Aggregate (10mm to 20mm)	Crumb Rubber (63µ to 4mm)	Rubber Chips (5mm to 10mm)	Rubber Chips (10mm to 14mm)
1	Control Mix (CM)	100%	100%	100%	0%	0%	0%
2	CR25 - 25% Crumb Rubber	75%	100%	100%	25%	0%	0%
3	CR50 - 50% Crumb Rubber	50%	100%	100%	50%	0%	0%
4	CR75 - 75% Crumb Rubber	25%	100%	100%	75%	0%	0%
5	CR100 - 100% Crumb Rubber	0%	100%	100%	100%	0%	0%
6	SRC25 - 25% Shredded Rubber Chips	100%	75%	75%	0%	25%	25%
7	SRC50 - 50% Shredded Rubber Chips	100%	50%	50%	0%	50%	50%
8	SRC75 - 75% Shredded Rubber Chips	100%	25%	25%	0%	75%	75%
9	SRC100 - 100% Shredded Rubber Chips	100%	0%	0%	0%	100%	100%
10	CR/SRC25 - 25% Crumb Rubber and Shredded Rubber Chips	75%	75%	75%	25%	25%	25%
11	CR/SRC50 - 50% Crumb Rubber and Shredded Rubber Chips	50%	50%	50%	50%	50%	50%

Tables 3.3 and 3.4: Control mix contents / Table of concrete mixes – Magro (2011)

Material	Quantities (per m^3)
Cement (kg)	345
Water(kg/ltr)	190
Fine Aggregate (kg)	670
Coarse Aggregate 5-10mm (kg)	340
Coarse Aggregate 10-20mm (kg)	670

Water-Cement Ratio	0.55

Mix No.	Mix Type	Fine Aggregate (63µ to 4mm)	Coarse Aggregate (5mm to 10mm)	Coarse Aggregate (10mm to 20mm)	Crumb Rubber (63µ to 4mm)	Rubber Chips (5mm to 10mm)	Rubber Chips (10mm to 14mm)
1	Control Mix (CM)	100%	100%	100%	0%	0%	0%
2	CR25 - 25% Crumb Rubber	75%	100%	100%	25%	0%	0%
3	CR50 - 50% Crumb Rubber	50%	100%	100%	50%	0%	0%
4	SRC25 - 25% Shredded Rubber Chips	100%	75%	75%	0%	25%	25%
5	SRC50 - 50% Shredded Rubber Chips	100%	50%	50%	0%	50%	50%
6	CR/SRC25 - 25% Crumb Rubber and Shredded Rubber Chips	75%	75%	75%	25%	25%	25%

Tables 3.5 and 3.6: Control mix contents / Table of concrete mixes – Abdilla (2012)

Material	Quantities (per m^3)
Cement (kg)	345
Water(kg/ltr)	190
Fine Aggregate (kg)	585
Coarse Aggregate 5-10mm (kg)	390
Coarse Aggregate 10-20mm (kg)	780

Water-Cement Ratio	0.55

Mix No.	Mix Type	Fine Aggregate (63µ to 4mm)	Coarse Aggregate (5mm to 10mm)	Coarse Aggregate (10mm to 20mm)	Crumb Rubber (63µ to 4mm)	Rubber Chips (5mm to 10mm)	Rubber Chips (10mm to 14mm)
1	Control Mix (CM)	100%	100%	100%	0%	0%	0%
2	CR25 - 25% Crumb Rubber	75%	100%	100%	25%	0%	0%
3	CR50 - 50% Crumb Rubber	50%	100%	100%	50%	0%	0%
4	SRC25 - 25% Shredded Rubber Chips	100%	75%	75%	0%	25%	25%
5	SRC50 - 50% Shredded Rubber Chips	100%	50%	50%	0%	50%	50%
6	CR/SRC25 - 25% Crumb Rubber and Shredded Rubber Chips	75%	75%	75%	25%	25%	25%

These three studies collectively offer a broad dataset covering ascending increments of rubber content in concrete. All three studies share similar water-cement ratios and aggregate contents, allowing for meaningful comparisons between regular concrete and rubberised concrete. Particular attention has been given to compressive strength and flexural performances of the above mixes, forming a benchmark against which the results of this study can be evaluated.

3.2 Compressive Strength Performance of Concrete with Replacement Aggregates

The compressive strength of a mix after 7 and 28 days provides insight into concrete's quality. This parameter is widely reported across all three mentioned studies, with all three researchers having evaluated the effects of natural aggregate replacement on concrete's compressive strength. The results presented by Magro (2011), Abdilla (2012), and Scicluna (2010) consistently demonstrate that the inclusion of rubber, whether in crumb or shredded chip form, produces considerable reductions in compressive strength when compared to the respective control mixes. The extent of this reduction is influenced by the percentage replacement, particle size and grade, and the fine/coarse aggregate fraction.

3.2.1 Influence of Rubber Content on Compressive Strength

Across all three studies, increasing concrete's rubber content led to a progressive reduction in compressive strength. This trend could be noticed in both mixes containing crumb rubber replacing fine aggregate, and mixes containing shredded rubber replacing coarse aggregate.

At 25% crumb rubber replacement (CR25), all three studies reported a noticeable yet moderate decline in compressive strength in respect to their control mixes. The reduction became significantly more apparent at 50% (CR50), with mixes exhibiting reduced load-resisting capabilities and higher overall deformation at failure. Scicluna (2010) tested higher replacement mixes including CR75 and CR100. These mixes exhibited severe reductions in compressive strength, in some cases rendering the material unsuitable for structural applications. These results highlight the strong

influence regular fine aggregate has on concrete's compressive strength, as the gradual replacement with crumb rubber particles substantially disrupts the continuity and stiffness of the cementitious mix.

Similar strength reductions were noticed in shredded rubber replacement mixes (SRC), although in this case, the magnitude was sometimes less severe than the fine aggregate replacement mixes at lower percentage replacement levels (Scicluna, 2010). Just like the crumb rubber replacement mixes, at 25% shredded rubber chip replacement (SRC25), a considerable reduction in compressive strength was reported, which was later attributed to the lower stiffness and poorer interfacial bonding between the rubber chips and the cement. Higher percentage replacement mixes including SRC50, SRC75, and SRC100 resulted in exponential reductions in compressive capacity.

Mixed crumb rubber and shredded rubber mixes (CR/SRC) consistently exhibited lower compressive strengths than individual aggregate replacement mixes, demonstrating that concurrent reductions in both aggregate phases may lead to a more substantial weakening of the concrete matrix.

3.2.2 Comparative Analysis Between Research Studies

Magro (2011) and Abdilla (2012) investigated the same set of replacement levels (CR25, CR50, SRC25, SRC50, and CR/SRC25), enabling direct comparisons. In fact, both researchers reported comparable % reductions in compressive strength at each replacement increment, demonstrating consistency between both studies. Magro (2011) observed that CR25 exhibited the smallest % loss in compressive strength, reporting a reduction of 14.9% relative to her control mix. Furthermore, Magro (2011) deduced that only two of the mixes retained compressive strength levels suitable for structural applications, those being CR25 and SRC25. Higher replacement percentages, especially in crumb rubber mixes, showed exponential strength reductions as well as weaker matrix cohesion. Magro (2011) eventually concluded that CR25 remained the strongest mix when considering overall robustness and consistency in this mix's performance across differing material conditions.

Scicluna (2010) on the other hand evaluated compressive strength for a variety of mixes containing crumb rubber (CR), shredded rubber chips (SRC), and mixed chips/crumb rubber (CR/SRC) at replacements levels of 25%, 50%, 75%, and 100%. Once again, the two most notable mixes included CR25 and SRC25, which stood out as the strongest performing mixes. Both mixes indicated significantly smaller reductions in compressive strength relative to mixes consisting of 50%, 75%, and 100% rubber replacement levels, the latter of which (100percentage replacement) dropped so low that CR100 was excluded from further testing due to impractically weak behaviour. Scicluna's (2010) results proved that SRC mixes show a more linear and controlled reduction in strength as rubber percentage replacement levels increase, with SRC25 performing comparably or even better than CR25. Once again, CR25 produced the most optimal results amongst the crumb rubber mixes, being deduced as the only viable strength-retaining mix.

3.3 Flexural Performance of Concrete with Replacement Aggregates

The flexural behaviour and performance of concrete provide insight into the tensile response, ductility, and crack development of concrete. The rubberised concrete samples tested by Scicluna (2010), Magro (2011), and Abdilla (2012) exhibited different flexural characteristics relative to their control mix, likely due to the elasticity and low stiffness present in rubber particles.

3.3.1 Influence of Rubber Content on Flexural Behaviour

As rubber content in concrete was increased, overall flexural strength decreased. The magnitude of this reduction and changes in failure mode ultimately came down to the quantity and type of rubber percentage replacement.

Crumb rubber mixes at low replacement levels (CR25) reported a steady decrease in flexural strength of concrete beam samples across all studies. However, these mixes generally retained a portion of their load-carrying capacity unlike higher percentage replacement mixes (CR50, CR75, and CR100), where the overall load-carrying capacity had begun to drop drastically. It was deduced that the addition of crumb

rubber had reduced the stiffness of the tension zone and weakened the interfacial transition zone (ITZ), leading to lower ultimate loads during testing.

Furthermore, replacement mixes CR50 and beyond had exhibited an increase in their deflection capacity, although flexural strength was sharply decreasing as rubber percentage replacement increased. Scicluna (2010) reported highly ductile behaviour in his CR75 and CR100 mixes, with both samples exhibiting large deformations prior to failure. This indicates that crumb rubber strongly influences the reduction of tensile stiffness while promoting deformability.

SRC mixes with low percentage replacements (SRC25 and SRC50) exhibited moderate reductions in flexural strength. The large particle size attributed to SRC introduced weak inclusions within the concrete matrix, causing premature crack pattern initiation when subject to bending in comparison to the CR samples. Nonetheless, SRC test samples generally exhibited greater post-cracking deformation compared to their control mix counterparts. Scicluna (2010) documented how SRC75 and SRC100 demonstrated flexural performances were dominated by rubber behaviour, with significantly reduced ultimate moments, yet substantial rotational capacity prior to failure.

Combined replacement mixes (CR/SRC) endured cumulative effects from both crumb and shredded rubber particle types, like the way these mixes reacted to compressive loading as mentioned above. Generally, these mixes consistently produced lower flexural strengths than individual aggregate replacement mixes yet still producing the highest ductility amongst all tested mixes. This may be attributed to the simultaneous reduction in stiffness in both tension and compression zones, leading to lower bending resistance, but significantly improved energy absorption capabilities.

It may be concluded that the flexural behaviour of rubberised concrete is characterised by decreased ultimate moment capacity, but enhanced deformability and post-cracking resistance. These properties become more evident as rubber content increases.

3.3.2 Comparative Analysis Between Research Studies

A cross-comparison of flexural test results from Scicluna (2010), Magro (2011), and Abdilla (2012) shows a consistent trend that aligns with the compressive strength behaviour of their respective concrete samples. Two mixes in particular stand out regarding concrete performance:

- 25% Crumb rubber replacement mix – CR25
- 25% Shredded rubber chip replacement mix – SRC25

Both 25% aggregate replacement mixes consistently outperformed higher percentage replacement mixes throughout all three studies.

Scicluna (2010) conducted a series of four-point flexural tests on beams consisting of CR, SRC, and CR/SRC aggregates replacing fine and coarse aggregates respectively. Among the crumb rubber mixes, CR25 achieved the highest flexural strength, recording a mean flexural strength of 12.9 kN (3.7 MPa) relative to the 13.5 kN (3.7 MPa) obtained by his control beam. CR25 outperformed higher crumb rubber replacement mixes in this regard:

- CR50 – 10 kN (2.8 MPa)
- CR75 – 6.8 kN (1.9 MPa)

Furthermore, Scicluna (2010) observed that CR25 was the only crumb rubber mix to fail in a brittle manner, like that of the control mix. This indicates that the CR25 beam managed to retain adequate stiffness and moment capacity to behave elastically rather than plastically. On the other hand, CR50 and CR75 mixes reportedly behaved in an excessively ductile, soft, and cohesive manner, with both beam samples exhibiting pronounced post-cracking deformation, yet drastically reduced flexural strength.

In parallel, SRC25 outperformed SRC50, SRC75, and SRC100:

- SRC25 – 11.8 kN (3.4 MPa)
- SRC50 – 10.1 kN (2.8 MPa)
- SRC75 – 7.2 kN (2.1 MPa)
- SRC100 – 4.9 kN (1.4 MPa)

As discussed previously, combined replacement mixes (CR/SRC) generally produced lower flexural strengths than CR and SRC mixes:

- CR/SRC25 – 10.8 kN (3.0 MPa)
- CR/SRC50 – 7.0 kN (2.0 MPa)

Magro's (2011) flexural test results further demonstrated how 25% rubber replacement was generally the superior replacement level in concrete under flexure. In her case, SRC25 outperformed CR25 with regards to their ultimate flexural load.

Table 3.7: Four-point flexural test results (Magro, 2011)

Slump	Testing Day	Specimen	Flexural Load (kN)
30	28	CM	70.87
20	28	CR-25	65.46
40	28	CR-50	61.22
20	28	SRC-25	67.33
10	28	SRC-50	46.55
10	28	CR/SRC-25	53.28

Magro (2011) reported a characteristic decline in flexural strength with increasing rubber content, but emphasised that this loss in flexural strength was consistently smaller in the crumb rubber mixes than in the shredded rubber chip mixes at identical replacement percentages. Magro (2011) once again highlighted how the 25percentage replacement mixes (CR25 and SRC25) showed the most optimal balance between load-carrying capacity and deflection behaviour, while higher percentage replacement mixes suffered excessive reductions in modulus of rupture (MOR), exhibiting premature cracking in the process. She deduced that CR25 preserved the most conventional flexural strength pattern, with a limited elasto-plastic region and a relatively sudden, brittle failure, demonstrating that her CR25 mix retained significant stiffness and resembled the structural behaviour of the control beam more accurately than any other mix. This deduction aligns with that of Scicluna (2010), who reported similar findings in this regard.

3.4 Summary of Findings from Previous Research

When summarising both compressive strength and flexural strength test results conducted by Scicluna (2010), Magro (2011), and Abdilla (2012), clear behavioural trends emerge across all three studies. Generally, the inclusion of rubber, regardless

of type or particle size, resulted in measurable reductions in both compressive and flexural strength in comparison to their relative control mixes. The extent of strength loss increased proportionally to the increase in rubber content added to the mix, which ultimately replaced natural aggregates typically used to aid in concrete's compressive and flexural performances. High-level replacement mixes (≥50%) consistently exhibited significant reductions in stiffness, load-bearing capacity (peak strength), as well as overall structural integrity. Moreover, bonding issues between the rubber particles and cement were frequently observed. On the other hand, increased rubber content enhanced ductility and deformation capacity of concrete.

Crumb rubber mixes (CR) demonstrated progressively weaker performance as percentage replacements increased, particularly due to the disruption of the fine aggregate matrix and the reduction in stiffness provided by the rubber particles. Shredded rubber chip mixes (SRC) behaved similarly in this regard, though higher percentage replacement mixes seemed to have a more significant drop-off in overall structural integrity. This could come down to poor bonding between SRC and cement, which is not as prevalent in CR mixes. Meanwhile, combined replacements (CR/SRC) consistently produced the lowest compressive and flexural performances at comparable replacement levels, confirming the cumulative weakening effects caused by replacing both fine and coarse aggregate fractions simultaneously.

Table 3.8: Aggregate replacement effect on 28-day cube compressive strength – Past research

Researcher	Mix	Compressive Strength (MPa)
Scicluna (2010)	CM	41.20
	CR25	31.70
	CR50	28.90
	SRC25	31.60
	SRC50	24.30
	CR/SRC25	25.10
Magro (2011)	CM	33.26
	CR25	28.30
	CR50	17.48
	SRC25	20.90
	SRC50	12.24
	CR/SRC25	12.12

Abdilla (2012)	CM	31.25
	CR25	28.84
	CR50	17.50
	SRC25	19.35
	SRC50	10.56
	CR/SRC25	14.53

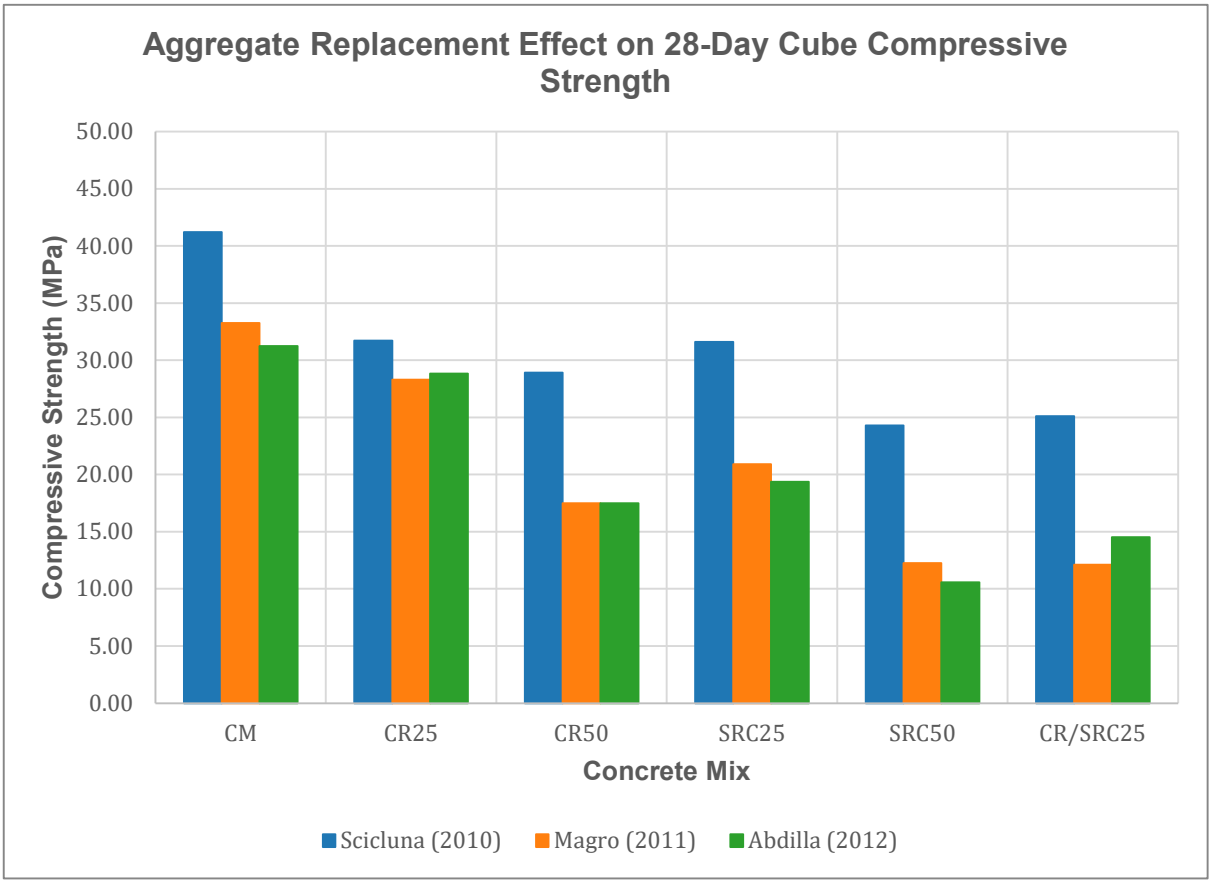

Figure 3.1: Aggregate replacement effect on 28-day cube compressive strength – Past research

Despite these general strength reductions, past research indicates that two mixes consistently stood out as the strongest performing modified concrete across all three studies:

- 25% Crumb rubber replacement mix – CR25
- 25% Shredded rubber chip replacement mix – SRC25

Once again, both CR25 and SRC25 demonstrated significantly smaller reductions in compressive strength and flexural strength compared to higher percentage replacement mixes. Both mixes retained substantially high ultimate loads and stiffness, exhibiting cracking patterns and failure modes that closely resembled conventional concrete.

Between the two mixes, CR25 emerged as the most consistently reliable mix throughout the three studies. Magro (2011) and Abdilla (2012) reported that CR25 experienced the smallest reduction in compressive strength out of all their tested mixes. Moreover, CR25 produced the most conventional flexural response in Magro's (2011) case, reporting a relatively brittle failure mode that closely resembled that of the control beam. Scicluna (2010) reiterates this observation, noting that CR25 was the only crumb rubber mix to retain sufficient stiffness and exhibit an elastic-brittle failure pattern, unlike the excessively ductile behaviour of higher percentage replacement mixes. Finally, Abdilla (2012) further supports these observations by reinforcing the robustness of CR25, through his own independent tests.

While SRC25 also performed strongly, particularly in flexure, its behaviour varied slightly more than CR25's, suggesting generally higher variability relative to finer crumb rubber mixes. Furthermore, SRC25's mechanical responses, particularly under flexure, delved further away from regular aggregate concrete than CR25 did.

For these reasons, CR25 was selected as the final mix to be investigated in this study. Its selection is supported by its superior balance between strength retention and deformation capacity along with its consistency and reliability demonstrated across multiple independent research efforts. In conclusion, CR25 provides an optimal basis for evaluating the structural potential of rubberised concrete under cyclic loading, albeit compressive or flexural.

4. Research Methodology

4.1 Aim

The aim of this dissertation was to evaluate the mechanical performance of rubberised concrete, with particular emphasis on its cyclic performance and its suitability for use in seismically resilient structural components. This study focused solely on the behaviour of concrete containing 25% crumb rubber replacement of fine aggregate (CR25), which was identified as the most structurally viable rubberised mix in Scicluna (2010), Magro (2011), and Abdilla's (2012) research studies.

The objective was to assess how CR25 performs under cyclic compressive and flexural loading when compared to a conventional control mix, and to determine whether the enhanced ductility typically associated with rubberised concrete aids in overall seismic resilience. To achieve this, casting and testing of the following concrete samples was involved, including:

- 12 cubes
- 8 beams
- 8 short columns

This chapter involves details on the mix design used, as well as the testing procedures carried out on said mixes. Preliminary investigations, mix preparations, and casting of all 28 specimens were carried out at Ballut Blocks Ltd. in Naxxar. All forms of testing were then carried out at the civil engineering laboratory within the Faculty for the Built Environment.

4.2 Concrete Design Mixes Considered

This dissertation aimed to follow up on Magro's (2011) findings. From her six mixes, two were chosen for further investigation. These mixes included a control mix and a CR25 mix acting as the only rubber aggregate replacement mix throughout the dissertation. CR25 was chosen on the basis of cube compressive strength, flexural strength, and flexural responsiveness from Scicluna (2010) and Magro's (2011) research. All variables considered in the mix design and investigation were kept identical to those adopted by Magro (2011), wherever possible.

Table 4.1: Table of concrete mixes

Mix no.	Mix Type	Fine Aggregate (63µ to 4mm)	Coarse Aggregate (5mm to 10mm)	Coarse Aggregate (10mm to 20mm)	Crumb Rubber (63µ to 4mm)	Rubber Chips (5mm to 10mm)	Rubber Chips (10mm to 14mm)
1	Control Mix (CM)	100%	100%	100%	0%	0%	0%
2	CR25 - 25% Crumb Rubber	75%	100%	100%	25%	0%	0%

4.3 Preliminary Investigations

The investigations carried out at the Faculty laboratory included:

- Sieving of crumb rubber
- Preparation and casting of mixes for column-capping elements (Sika mix)
- Cube compressive strength tests
- Column static compressive strength tests
- Column cyclic compressive strength tests
- Beam static four-point flexural strength tests
- Beam cyclic four-point flexural strength tests
- Sika mix compressive strength tests
- Sika mix flexural strength tests

4.3.1 Materials

4.3.1.1 Cement

CEM II Ordinary Portland Cement was used in both control and rubber mixes, conforming to MSA EN 187-1:200. All cement was provided on-site at Ballut Blocks Ltd. in Naxxar.

Regarding the column-capping elements, SikaGrout S55 cementitious structural mortar was brought to the Faculty laboratory in sacks of 25kg and stored on wooden pallets until use.

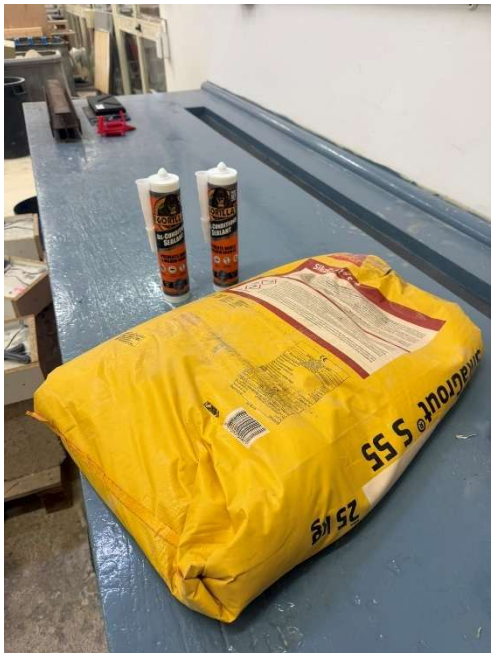

Figure 4.1: SikaGrout S55 cementitious structural mortar (25kg)

4.3.1.2 Natural Aggregate

Samples of natural aggregate; sand, 5mm – 10mm and 10mm – 20mm spalls were collected and provided by Ballut Blocks Ltd. and stored at their facilities until use. Both sets of spalls were sieved prior to storage, ensuring they fell in their respective 5mm – 10mm and 10mm – 20mm ranges. No sieving was performed on the sand samples.

4.3.1.3 Water

All water used for experimentation was tap water provided by Ballut Blocks Ltd. and the civil engineering laboratory within the Faculty for the Built Environment.

4.3.1.4 Shredded Rubber Tyres

The recycled rubber aggregate used within both mixes consisted of crumb rubber sourced from end-of-life vehicle tyres. At the time of this dissertation, conventional crumb rubber produced through mechanical tyre shredding was not being manufactured in Malta. As a result, crumb rubber was sourced from Three Eight Nine Co. Ltd. (389 Co. Ltd.), a local supplier specialising in artificial turf systems and pitch

installations. The material supplied contained comparable physical and mechanical characteristics with conventional crumb rubber, consisting of rubber with a particle size range of approximately 2mm – 5mm. This crumb rubber alternative is commonly used as infill material in synthetic sports surfaces, originating from recycled vehicle tyres and undergoing mechanical processing similar to that used in the production of conventional crumb rubber.

Figure 4.2: Sack of crumb rubber provided by Three Eight Nine Co. Ltd. (389 Co. Ltd.)

Although commercially classified as pitch rubber, the chosen material is functionally equivalent to conventional crumb rubber in terms of origin, composition, and mechanical behaviour. This implies that the chosen material contains rubber particles that exhibit low stiffness, high elasticity, low density, and hydrophobic surface characteristics, making it a consistent alternative to traditional crumb rubber sources. Furthermore, the 2mm – 5mm particle size range falls within the upper bound of crumb rubber used in all three previously mentioned studies, where crumb rubber was a replacement for fine aggregate.

Around 200kg of rubber aggregate was transported to the Faculty laboratory, where it was sieved using a 4mm sieve at the top and a 63μm sieve at the bottom, with a pan to catch any excess material passing through the 63μm sieve. The process was relatively easy since only a small amount of rubber was retained on the 4mm sieve, and unwanted foreign materials and silts were easily filtered out through both sieve

sizes. Upon completion, the remaining rubber material was transported to Ballut Blocks Ltd. in Naxxar and stored there until use.

Figures 4.3 and 4.4: Sieves present at Faculty laboratory / 4mm and 63µm sieves used to sieve crumb rubber

Figure 4.5: Excess foreign materials and silts filtered out through sieving crumb rubber

4.3.2 Concrete Design Mix

The concrete design mix was based on the mix proportions used by Magro (2011), who in turn based hers on those used by Scicluna (2010). All mix proportions were found by means of the design of normal concrete mixes, otherwise known as the DoE Method. The control mix was designed to achieve a target compressive strength of 35 MPa at 28 days and a slump of 10mm to 30mm. A water-cement ratio of 0.55 was used in the control design mix.

Table 4.2: Control design mix contents

Material	Quantities (per m^3)
Cement (kg)	345
Water(kg/ltr)	190
Fine Aggregate (kg)	674
Coarse Aggregate 5-10mm (kg)	337
Coarse Aggregate 10-20mm (kg)	673
Water-Cement Ratio	0.55

4.4 Preparation of Experimental Concrete Test Samples

The preparation of the experimental test samples was carried out at Ballut Blocks Ltd., where the casting of cubes, beams, and short columns took place.

4.4.1 Materials

4.4.1.1 Cement

As mentioned previously, CEM II Ordinary Portland Cement was used in both control and rubber mixes, conforming to MSA EN 187-1:200. All cement was provided on-site at Ballut Blocks Ltd. in Naxxar and weighed accordingly prior to mixing.

4.4.1.2 Natural Aggregate

As mentioned previously, the following natural aggregate components were used:

- Sand

- 5mm – 10mm natural coarse aggregate
- 10mm – 20mm natural coarse aggregate

The aggregate was weighed and transported to the area where all specimens were going to be casted.

4.4.1.3 Water

All water used for experimentation was tap water provided by Ballut Blocks Ltd.

4.4.1.4 Shredded Rubber Tyres

The sieved crumb rubber was transported to Ballut Blocks Ltd. in sacks on the day of casting.

4.5 Beam Steel Reinforcement

Preliminary beam reinforcement calculations were carried out in accordance with MSA EN 1992-1-1:2004. These were carried out by using the cube compressive strengths obtained by Magro (2011) during her study. The characteristic design compressive strength was found by using the 28-day compressive strength and the coefficient of variation. The maximum area of the beam reinforcement was calculated by limiting the neutral axis of the beam to 0.617d (beam measurements: 0.2m x 0.25m x 4m). An area of reinforcement less than the maximum area was chosen to ensure that the neutral axis was always above the limiting value of 0.617d, so that the steel would reach its yielding point. Moreover, this was a precautionary step taken in case the cube compressive strength test results carried out in this dissertation would end up lower than those of Magro (2011). The characteristic design compressive strength was used to calculate the moment of resistance and shear resistance of the beam. The load at which the beam would fail in bending and shear were found, to ensure that the beam would always fail in bending rather than in shear given the provided reinforcement (Magro, 2011).

The calculations were worked out again using the cube compressive strengths achieved during this dissertation to find the load at which the beam would fail. The

calculations were worked once with the partial safety factors stated in MSA EN 1992-1-1:2004 and another time using a unit value for all partial safety factors. When the four-point flexural tests were carried out on the beams, the model of uncertainty parameter was worked out for each beam by dividing the actual failure load by the predicted failure load. These calculations may be found in Appendix 6.

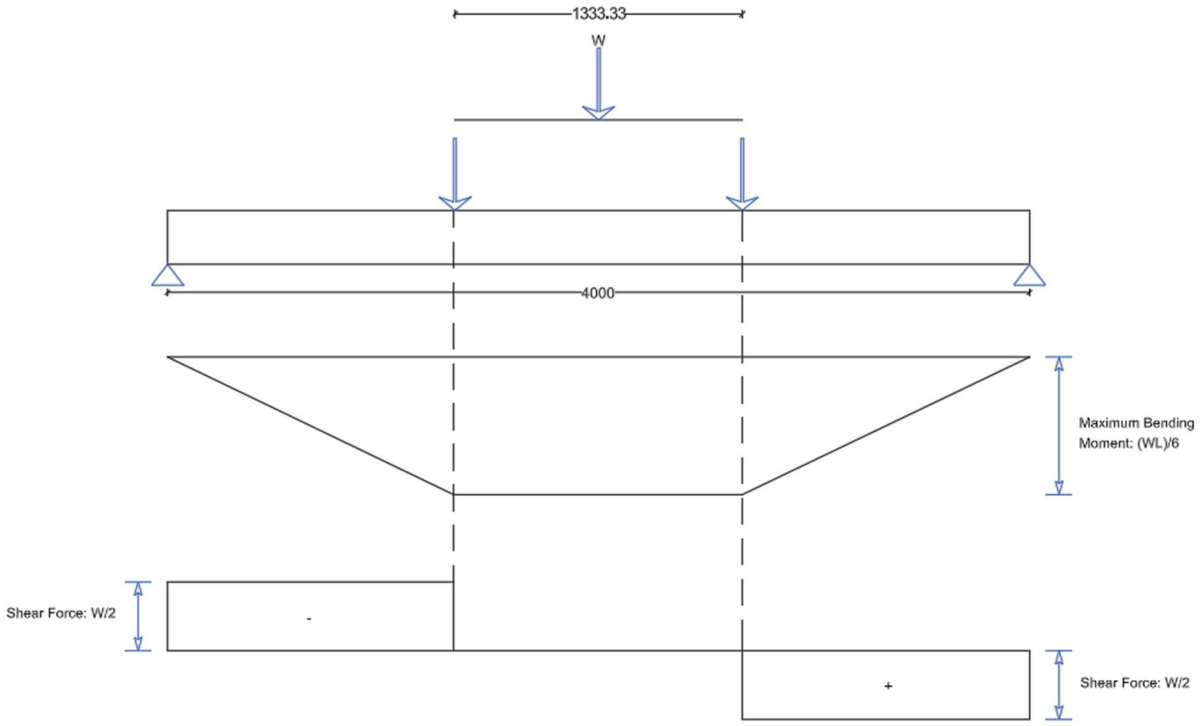

Figure 4.6: Bending moment and shear force diagram

The reinforcement cage was set up as shown in Figure 4.7 below. Two steel strain gauges of type FLA-10-11-5L were attached to the steel cage, one on the top reinforcement, and another on the bottom reinforcement. The reinforcement was grinded down lightly using abrasive paper to achieve a smooth surface to comprise the gauge position. The surface was then cleaned with acetone and dried with a cloth. This step was repeated until the cloth came away clean, indicating that the area was no longer contaminated by residual grinded steel material. The steel strain gauges were fixed with a strain gauge adhesive (CN). Once the strain gauge adhesive cured, the strain gauge wire was covered with electrical tape at multiple points to prevent pulling and ripping of the strain gauge wire during the casting and hardening of concrete. Moreover, a layer of melted wax covered the strain gauge to protect it from concrete, keeping it stuck in place. The strain gauges were checked before and after

attaching them to the steel reinforcement by means of an ohmmeter to make sure that they worked and registered a resistance of 120 ± 0.5 ohms.

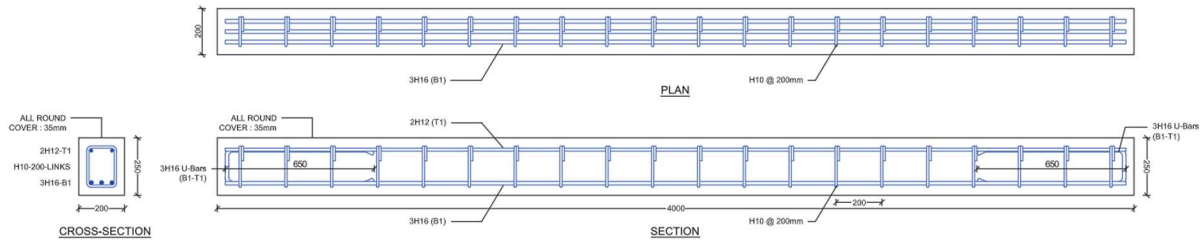

Figure 4.7: Beam sample used for all flexural tests

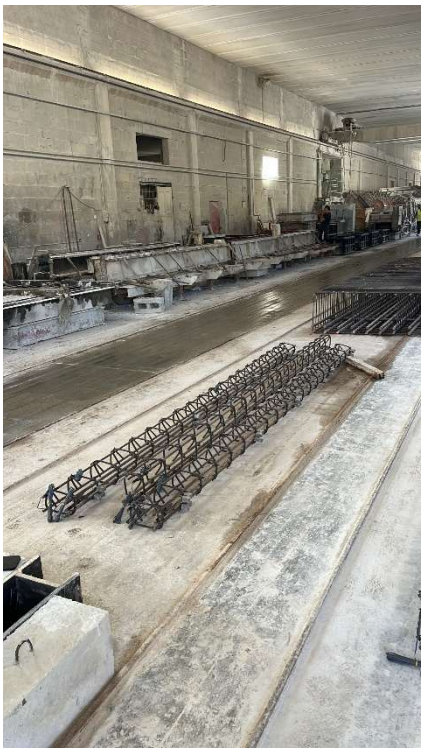

Figures 4.8 and 4.9: Beam reinforcement cages laid out on-site

4.6 Short Column Steel Reinforcement

The reinforced concrete short column specimens were designed with a cross-section of 200mm x 200mm and a height of 400mm, as depicted in Figure 4.10. The primary reason for these column dimensions came down to laboratory rig constraints, with the maximum allowable specimen height within the compression testing machine being 500mm. The chosen 400mm sample height allowed for adequate clearance for

seating, alignment, load application, and measuring of overall contraction of the short columns. In addition to rig restraints, the short nature of the columns would in theory have allowed for a low slenderness ratio, ensuring that failure would have been governed by material behaviour under axial compression, rather than instability or buckling effects (minimising end effects and eccentricities).

Longitudinal reinforcement was provided in the form of 4H12 vertical bars, cranked inwards at both ends as shown in Figure 4.10. This was done to ensure proper anchorage within the short specimen length provided, as well as to prevent premature spalling of the end concrete covers of the specimens. The reinforcement ratio was selected to represent nominal longitudinal reinforcement according to EN 1992-1-1 (Eurocode recommendations for compression members). The final short column design contained a reinforcement ratio (ρ) of approximately 1.13%, which falls within the accepted nominal range of 0.8% - 1.5%. Nominal reinforcement was necessary to ensure that the short columns exhibited reinforced concrete behaviour without excessive steel contributions. This was essential when comparing results between the control columns and rubberised columns.

Transverse reinforcement came in the form of H10 closed links at approximately 140mm centres, resulting in three links throughout the short column's span as shown in Figure 4.10. These links were added to restrain the vertical bars and prevent premature bar buckling. The selected link spacing of 140mm satisfies Eurocode detailing principles for transverse reinforcement in compression members and was therefore appropriate for the short column configuration.

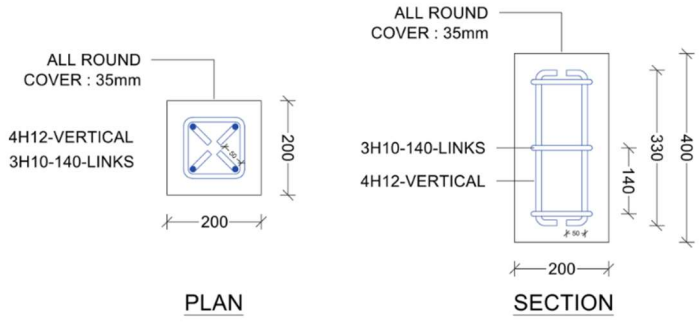

Figure 4.10: Short column sample used for all short column compressive tests

A concrete cover of 35mm was adopted at all ends of the short column design. This ensured adequate embedment of the steel reinforcement, preventing early exposure of the steel in case of concrete surface spalling during testing.

Each set of vertical reinforcement required the attachment of a strain gauge of type FLA-10-11-5L, which was attached to the lower end interior-facing side of one of the vertical bars (one steel strain gauge per short column sample). The reinforcement was grinded down lightly using abrasive paper to achieve a smooth surface to comprise the gauge position. The surface was then cleaned with acetone and dried with a cloth. This step was repeated until the cloth came away clean, indicating that the area was no longer contaminated by residual grinded steel material. The steel strain gauges were fixed with a strain gauge adhesive (CN). Once the strain gauge adhesive cured, the strain gauge wire was covered with electrical tape at multiple points to prevent pulling and ripping of the strain gauge wire during the casting and hardening of concrete. Moreover, a layer of melted wax covered the strain gauge to protect it from concrete, keeping it stuck in place. The strain gauges were checked before and after attaching them to the steel reinforcement by means of an ohmmeter to make sure that they worked and registered a resistance of 120 ± 0.5 ohms.

Figures 4.11, 4.12, and 4.13: Short column reinforcement cage / Attachment of steel strain gauge / Addition of melted wax layer to strain gauge

4.7 Concrete Design Mix Methodology

4.7.1 Preparation of Mix Ingredients

Each mix material was weighed using a balance beam scale at Ballut Blocks Ltd. and prepared in separate sacks for mixing in a truck-mounted concrete mixer.

4.7.2 Concrete Mixing

The concrete mixer was cleaned and moistened internally to remove unwanted residual material from previous mixes and to prevent water absorption from the fresh mix. The mix materials were then added to the drum mixer in the following order:

i. Coarse aggregate
ii. Fine aggregate
iii. Crumb rubber (if specified)
iv. Water (added gradually)
v. Cement

4.7.3 Casting of Specimens

For each mix design, the following specimens were cast for testing on hardened concrete:

- 6 cubes measuring 150mm by 150mm by 150mm to be tested at 7 and 28 days
- 4 beams measuring 200mm by 250mm by 4000mm to be tested at 28 days
- 4 columns measuring 200mm by 200mm by 400mm to be tested at 28 days

The cube moulds consisted of pre-oiled plastic moulds. All sets of beam and short column moulds consisted of marine plywood shuttering, shuttered from three sides to obtain the required sample dimensions. The sample moulds were cleaned and greased internally prior to lowering the reinforcement cages into their respective moulds. As the concrete was being poured, it was vibrated at multiple points using a vibrator. In the case of the short columns, the areas containing the steel strain gauges were carefully vibrated due to the strain gauge wires.



Figures 4.14, 4.15, and 4.16: Pre-oiled plastic cube moulds / Beam moulds with steel cages / Short column moulds with steel cages



Figures 4.17, 4.18, and 4.19: Casting process / Vibrating of concrete / Addition of hooks for ease of transportation



Figures 4.20, 4.21, and 4.22: Mix sample used for cube casting / Compacting concrete cubes with a tamping rod / Labelling of samples

4.7.4 Concrete Curing

A layer of polythene sheeting was placed over all cube, beam, and short column samples after casting to avoid water evaporation. The cubes were left in the moulds for 24 hours before being transported to the Faculty laboratory to be de-moulded and cured in a tank filled with tap water at a constant temperature for the additional curing time prior to 7-day and 28-day tests. Regarding the beam and short column samples, water was poured on all sixteen samples 24 hours after casting to prevent the occurrence of surface cracks. All sixteen samples were stored at Ballut Blocks Ltd. in Naxxar for approximately two weeks before being transported to the Faculty laboratory prior to 28-day tests.

Figures 4.23 and 4.24: Cubes after de-moulding / Curing process of cubes

4.7.5 Preparation of Short Column Capping Mix and Test Samples

The short columns needed to be capped at both ends prior to testing to ensure uniform load transfer through flat end surfaces of each sample. This comes down to potential geometric inaccuracies and unevenness caused by the original casting of the short column samples, where marine plywood moulds were used, risking eccentric loading, unwanted stress concentrations, and possibly premature failure during testing. To mitigate these risks, a high-strength cementitious capping layer was applied to both ends of each column specimen.

The selected capping mix material was SikaGrout S55, a high-strength repair mortar. This material was chosen due to its high compressive strength capabilities relative to the column concrete, particularly the rubberised column concrete. Furthermore, SikaGrout S55 exhibits good adhesion properties, an important characteristic considering the need for bonding with the column concrete. This capping layer ensured that its compressive strength exceeded that of the short columns, implying that failure during testing occurred within the concrete specimen itself rather than within the capping layer.

White melamine chipboard moulds were attached at one end of each short column, and a transparent sealer was applied at the inner vertices of the mould, to ensure that the moulds were tightly sealed prior to casting. The column ends were cleaned of any dust and other loose particles.

Figure 4.25: Capping layer moulds attached to short column ends

The Sika S55 mix was prepared in accordance with the manufacturer's guidelines, consisting of a water-cement ratio of 0.15.

The capping layers were then cast at one end of each short column to form a 5mm uniform capping layer. Care was taken to ensure the capping surfaces were level and perpendicular to the column axis. After three days, the opposite ends of the column were also cast. Prism samples were cast from the same mix as the first capping cast, which were left to cure under controlled laboratory conditions for 28 days, like those experienced by the concrete cubes.



Figures 4.26, 4.27, and 4.28: Sika S55 capping layer cast / Polythene sheeting cover to prevent water evaporation / Casting of prism samples in steel moulds

4.8 Tests on Hardened Concrete

4.8.1 Concrete Cube Compressive Strength

The compressive strengths of all cube specimens were obtained by means of a compression testing machine at the Faculty laboratory, where the cubes were loaded in compression until breaking at failure. Two sets of six cubes were tested at 7 and 28 days from the day of casting, totalling twelve cube compression tests. The cubes were removed from the water tank and dried with a cloth prior to having their face dimensions measured (length, width, and height) by means of a digital veneer calliper. Furthermore, the weight of each cube was also recorded using an electronic balance. A 3000kN automatic testing machine was used, loading each cube specimen at a rate of 0.6 MPa/s. The tests on the cube specimens were carried out in accordance with the latest code, MSA EN 12390-3:2019.

4.8.2 Flexural Strength of Rubberised Reinforced Concrete Beams

4.8.2.1 Beam Preparation for Testing

The beams were transported from Ballut Blocks Ltd. to the Faculty laboratory and stored on timber packers. Prior to testing, the beams were prepared in relation to the tests that were set to be carried out. This included the marking of centre lines across the top faces of all beams using a permanent marker to indicate where the concrete

strain gauges had to be fixed. Moreover, lines were marked at both beam 1/3 spans (1.33m from each beam end) to be used as bearing plate markers during testing.

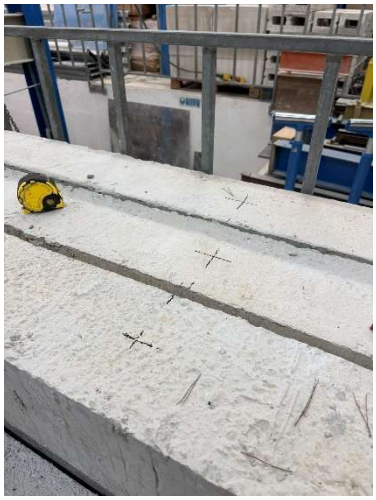

Figure 4.29: Marking of beam centres

An area larger than the concrete strain gauge was smoothened out using abrasive paper, and any loose particles were brushed off. The surface was then cleaned with acetone and dried with a cloth. This step was repeated until the cloth came away clean, indicating that the area was no longer contaminated by residual concrete dust particles. A concrete strain gauge of type PL-60-11-5L was then attached to the centre of the compression face of the 4m beam by means of a strain gauge adhesive (CN). The strain gauge was kept pressed down until the adhesive cured. At this point, electrical tape was applied to the wire at multiple points, to prevent the strain gauge from ripping off in case of pulling. The strain gauges were checked before and after attaching them to the concrete face by means of an ohmmeter to make sure that they worked and registered a resistance of 120 ± 0.5 ohms.

All beam samples were coated with multiple layers of industrial lime paste (ġir). Approximately two to three layers of industrial lime paste were added with minimum intervals of 6 hours between each coat. This process was carried out to ensure that any cracks developed on major beam faces during testing could be observed more clearly.

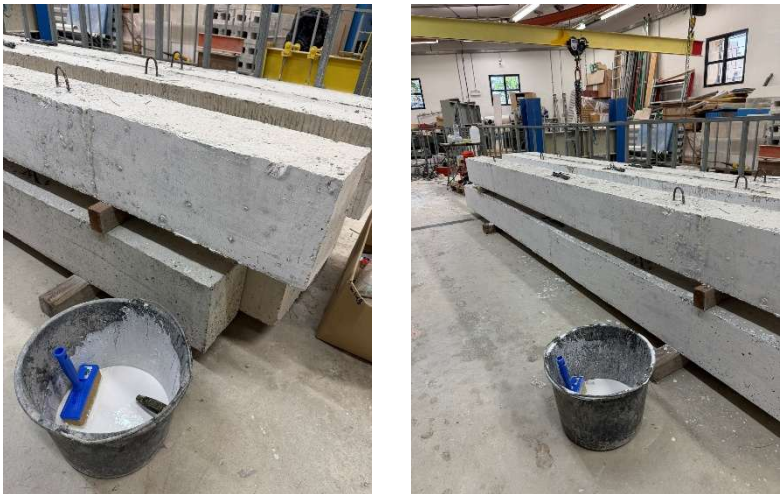

Figure 4.30: Addition of industrial lime paste

4.8.2.2 Four-Point Loading Flexural Test Set-up

All eight beam samples were moved and lowered into the testing rig by means of the Faculty laboratory overhead crane. The testing rig was set up beforehand to accommodate a beam span of 4m. For every test, a concrete beam specimen was lowered onto two perpendicular steel beams containing two stacked steel bearing plates for each steel beam, acting as the concrete beam end supports during testing. Each set of steel bearing plates contained a layer of rubber sheeting, purposefully set out to achieve a smooth surface between the perpendicular steel beam and the end bearing plates.

A flat bar was gently hammered approximately at mid span of the beam, acting as a placeholder for two linear variable differential transformers (LVDTs), which were placed at each side of the beam with their ends resting on top of the flat metal bar.

Another two sets of steel bearing plates were placed at 1/3 of the overall beam length (1.33m from each beam end), using the lines marked beforehand as placeholders. These plates were used to evenly distribute load at each point through a spreader beam. Once again, both sets of bearing plates contained a layer of rubber sheeting. The load was applied through a 200kN load cell, which was attached to a 600kN hydraulic jack. An intermediary steel plate was placed on top of the spreader beam's mid span and directly under the jack, to act as the first point of contact as the jack started to extend.

The concrete strain gauges were attached to the data logger for each test, which in turn was attached to a data logger. Prior to testing, each strain gauge was once again checked with an ohmmeter to ensure they were working correctly, exhibiting a resistance of 120 ± 0.5 ohms. The load cell was also attached to the data logger. On the other hand, the LVDTs were attached to the data logger by means of a CA522 card. All readings were recorded on Autosoft 3000.

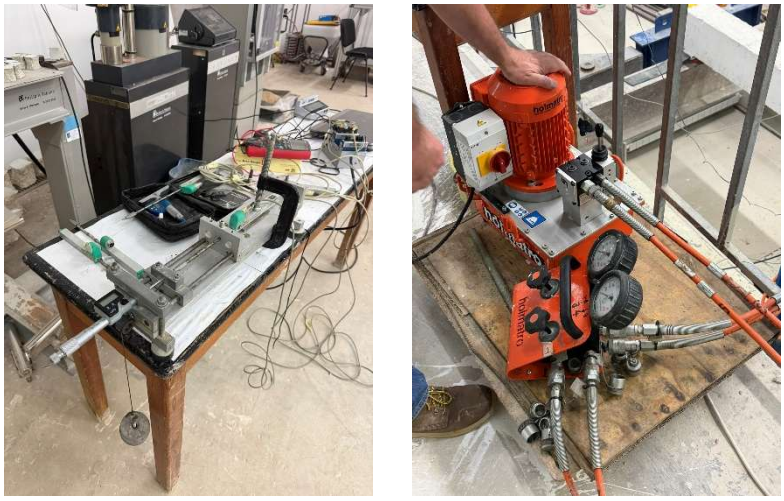

Figures 4.31 and 4.32: Preparation of LVDTs / Hydraulic jack

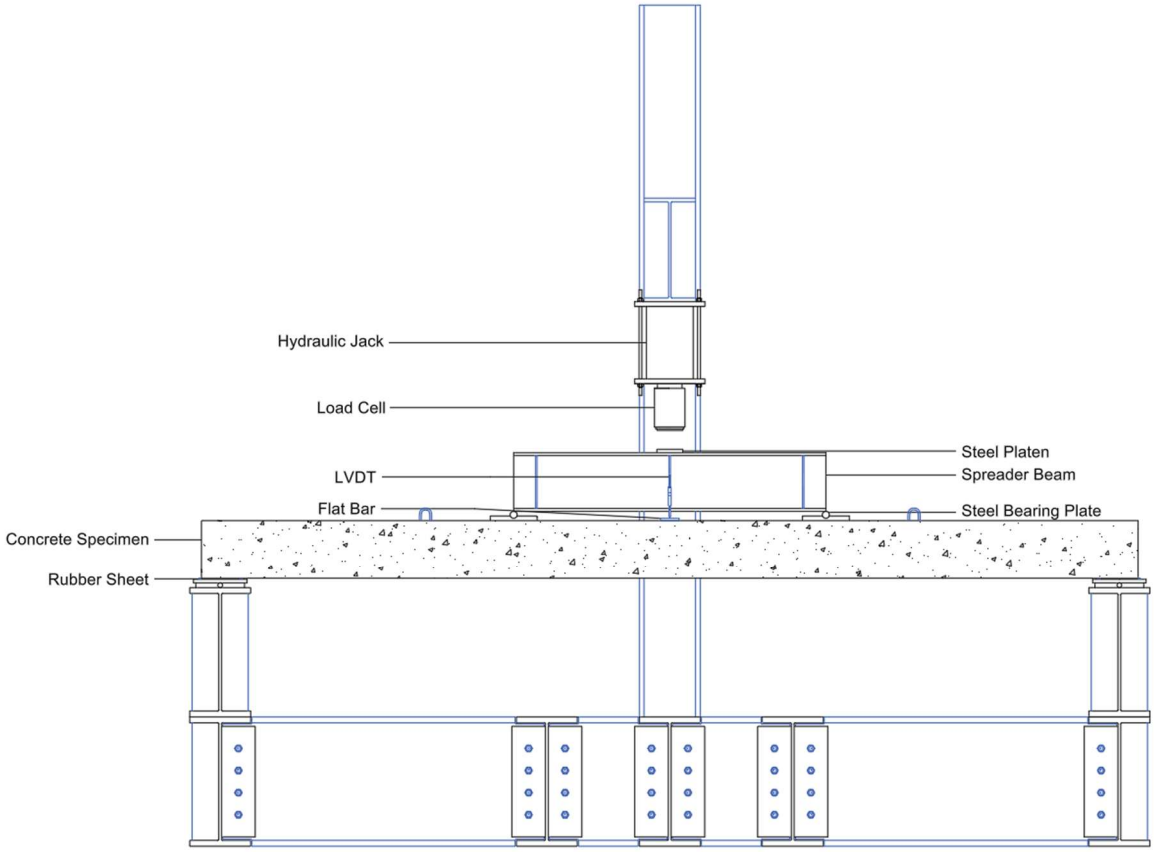

Figure 4.33: Flexural test set-up

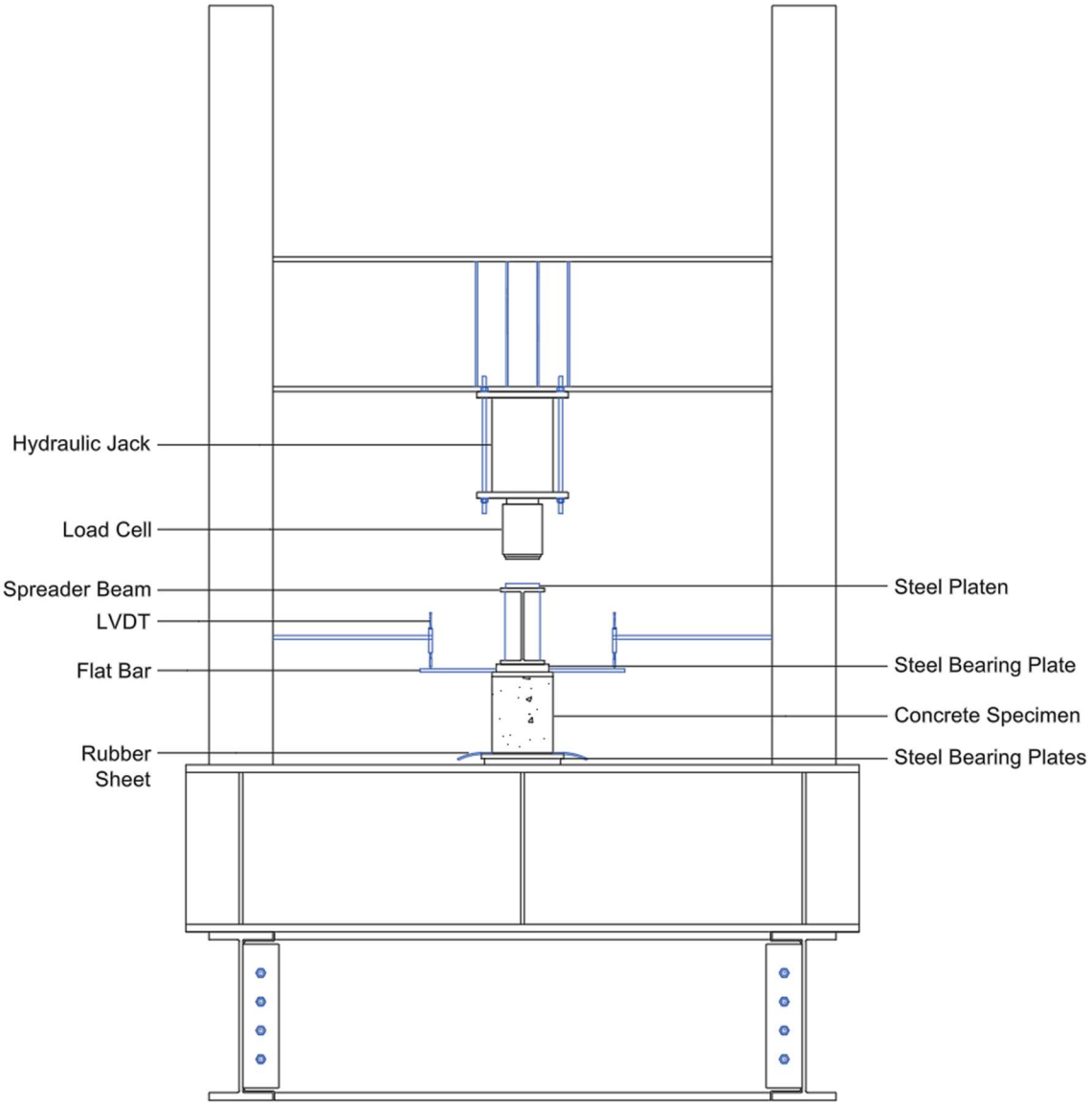

Figure 4.34: Flexural test set-up

4.8.2.3 Static Four-Point Loading Flexural Test Procedure

After setting up the testing rig accordingly, some final procedures needed to be taken before each static four-point flexural test. This involved the calibration of both LVDTs, the load cell, the steel strain gauge, and the concrete strain gauge on Autosoft 3000.

The test procedure began by applying load at a slow rate until the telescopic jack was barely in contact with the intermediary steel plate on top of the spreader beam. A load rate of approximately 2kN every two minutes was adhered to throughout the entire procedure. Any appearing hairline cracks were marked and labelled at every load interval until it was deemed unsafe to remain physically present in the testing pit. After

failure of each sample, the telescopic jack was gently lifted off the spreader beam and switched off. All relevant data was then compiled. Strain measurements were verified through the use of multiple gauges collectively on both concrete and reinforcement, allowing for a cross-comparison of strain development against load displacement responses. Unfortunately, the steel strain gauges did not produce meaningful results throughout, hence being excluded from all flexural tests. Otherwise, no noteworthy issues were documented throughout all four static four-point flexural tests.

4.8.2.4 Cyclic Four-Point Loading Flexural Test Procedure

Like their respective static tests, all four cyclic four-point flexural tests required minor calibration prior to each individual sample test. This involved the calibration of both LVDTs, the load cell, and the concrete strain gauge on Autosoft 3000.

The test procedure began by applying load at a slow rate until the telescopic jack was barely in contact with the intermediary steel platen on top of the spreader beam. The ultimate failure loads (W_{ult}) obtained for both control and rubber static four-point flexural tests were used as bases for cyclic loading for each respective mix.

Table 4.3: Cyclic four-point flexural tests – Loads and cycles

Sample	10% x W_{ULT} (kN)	30% x W_{ULT} (kN)	50% x W_{ULT} (kN)	70% x W_{ULT} (kN)	90% x W_{ULT} (kN)	W_{ULT} Static Test (kN)
CM-A-5	8.58 *(5 cycles)*	25.74 *(5 cycles)*	42.91 *(5 cycles)*	60.07 *(5 cycles)*	77.23 *(5 cycles)*	85.82 *(5 cycles)*
CM-B-10	8.58 *(10 cycles)*	25.74 *(10 cycles)*	42.91 *(10 cycles)*	60.07 *(10 cycles)*	77.23 *(10 cycles)*	85.82 *(10 cycles)*
CR25-A-5	7.19 *(5 cycles)*	21.58 *(5 cycles)*	35.97 *(5 cycles)*	50.36 *(5 cycles)*	64.75 *(5 cycles)*	71.95 *(5 cycles)*
CR25-B-10	7.19 *(10 cycles)*	21.58 *(10 cycles)*	35.97 *(10 cycles)*	50.36 *(10 cycles)*	64.75 *(10 cycles)*	71.95 *(10 cycles)*

Loads were manually applied, starting by reaching 10% of the respective static ultimate load (10%.W_{ult}) for each beam. This load was held for approximately one minute before unloading the beam down to approximately 1kN. Once unloaded, load was immediately applied until reaching 10%.W_{ult}. This process was repeated until completing five or ten cycles, depending on which sample was being tested.

After completing the necessary desired cycles, load was increased until reaching 30%.W_{ult}. From this point on, all samples were unloaded until approximately 10%.W_{ult}, which became the new base load for each test. The sequence of cycle rates adhered to throughout all four tests may be found in Table 4.3 above. This cycle sequence carried on until failure for each specimen.

Any appearing hairline cracks were marked and labelled at every load interval until it was deemed unsafe to remain physically present in the testing pit. After failure of each sample, the telescopic jack was gently lifted off the spreader beam and switched off. All relevant data was then compiled. Strain measurements were verified through the use of multiple gauges collectively on both concrete and reinforcement, allowing for a cross-comparison of strain development against load displacement responses.

During the second control test (CM-B-10), one of the Faculty laboratory's emergency switches was set off thirteen minutes into the test, temporarily cutting off power to the testing rig for approximately five minutes. At this point, loading was still being applied up until 10%.W_{ult}.

4.8.3 Compressive Strength of Rubberised Reinforced Concrete Short Columns

4.8.3.1 Short Column Preparation for Testing

The short columns were transported from Ballut Blocks Ltd. to the Faculty laboratory and stored on timber pallets. Prior to testing, the short columns were prepared in relation to the tests that were set to be carried out. Centre lines were marked across one of the longitudinal faces using a permanent marker to indicate where the concrete strain gauges had to be fixed.

An area larger than the concrete strain gauge was smoothened out using abrasive paper, and any loose particles were brushed off. The surface was then cleaned with acetone and dried with a cloth. This step was repeated until the cloth came away clean, indicating that the area was no longer contaminated by residual concrete dust particles. A concrete strain gauge of type PL-60-11-5L was then attached on the marked centre lines of the short columns by means of a strain gauge adhesive (CN). The strain gauge was kept pressed down until the adhesive cured. At this point,

electrical tape was applied to the wire at multiple points, to prevent the strain gauge from ripping off in case of pulling. The strain gauges were checked before and after attaching them to the concrete face by means of an ohmmeter to make sure that they worked and registered a resistance of 120 ± 0.5 ohms.

Figure 4.35: Position of concrete strain gauge on short column sample

4.8.3.2 Short Column Compression Test Set-up

All eight short columns were transported to the compression testing area by means of a palletiser. A 4000kN automatic compression testing machine was used for all tests. Each column sample was gently lifted into place, ensuring their centres aligned with the compression machine's hydraulic base plate. Two steel platens were placed on top of each sample within the testing machine, acting as the first point of contact upon loading the sample.

An LVDT was incorporated into the set-up by means of an adjustable steel stand, which allowed for vertical movement of the LVDT when calibrating prior to every test. The LVDT's end was rested at the rear corner of the hydraulic base plate, allowing for the measuring of column contraction during testing.

Both steel and concrete strain gauges were attached to the data logger for each test. Prior to testing, each strain gauge was once again checked with an ohmmeter to

ensure they were working correctly, exhibiting a resistance of 120 ± 0.5 ohms. The load cell and LVDT were attached directly to the data logger.

Figure 4.36: Short column compressive strength testing set-up

4.8.3.3 Static Short Column Compression Test Procedure

After setting up the testing rig accordingly, some final procedures needed to be taken before each short column compression test. This involved the calibration of the LVDT, the load cell, and the strain gauges on the data logger.

The test procedure began by applying load at a slow rate until the end plate within the compression testing machine was barely in contact with the intermediary steel platens on top of the concrete sample. A load rate of 5000 N/s was applied throughout the entire procedure. After failure of each sample, the hydraulic base plate was lowered until the concrete sample was fully unloaded. At this point, the machine was switched off and cleaned of loose concrete material before stacking the next short column within the testing machine. All relevant data was then compiled. Strain measurements were verified through the use of multiple gauges collectively on both concrete and reinforcement, allowing for a cross-comparison of strain development against load displacement responses. Sample CR25-B had a faulty steel strain gauge which was excluded from the final results.

4.8.3.4 Cyclic Short Column Compression Test Procedure

Like their respective static tests, all four cyclic compression tests required minor calibration prior to each individual sample test. This involved the calibration of the LVDT, the load cell, and the strain gauges on the data logger.

The test procedure began by applying load at a slow rate until the end plate within the compression testing machine was barely in contact with the intermediary steel platens on top of the concrete sample. A load rate of 5000 N/s was applied throughout the entire procedure. The ultimate failure loads (W_{ult}) obtained for both control and rubber static compression tests were used as bases for cyclic loading for each respective mix.

Table 4.4: Cyclic column compressive tests – Loads and cycles

Sample	10% x W_{ULT} (kN)	30% x W_{ULT} (kN)	50% x W_{ULT} (kN)	70% x W_{ULT} (kN)	90% x W_{ULT} (kN)	W_{ULT} Static Test (kN)
CM-A-5	102.10 *(5 cycles)*	306.29 *(5 cycles)*	510.48 *(5 cycles)*	714.47 *(5 cycles)*	918.86 *(5 cycles)*	1020.95 *(5 cycles)*
CM-B-10	102.10 *(10 cycles)*	306.29 *(10 cycles)*	510.48 *(10 cycles)*	714.47 *(10 cycles)*	918.86 *(10 cycles)*	1020.95 *(10 cycles)*
CR25-A-5	44.52 *(5 cycles)*	133.56 *(5 cycles)*	222.60 *(5 cycles)*	311.64 *(5 cycles)*	400.68 *(5 cycles)*	445.20 *(5 cycles)*
CR25-B-10	44.52 *(10 cycles)*	133.56 *(10 cycles)*	222.60 *(10 cycles)*	311.64 *(10 cycles)*	400.68 *(10 cycles)*	445.20 *(10 cycles)*

Loads were inputted into the system, which in turn automatically loaded/unloaded the sample. Like the cyclic flexural test procedures, loading started at 10% of the respective static ultimate load (10%.W_{ult}) for each short column. This load was held for approximately one minute before unloading the short column down to approximately 10kN. Once unloaded, load was immediately applied until reaching 10%.W_{ult}. This process was repeated until completing five or ten cycles, depending on which sample was being tested.

After completing the necessary desired cycles, load was increased until reaching 30%.W_{ult}. From this point on, all samples were unloaded until 10%.W_{ult}, which became the new base load for each test. The sequence of cycle rates adhered to throughout all four tests may be found in Table 4.4 above. This cycle sequence carried on until failure for each specimen.

After failure of each sample, the hydraulic base plate was lowered until the concrete sample was fully unloaded. At this point, the machine was switched off and cleaned of loose concrete material before stacking the next short column within the testing machine. All relevant data was then compiled. Strain measurements were verified through the use of multiple gauges collectively on both concrete and reinforcement, allowing for a cross-comparison of strain development against load displacement responses. No noteworthy issues were documented throughout all four cyclic compression tests.

4.8.4 Capping Mix for Compression and Flexural Strength Test Samples

As mentioned previously, samples of the capping mix for the short column concrete samples were cast and left to cure for 28 days. A total of three prism samples were to be tested in flexure and compression once finalising the curing process. Once cured, all samples were removed from the water tank and dried, weighed, and measured the same way the concrete cubes had been. Lines were marked on each prism (centre line and two lines at 50mm from each side of centre line), clearly indicating where they would be positioned during three-point flexural testing.

Figures 4.37 and 4.38: Measuring, weighing, and marking of three prism samples

4.8.4.1 Capping Mix for Three-Point Flexural Test Procedure

The prism sample was positioned accordingly in the three-point flexural testing machine. The loading rate applied for the three-point flexural test was 50 N/s,

conforming to EN 1015-11:1999, which specifies controlled and uniform load application for hardened mortar. This standard loading rate was applied with guidance from the Faculty Laboratory technicians, who ensured that the 50 N/s load rate was used in standard practice for this particular test, ensuring repeatable and reliable results. Load was applied uniformly over the width of the prism. Upon failure, the maximum failure load was recorded, and both halves of each prism were kept for further compression strength tests. As may be seen in Figure 4.39, the testing machine consisted of two bottom steel supporting rollers and a top roller applying the flexural load to each specimen. The rollers remained equidistant, exhibiting slight tilting characteristics, aiding against torsion and uneven stress distribution. Moreover, the ability for the steel rollers to tilt helped accommodate for potential misalignments when positioning the samples.

Figure 4.39: Three-point flexural test set-up

4.8.4.2 Capping Mix for Compression Test Procedure

Compressive strength tests were performed on a total of six samples, which consisted of the broken halves resulting from the prior flexural strength tests carried out. Each prism half was positioned accordingly within the compression testing machine, having compression contact areas of approximately 80mm x 40mm. A load rate of 2400 N/s was applied to each sample until failure, conforming to EN 1015-11:1999, which specifies controlled and uniform load application for hardened mortar. This standard loading rate was applied with guidance from the Faculty Laboratory technicians, who ensured that the 2400 N/s load rate was used in standard practice for this particular

test, ensuring repeatable and reliable results. Upon failure, the maximum failure load was recorded.

Figure 4.40: Compressive strength test set-up

4.9 Final Classification of Mixes and Samples

Table 4.5: Final classification of mixes and samples

Mix No.	Mix Type	% Crumb Rubber	Name	Test	Test Day	Sample Name
1	Control Mix	0%	CM	Cube Compression	7	CM-7-A
					7	CM-7-B
					7	CM-7-C
				Cube Compression	28	CM-28-A
					28	CM-28-B
					28	CM-28-C
				Static Flexure	28	CM-A
					28	CM-B
				Cyclic Flexure	28	CM-A-5
					28	CM-B-10
				Static Compression	28	CM-A
					28	CM-B
				Cyclic Compression	28	CM-A-5
					28	CM-B-10

2	Crumb Rubber Mix	25%	CR25	Cube Compression	7	CR25-7-A
					7	CR25-7-B
					7	CR25-7-C
				Cube Compression	28	CR25-28-A
					28	CR25-28-B
					28	CR25-28-C
				Static Flexure	28	CR25-A
					28	CR25-B
				Cyclic Flexure	28	CR25-A-5
					28	CR25-B-10
				Static Compression	28	CR25-A
					28	CR25-B
				Cyclic Compression	28	CR25-A-5
					28	CR25-B-10

3	SikaGrout S55 Mix	0%	SIKAM	Flexure	28	SIKAM-28-A
					28	SIKAM-28-B
					28	SIKAM-28-C
				Compression	28	SIKAM-28-A-1
					28	SIKAM-28-A-2
					28	SIKAM-28-B-1
					28	SIKAM-28-B-2
					28	SIKAM-28-C-1
					28	SIKAM-28-C-2

5. Results and Discussion

5.1 Concrete Cube Compressive Strength Tests

5.1.1 Control Design Mix

The control mix was cohesive and workable. A visual inspection of the control cube specimens revealed a high degree of compaction, with minimal surface voids generally appearing throughout. The same may be said for the internal parts of the cubes after being crushed. The shape adopted by the cubes after crushing showed that the mix was homogenous.

Table 5.1: Concrete Cube compressive strengths – Control design mix

Mix 1 - CM (control mix)			
Testing Day	**Sample Name**	**Cube Compressive Strength (MPa)**	**Mean Cube Compressive Strength (MPa)**
7	CM-7-A	24.15	24.58
7	CM-7-B	25.28	
7	CM-7-C	24.32	
28	CM-28-A	24.00	25.00
28	CM-28-B	26.34	
28	CM-28-C	24.66	

Figure 5.1: Crushed cubes - Control design mix

5.1.2 25% Crumb Rubber Concrete Design Mix (CR25)

Upon visual inspection, the crumb rubber mix proved to be quite workable – even more so than the control mix. An overall decrease in mechanical bonding was evident upon the addition of crumb rubber. This was due to the loss of fine aggregate in the mix, resulting in a lack of mechanical bonding between crumb rubber and cement paste. The surface of the rubberised cube specimens made this evident, as crumb rubber was left exposed and uncovered by the cement paste. Small voids were observed on the cube surfaces, which were possibly a result of the compacting of concrete during casting forming air bubbles on the surface. The most notable aspect of the rubberised concrete cubes was the overall dampness observed on the cube surfaces. This could be due to the hydrophobic nature of rubber particles, which in turn repelled water. The water-cement ratio of 0.55 might have also affected this, as the loss of fine aggregate decreased water absorption throughout the mix. The cured cubes were easily chipped at the edges, showing a lack of toughness at the edges of the specimens. Compressive failure of the rubber specimens was not typical to that of conventional concrete. In this case, failure proved to be more ductile and less abrupt than the failure exhibited by the control cubes.

Table 5.2: Concrete Cube compressive strengths – CR25 design mix

Mix 2 - CR25 (25% crumb rubber mix)			
Testing Day	**Sample Name**	**Cube Compressive Strength (MPa)**	**Mean Cube Compressive Strength (MPa)**
7	CR25-7-A	7.98	8.12
7	CR25-7-B	8.05	
7	CR25-7-C	8.32	
28	CR25-28-A	9.26	8.71
28	CR25-28-B	8.60	
28	CR25-28-C	8.26	

Figure 5.2: Crushed cubes – CR25 design mix

Figure 5.3: Evidence of weak mechanical bonding (ease of crumbling) – CR25

Figures 5.4 and 5.5: Crushed CR25 vs CM / Failure of CM vs CR25

5.1.3 Concrete Cube Compressive Strength Tests - Results and Observations

Three cubes of both mixes were cast and tested in compression at 7 and 28 days from the day of casting. Figure 5.6 shows how the mean cube compressive strength of each mix varied on each day of testing.

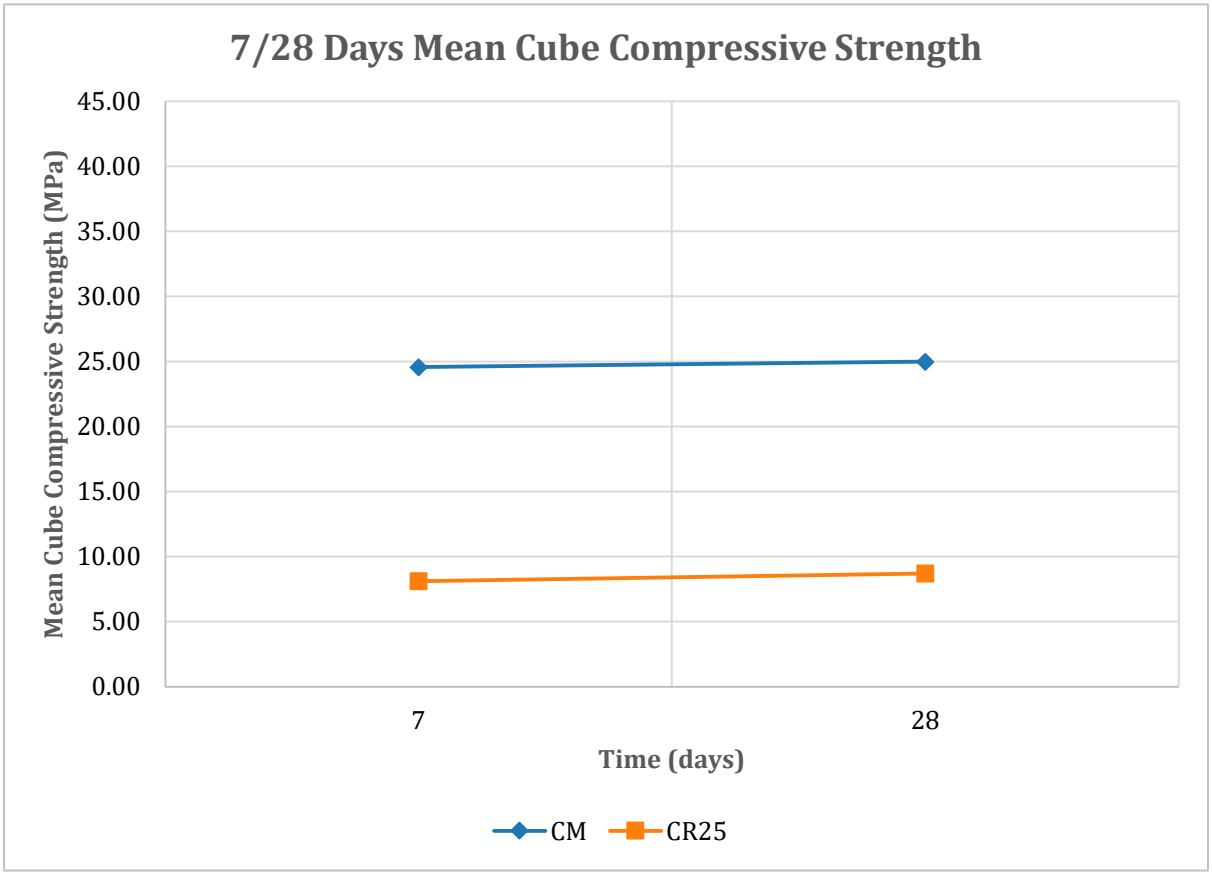

Figure 5.6: Mean concrete cube compressive strengths (MPa) for 7 days and 28 days

Figure 5.6 shows how the control mix (CM) exhibited a considerably higher compressive strength at both 7 days and 28 days in comparison with the crumb rubber mix (CR25). Although the 25% crumb rubber mix (CR25) exhibited a lower compressive strength, its increase in strength from 7 to 28 days was like that of the control mix. Contrary to Scicluna (2010), Magro (2011), and Abdilla's (2012) findings, CR25 did not retain sufficient compressive strength, producing an overall decrease of 65.16% from CM's compressive strength at 28 days. This possibly occurred due to the high water-cement ratio used within the mix (0.55), which was evidently too high. As mentioned previously, the high water content weakened the concrete matrix and the ITZ, which resulted in a significant drop in compressive strength in the CR25 mix.

Table 5.3 along with Figures 5.7 and 5.8 show a comparison of cube compressive strengths for CM and CR25 respectively.

Table 5.3: Comparison of concrete cube compressive strengths across past studies

Researcher	Mix	Mean Compressive Strength (MPa)	Day
Scicluna (2010)	CM	33.00	7
	CM	41.20	28
	CR25	25.80	7
	CR25	31.70	28
Magro (2011)	CM	30.58	7
	CM	33.26	28
	CR25	26.10	7
	CR25	28.30	28
Abdilla (2012)	CM	26.48	7
	CM	31.25	28
	CR25	24.09	7
	CR25	29.61	28
Test Results	CM	24.58	7
	CM	25.00	28
	CR25	8.12	7
	CR25	8.71	28

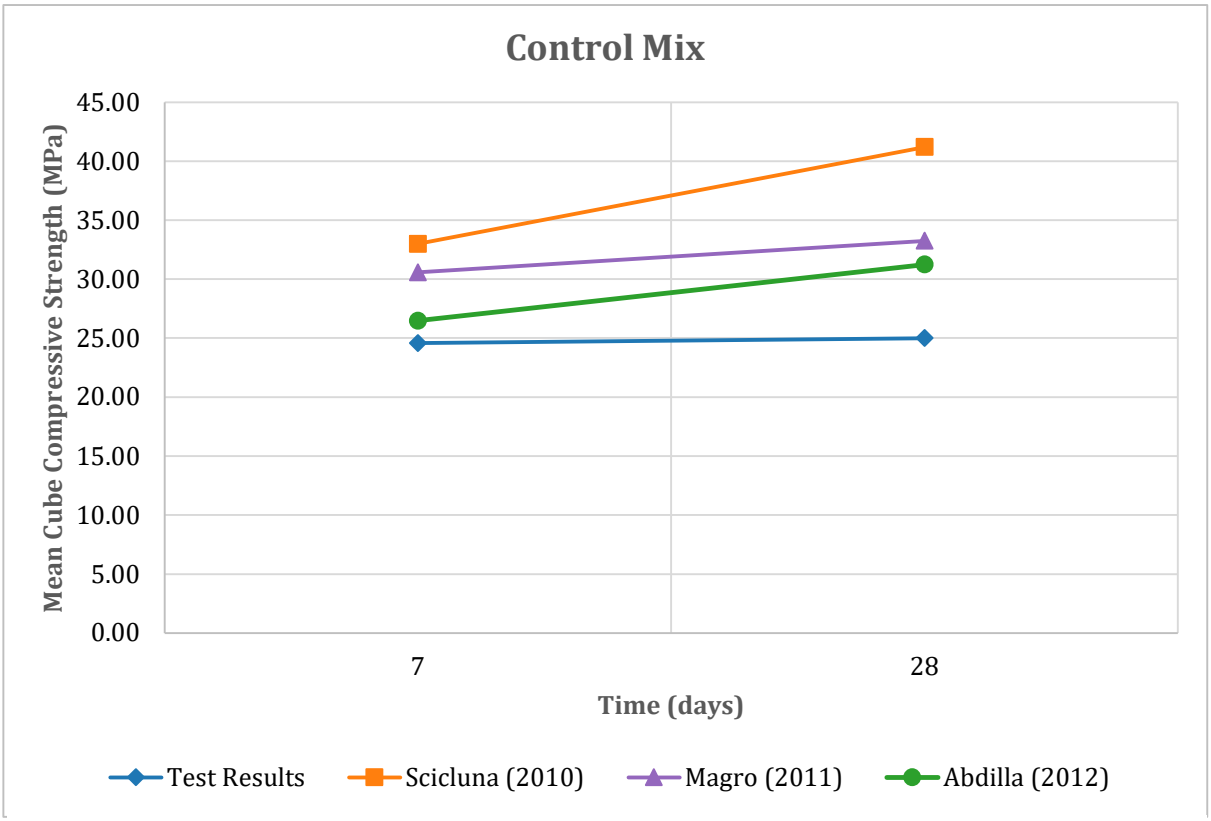

Figure 5.7: Comparison of CM compressive strengths across past studies

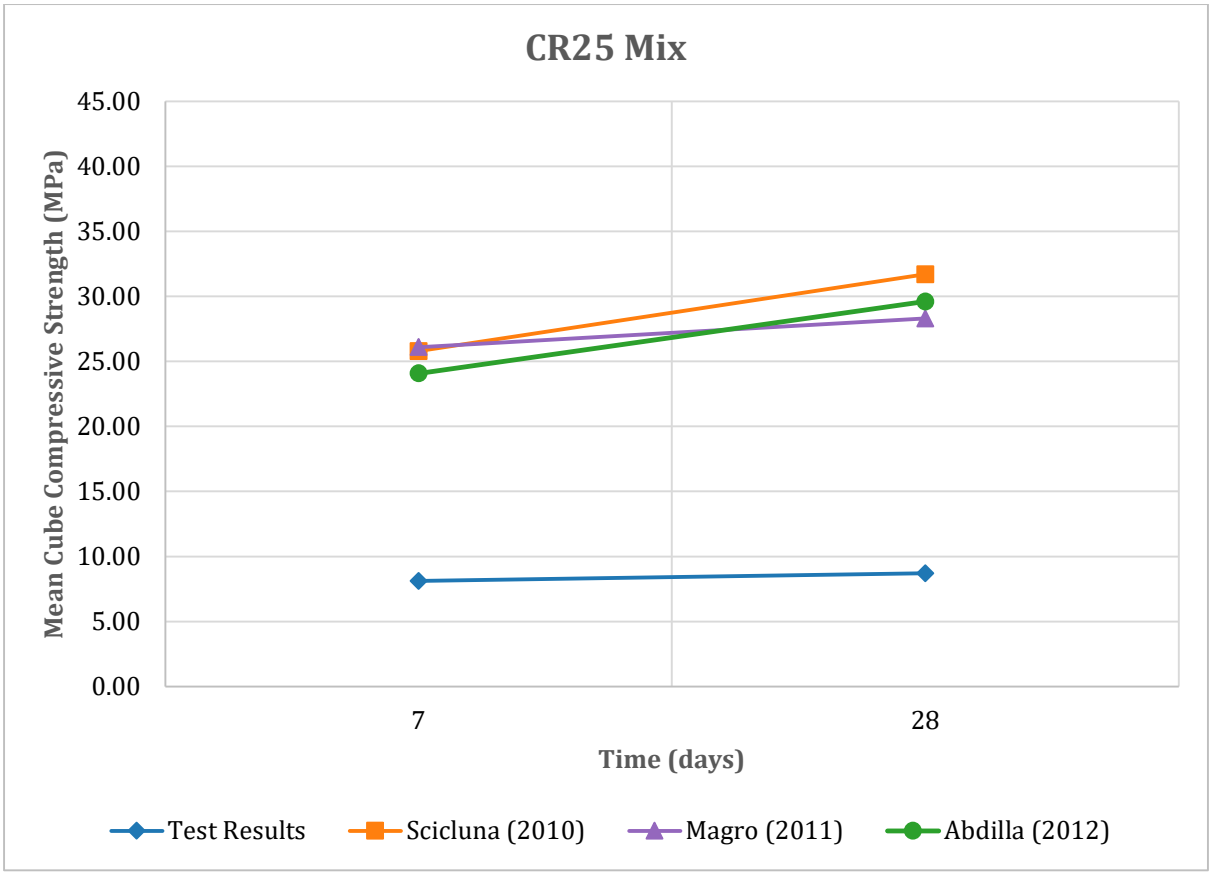

Figure 5.8: Comparison of CR25 compressive strengths across past studies

As may be seen in Figures 5.7 and 5.8 above, both sets of tests produced low compressive strengths compared to past research. This was mostly notable in the CR25 mix, suffering a steep drop off from 31.7 MPa, 28.3 MPa, and 29.61 MPa obtained by Scicluna (2010), Magro (2011), and Abdilla (2012) respectively – resulting in a mean cube compressive strength of 8.71 MPa at 28 days. Moreover, as may be seen in both figures, the increase in compressive strength from 7 to 28 days in both mixes was not as prevalent as the strength increases observed throughout past research.

All these observations conclude an overall decrease in compressive strength throughout both mixes produced in this study. This decrease, irrespective of rubber content or type of crumb rubber used could be due to a number of reasons. Although the type of natural coarse aggregate used in all studies consisted of Upper Coralline Limestone, the fluctuation in results shows that aggregate used in other studies could have possessed better qualities than the aggregate used in this study. As the different aggregates came from a variety of rock sources, the properties of the parent rock, such as specific density, hardness, physical stability, and chemical and mineral

composition, were ultimately different. The maximum coarse aggregate size of 20mm also differed to the 14mm used by Scicluna (2010), who coincidentally obtained the best cube compressive strengths throughout all past research. Although the water-cement ratio was kept the same (0.55) in all investigations, the free water content and cement content varied next to Scicluna's (2010) mix, as these are based on the maximum aggregate size. Using 20mm aggregate generally produces a lower surface area to be wetted per unit mass. This could have ultimately lowered the mix's strength, since more free water was present in the mix. Another factor affecting the obtained results could relate to the variety in sourced rubber, implying that the pitch rubber used in this study could have possessed higher hydrophobic capabilities relative to past studies.

Table 5.4: Concrete Cube Data at 7 days and 28 days

Sample Type	Sample Tested	Length (mm)	Breadth (mm)	Width (mm)	Weight (Kg)
Control Cube	CM-7-A	150.65	150.81	152.77	7.10
Control Cube	CM-7-B	150.17	150.52	151.24	7.13
Control Cube	CM-7-C	150.55	150.39	152.56	7.12
Rubberised Cube	CR25-7-A	150.45	150.55	153.13	6.05
Rubberised Cube	CR25-7-B	150.33	150.54	151.65	6.02
Rubberised Cube	CR25-7-C	150.18	150.21	152.61	5.99

Sample Type	Sample Tested	Length (mm)	Breadth (mm)	Width (mm)	Weight (Kg)
Control Cube	CM-28-A	150.82	150.75	151.38	7.15
Control Cube	CM-28-B	150.59	150.10	151.18	7.12
Control Cube	CM-28-C	150.42	150.80	149.95	7.18
Rubberised Cube	CR25-28-A	150.69	150.16	153.63	6.09
Rubberised Cube	CR25-28-B	150.25	150.40	151.99	6.01
Rubberised Cube	CR25-28-C	150.43	150.10	152.46	6.01

5.2 Capping Mix for Flexural and Compressive Strength Tests

As mentioned previously, SikaGrout S55 cement was chosen for the short column capping mix, with the aim of avoiding premature failure of the column capping layers during the short column compressive tests. Therefore, the primary requirement for the capping material was that its mechanical strength exceeded that of the column concrete so that failure during compression testing would be governed exclusively by the behaviour of the concrete column rather than by crushing or cracking of the capping layer. To understand this, SikaGrout S55 prism samples (SIKAM) were testing in both flexure and compression. Tables 5.5 and 5.6 highlight the outcomes of both testing procedures.

Table 5.5: SIKAM prism three-point loading flexural strengths

Mix 3 - SIKAM (sikagrout S55 mix)			
Testing Day	**Sample Name**	**Prism Flexural Strength (MPa)**	**Mean Prism Flexural Strength (MPa)**
28	SIKAM-28-A	11.10	10.47
28	SIKAM-28-B	9.54	
28	SIKAM-28-C	10.78	

Table 5.6: SIKAM prism compressive strengths

Mix 3 - SIKAM (sikagrout S55 mix)			
Testing Day	**Sample Name**	**Prism Compressive Strength (MPa)**	**Mean Prism Compressive Strength (MPa)**
28	SIKAM-28-A-1	88.06	89.23
28	SIKAM-28-A-2	94.09	
28	SIKAM-28-B-1	87.74	
28	SIKAM-28-B-2	84.23	
28	SIKAM-28-C-1	90.16	
28	SIKAM-28-C-2	91.12	

As may be seen in Table 5.6, the mean compressive strength of SIKAM at 28 days was 89.23 MPa, which significantly exceeded the mean compressive strength of the CM cubes at the same day from casting (25 MPa). This represents a compressive strength ratio of more than 3.5:1, confirming that the grout mix possessed a substantially higher compressive strength capacity than the column concrete, and

ensuring that the capping layer would not have become a governing failure mechanism during future compressive tests.

Similarly, the mean flexural strength of SIKAM at 28 days was 10.47 MPa, indicating adequate stiffness and crack resistance. These characteristics made the material capable of maintaining structural integrity under high bearing stresses and minor bending effects caused at the column-steel platen interface. Moreover, these results further supported the suitability of the capping material in relation to uniform stress transfer during axial loading.

Table 5.7: Prism data at 28 days

Sample Type	Sample Tested	Length (mm)	Breadth (mm)	Width (mm)	Weight (Kg)
Capping Mix	SIKAM-28-A	160.23	40.30	40.29	0.59
Capping Mix	SIKAM-28-B	160.15	40.19	40.06	0.59
Capping Mix	SIKAM-28-C	160.28	40.22	40.51	0.61

5.3 Static Four-Point Loading Flexural Strength Tests

5.3.1 Test Results

Table 5.8 shows the static flexural failure load of all four reinforced concrete beam samples after 28 days from casting.

Table 5.8: Static four-point loading flexural test results

Sample Type	Sample Tested	Time (s)	Average LVDT (mm)	Compressive Concrete Strain (µm/m)	Load (kN)	Mean Ultimate Load (W_{ULT})
Control Beam	CM-A	9143.49	63.86	-0.001655	86.86	85.82
Control Beam	CM-B	9877.15	59.56	-0.002058	84.77	
Rubberised Beam	CR25-A	8274.11	65.50	-0.001359	71.63	71.95
Rubberised Beam	CR25-B	7752.11	60.50	-0.002541	72.26	

The control beams (CM) failed with the highest mean ultimate flexural load (85.82kN), with sample CM-A achieving the highest overall failure load of 86.86kN. On the other hand, the 25% rubber replacement beam samples (CR25) failed with a mean ultimate load of 71.95kN, recording a 16.16% reduction in flexural strength relative to CM. When compared to the reduction in compressive strength exhibited by the CR25 cubes

from the CM cubes, one may observe that the reduction in cube compressive strength was substantially greater (65.16% at 28 days) than the overall flexural strength reduction.

When compared to Magro's (2011) static flexural test results, both CM and CR25 tested in this study exhibited higher ultimate flexural capacities. As may be seen in Figure 5.9, CM beams achieved a mean ultimate flexural load of 85.82kN compared to 70.87kN reported by Magro (2011), resulting in an increase of 21.1% relative to her CM beam result. Similarly, CR25 beams achieved a mean ultimate flexural load of 71.95kN compared to 65.46kN reported by Magro (2011), resulting in an increase of 9.9% relative to her work. These improvements in flexural performance are particularly noteworthy given that the cube compressive strengths obtained in this study were marginally lower than the corresponding cube strengths reported by Magro (2011). This indicates that the higher flexural capacities obtained during this study are therefore not a result of superior concrete strength, but rather to differences in beam detailing adopted in both studies.

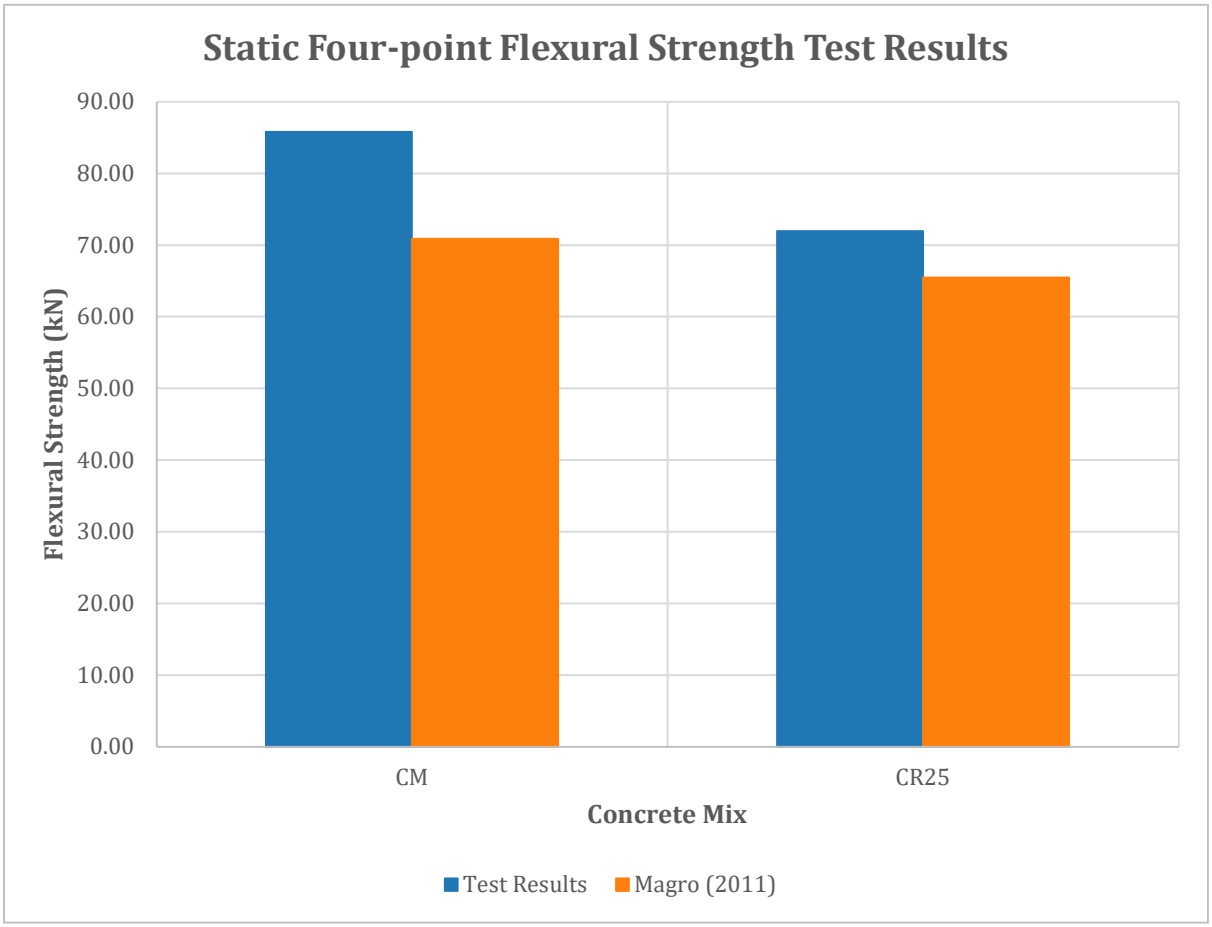

Figure 5.9: Static four-point loading flexural strength test results – Comparison with Magro (2011)

The main variable between both experimental studies came in the inclusion of one bottom longitudinal reinforcement bar (H16) in the beams used in this study. The primary purpose of this additional reinforcement was to ensure that beam failure occurred predominantly due to concrete crushing in the compression zone of the beam, rather than premature yielding of the tensile reinforcement. This in turn was necessary to investigate the brittle nature of failure of reinforced concrete beams, which was not as predominant in Magro's (2011) study, where the combination of higher cube compressive strengths and less tension reinforcement caused a ductile failure mode as opposed to the semi-brittle failure mode achieved during this study. In other words, this testing approach was adopted to allow for a more direct assessment of concrete material behaviour, particularly the influence of crumb rubber on compressive and post-peak response, rather than having the results dictated by steel yielding. Consequently, this variation highlights the significant role of steel reinforcement in flexural test outcomes.

5.3.2 Static Four-Point Loading Flexural Strength Tests – Observations

5.3.2.1 Control Beams (CM)

Figure 5.10 showcases the failure mode presented by both CM beam samples, which was deduced to be flexural failure typical to that presented in conventional reinforced concrete beams. The central third compression zone of each beam was crushed, with intensified crushing occurring towards one of the beam thirds. This could be due to local effects present in the beam. This may be observed in Figure 5.10, where failure still occurred within the central compression third of the beam, yet being a few centimetres away from one of the spreader's points of contact with the beam.

A series of vertical cracks formed throughout the span of each beam, predominantly originating from the beam's tension zone (maximum bending moment zone). The cracks formed in the central third of the beam (towards both beam thirds) were substantially wider, becoming more hairline away from the central zone of the 4m beam.

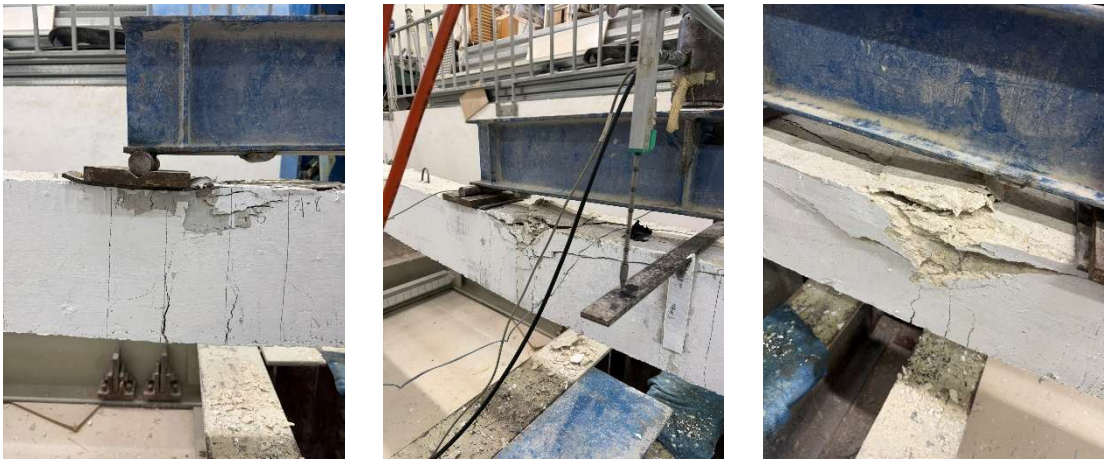

Figure 5.10: Control beam failure

5.3.2.2 25% Crumb Rubber Beams (CR25)

Figure 5.11 showcases the failure mode presented by both CR25 beam samples. Once again, beam failure did not occur in the centre, but at approximately one third of the beam, close to one of the spreader's points of contact with the beam. This may be observed in Figure 5.11. The central one third compression zone of the beam was also crushed like the CM beam.

A series of vertical cracks formed throughout the span of each beam, predominantly originating from the beam's tension zone (maximum bending moment zone). The cracks formed in the central third of the beam (towards both beam thirds) were substantially wider, becoming more hairline away from the central zone of the 4m beam. Generally, the observed vertical cracks were wider than those observed in the CM beam samples. Crushing of the compression concrete cover was also more severe, aligning with the weaker cube compressive strengths exhibited by CR25 relative to the CM cube compressive strengths.

Upon failure, crumbling of the top and bottom beam covers was evident, indicating weaker concrete and mechanical bonding due to the presence of rubber content. This may be observed in Figure 5.11.

Figure 5.11: CR25 beam failure

5.3.3 Static Four-Point Loading Flexural Strength Tests – Deflection

Figures 5.12, 5.13, and 5.14 show the deflection curves for all four static four-point flexural tests, consisting of two control beams and two rubberised beams. Magro's (2011) deflection curves for CM and CR25 were also added for comparative purposes.

5.3.3.1 Deflection – Control Beam Samples (CM)

Magro (2011) achieved higher stiffness in her control beam, as may be seen by the steepness of her gradient on Figure 5.12. This is probably due to the strength of her control mix in relation to the control mix produced in this study. After reaching the elastic limit, one may observe a long plateau within Magro's (2011) elasto-plastic region until reaching the peak load (70.87kN) prior to failing in a ductile manner.

The CM beam deflection curves achieved during this study exhibit less stiffness than Magro's (2011), which was to be expected considering the differences in cube compressive strengths as discussed previously. However, both CM beam samples reached a higher peak load than Magro's (2011) CM beam sample, before failing in a semi-brittle manner relative to Magro's (2011) ductile failure mode. This indicates that even though the CM cube compressive strengths achieved in this study decreased by approximately 24.83% from Magro's (2011), the additional bottom longitudinal reinforcement bar (H16) compensated for this decrease in concrete strength. The shorter elasto-plastic plateaus achieved in this study showcase a more brittle failure mode relative to Magro's (2011), which may also be attributed to the additional provided steel reinforcement within the beam specimens. As discussed previously, this was done purposely to investigate the brittle mode of failure within the beam samples produced, by inducing the beam samples to fail by concrete crushing rather than premature steel yielding. The results prove that this was achieved.

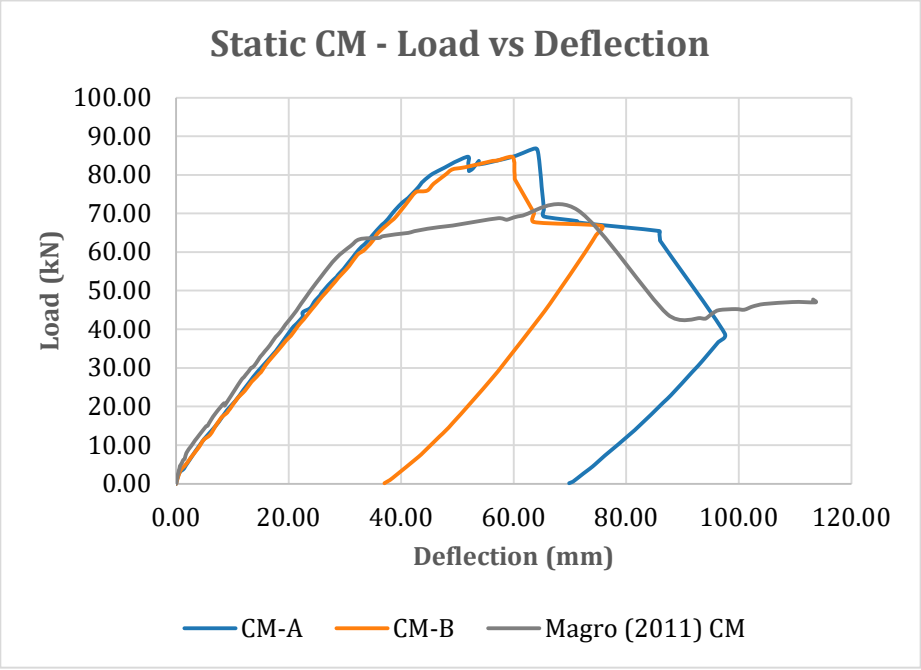

Figure 5.12: Static four-point CM deflection curves

5.3.3.2 Deflection – 25% Crumb Rubber Beam Samples (CR25)

As may be expected, Magro's (2011) CR25 beam deflection curve followed a similar path to that of her CM beam curve, up until the point where the CR25 beam began to

fail (≈45mm deflection). After reaching the beam's peak load (65.46kN), one may observe a ductile mode of failure before failing abruptly.

Once again, the CR25 beam deflection curves achieved during this study exhibit less stiffness than Magro's (2011), which was to be expected considering the differences in cube compressive strengths as discussed previously. Furthermore, the CR25 beam samples proved to be substantially less stiff than the CM beam samples produced in this study, which was to be expected considering how much weaker the CR25 concrete was than the CM concrete. This may be seen in the gradients produced by both beam sample types in Figure 5.14, where the CR25 gradients are much less steep than those exhibited by CM. In Magro's (2011) case, both CM and CR25 followed the same gradient path upon being loaded, indicating similar mix stiffnesses.

However, both CR25 beam samples in this study reached a higher peak load than Magro's (2011) CR25 beam sample, before failing in a semi-ductile manner. This indicates that even though the CR25 cube compressive strengths achieved in this study decreased by approximately 69.22% from Magro's (2011), the additional bottom longitudinal reinforcement bar (H16) compensated for this decrease in concrete strength.

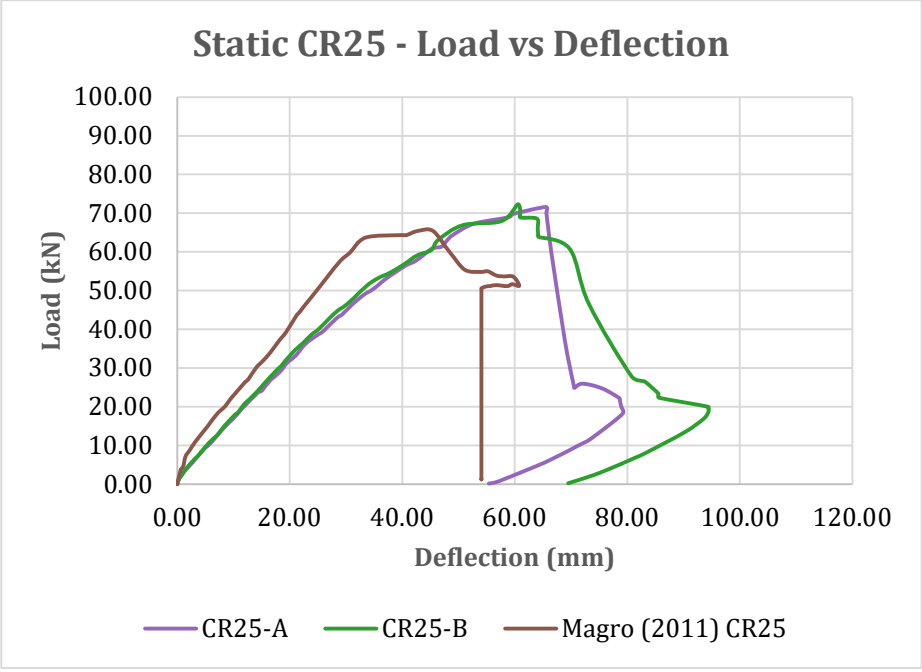

Figure 5.13: Static four-point CR25 deflection curves

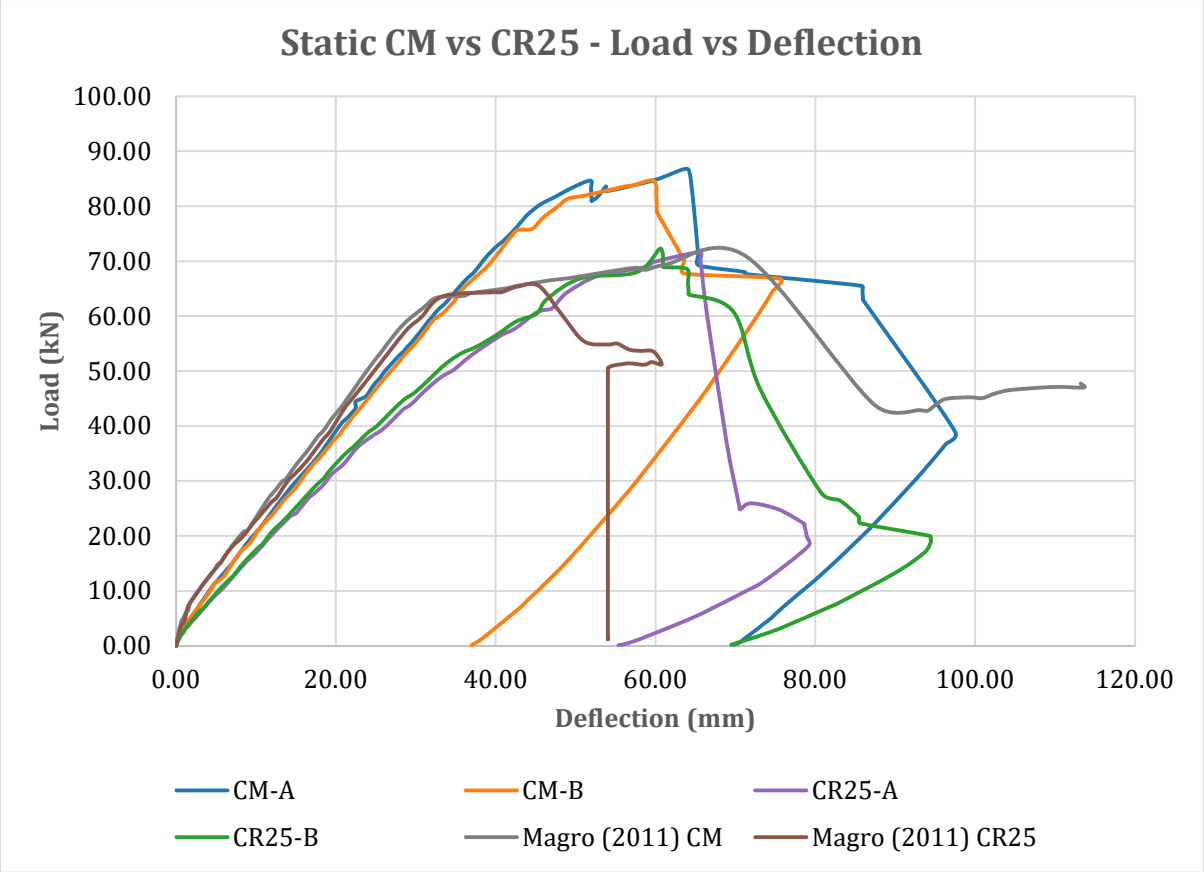

Figure 5.14: Static four-point CM vs CR25 deflection curves

5.4 Cyclic Four-Point Flexural Strength Tests

5.4.1 Test Results

Table 5.9 shows the cyclic flexural failure load of all four reinforced concrete beam samples after 28 days from casting.

Table 5.9: Cyclic four-point flexural test results

Sample Type	Sample Tested	Time (s)	Average LVDT (mm)	Compressive Concrete Strain (µm/m)	Load (kN)	Mean Ultimate Load (W_{ULT})
Control Beam	CM-A-5	5394.26	58.07	-0.001524	83.43	84.29
Control Beam	CM-B-10	9593.11	69.37	-0.003025	85.14	
Rubberised Beam	CR25-A-5	4454.16	58.89	-0.001626	69.50	67.40
Rubberised Beam	CR25-B-10	7182.41	53.18	-0.003374	65.30	

Like the static tests, the CM beam samples failed at a higher flexural load than the CR25 samples, recording a mean ultimate load of 84.29kN as opposed to 67.40kN

obtained by the CR25 samples. As may be seen in Figure 5.15, CR25 suffered a higher decrease in flexural strength capacity when subjected to cyclic loading as opposed to CM:

- CM beam samples – Approximately 1.78% strength reduction
- CR25 beam samples – Approximately 6.32% strength reduction

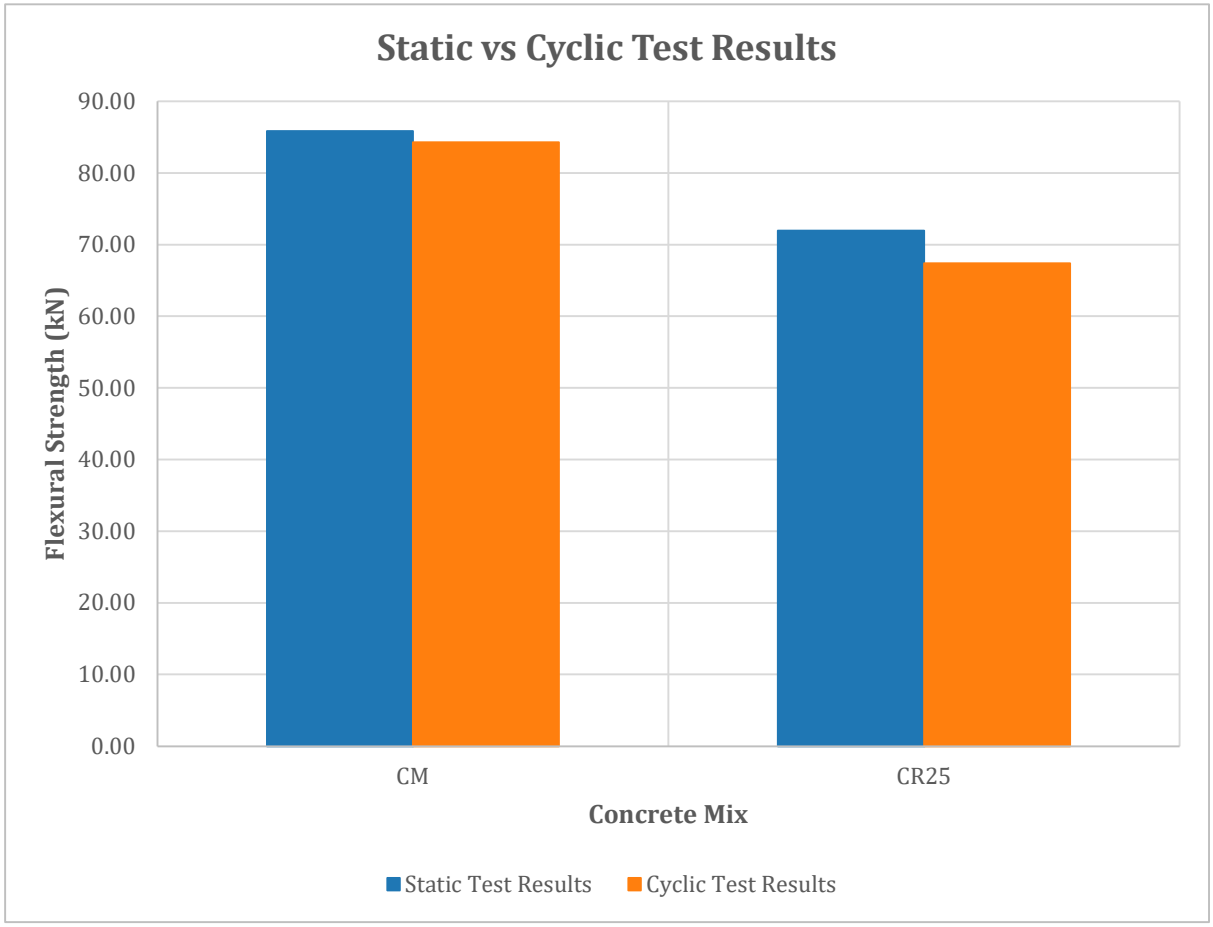

Figure 5.15: Static vs cyclic mean ultimate loads

Table 5.10 depicts how many cycles each beam sample underwent during testing, with the last cycle indicating the failure cycle for that sample. One may notice that both CM beam samples only failed once reaching 100%.W_{ult} of the static ultimate load (approximately 85.82kN), whilst the CR25 beam samples failed in the 90%.W_{ult} region. This indicates that the CM beams retained sufficient stiffness and fatigue resistance to withstand repeated loading without experiencing premature degradation. In contrast, the CR25 beams exhibited that while they could tolerate repeated loading at moderate stress levels, their reduced stiffness and flexural strength result in earlier specimen failure under high-amplitude cyclic loading. This indicates that CR25

endured accelerated stiffness degradation and crack propagation as loading increased in comparison to CM. This behaviour is consistent with the known effects of crumb rubber incorporation in concrete, which reduces peak strength, but increases overall deformability and energy dissipation. Under high cyclic stress levels, the reduced tensile stiffness of the rubberised concrete led to faster structural degradation and premature loss regarding load-carrying capacity relative to CM.

Table 5.10: Number of cycles per sample

Sample	10% x W_{ULT}	30% x W_{ULT}	50% x W_{ULT}	70% x W_{ULT}	90% x W_{ULT}	W_{ULT} Static Test
CM-A-5	5	5	5	5	5	1
CM-B-10	10	10	10	10	10	1
CR25-A-5	5	5	5	5	1	-
CR25-B-10	10	10	10	10	4	-

5.4.2 Cyclic Four-Point Loading Flexural Tests – Observations

Visual observations during testing indicated that the overall crack formation patterns on both sample types were consistent with those observed during the corresponding static flexural tests. Once again, a series of vertical cracks formed throughout the span of each beam, predominantly originating from the beam's tension zone (maximum bending moment zone). The cracks formed in the central third of the beam (towards both beam thirds) were substantially wider, becoming more hairline away from the central zone of the 4m beam. Generally, the observed vertical cracks were wider than those observed in the CM beam samples.

In CM's case, once these cracks formed, they remained clearly visible during unloading, with limited crack closure observed between successive load cycles. As cyclic loading progressed, residual deflections accumulated, indicating a permanent loss of stiffness and reduced ability of the beams to recover their original geometry after unloading.

In CR25's case, a noticeably different deformation response under cyclic loading was observed. Although crack formations were similar to those observed the static flexural tests, the CR25 beams demonstrated improved crack closure and shape recovery during unloading at each increase in load. This behaviour was consistently observed

across all unloading cycles prior to the 90%.W_{ult} region, where deformation began to become more evident prior to total failure.

The enhanced shape recovery observed in the CR25 beams is attributed to the elastic nature of the crumb rubber particles. While this did not prevent crack formation under higher loads, it contributed to improved deformation reversibility and reduced permanent damage accumulation during cyclic loading at medium to lower loads (≤ 70%.W_{ult}). These observations highlight the contrasting behavioural characteristics between conventional and rubberised concrete when subjected to repeated flexural loading.

Figure 5.16: CM beam failure

Figure 5.17: CR25 beam failure

5.4.3 Cyclic Four-Point Loading Flexural Strength Tests – Deflection

5.4.3.1 Deflection – Control Beams (CM)

As shown in Figure 5.20, the CM beam samples retained a relatively high level of stiffness under cyclic loading when compared to their corresponding static four-point flexural tests. This is indicated by the average load–deflection gradients of both CM-A-5 and CM-B-10, which overlap their static counterparts. The similarity between cyclic and static behaviour indicates that repeated loading did not significantly alter the flexural response of the control beams within a cyclic environment. Like their static counterparts, semi-brittle failure mode was observed in both specimens, particularly in CM-A-5, whose behaviour closely resembled that recorded during static testing.

Furthermore, the load–deflection data exhibited by CM-A-5 and CM-B-10 overlapped up to a deflection of approximately 55mm, beyond which CM-A-5 began to fail, diverging from CM-B-10's load-deflection curve path. Despite the difference in the number of applied cycles, both specimens achieved comparable peak loads, suggesting that increasing the number of cycles from five to ten did not significantly influence the ultimate flexural capacity of the CM beams in this case. This indicates that CM exhibited sufficient resistance to cyclic degradation during testing.

As may be seen in Figure 5.20, a semi-brittle failure mode is prevalent in both CM beam samples, particularly in CM-A-5, which was very similar to the corresponding static tests. One must note that the total number of cycles applied to each specimen was constrained by practical time considerations, requiring the tests to be completed within a feasible laboratory timeframe. This implies that increasing the number of cycles per load increment would build on the deflection results discussed above.

5.4.3.2 Deflection – 25% Crumb Rubber Beams (CR25)

Unlike the CM beam samples, the CR25 beam samples did not retain a high level of stiffness under cyclic loading when compared to their corresponding static four-point flexural tests. As may be seen in Figure 5.21, stiffness in both CR25 samples was retained until approximately 35mm of deflection, corresponding to 70%.W_{ult} in the cyclic loading protocol. At this point, both samples' gradients start to delve away from the corresponding static curve gradients and becoming less steep in the process,

indicating a loss in stiffness which accumulated as each sample was reloaded every cycle. However, the CR25 beams proved to retain their form better than the CM samples. This is shown during the unloading phases of each cycle, where deflection in the CR25 curves decreases substantially relative to the CM curves even though CR25 lost stiffness more easily when loaded. This factor indicates that CR25 produced a more flexible mix than that of CM, being able to dissipate energy mor efficiently as a result.

Unlike the CM beam samples, the CR25 beam samples did not manage to reach the peak loads achieved in their corresponding static four-point flexural tests. This is once again attributed to the lower stiffness present in rubberised concrete, which promoted structural degradation as loading cycles accumulated. This caused the CR25 beams to fail prematurely in comparison with their static counterparts.

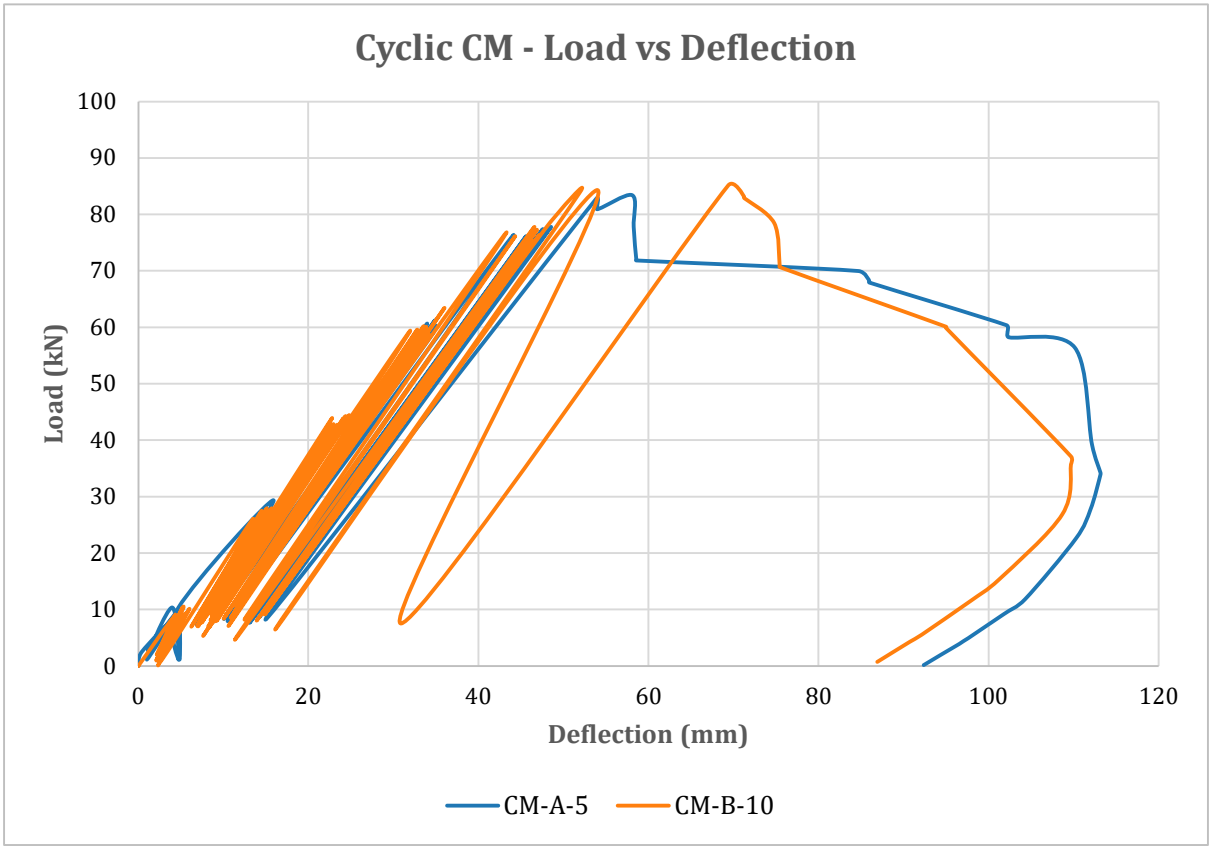

Figure 5.18: Cyclic four-point CM deflection curves

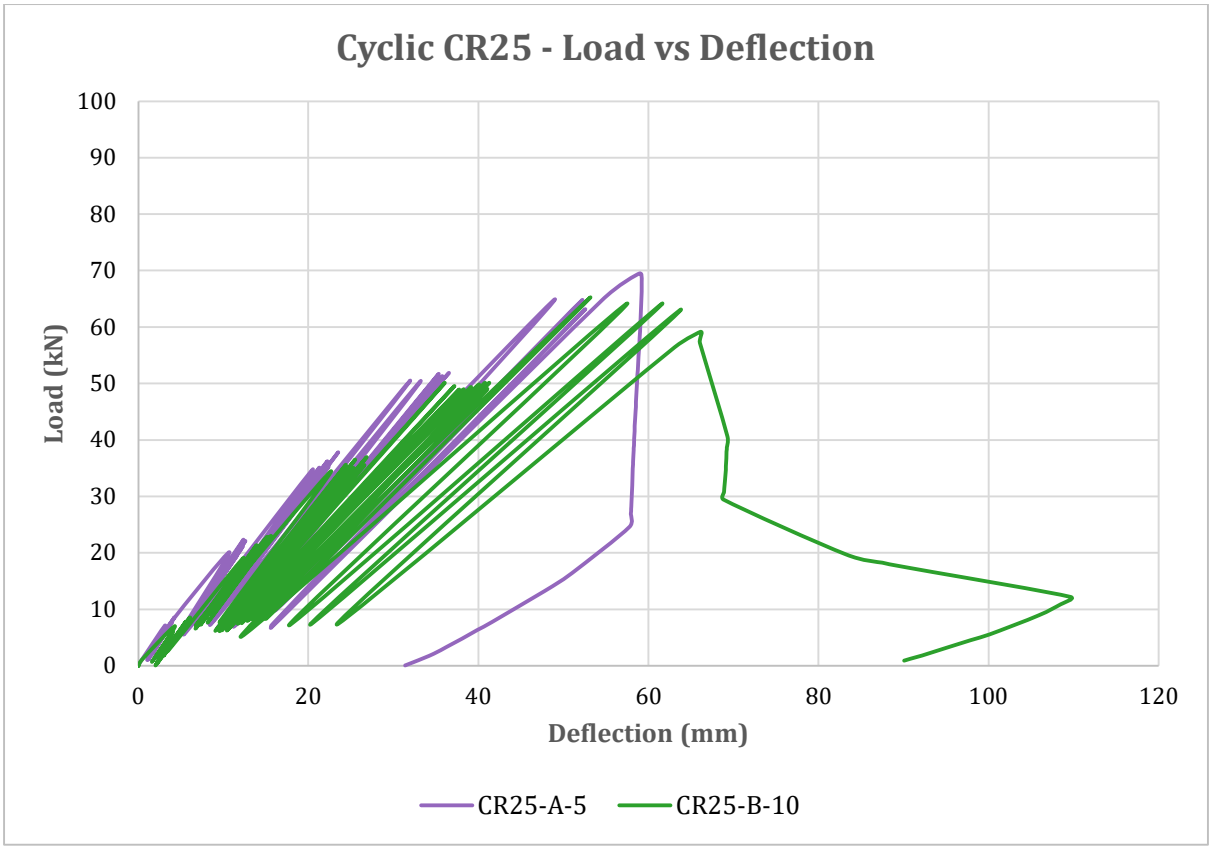

Figure 5.19: Cyclic four-point CR25 deflection curves

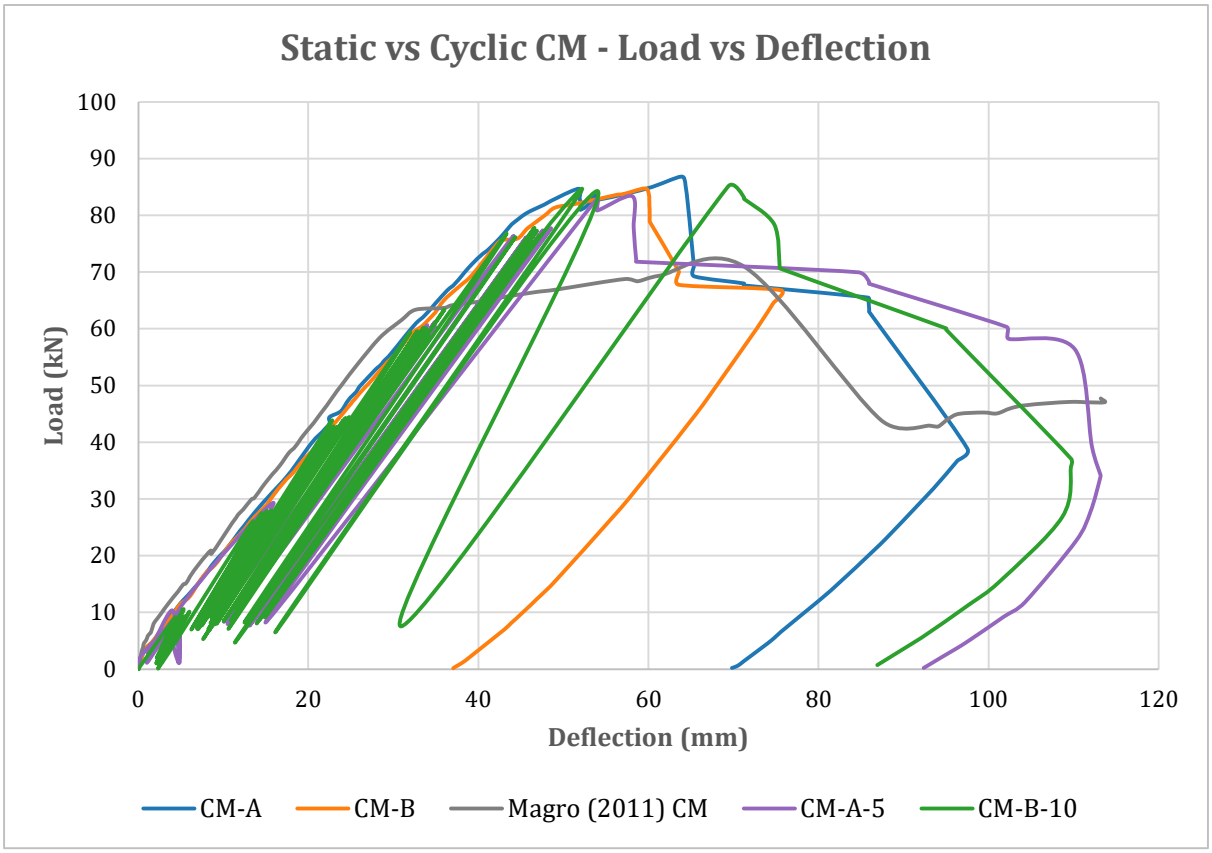

Figure 5.20: Static vs Cyclic four-point CM deflection curves

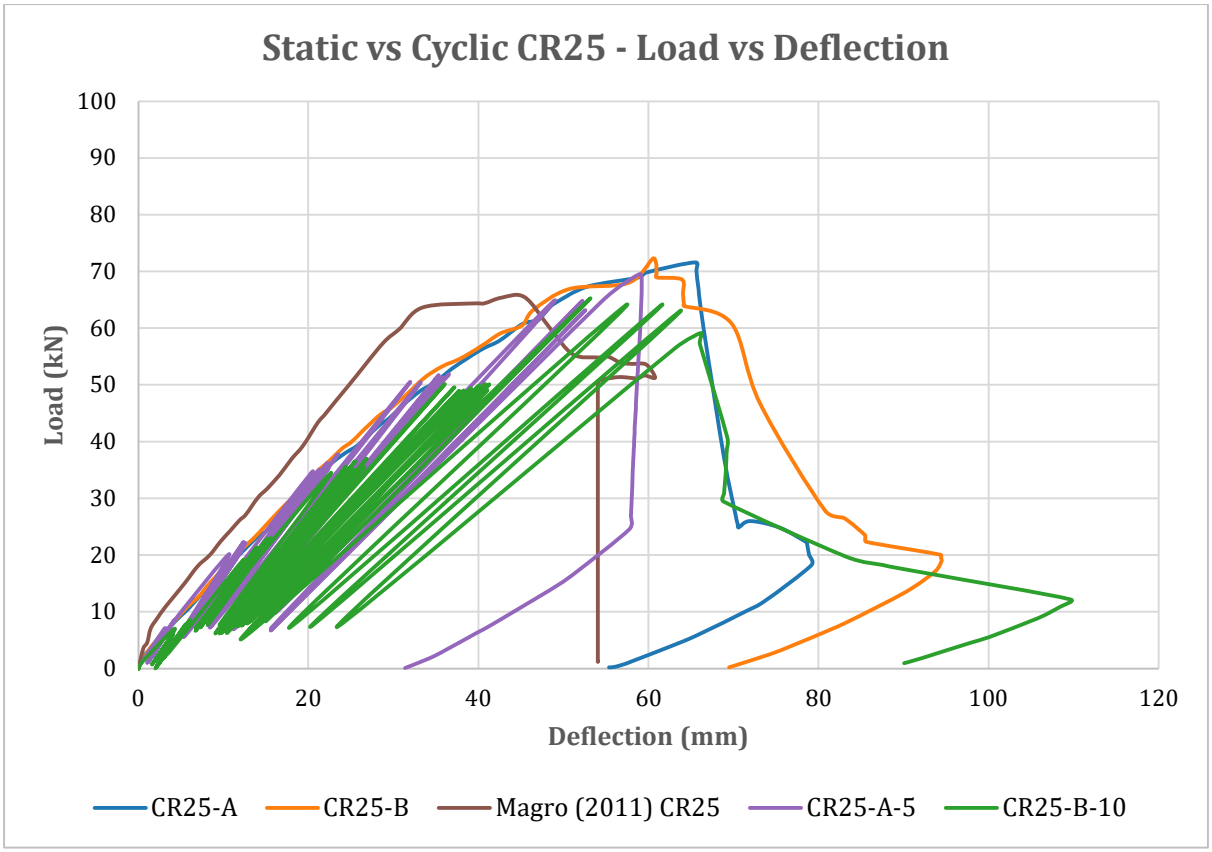

Figure 5.21: Static vs Cyclic four-point CR25 deflection curves

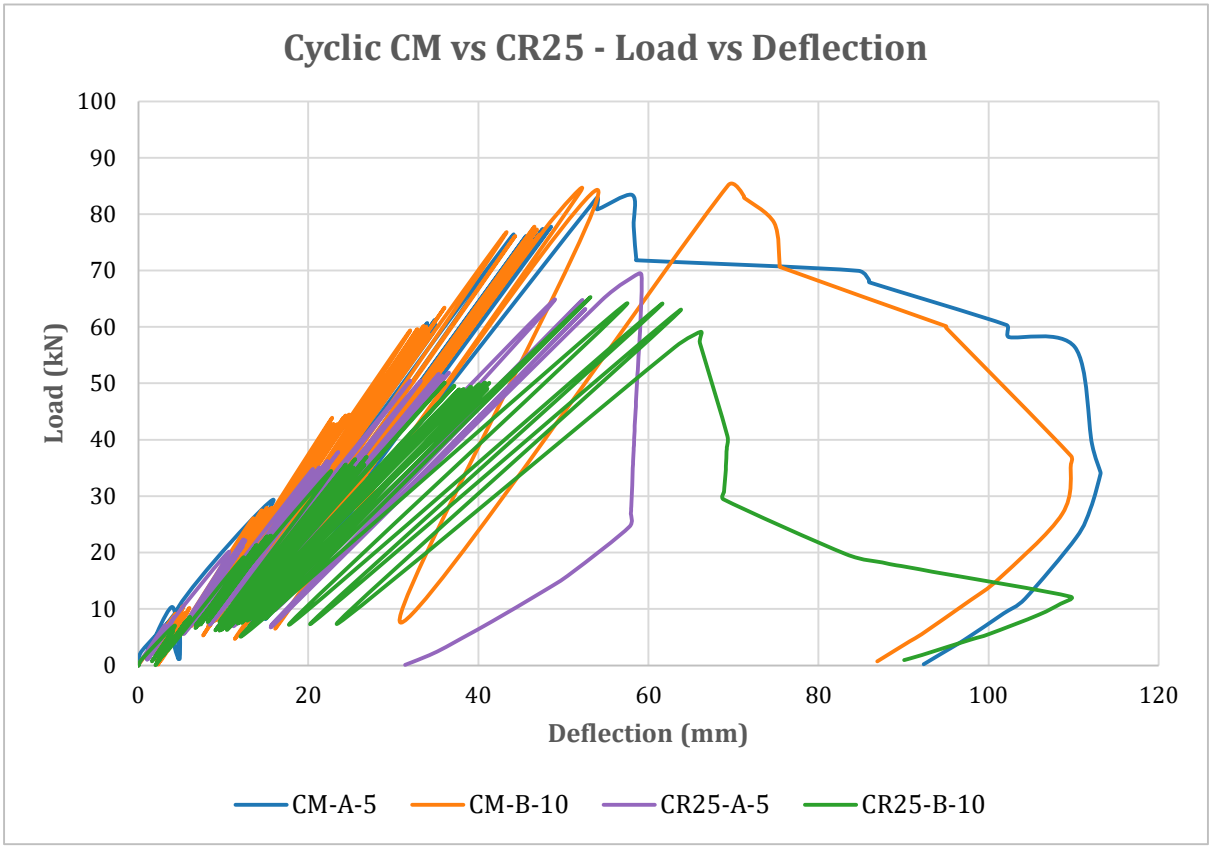

Figure 5.22: Cyclic four-point CM vs CR25 deflection curves

5.5 Static Short Column Compressive Strength Tests

5.5.1 Test Results

Table 5.11 shows the static compressive strengths of all four reinforced concrete short column samples after 28 days from casting.

Table 5.11: Static short column compressive strength results

Sample Type	Sample Tested	Time (s)	LVDT 1 (mm)	Comp. Steel Strain (µm/m)	Comp. Concrete Strain (µm/m)	Load (kN)	Mean Ultimate Load (W_{ULT})
Control Column	CM-A	214.80	2.47	-1136.00	-2689.70	1079.10	1020.95
Control Column	CM-B	187.20	2.92	-656.20	-387.50	962.80	
Rubberised Column	CR25-A	94.90	2.70	-677.60	-577.60	478.20	445.20
Rubberised Column	CR25-B	81.30	1.92	-	-424.40	412.20	

The control columns (CM) failed with the highest compressive load, recording a mean ultimate compressive load of 1020.95kN. The 25% crumb rubber columns (CR25) failed with a mean ultimate compressive load of 445.20kN, recording a compressive strength decrease of 56.39% from the CM column samples.

5.5.2 Static Short Column Compressive Strength Tests – Observations

5.5.2.1 Control Short Columns (CM)

Figure 5.23 showcases the failure mode presented by both CM column samples, which was deduced to be compressive failure typical to that presented in conventional reinforced concrete short columns. The primary mode of failure came in the form of concrete crushing within the column body, typical of reinforced short columns subjected to concentric compressive loading. Cracks were first observed in the central regions of the column height, which eventually progressed outwards. As loading increased, vertical splitting cracks developed along the column faces, extending along the columns' height. Prior to failure, these vertical cracks became more pronounced, and the concrete cover began to spall towards the columns' mid-heights. Column failure remained governed by material crushing rather than instability, confirming that both samples behaved as intended, and that the observed response was representative of compressive concrete failure. The SIKAM capping layers remained intact as expected, with little to no signs of structural degradation.

Figure 5.23: CM short column failure

5.5.2.2 25% Crumb Rubber Short Columns (CR25)

Figure 5.24 showcases the failure mode presented by both CR25 column samples. Once again, concrete crushing of the concrete body was predominant, making the CR25 samples consistent with the behaviour of reinforced concrete short columns subjected to predominantly concentric compressive loading. However, in comparison with their control counterparts, both CR25 column samples exhibited a more distributed and ductile cracking response prior to total failure.

Cracks were first observed in the central regions of the column height, which eventually progressed outwards. As loading increased, vertical splitting cracks developed along the column faces, extending along the column's height. These cracks were wider and more prevalent than those seen in the CM samples, extending along a greater portion of the column height and being accompanied by gradual spalling of the concrete cover towards the column's mid-height. Crack progression was observed to be less abrupt, indicating a more ductile mode of failure relative to the CM samples. Nonetheless, column failure remained governed by material crushing rather than instability or buckling, confirming that both samples behaved as intended, and that the observed response was representative of compressive concrete failure. Moreover, the enhanced crack formations observed indicate the influence of crumb rubber within the concrete mix.

Finally, the failed regions of the CR25 samples quickly crumbled upon failure and minor handling of the samples, which reinforced the argument made on the lack of mechanical bonding present in rubberised concrete. As may be observed in Figure 5.24, post-failure material was loose and silty at times, with rubber particles easily detaching from the cementitious matrix.

Once again, the SIKAM capping layers remained intact, with little to no signs of structural degradation.

Figure 5.24: CR25 short column failure

5.5.3 Static Short Column Compressive Strength Tests – End Displacement

Figure 5.25 shows the deflection curves for all four static compressive tests, consisting of two control short columns and two rubberised short columns.

Both CM column samples produced a stiffening effect during the early loading stages, meaning that the gradient of the load-end displacement curve starts out gradual, implying low apparent stiffness. As loading increased, the curve gradient steepened, implying a significant build-up in material stiffness.

As may be seen in Figure 5.25, column sample CM-A produced a load-end displacement curve distinctive of a typical short column response to compressive loading, resulting in a brittle mode of failure. On the other hand, CM-B exhibited a less typical load-end displacement curve, indicating that localised crushing prior to failure could have cushioned the sample's failure, albeit achieving a similar result to that of sample CM-A.

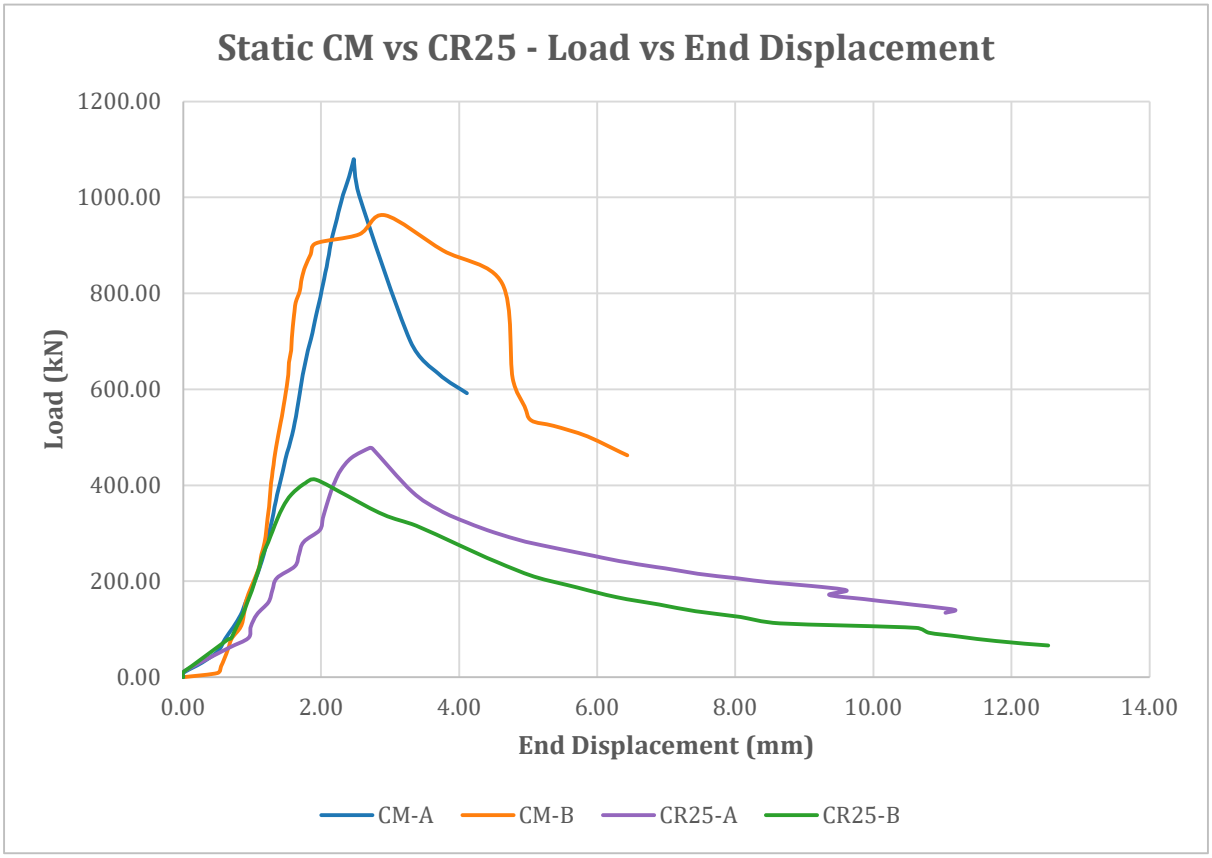

Figure 5.25: Static short column compressive test displacement curves

Both CR25 column samples exhibited a ductile failure response in their load-end displacement curves, which is indicative of the addition of rubber particles within the

concrete specimens. While the mean ultimate compressive load reduced by 56.39% relative to the control counterparts, the achieved ductile failure mode was deemed to be more advantageous in seismic scenarios. This is because failure occurred progressively over an extended displacement range rather than abruptly (brittle), which in turn provided an enhanced deformation capacity and a more gradual loss of load-bearing resistance. Such behaviour would be considered desirable under seismic loading in a real-life scenario, as it allows for energy dissipation and offers greater warning prior to collapse, thereby enhancing overall structural resilience and occupant safety.

5.6 Cyclic Short Column Compressive Strength Tests

5.6.1 Test Results

Table 5.12 shows the static compressive strengths of all four reinforced concrete short column samples after 28 days from casting.

Table 5.12: Cyclic short column compressive strength results

Sample Type	Sample Tested	Time (s)	LVDT 1 (mm)	Comp. Steel Strain (µm/m)	Comp. Concrete Strain (µm/m)	Load (kN)	Mean Ultimate Load (W_{ULT})
Control Column	CM-A-5	7924.20	2.12	-1465.90	-719.20	1153.90	926.20
Control Column	CM-B-10	5346.20	2.31	-1030.50	-73.00	698.50	
Rubberised Column	CR25-A-5	2616.40	2.14	-786.10	-833.60	400.60	355.80
Rubberised Column	CR25-B-10	4665.00	2.20	-604.40	-943.70	311.00	

The control columns (CM) failed with the highest compressive load, recording a mean ultimate compressive load of 926.20kN. The 25% crumb rubber columns (CR25) failed with a mean ultimate compressive load of 355.80kN, recording a compressive strength decrease of 61.58% from the CM column samples. This indicates a higher strength reduction than the static compressive strength test counterparts (56.39%). As may be seen in Figure 5.26, CR25 suffered a higher decrease in compressive strength capacity when subjected to cyclic loading as opposed to CM. This corresponds to the flexural strength test counterparts, where CR25 also suffered greater strength reductions than CM:

- CM short column samples – Approximately 9.28% strength reduction
- CR25 short column samples – Approximately 20.08% strength reduction

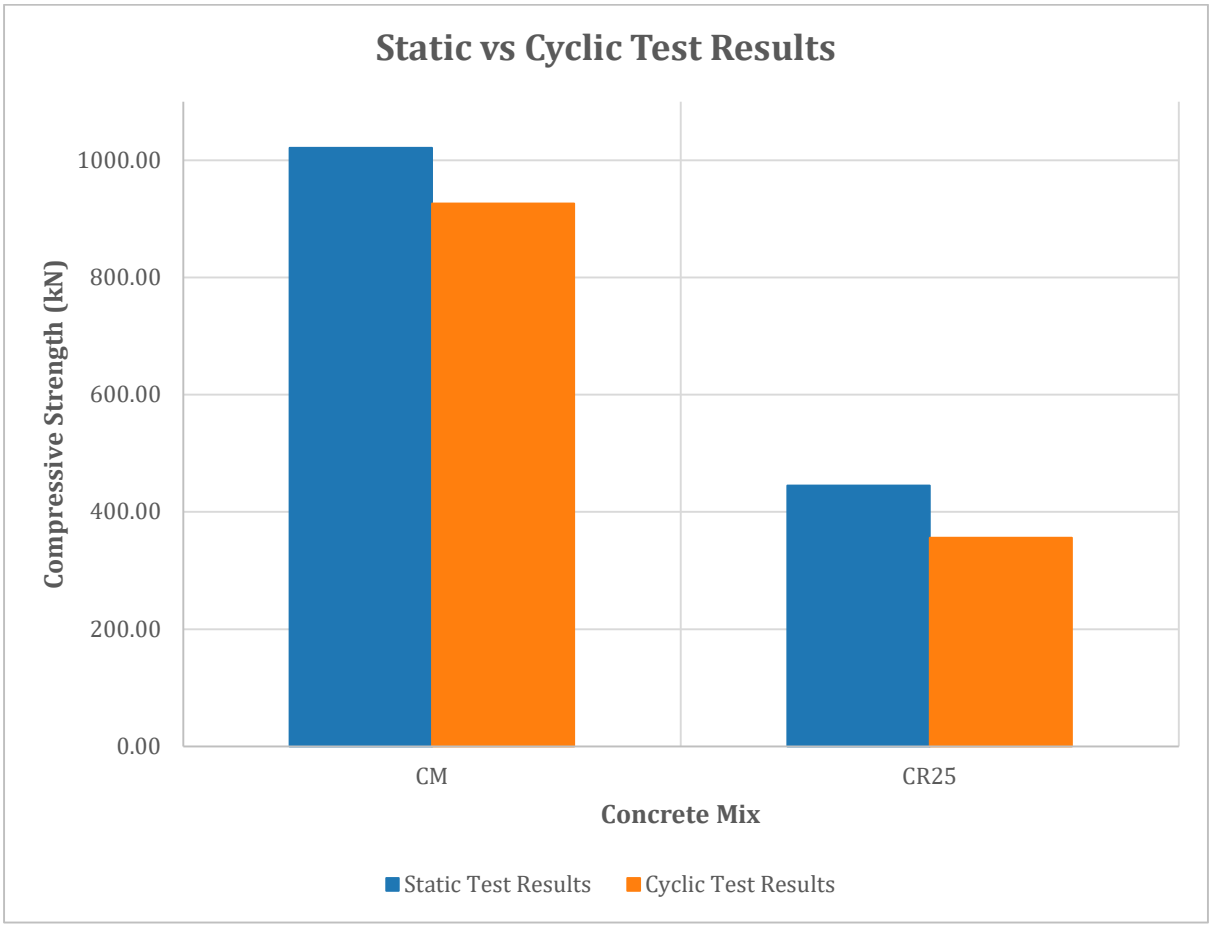

Figure 5.26: Static vs cyclic mean ultimate loads

Table 5.13 depicts how many cycles each column sample underwent during testing, with the last cycle indicating the failure cycle for that sample. One may notice that CM-A-5 managed to reach 100%.W_{ult} of the static ultimate load. This result was considered

to be irregular, since it somehow managed to bypass the ultimate load achieved in static testing, with total failure arriving at approximately 1153.90kN, while increasing the number of cycles to ten (CM-B-10) led to more realistic results, with the sample failing immediately after reaching the 70%.W_{ult} region. This indicates that the sample undergoing five cycles per load increment (CM-A-5) managed to retain full material stiffness relative to its static counterparts, while the sample undergoing ten cycles per load increment (CM-B-10) lost stiffness prematurely.

Meanwhile, the CR25 column samples failed in the 70%.W_{ult} - 90%.W_{ult} region. This indicates that CR25 endured accelerated stiffness degradation and crack propagation as loading increased in comparison to CM. This behaviour is consistent with the known effects of crumb rubber incorporation in concrete, which reduces peak strength, but increases overall deformability and energy dissipation. Under high cyclic stress levels, the reduced tensile stiffness of the rubberised concrete led to faster structural degradation and premature loss regarding load-carrying capacity relative to CM.

Table 5.13: Number of cycles per sample

Sample	10% x W_{ULT}	30% x W_{ULT}	50% x W_{ULT}	70% x W_{ULT}	90% x W_{ULT}	W_{ULT} Static Test
CM-A-5	5	5	5	5	5	5
CM-B-10	10	10	10	1	-	-
CR25-A-5	5	5	5	5	1	-
CR25-B-10	10	10	10	10	-	-

5.6.2 Cyclic Short Column Compressive Strength Tests – Observations

5.6.2.1 Control Short Columns (CM)

Figure 5.27 showcases the failure mode presented by both CM-A-5 and CM-B-10 control samples, which exhibited varying failure modes from one another.

Specimen CM-A-5 exhibited compressive failure typical to that presented in conventional reinforced concrete short columns. The primary mode of failure came in the form of concrete crushing within the column body, typical of reinforced short columns subjected to concentric compressive loading. Cracks were first observed in the central regions of the column height, which eventually progressed outwards. As loading increased, vertical splitting cracks developed along the column faces, extending along the columns' height. Prior to failure, these vertical cracks became

more pronounced, and the concrete cover began to spall towards the column's mid-height. Column failure remained governed by material crushing rather than instability, confirming that CM-A-5 behaved in a brittle manner, and that the observed response was representative of compressive concrete failure.

In contrast, specimen CM-B-10 exhibited a more ductile compressive failure mode. Failure developed progressively, with wider and more distributed vertical splitting cracks forming along the column faces prior to crushing. Concrete spalling occurred gradually relative to CM-A-5, indicating an increased ability of the specimen to accommodate deformation before failure.

Overall, the cyclic compression tests performed on CM short column samples demonstrated that even for conventional concrete columns, the mode of failure may vary from brittle to more ductile depending on the extent of cyclic loading, implying that the number of cycles endured by CM columns affects their behaviour and failure mechanisms. It must be said that an increase in the number of cycles would have been more ideal in a laboratory scenario. Like the cyclic flexural tests, the total number of cycles applied to each specimen was constrained by practical time considerations, requiring the tests to be completed within a feasible laboratory timeframe. This implies that increasing the number of cycles per load increment would build on the observations and results discussed above.

Figure 5.27: CM short column failure

5.6.2.2 25% Crumb Rubber Short Columns (CR25)

Figure 5.28 showcases the failure mode presented by both CR25-A-5 and CR25-B-10 samples, which exhibited similar modes of failure their static counterparts.

Once again, concrete crushing of the concrete body was predominant, making the CR25 samples consistent with the behaviour of reinforced concrete short columns subjected to predominantly concentric compressive loading. However, in comparison with their control counterparts, both CR25 column samples exhibited a more distributed and ductile cracking response prior to total failure. The main difference between cyclic and static testing was the peak load at which cracks began to propagate, since both cyclic CR25 column samples experienced this at lower peak loads than the static CR25 column samples.

Figure 5.28: CR25 short column failure

5.6.3 Cyclic Short Column Compressive Strength Tests – End Displacement

Figure 5.29 showcases the failure mode presented by both CM-A-5 and CM-B-10 control samples, which exhibited varying failure modes from one another. As mentioned previously, CM-A-5 presented irregular results since it achieved a higher ultimate load than its static counterparts. This indicates that after enduring thirty cycles of increasing load increments, it still achieved a higher compressive strength capacity than an identical sample undergoing static loading, implying that the addition of cyclic action did not affect the sample's stiffness capacity. CM-A-5 also failed in a brittle manner.

On the other hand, CM-B-10 failed after thirty cycles, as soon as it reached 70%.W_{ult}. As may be seen in Figure 5.29, the increased number of cycles at lower stress levels affected the sample's displacement, particularly when increasing the maximum load inflicted on the sample when entering the successive set of cycles. In other words, as load increased, overall displacement increased at a higher rate than CM-A-5, as may be seen by the gradient of the curve in some cases. This sample also failed in a very ductile manner, especially when considering the brittle nature of CM-A-5. Figure 5.29 shows that failure in CM-B-10 occurred progressively over an extended displacement range, even outperforming CR25-B-10 in this regard.

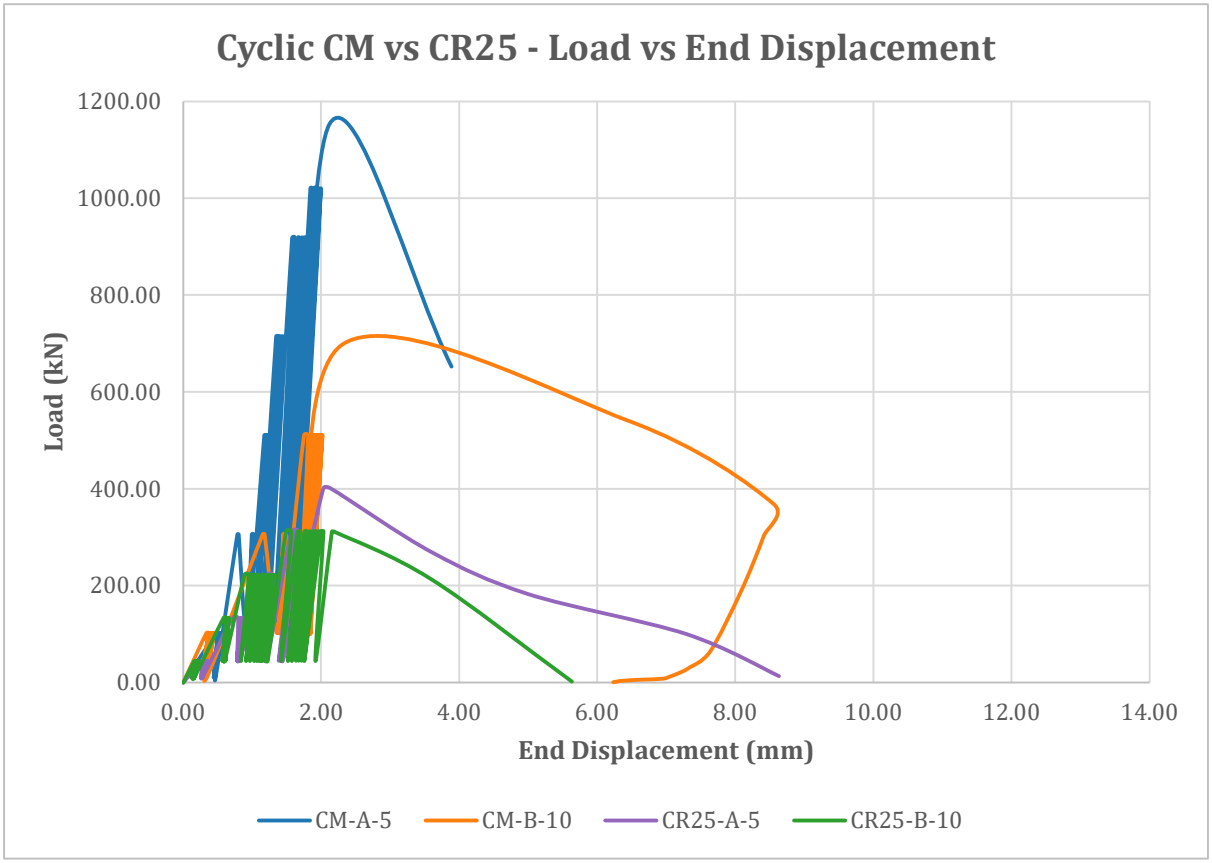

Figure 5.29: Cyclic short column compressive test displacement curves

When comparing CR25-A-5 and CR25-B-10 to their respective static counterparts, one may notice that both cyclic specimens failed with a lower peak load than the static specimens, particularly CR25-B-10. This indicates that the addition of cycles had an effect on material stiffness and degradation similar to the way the flexural beam samples were affected in the cyclic four-point flexural strength tests. Once again, both cyclic column samples behaved in a ductile manner which may be seen by the extended displacement range produced upon failure of each specimen. However, in

CR25-B-10's case this displacement range was generally shorter, even more so than CM-B-10.

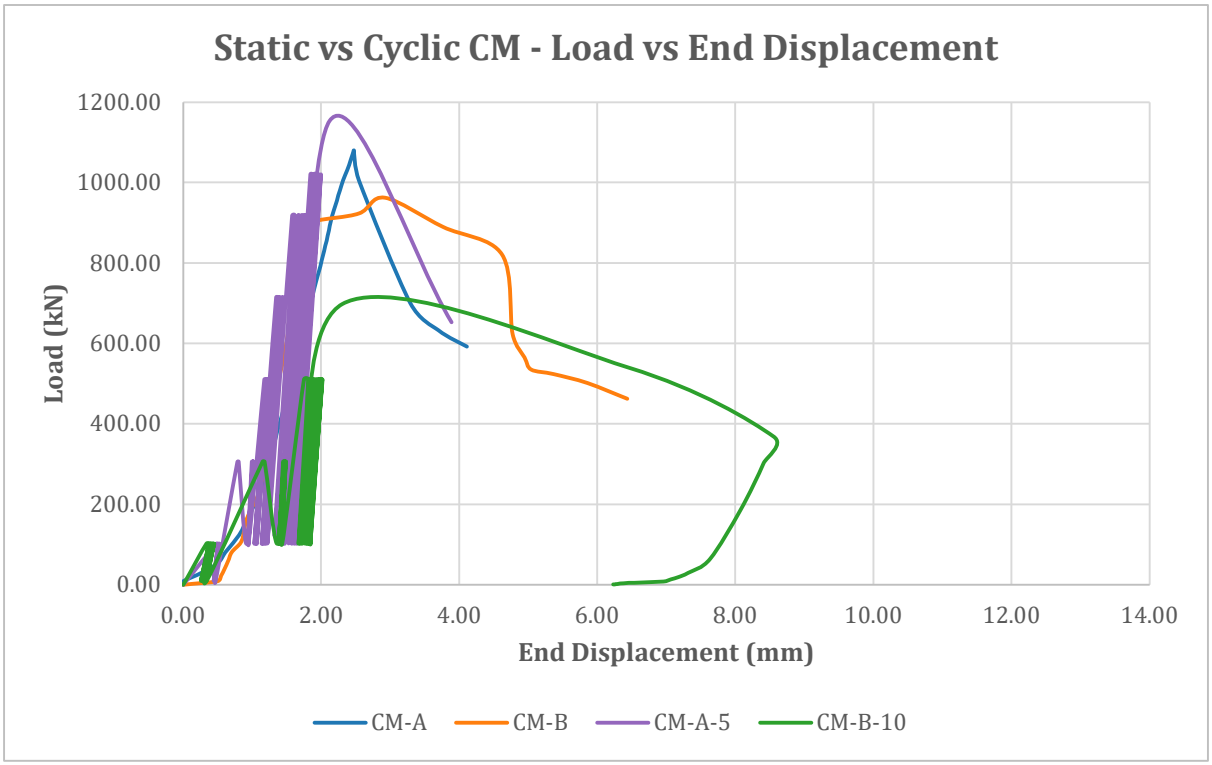

Figure 5.30: Static vs cyclic CM short column compressive test displacement

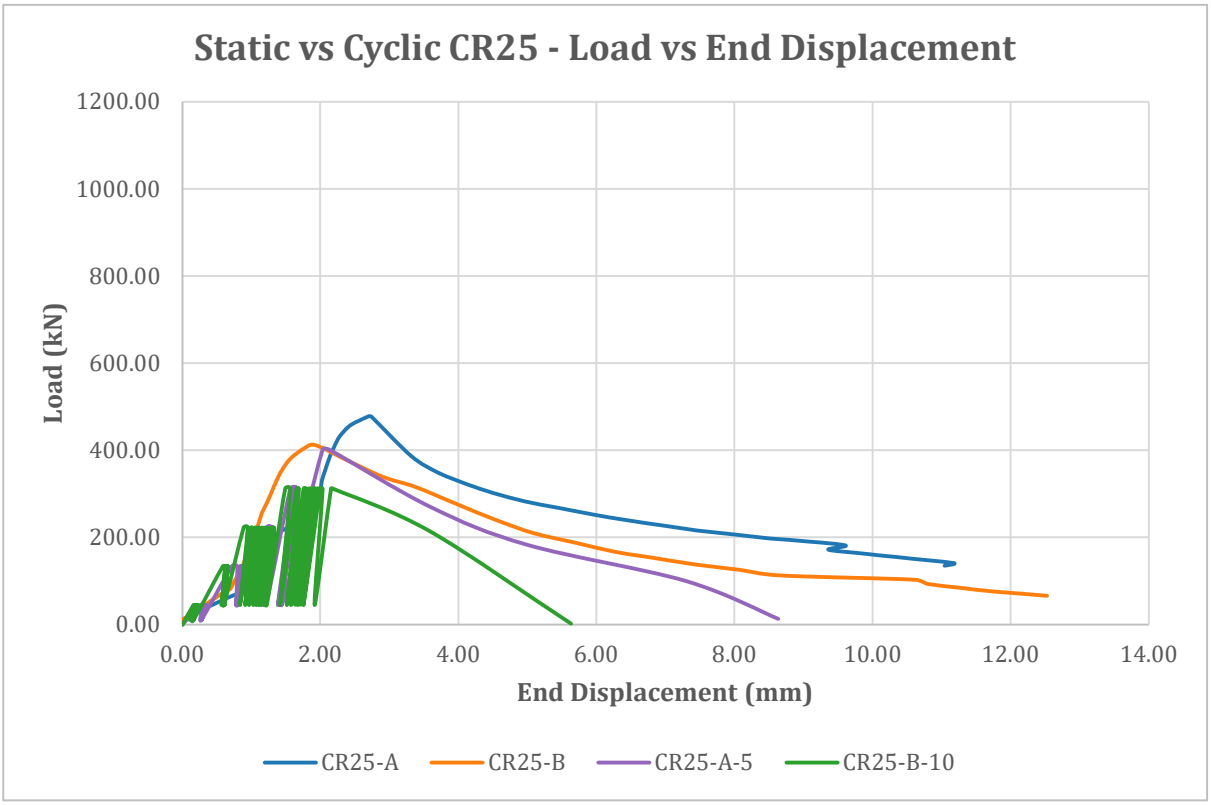

Figure 5.31: Static vs cyclic CR25 short column compressive test

6. Conclusions and Suggestions for Future Research Work

6.1 Overview

Following the research studies conducted by Scicluna (2010), Magro (2011), and Abdilla (2012), it was interesting to further investigate the properties of rubberised concrete, with particular attention being given to the cyclic performance and suitability of rubberised concrete in cyclic scenarios, typical of buildings subjected to cyclic loading. With particular emphasis on the findings of Magro (2011), this research study focused on a concrete design mix incorporating 25% crumb rubber replacement of fine aggregate (CR25), identified in previous research as the most structurally viable rubberised concrete design mix.

An experimental programme comprising of static concrete cube compressive strength tests, static and cyclic four-point loading flexural tests on reinforced concrete beams, and static and cyclic compressive strength tests on short reinforced concrete columns, was undertaken in this research study. The primary objective of this dissertation, therefore, was to evaluate the effects of rubber aggregate replacement on structural strength, stiffness, ductility, deformation capacity, and failure behaviour, particularly in scenarios representative of cyclic and/or seismic-type loading.

It is considered that the aims and objectives highlighted in Chapter 1 of this dissertation were successfully achieved, allowing for a more comprehensive assessment of the potential role of rubberised concrete in seismically resilient structural applications.

6.2 Conclusions

6.2.1 Experimental Methodology

The experimental methodology adopted in this research study was kept consistent with that used by Magro (2011) wherever possible, ensuring direct comparability between her results and the test results obtained in this research study. This included all material properties, design mix proportions, specimen dimensions (cubes and beams), and experimental testing procedures. These test parameters were

maintained, as closely as possible, with unavoidable variations being solely limited to aggregate sourcing and laboratory constraints.

The decision to focus solely on CR25 as the rubberised design mix representative with 25% crumb rubber replacement of fine aggregate was validated by previous research findings from all three afore-mentioned researchers, which consistently identified this particular design mix as the best-balanced concrete mix with respect to structural performance, deformation capacity and energy dissipation. Furthermore, the use of both static and cycling testing methods (as compared to the static testing only used in the three afore-mentioned research studies) allowed for a more realistic representation of structural performance for buildings subjected to seismic loading, thereby addressing a key research gap identified in earlier dissertations.

6.2.2 Test Results

6.2.2.1 Compressive Behaviour of Specimens

The results obtained from both cube and short column compressive strength tests confirm that CR25 exhibits a significant reduction in compressive strength relative to conventional concrete used in construction. However, this strength reduction is not consistent with the findings of Magro (2011), who documented that the CR25 test specimens experienced a small strength loss among all rubberised mixes investigated in her case. Under cyclic compressive conditions, rubberised concrete columns tested in this dissertation exhibited:

- Increased deformation capacity,
- Gradual stiffness degradation per cycle,
- More ductile behaviour and failure relative to the brittle failure modes observed in CM samples.

These observations align with the conclusions from the research study carried out by Magro (2011) regarding enhanced post-peak behaviour and deformation tolerance in rubberised concrete elements.

6.2.2.2 Flexural Behaviour of Beam Specimens

Similar to the cube and short column specimens, static flexural beam testing demonstrated that the CR25 beam specimens failed at lower ultimate loads relative to their CM Control Mix counterparts without any crumb rubber replacement of fine aggregate. Nevertheless, the overall flexural response observed was adequate, aligning with the corresponding conclusions made by Magro's (2011). Furthermore, the overall cracking patterns and failure modes of the CR25 beam specimens were comparable to those observed for the corresponding CM beams tested. Under cyclic flexural conditions, rubberised concrete beams exhibited:

- Earlier onset of stiffness degradation at higher stress cycles
- Improved crack closure when unloaded
- Reduced residual deflections at moderate load levels (≤ 70%.W_{ult}).

It was deduced that the elastic nature of crumb rubber particles contributed to enhanced shape recovery as well as improving the beams' ability to reverse deformation originating from cyclic loading, which was also briefly highlighted by Magro (2011).

6.2.2.3 Cyclic Performance and Ductility

A key observation throughout this study was how the introduction of cyclic loading highlighted the behavioural differences between conventional concrete and rubberised concrete structural elements. While the conventional concrete test specimens exhibited higher peak strengths, the rubberised concrete test specimens outperformed the former with regards to ductility, energy dissipation, and crack closure. Failure of the rubberised concrete test specimens was deemed to be progressive, with failure extending progressively over a longer displacement range. On the other hand, conventional concrete test specimens exhibited sudden and brittle failure responses. The ductile properties exhibited by the rubberised test specimens under cyclic loading is particularly relevant to seismic engineering applications, where deformation capacity and energy dissipation are critical design considerations.

6.3 Potential Use

Based on the conclusions made in this study, the 25% crumb rubber replacement concrete demonstrates limited potential for structural scenarios prioritising member strength. On the other hand, however, the 25% crumb rubber replacement concrete poses significant potential in applications prioritising ductility, energy dissipation, and deformation capacity.

In this respect, therefore, it may be concluded that potential applications of rubberised concrete include:

- Structural elements in seismic regions
- Bridge decks and structural components subjected to cyclic rolling loads such as ongoing traffic
- Vibration-sensitive structures
- Retrofitting and strengthening applications where energy absorption is essential.

The above-mentioned potential applications also align with the observations made by Magro (2011), in the sense that rubberised concrete should be regarded as a specialised structural material, rather than a direct replacement for conventional concrete in construction applications.

6.4 Suggestions for Future Research Work

While this research study provides valuable insights into the structural behaviour of rubberised concrete subjected to static or cyclic flexural or compressive loading, several other areas of research interest warrant further investigation:

1. **Extended Cyclic Testing** – Unfortunately, the number of cycles used in this dissertation had to be limited due to time constraints associated with long-term access to laboratory equipment, as mentioned several times throughout this dissertation, extended cyclic testing would help simulate better seismic and fatigue-type loading. This would entail producing longer cycles, as well as increasing the number of cycles induced on specimens per load increment.

2. **Durability and Long-Term Performance** – Creep, shrinkage, and long-term fatigue behaviour of rubberised concrete structural members under sustained cyclic loading would also require additional investigations.
3. **Bond and Interface Behaviour between Rubberised Concrete and Steel Reinforcement** – It would be interesting to investigate how rubberised concrete bonds with steel reinforcement in comparison with conventional concrete as well as potential ways to improve this bonding.
4. **Surface Treatment of Rubber Aggregates** – This would entail the addition of chemical and/or mechanical surface treatments to rubber particles (e.g. alkaline washing, cement coating, plasma treatment, etc.) in order to improve the bond between the rubber replacement aggregate and the cementitious matrix, which was deemed to be weak during this research study. In this way, improved mechanical bonding may mitigate strength losses experienced by rubberised concrete structural elements.

Bibliography

1. **Abdelaleem, A., Moawad, M., El-Emam, H., Salim, H. & Sallam, H.E.M.** (2024). Long term behavior of rubberized concrete under static and dynamic loads, *Case Studies in Construction Materials*, Volume 20.

2. **Abdilla, R.** (2012). *Shear Strength Assessment of Rubberised Concrete Beams*, University of Malta.

3. **ACI 374.1.** Acceptance Criteria for Moment Frames Based on Structural Testing, American Concrete Institute.

4. **BS EN 12390-3** (2019). *Testing hardened concrete – Part 3: Compressive strength of test specimens*, BSI Standards Publication.

5. **BS EN 12390-5** (2019). *Testing hardened concrete – Part 5: Flexural strength of test specimens*, BSI Standards Publication.

6. **BS EN 206** (2013+A2:2021). *Concrete – Specification, performance, production and conformity*, BSI Standards Publication.

7. **Caines, R., Kew, H. W., & Kenny, M. J.** (2004). *The use of recycled rubber tyres in concrete construction*.

8. **Eldin, N. N., & Senouci, A. B.** (1994). 'Measurement and prediction of the strength of rubberized concrete', *Cement and Concrete Composites*, 16(4).

9. **El-Gammal, A., Abdel-Gawad, A.K., El-Sherbini, Y. & Shalaby, A.** (2010). 'Compressive Strength of Concrete Utilizing Waste Tire Rubber', *Journal of Emerging Trends in Engineering and Applied Sciences*, pp. 96–99.

10. **Elghazouli, A.Y., Mujdeci, A., Bompa, D.V. & Guo, Y.T.** (2022). 'Experimental cyclic response of rubberised concrete-filled steel tubes', *Journal of Constructional Steel Research*, Volume 199.
11. **EN 1992-1-1** (2004). *Eurocode 2: Design of concrete structures – General rules and rules for buildings*.

12. **Kew, H.Y. & Kenny, M.J.** (2009). Developing viable products using recycled rubber tyres in concrete. In *Excellence in Concrete Construction through Innovation*, pp. 523–531, Taylor & Francis Group.

13. **Khorami, M., Ganjian, E., & Vafall, A.** (2007). 'Mechanical properties of concrete with waste tire rubbers as coarse aggregate', *Proceedings of the International Conference on Sustainable Construction Materials and Technologies*, Milwaukee, CBU, pp. 95–90.

14. **Langer, W. H.** (1988). *Natural Aggregates of the Conterminous United States*, U.S. Geological Survey Bulletin 1594.

15. **Magro, J. M.** (2011). *The Flexural Strength Assessment of Reinforced Concrete Beams using Rubberised Concrete*, University of Malta.

16. **Masvroulidou, M., & Figueiredo, J.** (2007). ‘Discarded tyre rubber as concrete aggregate: A possible outlet for used tyres’, *Global Nest Journal*, 12, pp. 359–367.

17. **Mehta, P. K., & Monteiro, P. J. M.** (2014). *Concrete: Microstructure, properties, and materials* (4th ed.), McGraw-Hill Education.

18. **Mohamed Amin, M. A., et al.** (2022). ‘Mechanical Behaviour of Concrete Containing Crumb Rubber as Partial Fine Aggregates Replacement’, *IOP Conference Series: Earth and Environmental Science*, 1022, 012043.

19. **Moore, P. & Booth, G.** (2015). *The Welding Engineer’s Guide to Fracture and Fatigue*, Woodhead Publishing, pp. 11–21.

20. **Nehdi, M., & Khan, A.** (2001). ‘Cementitious composites containing recycled tire rubber: An overview of engineering properties and potential applications’, *Cement, Concrete, and Aggregates*.

21. **Neville, A. M.** (2011). *Properties of concrete* (5th ed.), Pearson Education.

22. **Reda Taha, M. M., El-Dleb, A. S., Abd El-Wahab, M. A., & Abdel-Hameed, M. E.** (2008). ‘Mechanical, fracture, and microstructural investigations of rubber concrete’, *Journal of Materials in Civil Engineering*.

23. **Scicluna, S.** (2010). *The use of recycled waste tyre rubber in concrete*, University of Malta.

24. **Scott, E.** (2022). 'Tyres discarded in Amazonas need to be recycled in Paraná', *Tyre and Rubber Recycling*.

25. **Seifali Abbas-Abadi, M., Kusenberg, M., Mohamadzadeh Shirazi, H., Goshayeshi, B., & Van Geem, K.** (2022). 'Towards full recyclability of end-of-life tires: Challenges and opportunities', *Journal of Cleaner Production*, 374.

26. **Siddique, R., & Nehdi, M.** (2002). 'Properties of concrete containing scrap tire rubber – An overview'.

27. **Thomas, B. S., Gupta, R. C., Panicker, V. J., & Yang, J.** (2016). 'Recycling of waste tire rubber as aggregate in concrete: Durability-related performance', *Journal of Cleaner Production*, 112, pp. 504–513.

28. **Toutanji, H.** (1996). 'The Use of Rubber Tire Particles in Concrete to Replace Mineral Aggregates', *Cement and Concrete Composites*, pp. 135–139.

29. **Wang, J., Guo, Z., Zhang, P., Yuan, Q., & Guan, Q.** (2020). 'Fracture properties of rubberized concrete under different temperature and humidity conditions based on digital image correlation technique', *Journal of Cleaner Production*, 276.

30. **Xu, B., Bompa, D. V., & Elghazouli, A. Y.** (2020). 'Cyclic stress–strain rate-dependent response of rubberised concrete', *Construction and Building Materials*, 254.

31. **Xue, J., & Shinozuka, M.** (2013). 'Rubberized concrete: A green structural material with enhanced energy-dissipation capability', *Construction and Building Materials*, 42, pp. 196–264.

32. **Zongping, C., Jinjun, X., Yuliang, C., & Eric, M. L.** (2016). 'Recycling and reuse of construction and demolition waste in concrete-filled steel tubes: A review', *Construction and Building Materials*, 126.

Appendix 1: Material Characteristics

Control Concrete Mix Design

The DoE Design Method for conventional concrete mixes

Table A1.1: Control Design Mix

Stage 1	Item	Values
1	1.1 Characteristic Strength	25 N/mm^2 @ 28 days
	1.2 Target Mean Strength	33.26 N/mm^2
	1.3 Cement Strength Class	42.5
	1.4 Aggregate Type: Coarse	Crushed
	1.5 Aggregate Type: Fine	Crushed
	1.6 Free Water/Cement ratio	0.55
2	2.1 Maximum Aggregate Size	20
	2.2 Free water Content	0.55
3	3.1 Cement Content	345 kg/m^3
4	4.1 Concrete Density	2219 kg/m^3
	4.2 Total Aggregate Content	1010 kg/m^3
5	5.1 Proportion of fine aggregate	40%
	5.2 Fine Aggregate Content	674 kg/m^3
	5.3 Coarse Aggregate Content	1010 kg/m^3

Table A1.2: Control Design Mix Constituents

Material	Quantities (per m^3)
Cement (kg)	345
Water(kg/ltr)	190
Fine Aggregate (kg)	674
Coarse Aggregate 5-10mm (kg)	337
Coarse Aggregate 10-20mm (kg)	673
Water-Cement Ratio	0.55

Appendix 2: Test Results

Cube Compressive Strength Test Results

Sample Type	Sample Tested	Length (mm)	Breadth (mm)	Width (mm)	Weight (Kg)
Control Cube	CM-7-A	150.65	150.81	152.77	7.10
Control Cube	CM-7-B	150.17	150.52	151.24	7.13
Control Cube	CM-7-C	150.55	150.39	152.56	7.12
Rubberised Cube	CR25-7-A	150.45	150.55	153.13	6.05
Rubberised Cube	CR25-7-B	150.33	150.54	151.65	6.02
Rubberised Cube	CR25-7-C	150.18	150.21	152.61	5.99

Sample Type	Sample Tested	Length (mm)	Breadth (mm)	Width (mm)	Weight (Kg)
Control Cube	CM-28-A	150.82	150.75	151.38	7.15
Control Cube	CM-28-B	150.59	150.10	151.18	7.12
Control Cube	CM-28-C	150.42	150.80	149.95	7.18
Rubberised Cube	CR25-28-A	150.69	150.16	153.63	6.09
Rubberised Cube	CR25-28-B	150.25	150.40	151.99	6.01
Rubberised Cube	CR25-28-C	150.43	150.10	152.46	6.01

Mix 1 - CM (control design mix)			
Testing Day	**Sample Name**	**Cube Compressive Strength (MPa)**	**Mean Cube Compressive Strength (MPa)**
7	CM-7-A	24.15	24.58
7	CM-7-B	25.28	
7	CM-7-C	24.32	
28	CM-28-A	24.00	25
28	CM-28-B	26.34	
28	CM-28-C	24.66	

Mix 2 - CR25 (25% crumb rubber design mix)			
Testing Day	**Sample Name**	**Cube Compressive Strength (MPa)**	**Mean Cube Compressive Strength (MPa)**
7	CR25-7-A	7.98	8.12
7	CR25-7-B	8.05	
7	CR25-7-C	8.32	
28	CR25-28-A	9.26	8.71
28	CR25-28-B	8.60	
28	CR25-28-C	8.26	

Table A2.1: Control & CR Design Mix Test Results

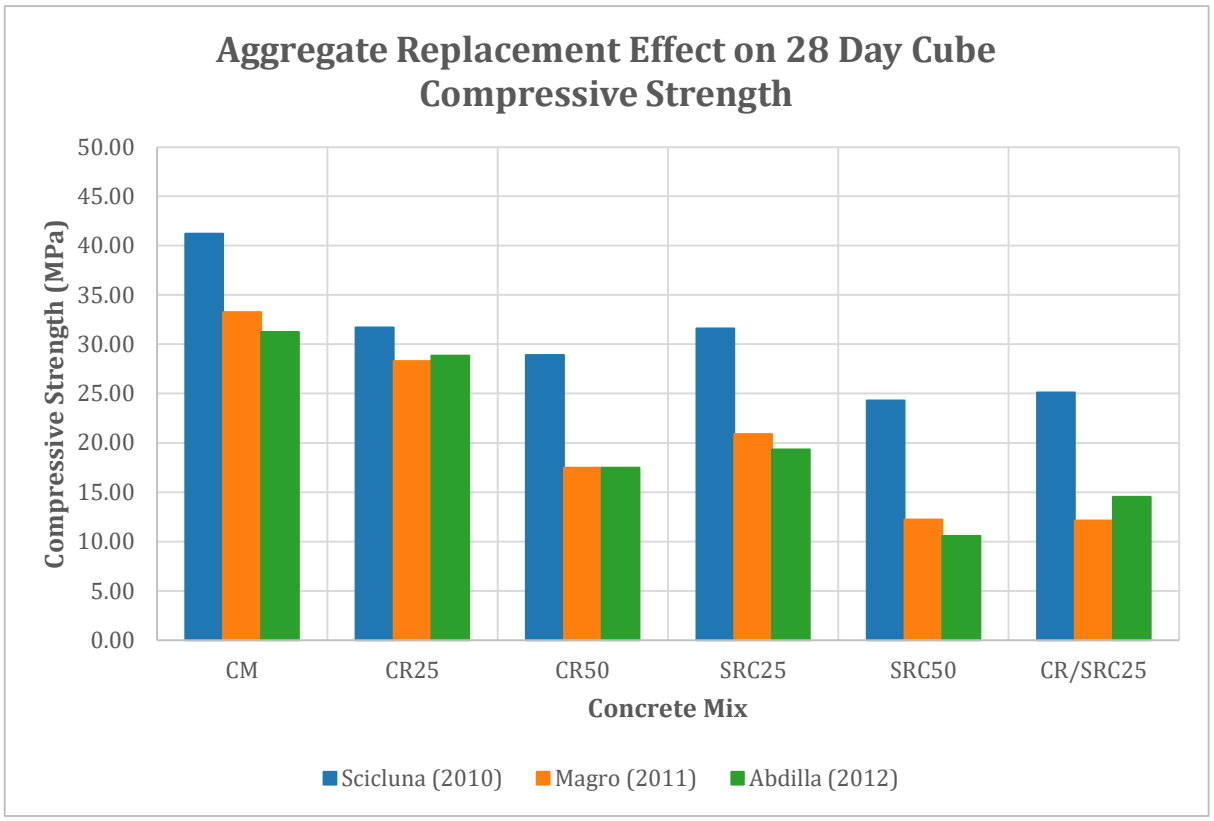

Figure A2.1: Aggregate Replacement Effect on 28 Day Cube Compressive Strength

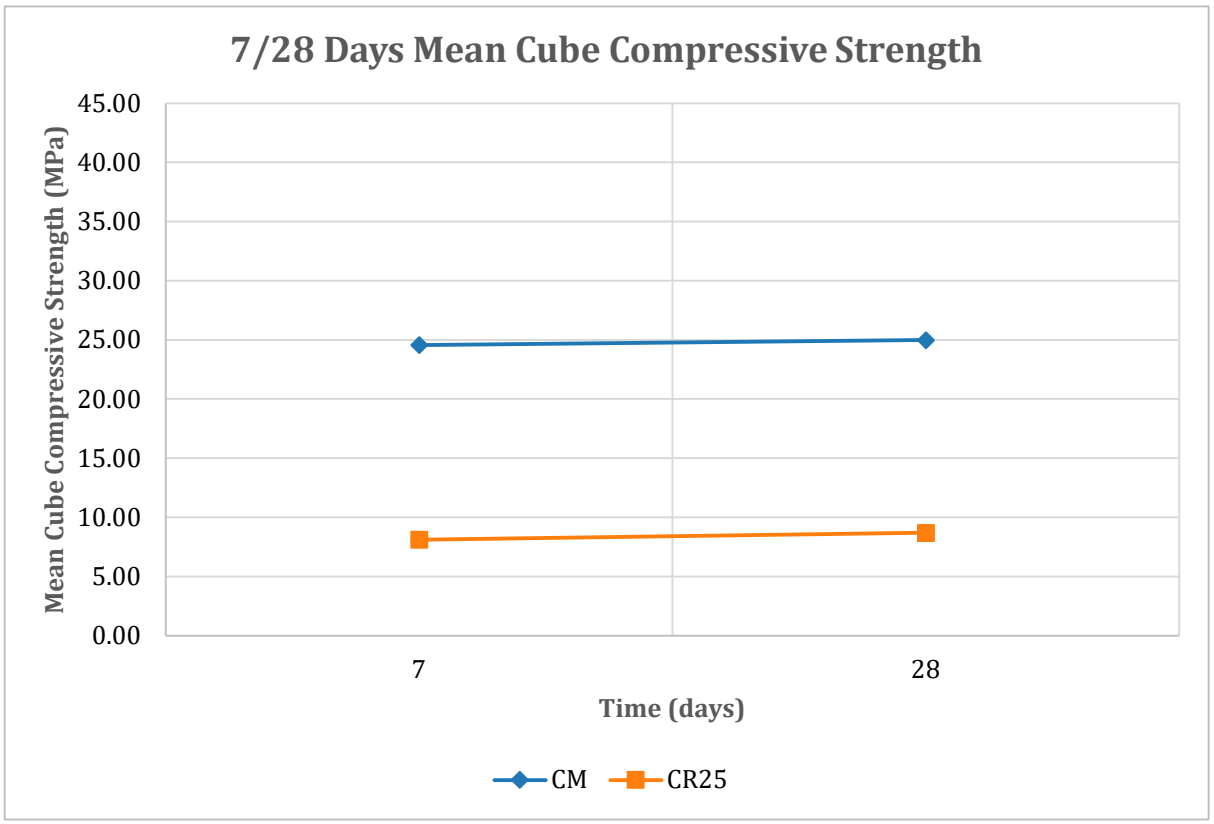

Figure A2.2: 7/28 Days Mean Cube Compressive Strength

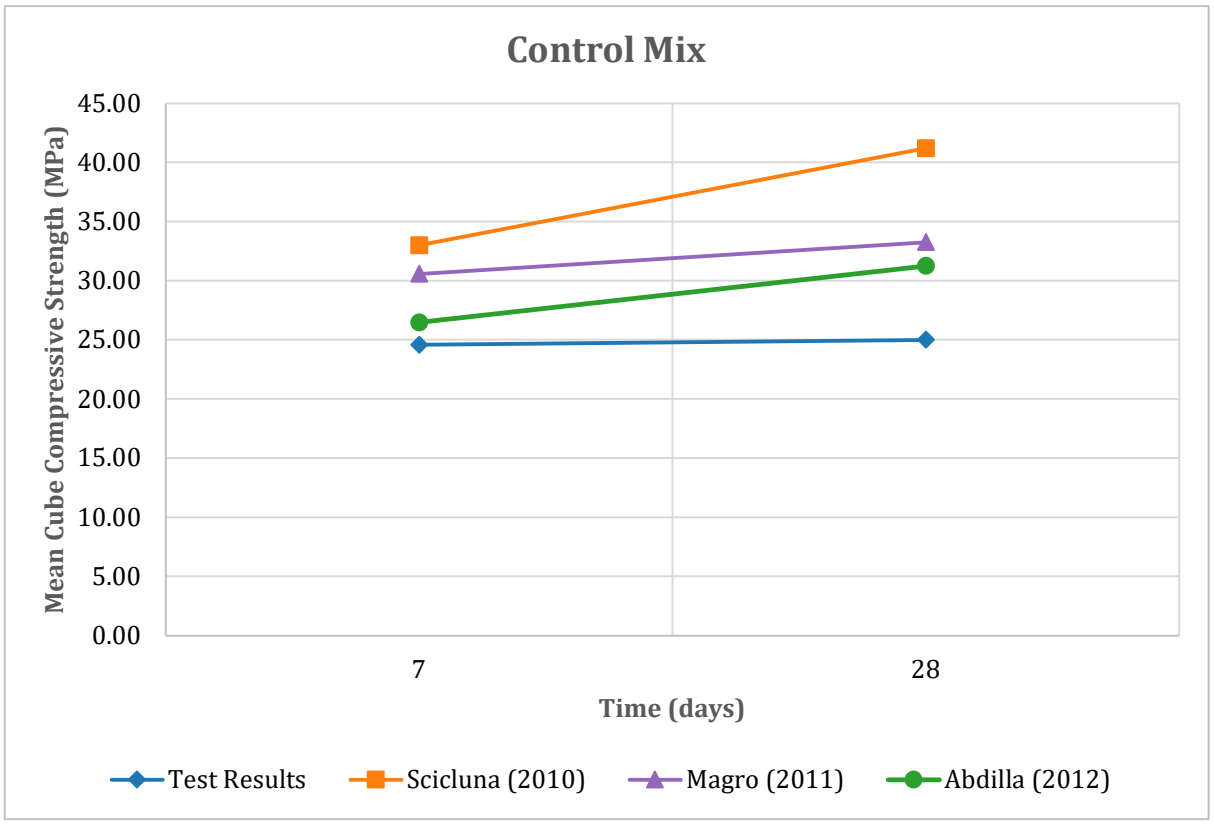

Figure A2.3: Control Design Mix Cube Mean Compressive Strengths

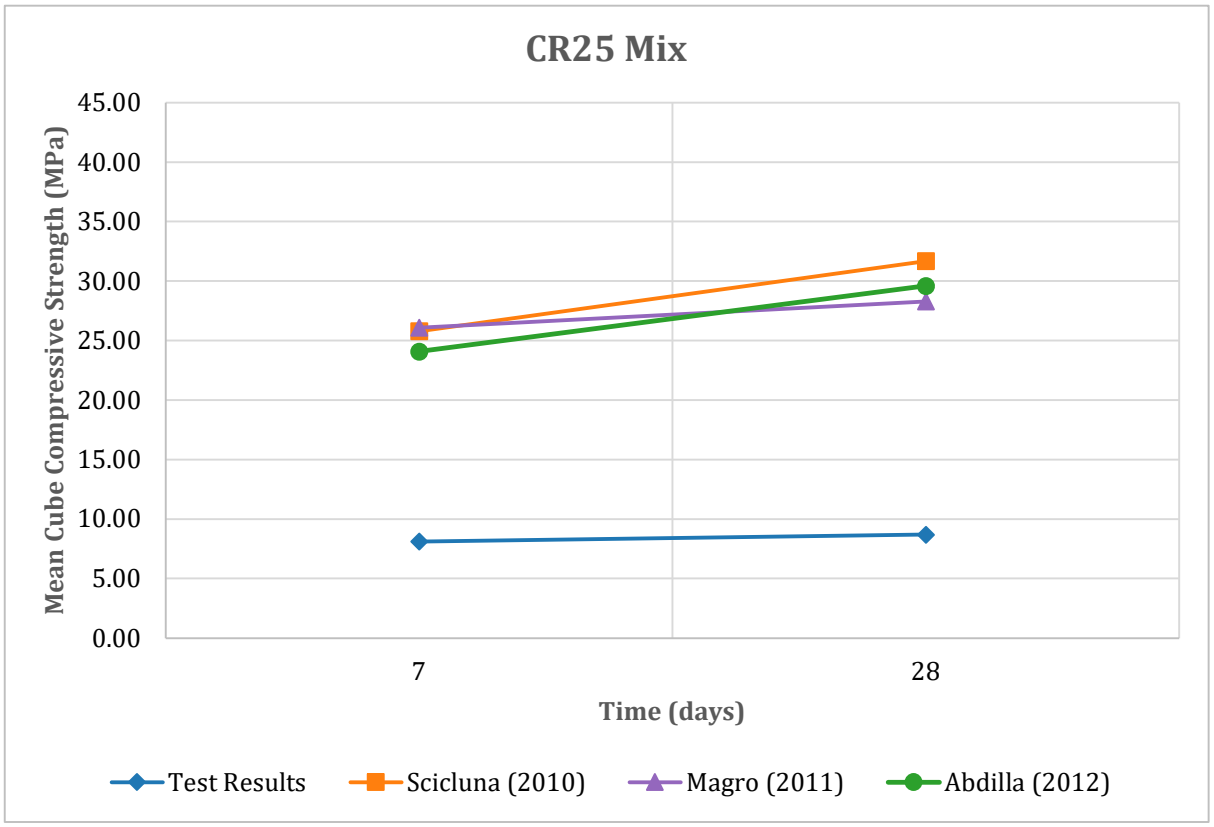

Figure A2.4: CR25 Design Mix Cube Mean Compressive Strengths

Appendix 3: Test Results

Prism Compressive and Flexural Strength Test Results

Table A3.1: Sika Mix Test Results

Sample Type	Sample Tested	Length (mm)	Breadth (mm)	Width (mm)	Weight (Kg)
Capping Mix	SIKAM-28-A	160.23	40.30	40.29	0.59
Capping Mix	SIKAM-28-B	160.15	40.19	40.06	0.59
Capping Mix	SIKAM-28-C	160.28	40.22	40.51	0.61

Mix 3 - SIKAM (sikagrout S55 mix)			
Testing Day	**Sample Name**	**Prism Compressive Strength (MPa)**	**Mean Prism Compressive Strength (MPa)**
28	SIKAM-28-A-1	88.06	89.23
28	SIKAM-28-A-2	94.09	
28	SIKAM-28-B-1	87.74	
28	SIKAM-28-B-2	84.23	
28	SIKAM-28-C-1	90.16	
28	SIKAM-28-C-2	91.12	

Mix 3 - SIKAM (sikagrout S55 mix)			
Testing Day	**Sample Name**	**Prism Flexural Strength (MPa)**	**Mean Prism Flexural Strength (MPa)**
28	SIKAM-28-A	11.10	10.47
28	SIKAM-28-B	9.54	
28	SIKAM-28-C	10.78	

Appendix 4: Four-Point Loading Flexural Beam Strength Test Results

Table A4.1:Four Point Loading Flexural Beam Strength Results

Sample Type	Sample Tested	Time (s)	Average LVDT (mm)	Compressive Concrete Strain (µm/m)	Load (kN)	Mean Ultimate Load (W_{ULT})
Control Beam	CM-A	9143.49	63.86	-0.001655	86.86	85.82
Control Beam	CM-B	9877.15	59.56	-0.002058	84.77	
Rubberised Beam	CR25-A	8274.11	65.50	-0.001359	71.63	71.95
Rubberised Beam	CR25-B	7752.11	60.50	-0.002541	72.26	

Sample Type	Sample Tested	Time (s)	Average LVDT (mm)	Compressive Concrete Strain (µm/m)	Load (kN)	Mean Ultimate Load (W_{ULT})
Control Beam	CM-A-5	5394.26	58.07	-0.001524	83.43	84.29
Control Beam	CM-B-10	9593.11	69.37	-0.003025	85.14	
Rubberised Beam	CR25-A-5	4454.16	58.89	-0.001626	69.50	67.40
Rubberised Beam	CR25-B-10	7182.41	53.18	-0.003374	65.30	

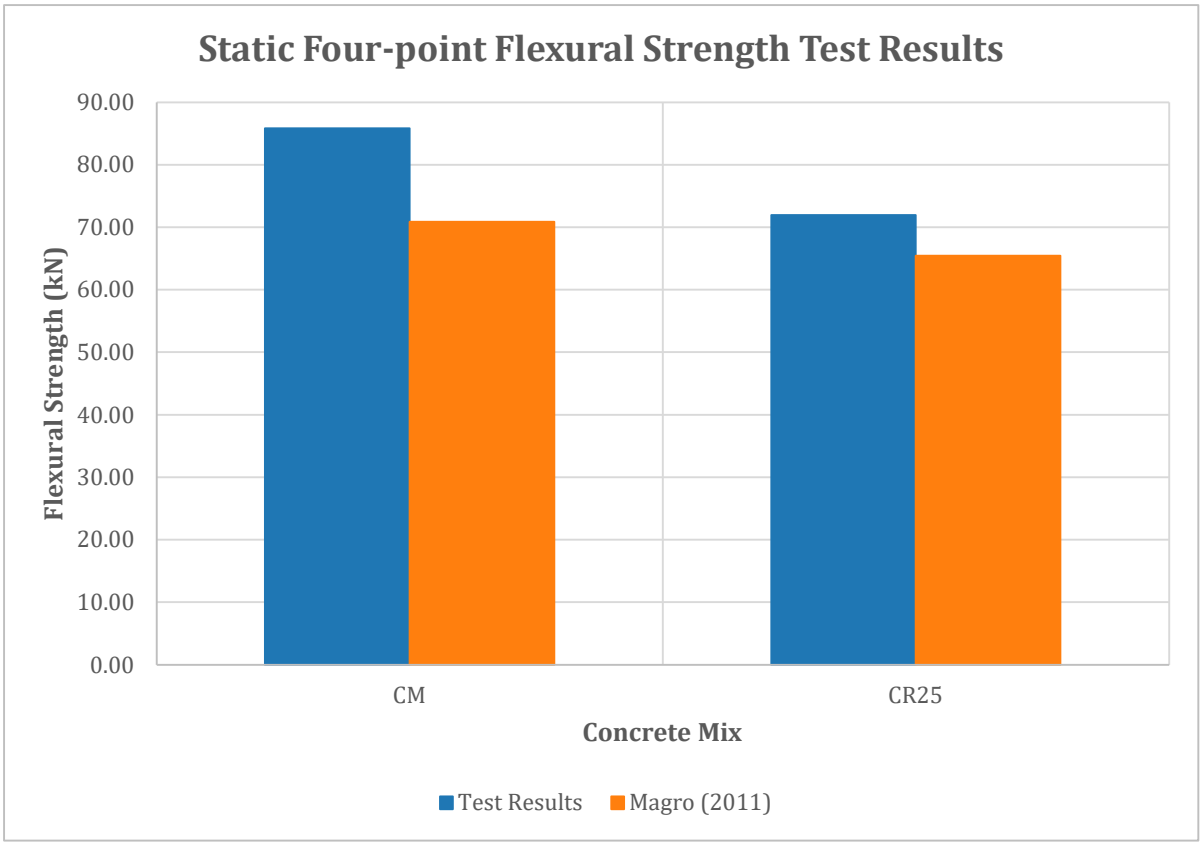

Figure A4.1: Four Point Loading Flexural Beam Strength Results - Comparison

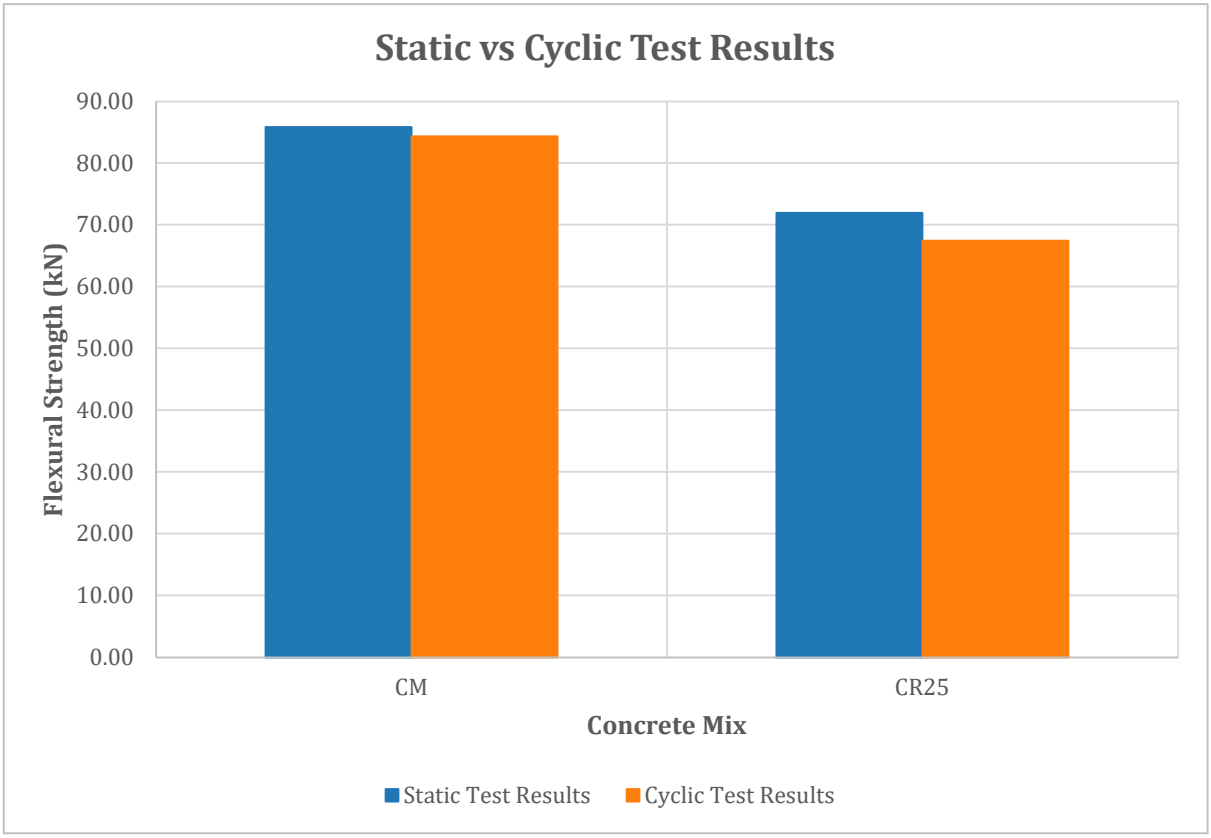

Figure A4.2: Static vs Cyclic Test Results - Comparison

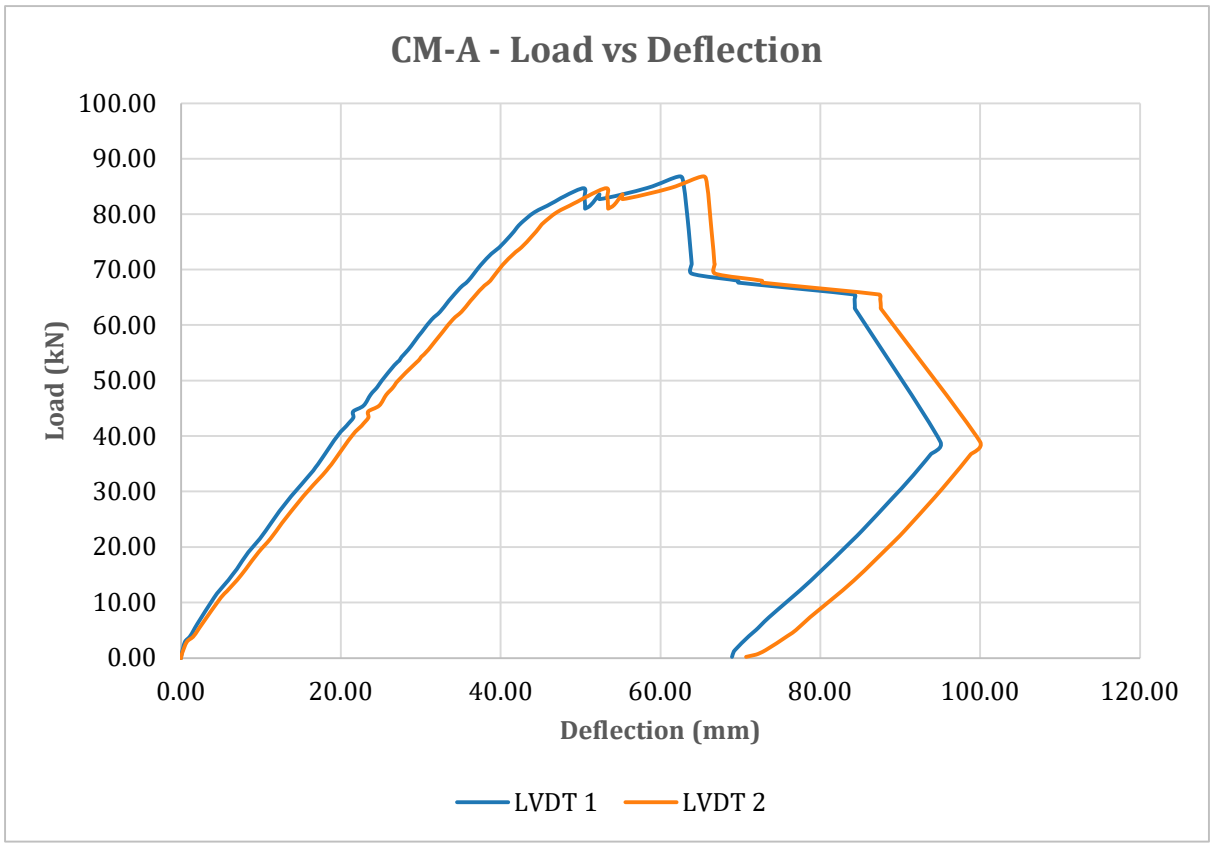

Figure A4.3: CM-A Deflection Curves

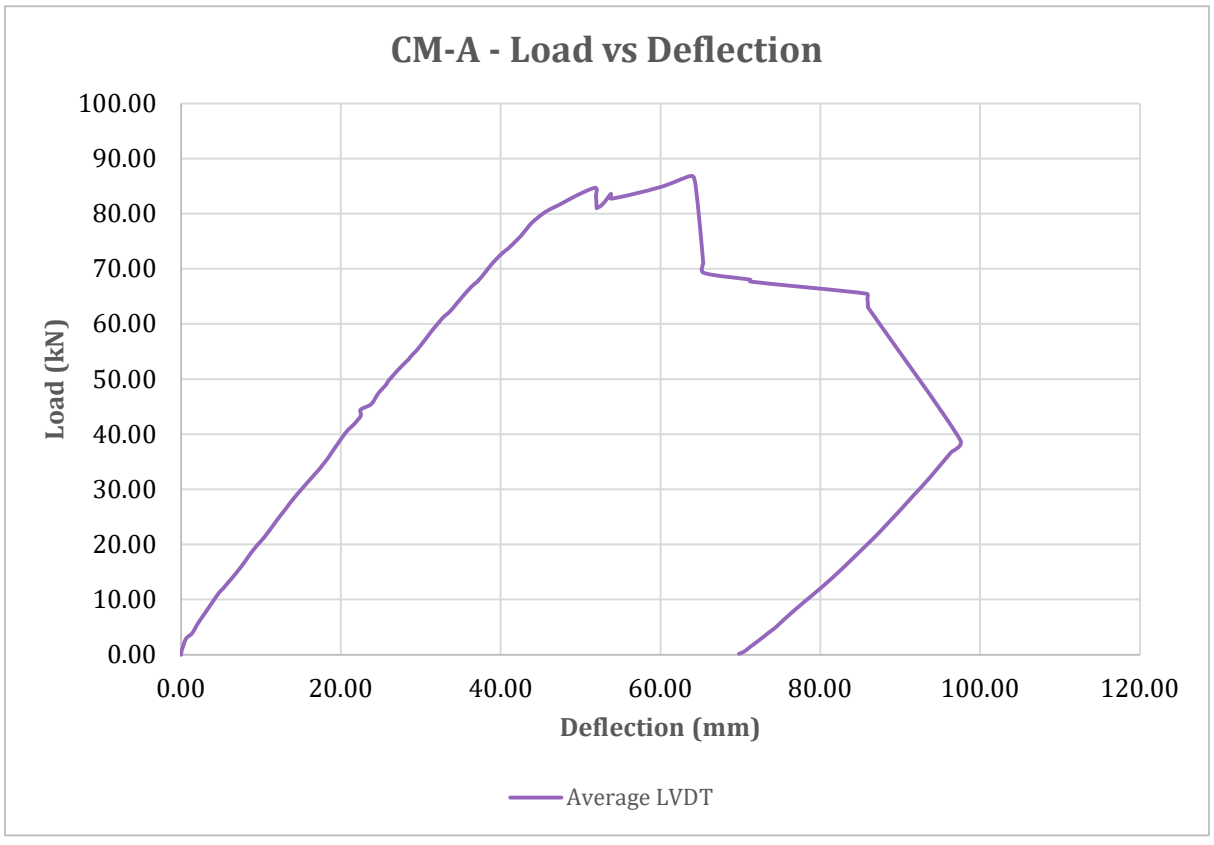

Figure A4.4: CM-A Deflection Curves - Average

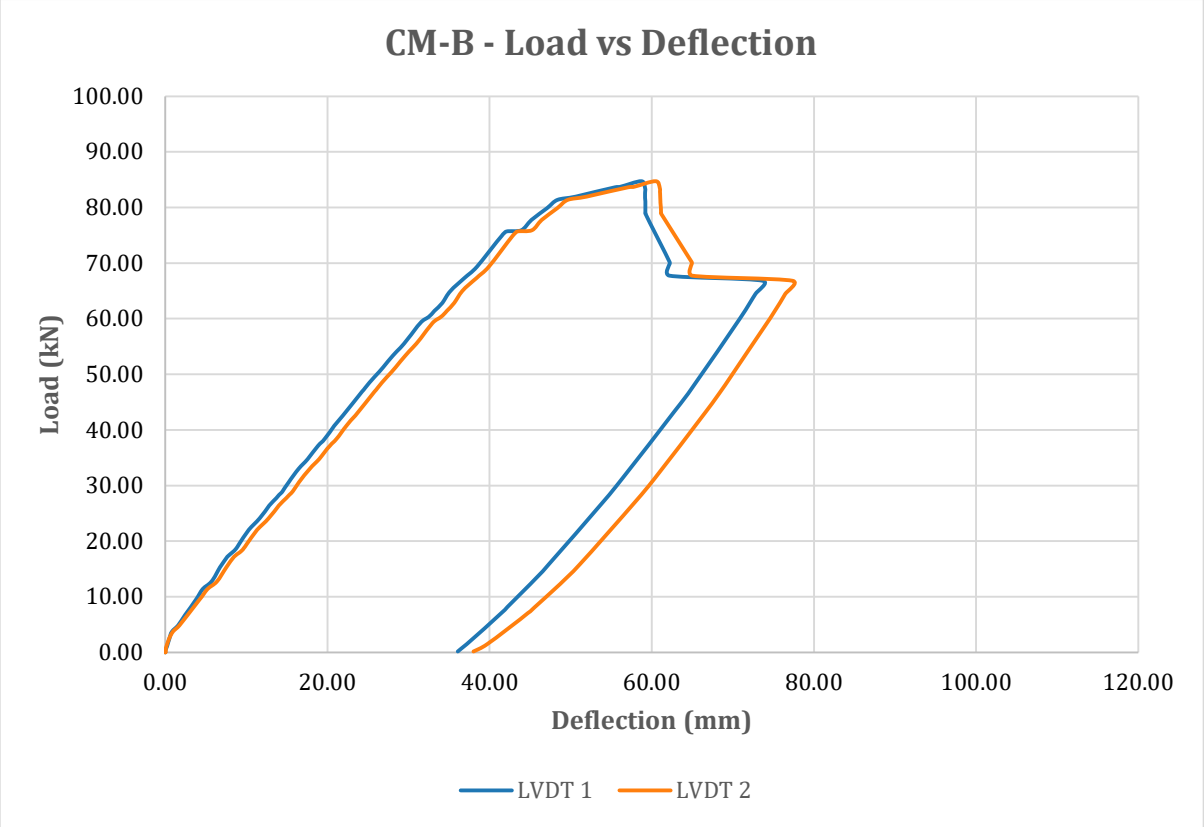

Figure A4.5: CM-B Deflection Curves

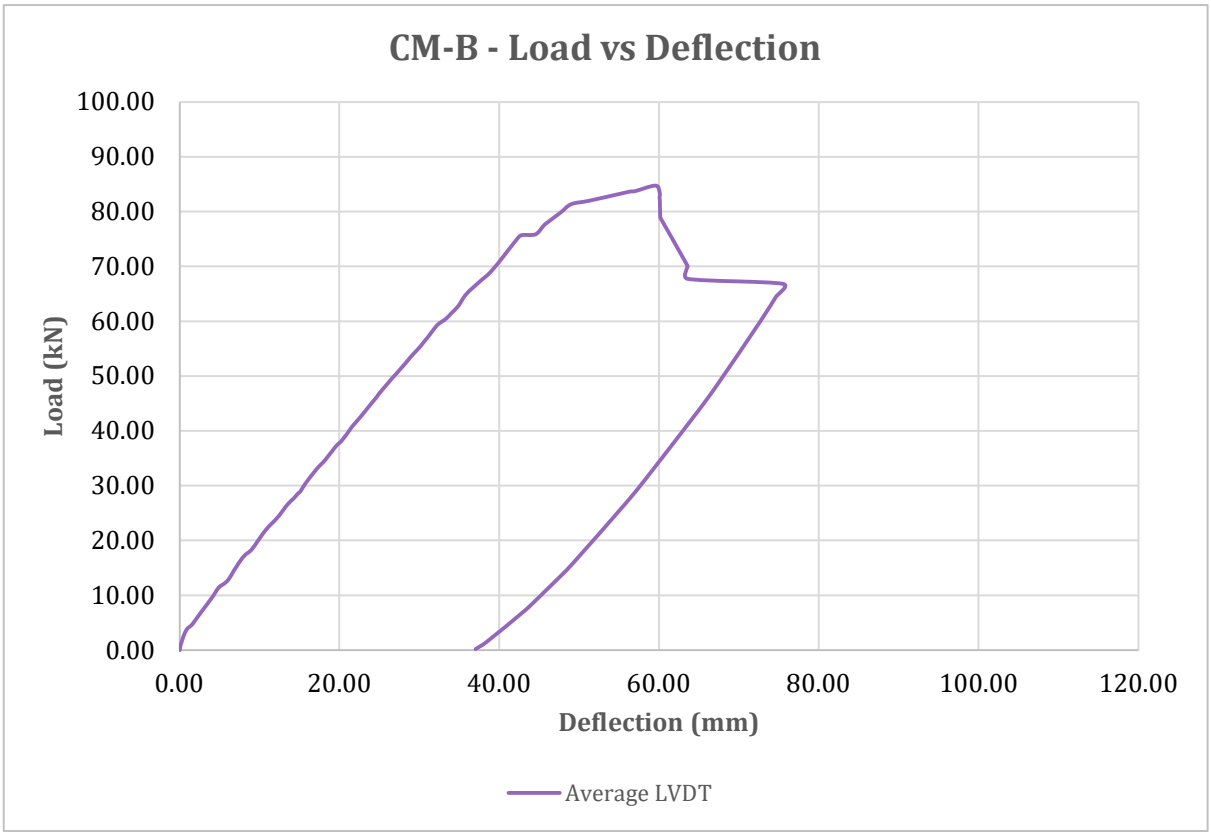

Figure A4.6: CM-B Deflection Curves - Average

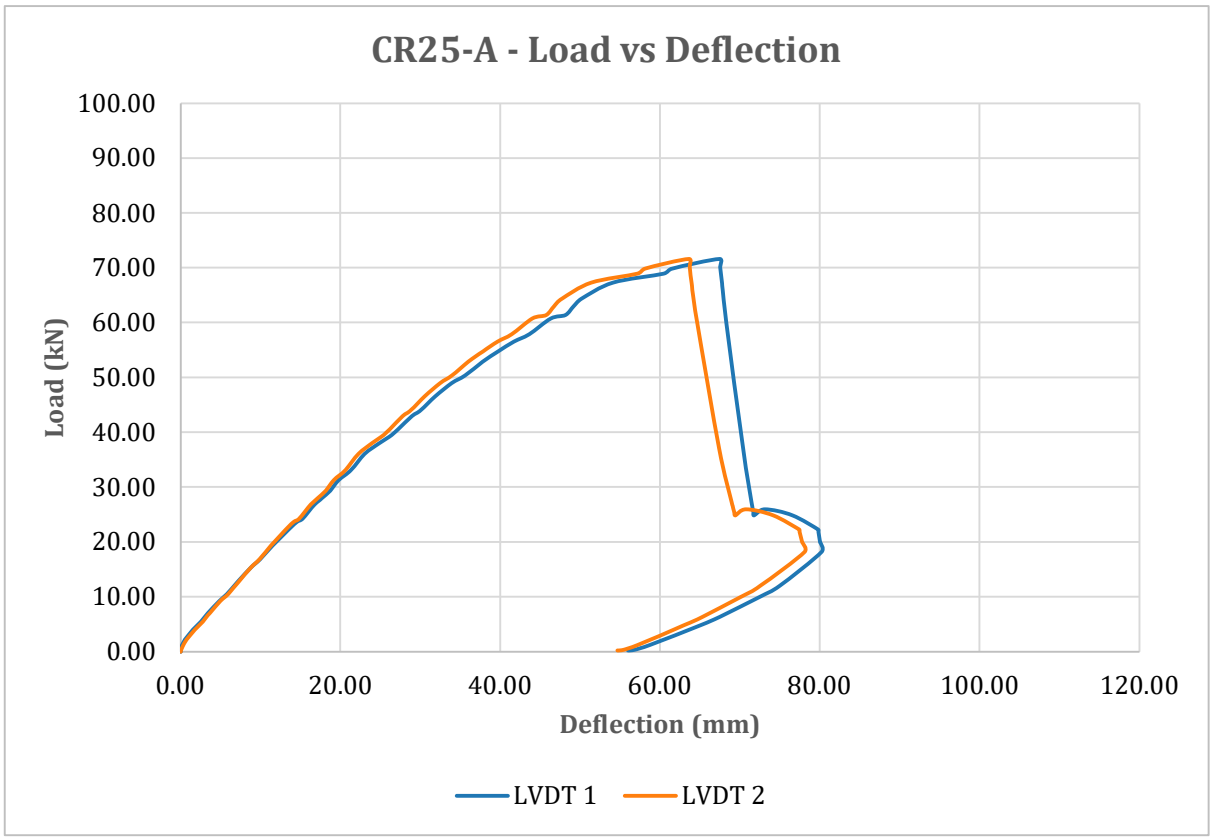

Figure A4.7: CR25-A Deflection Curves

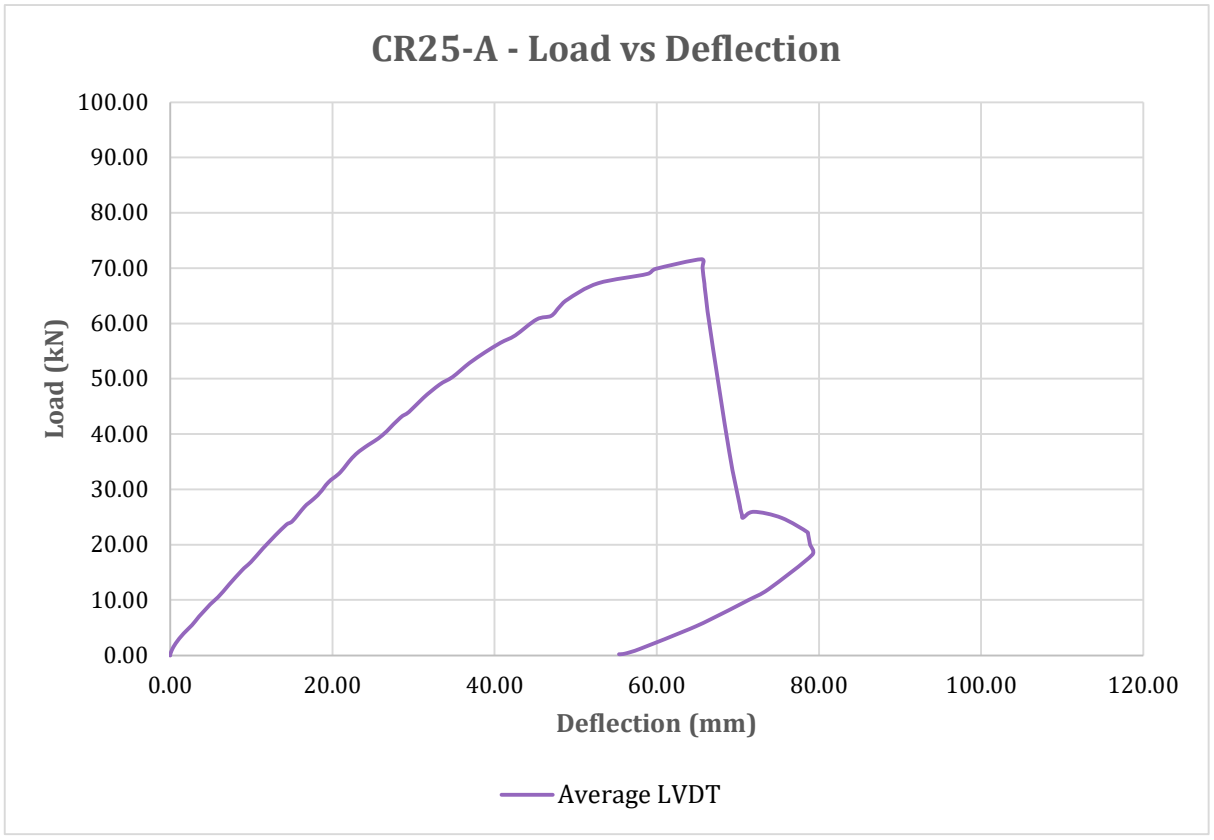

Figure A4.8: CR25-B Deflection Curves - Average

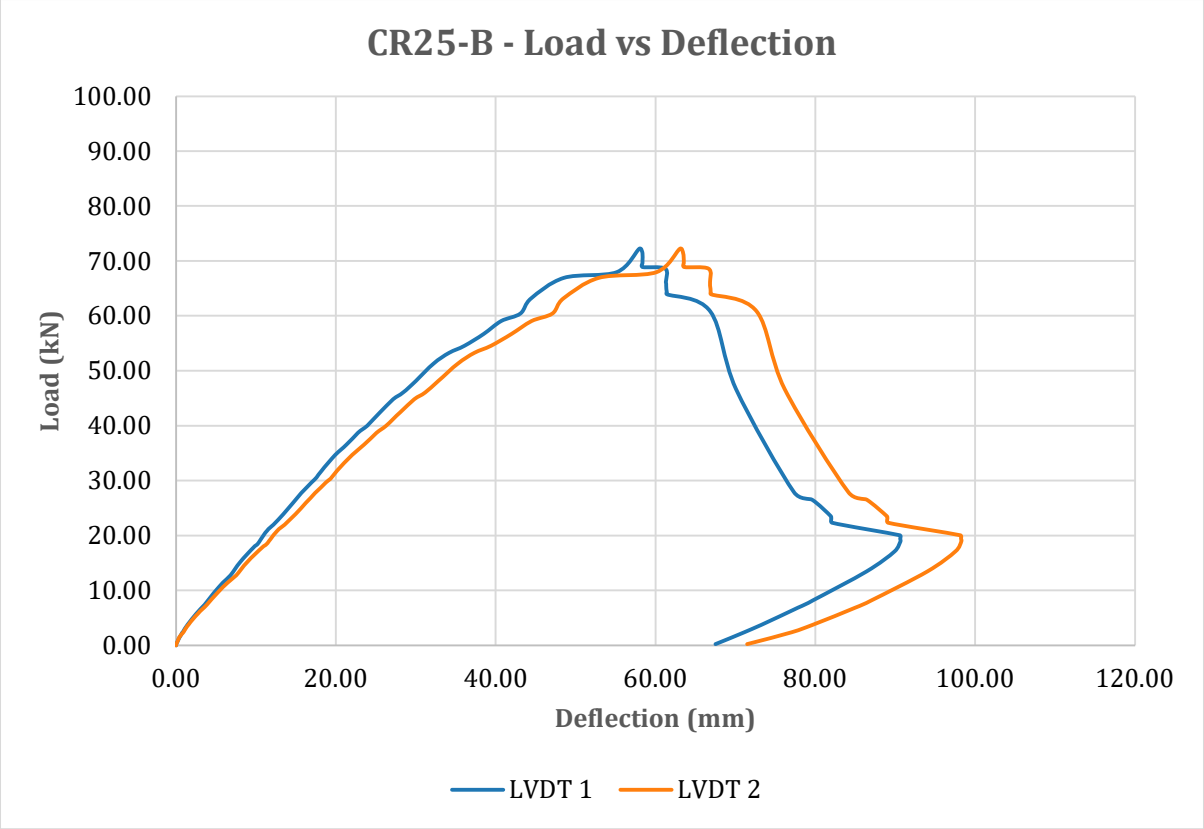

Figure A4.9: CR25-B Deflection Curves

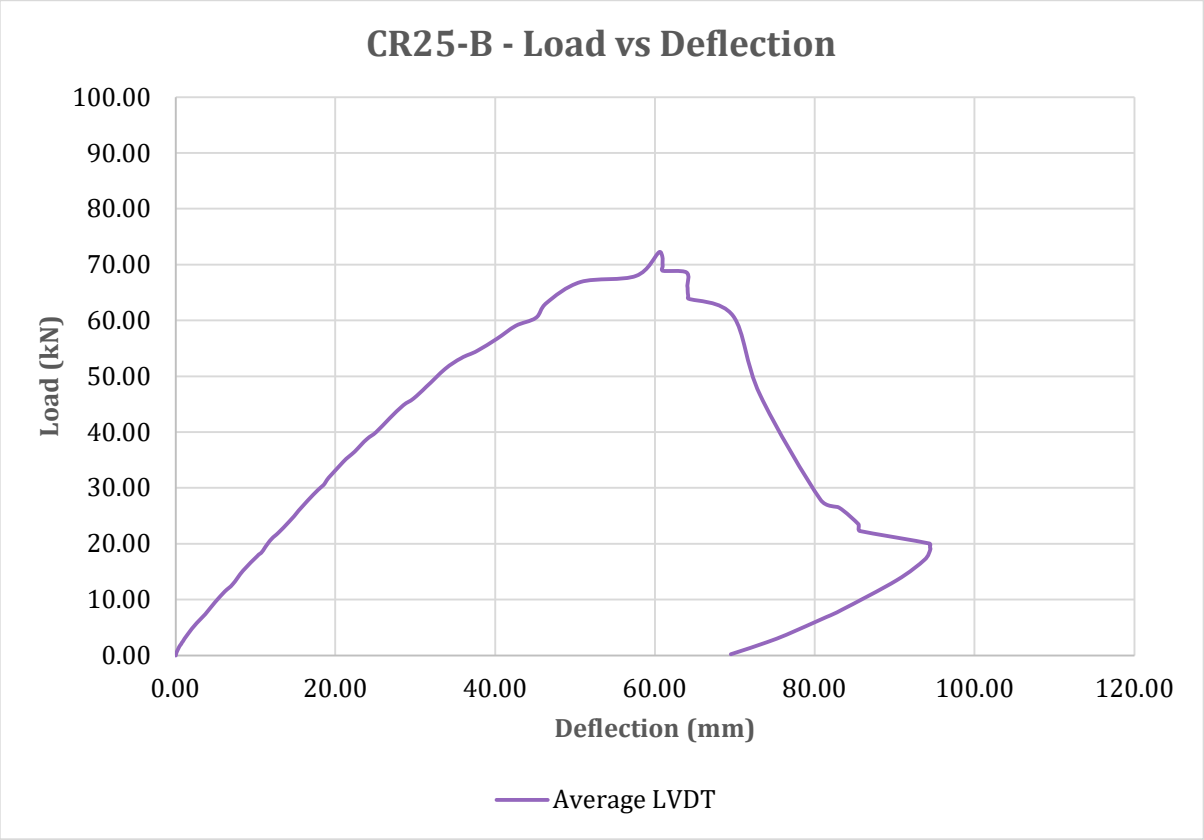

Figure A4.11: CR25-B Deflection Curves - Average

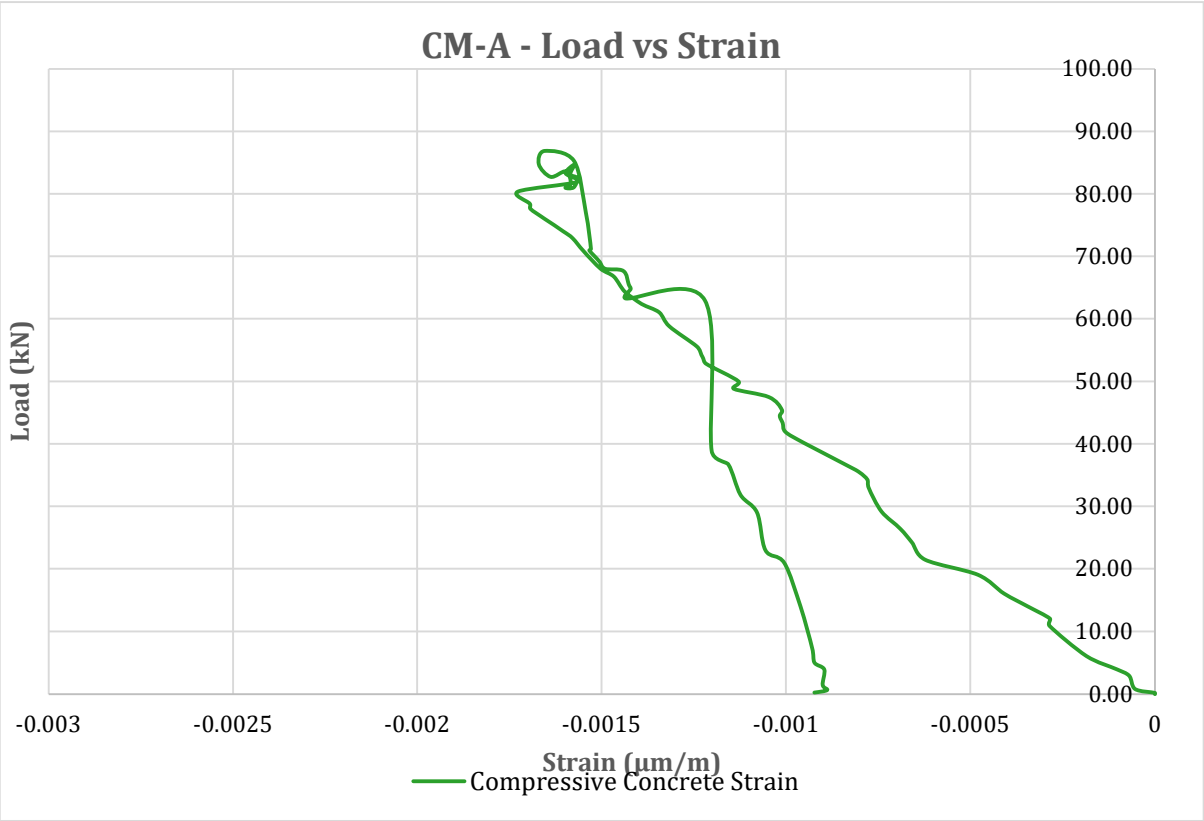

Figure A4.12: Compressive Concrete Strain for CM-A Beam

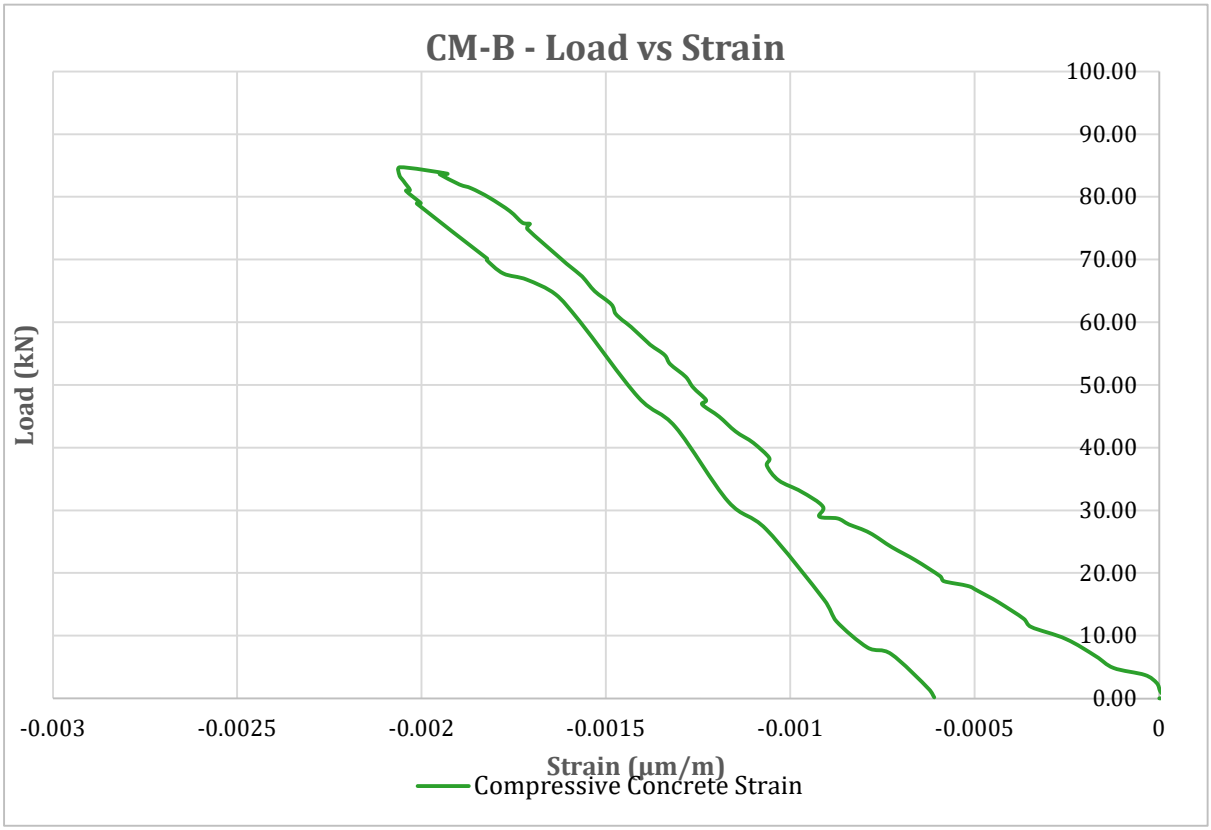

Figure A4.13: Compressive Concrete Strain for CM-B Beam

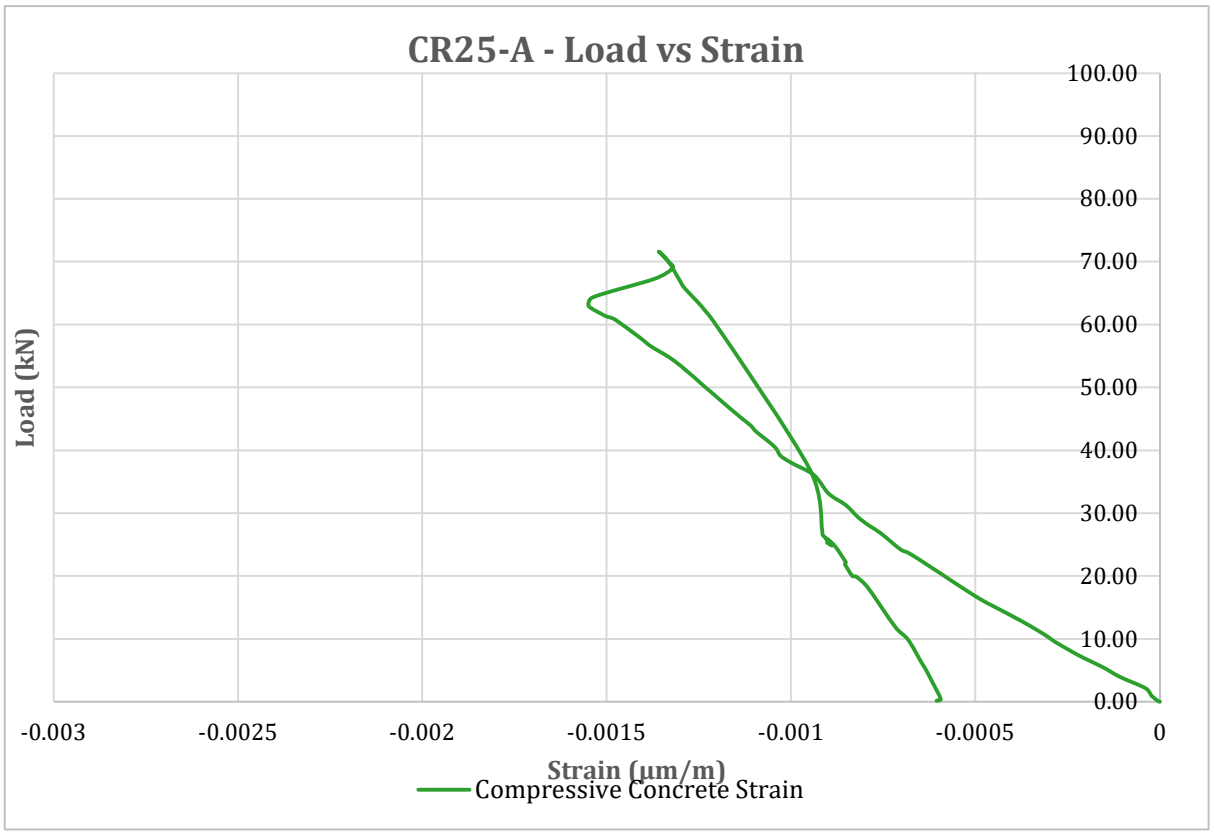

Figure A4.14: Compressive Concrete Strain for CR25-A Beam

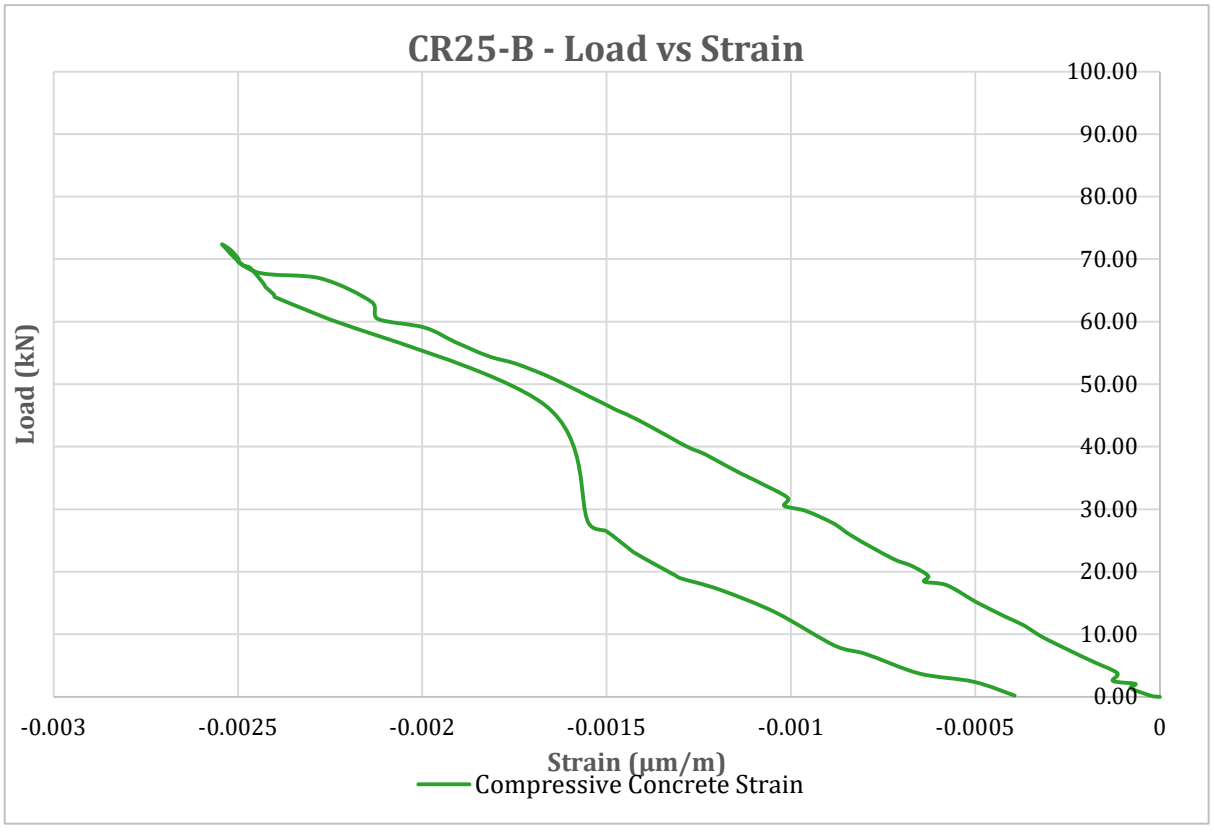

Figure A4.15: Compressive Concrete Strain for CR25-B Beam

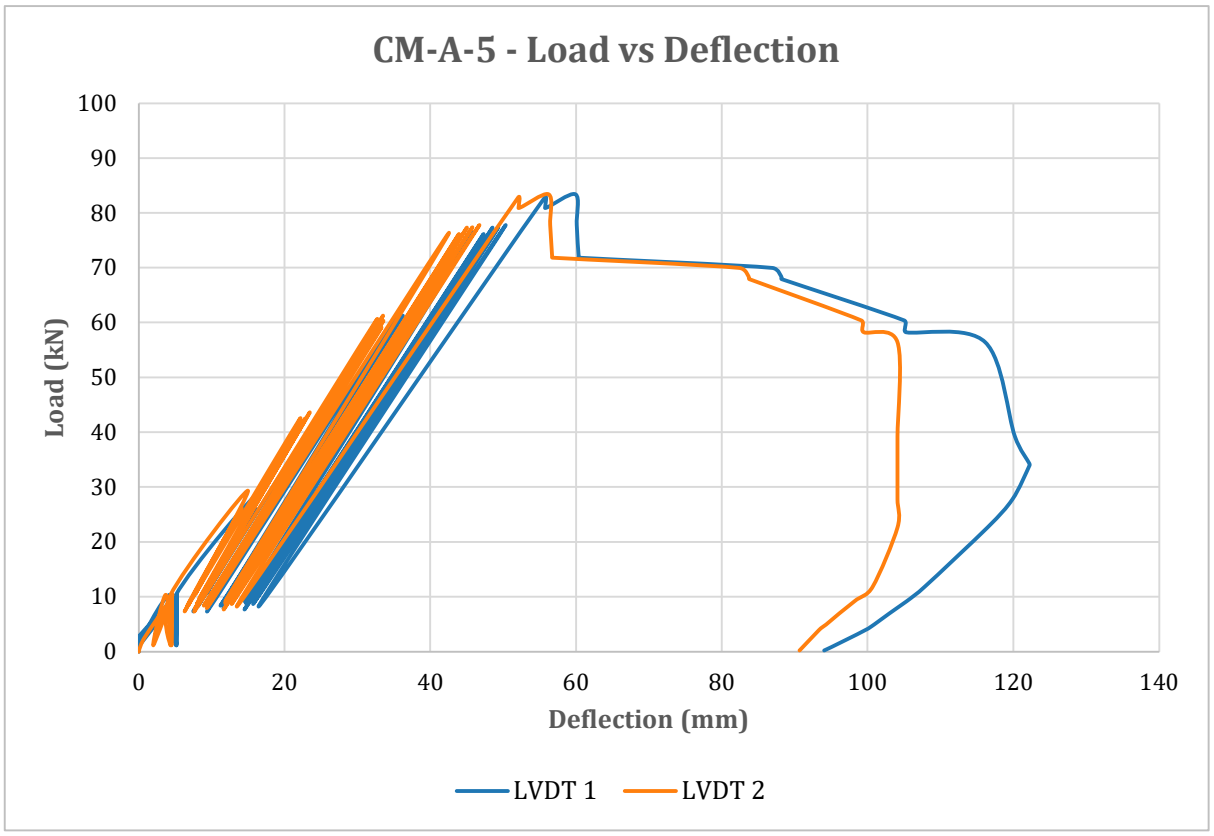

Figure A4.16: CM-A-5 Deflection Curves

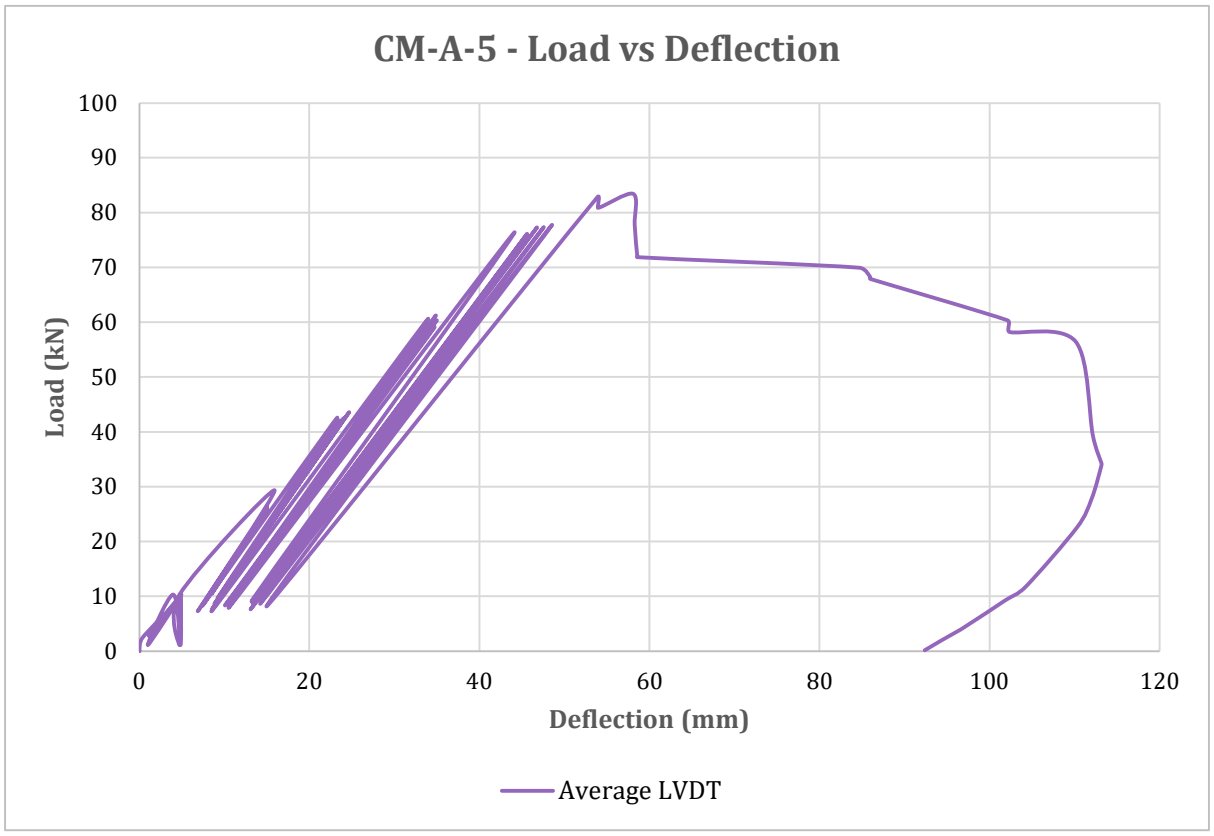

Figure A4.17: CM-A-5 Deflection Curves - Average

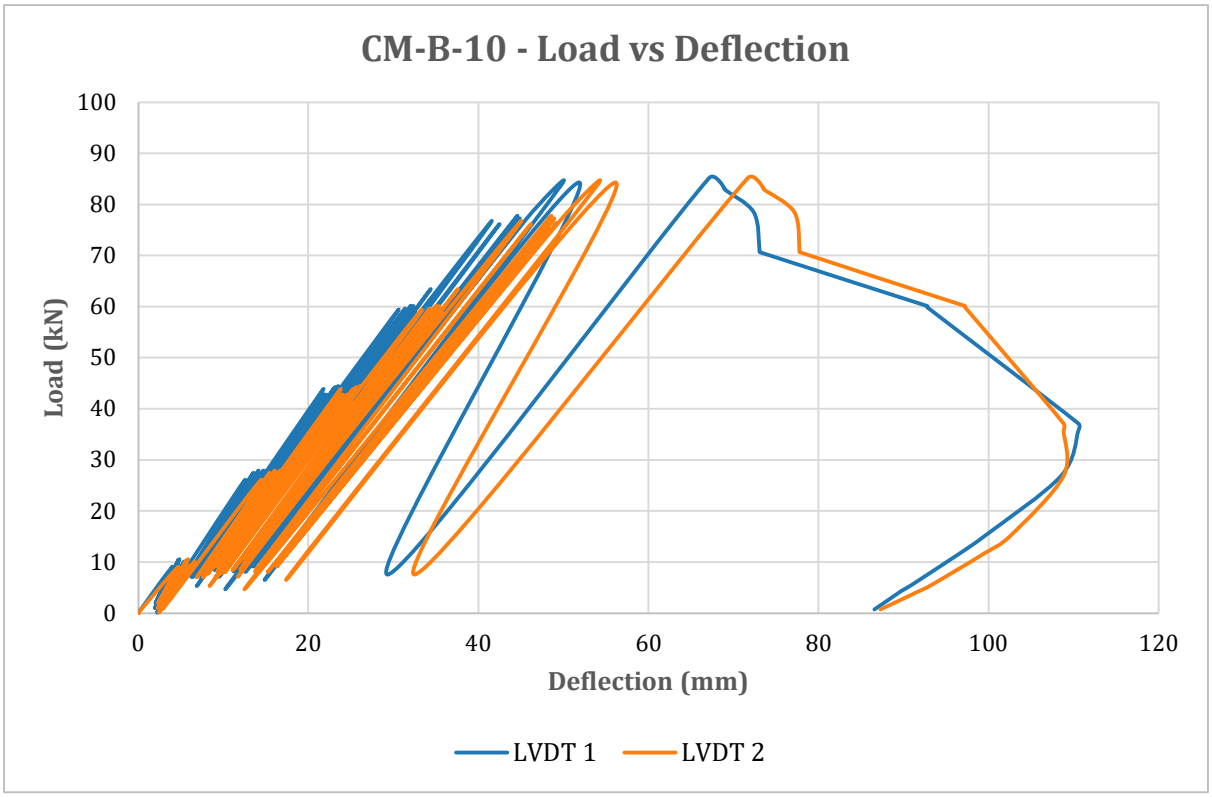

Figure A4.19: CM-B-10 Deflection Curves

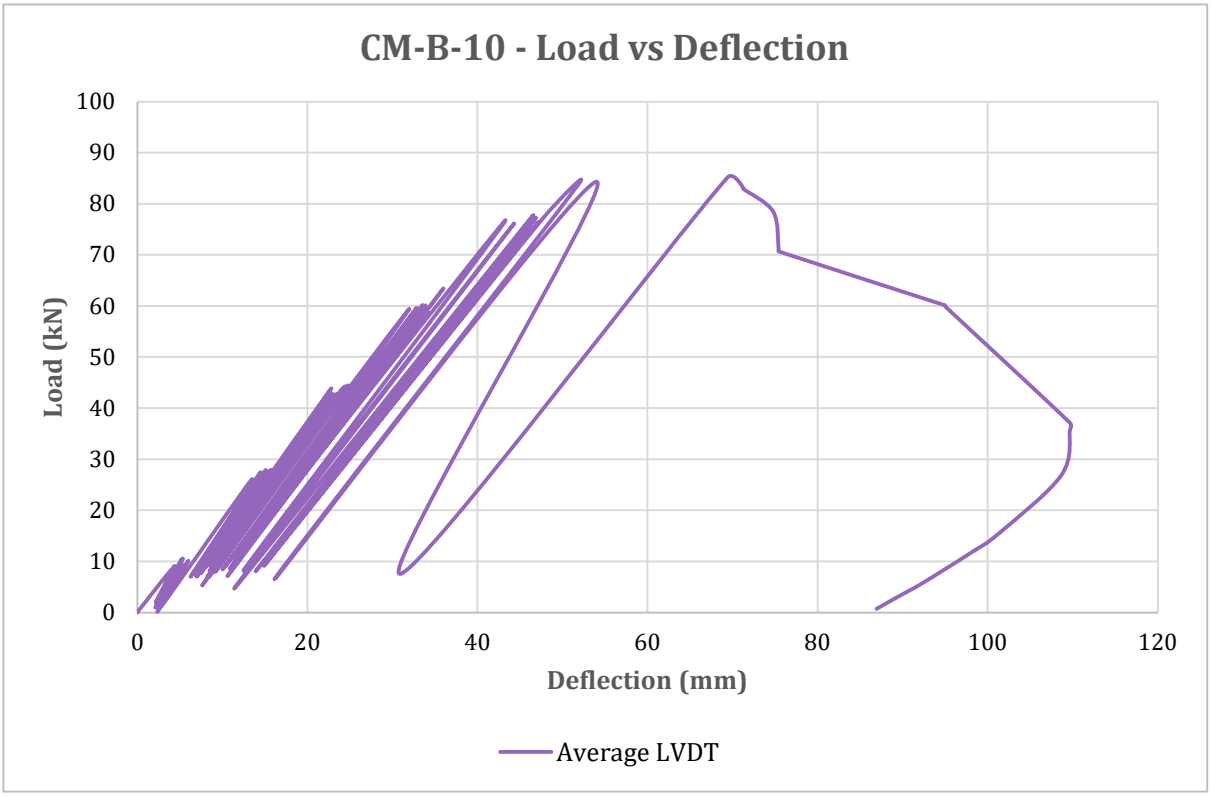

Figure A4.20: CM-B-10 Deflection Curves - Average

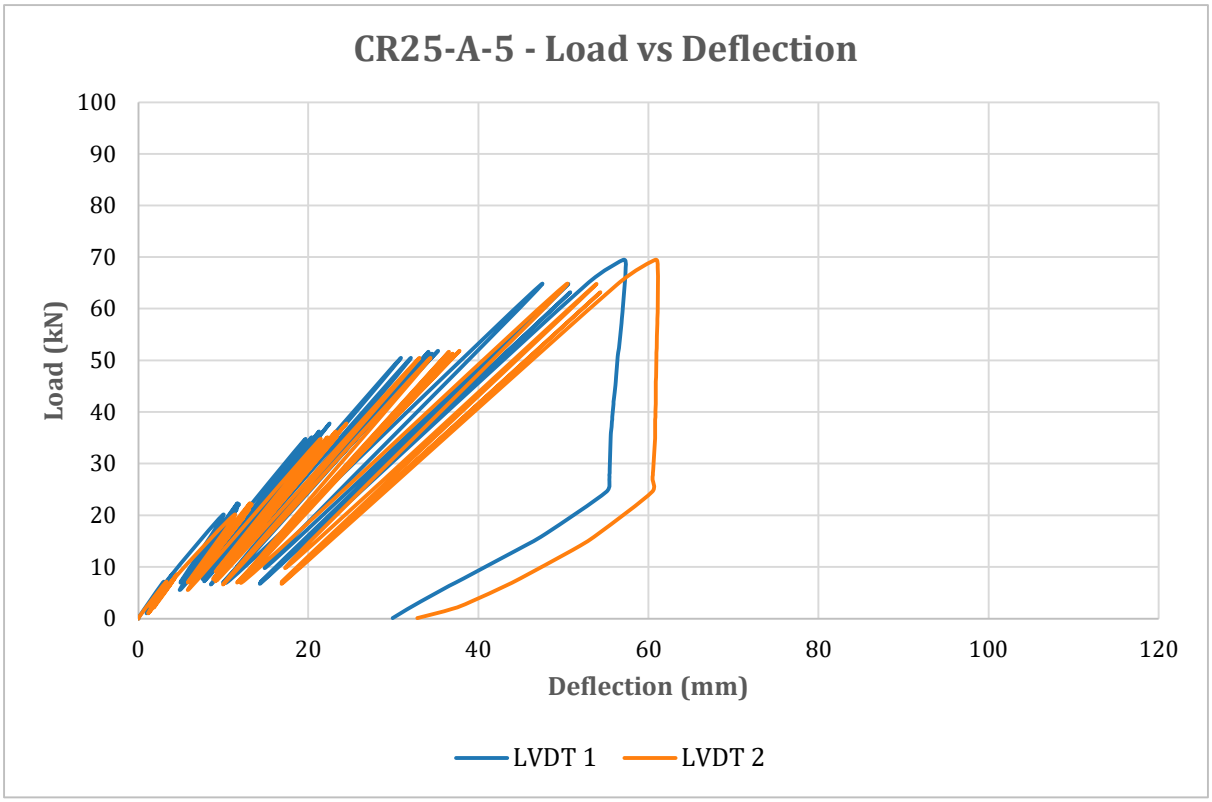

Figure A4.21: CR25-A-5 Deflection Curves

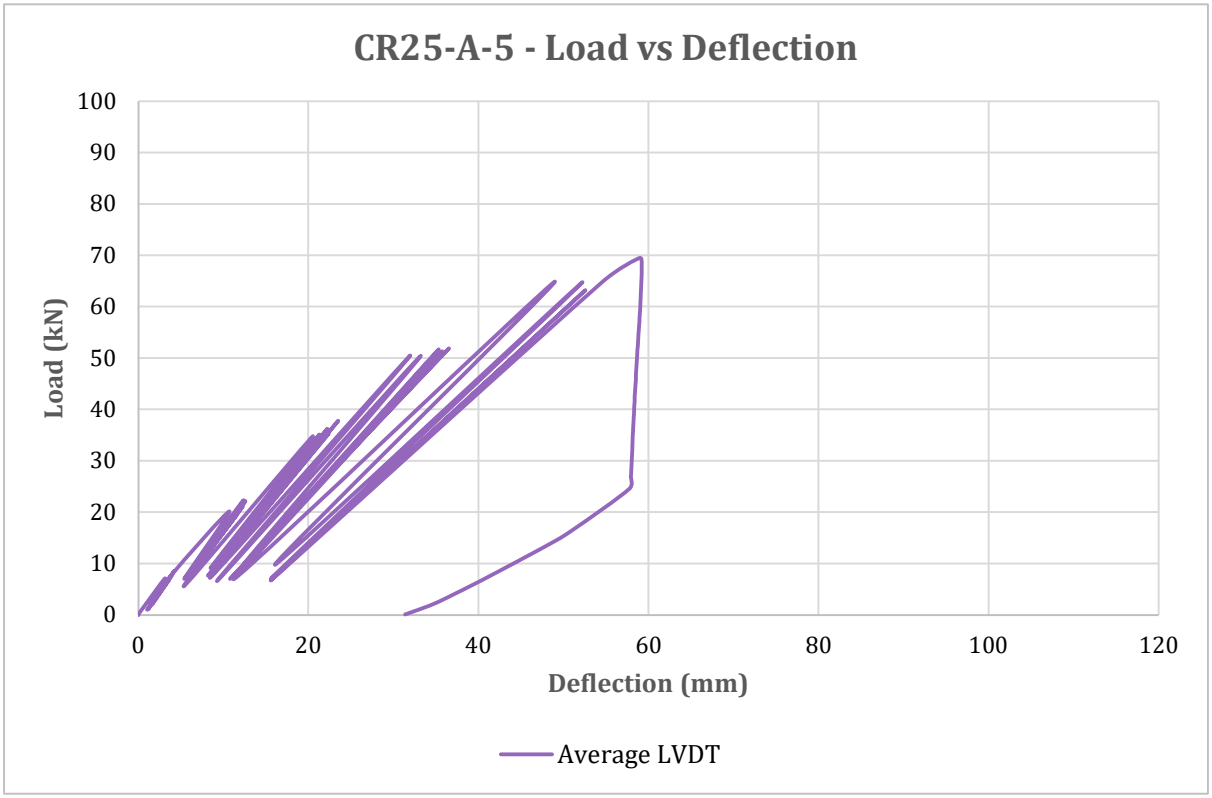

Figure A4.22: CR25-A-5 Deflection Curves - Average

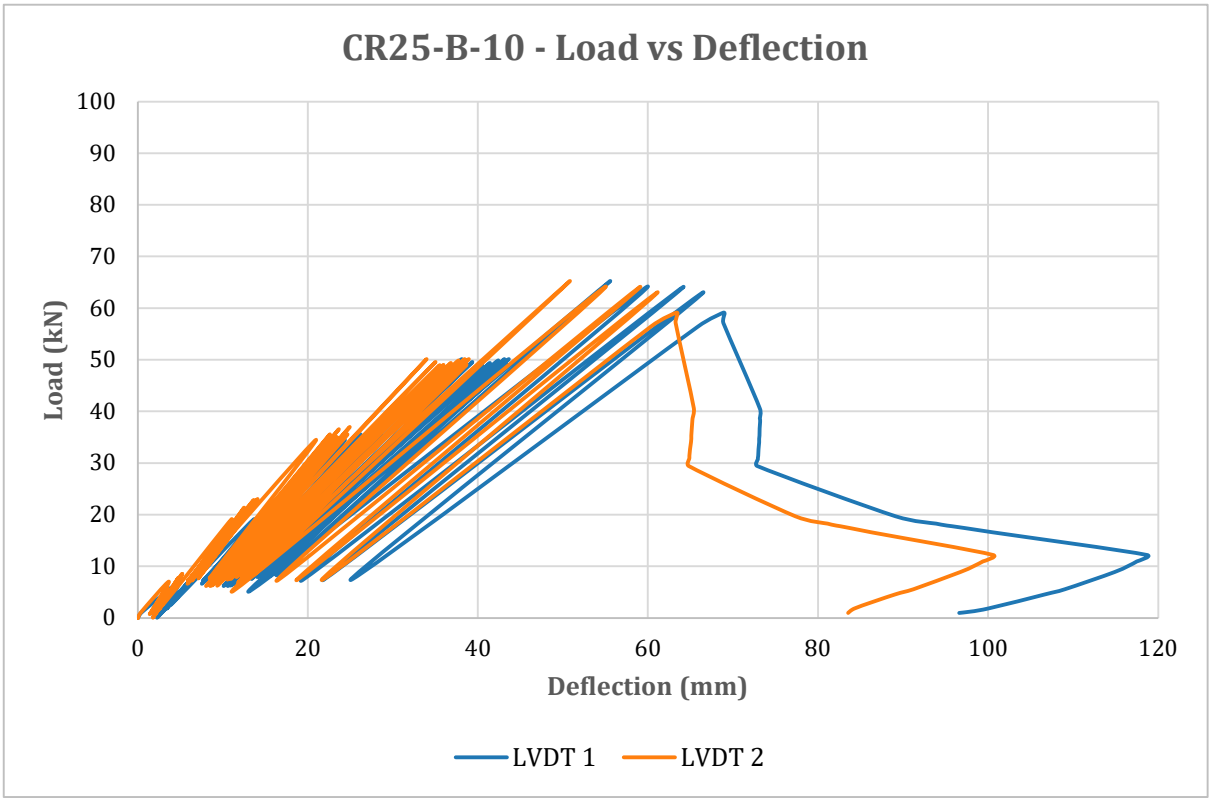

Figure A4.23: CR25-B-10 Deflection Curves

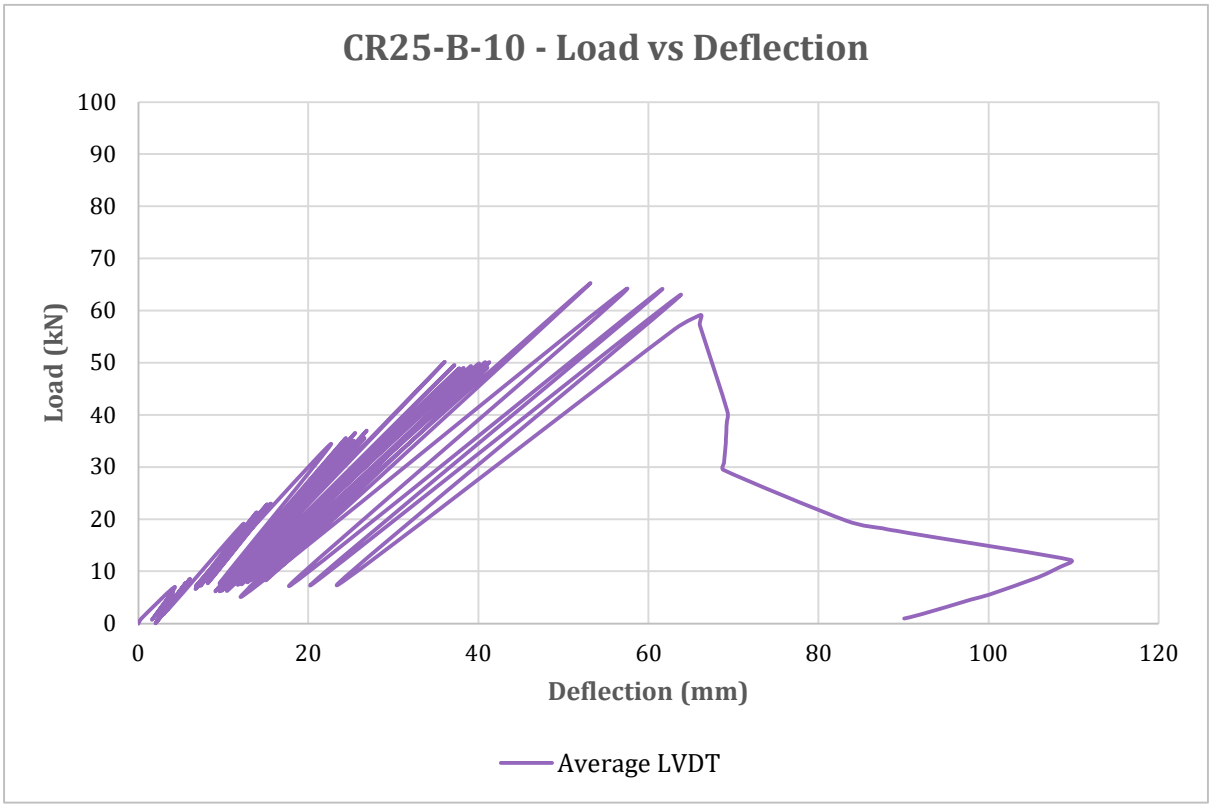

Figure A4.24: CR25-B-10 Deflection Curves - Average

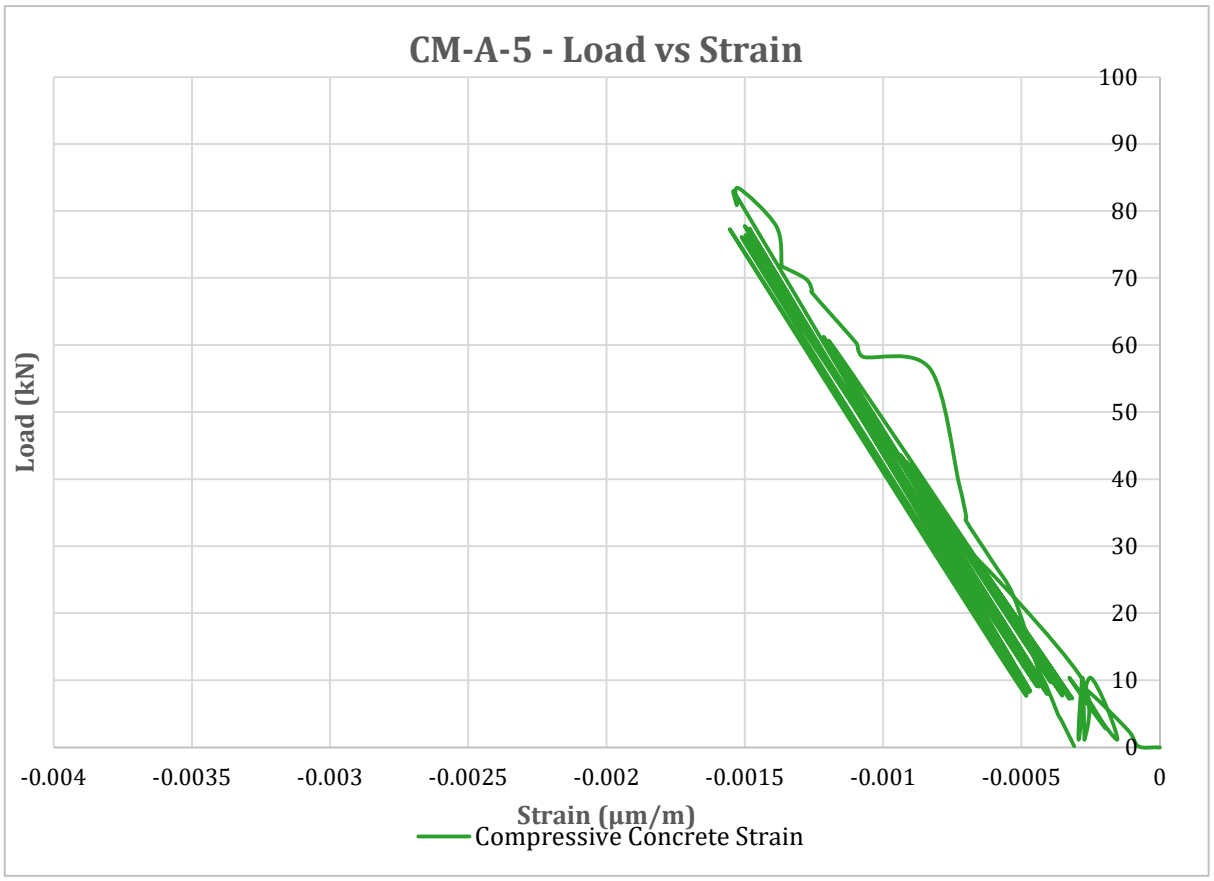

Figure A4.25: Compressive Concrete Strain for CM-A-5 Beam

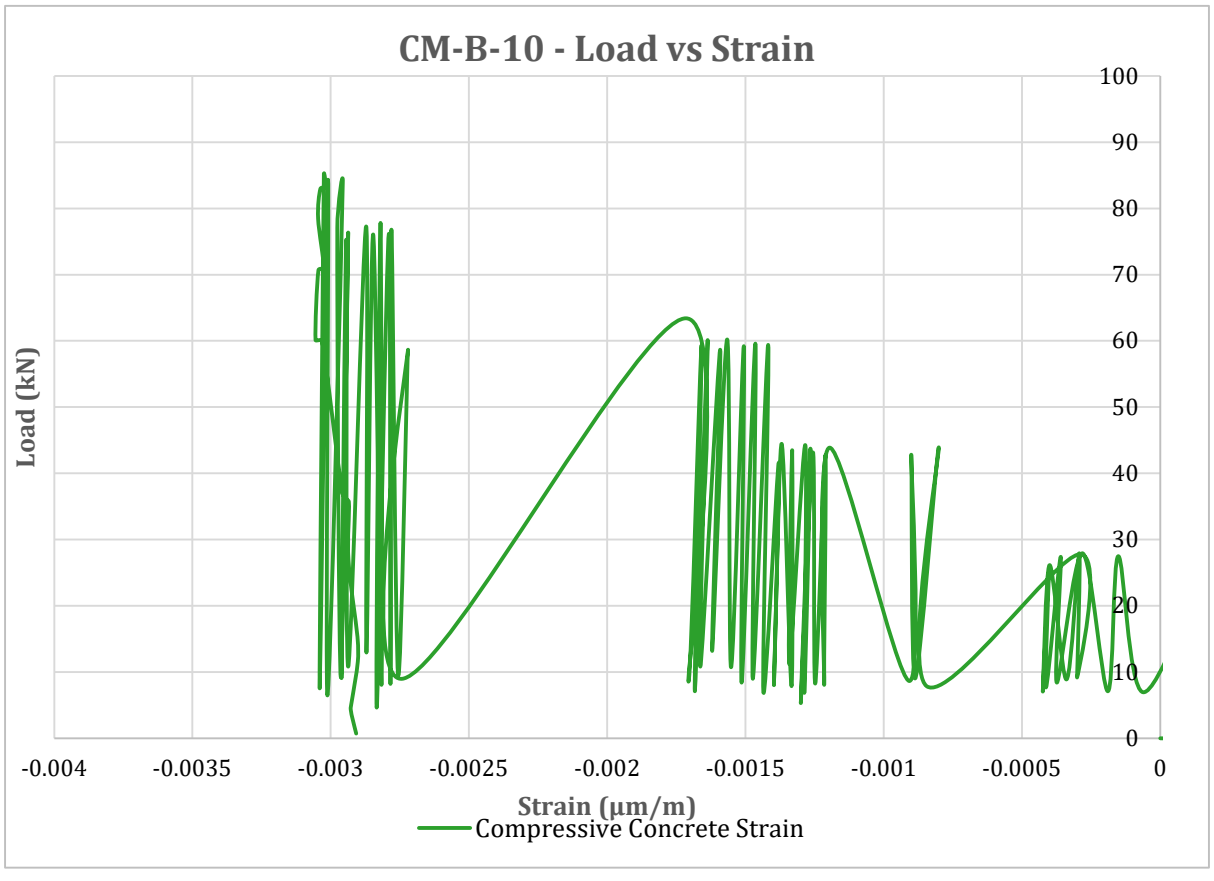

Figure A4.26: Compressive Concrete Strain for CM-B-10 Beam

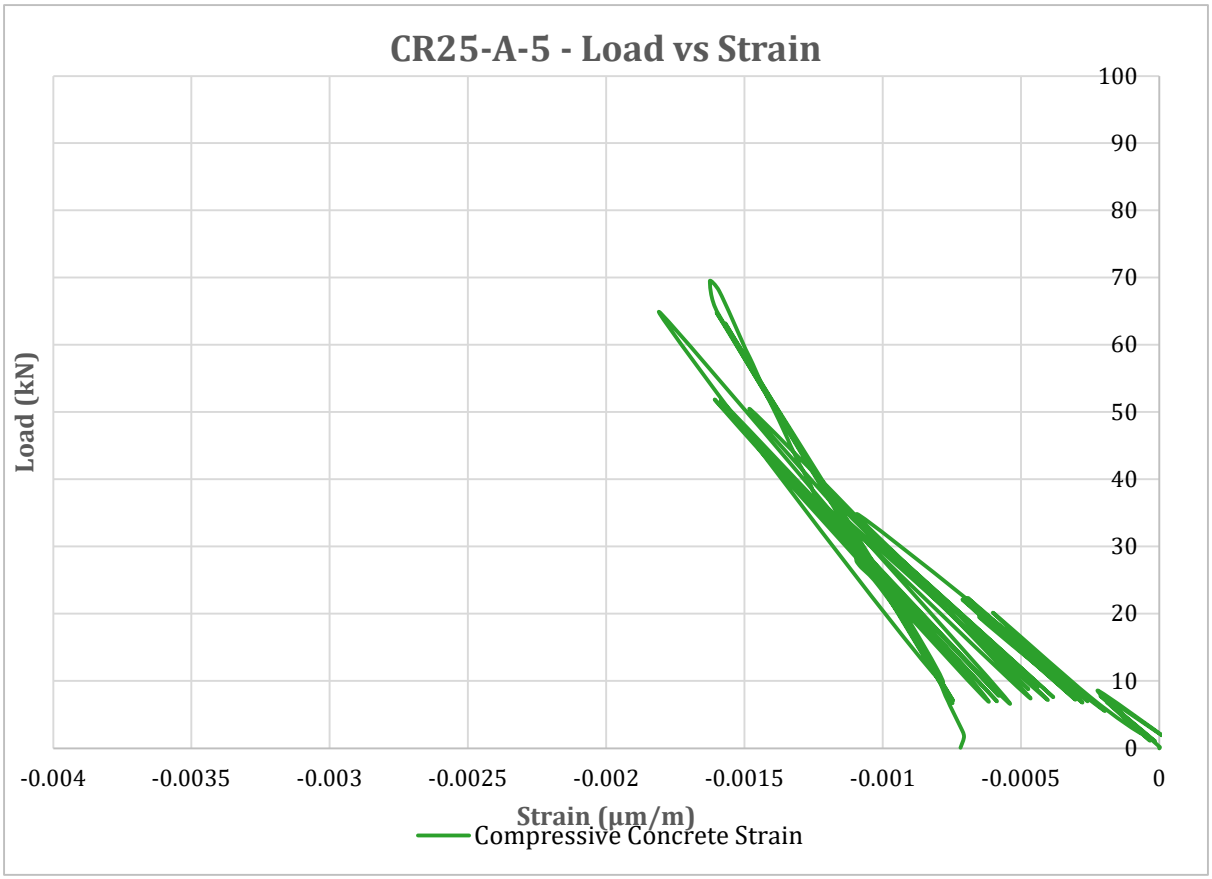

Figure A4.27: Compressive Concrete Strain for CR25-A-5 Beam

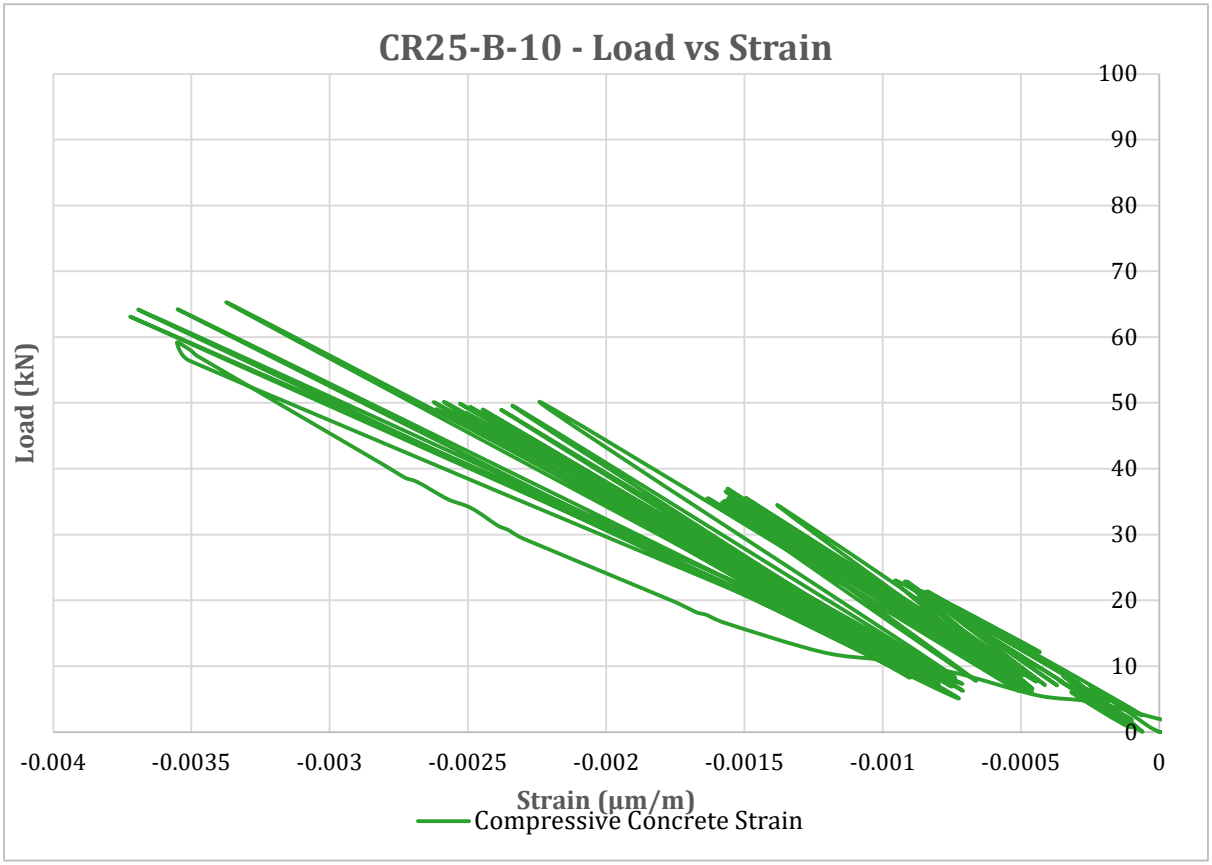

Figure A4.28: Compressive Concrete Strain for CR25-B-10 Beam

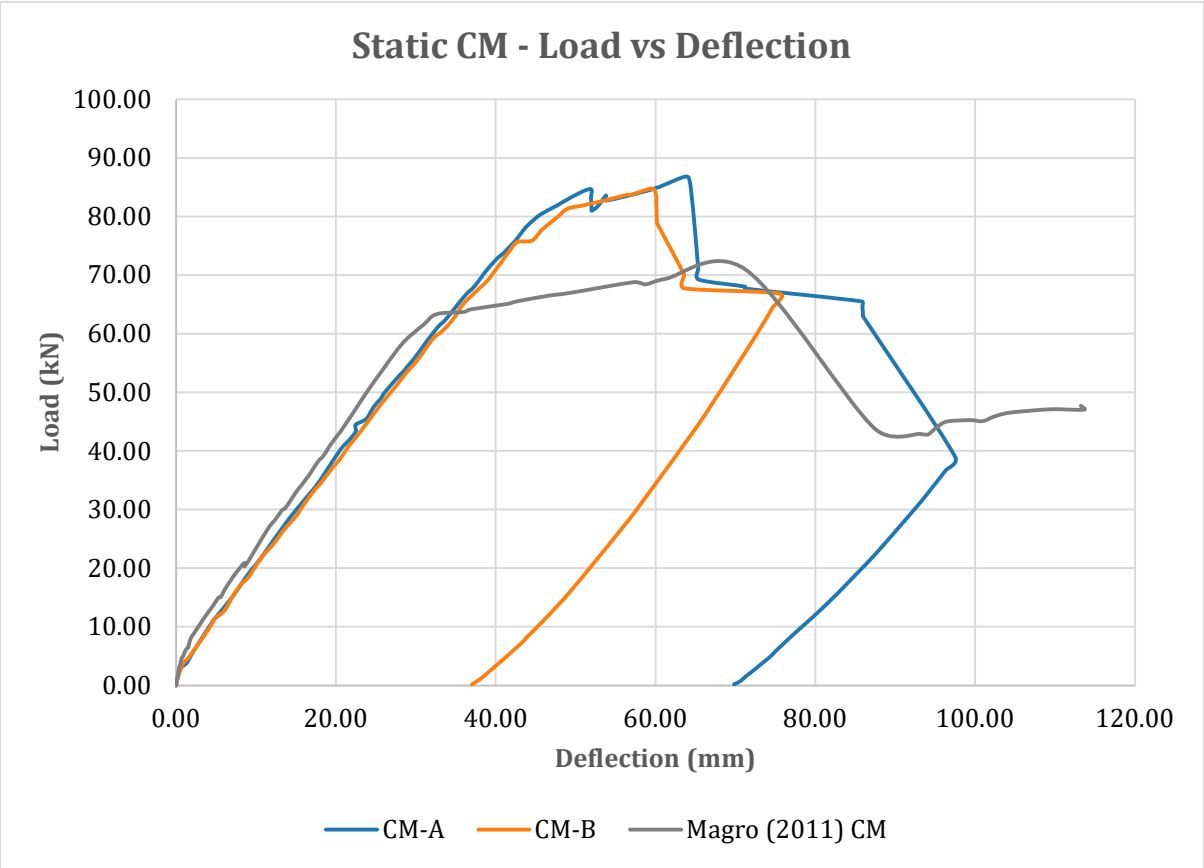

Figure A4.29: Static CM Deflection Curves

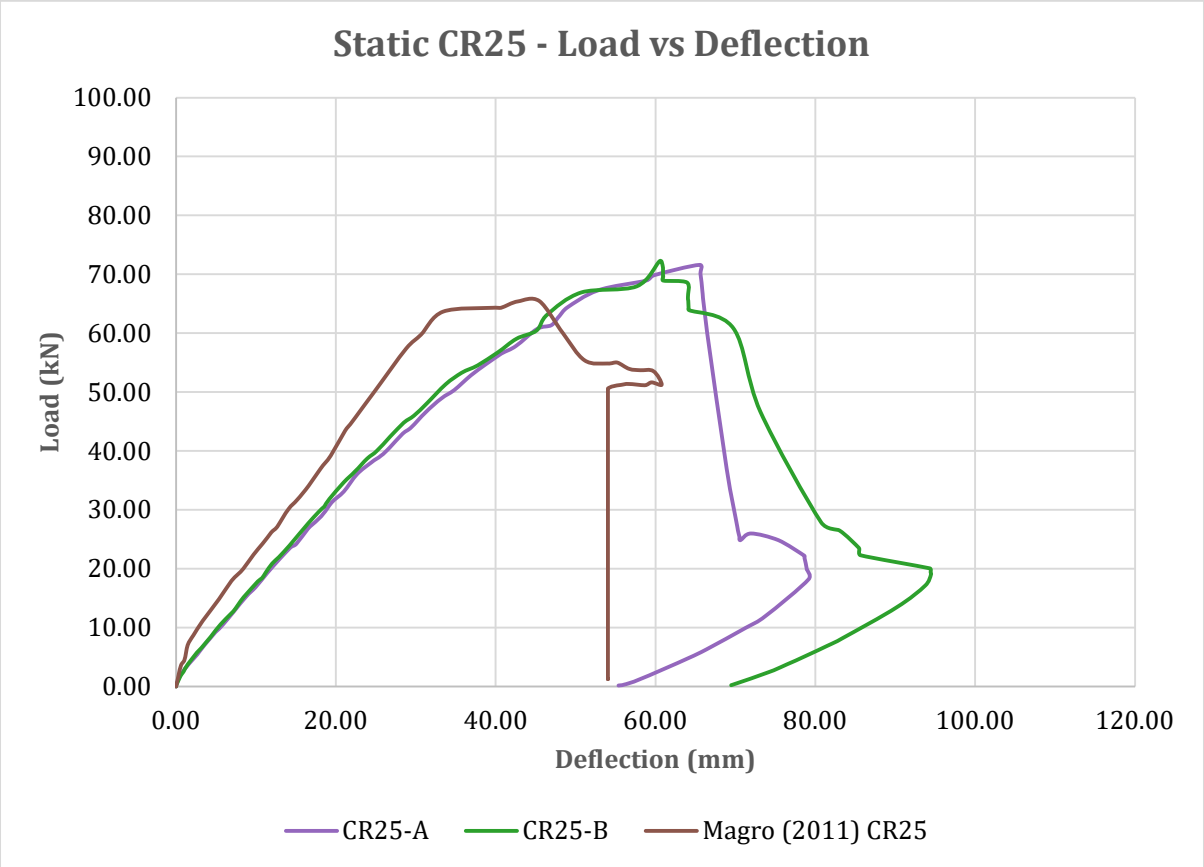

Figure A4.30: Static CR25 Deflection Curves

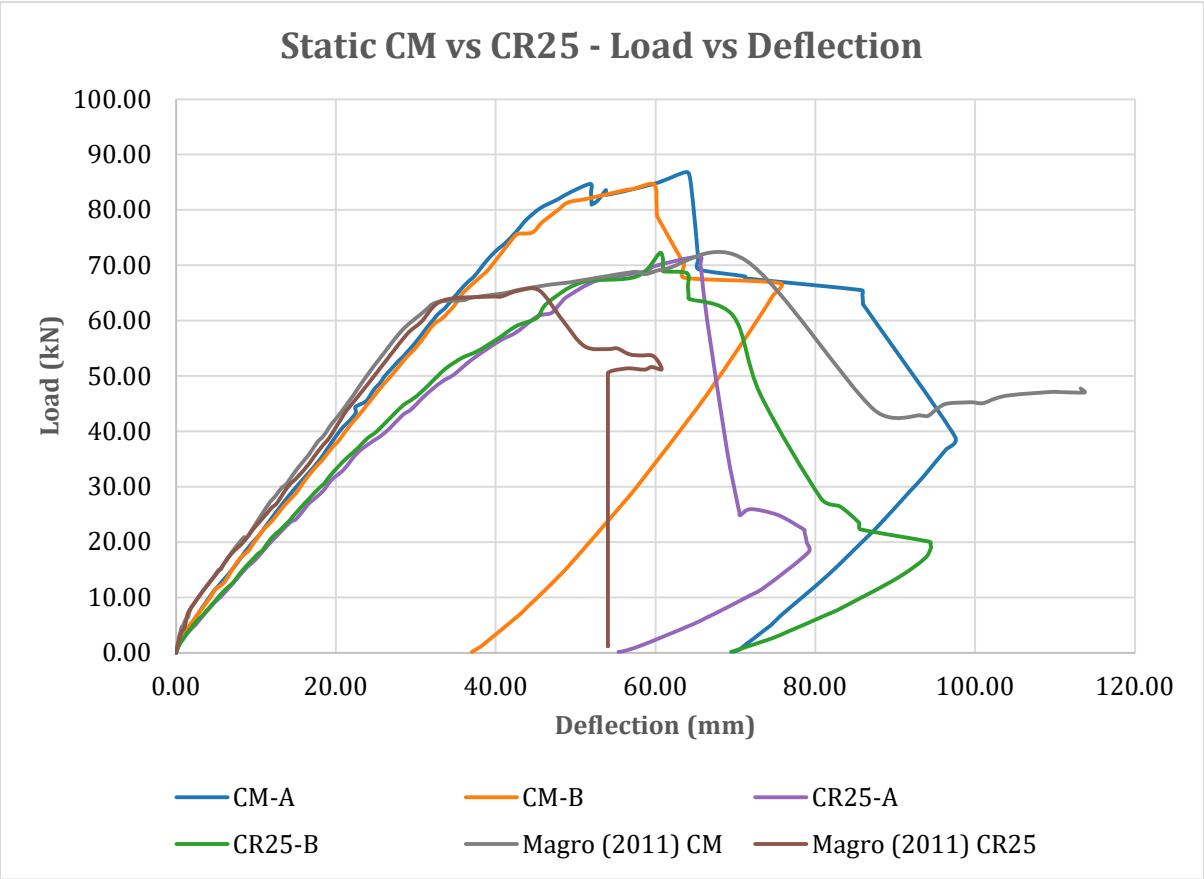

Figure A4.31: Static CM vs CR 25 Deflection Curves

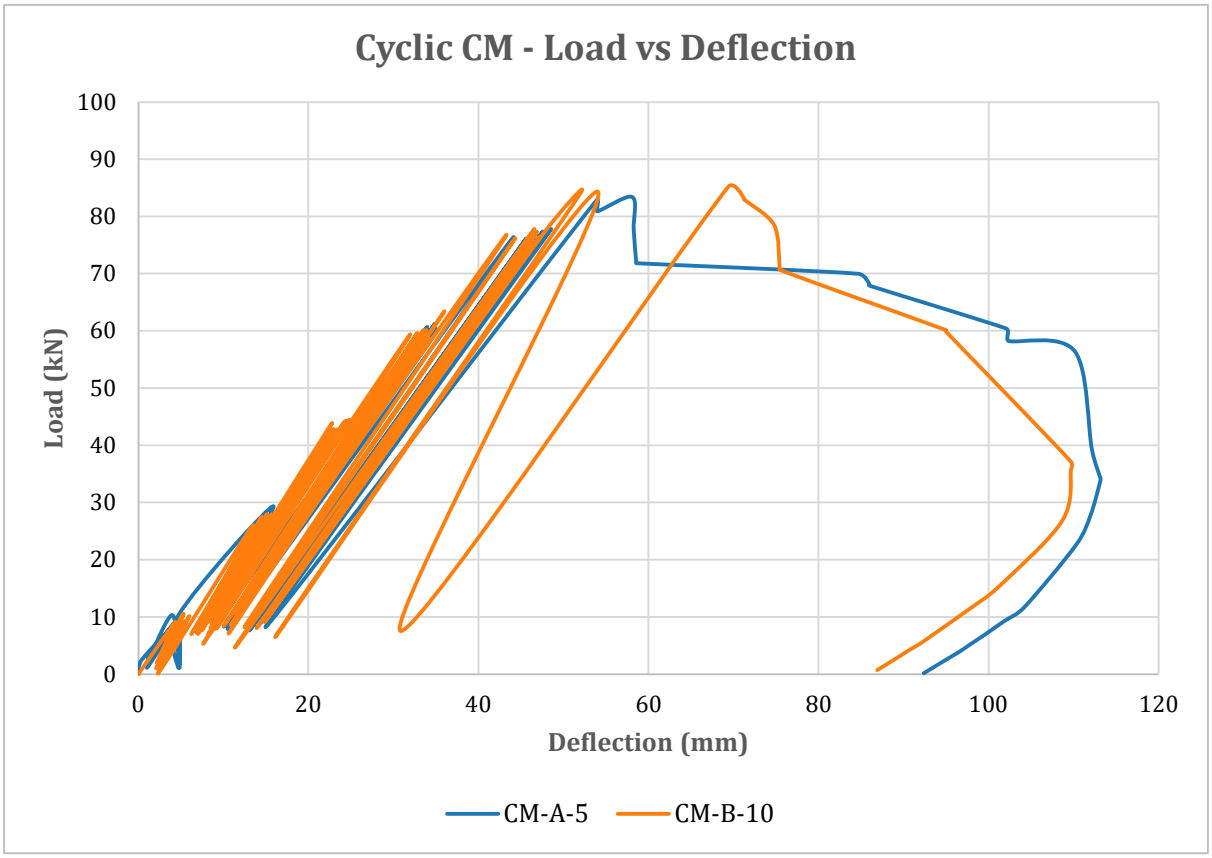

Figure A4.32: Cyclic CM Deflection Curves

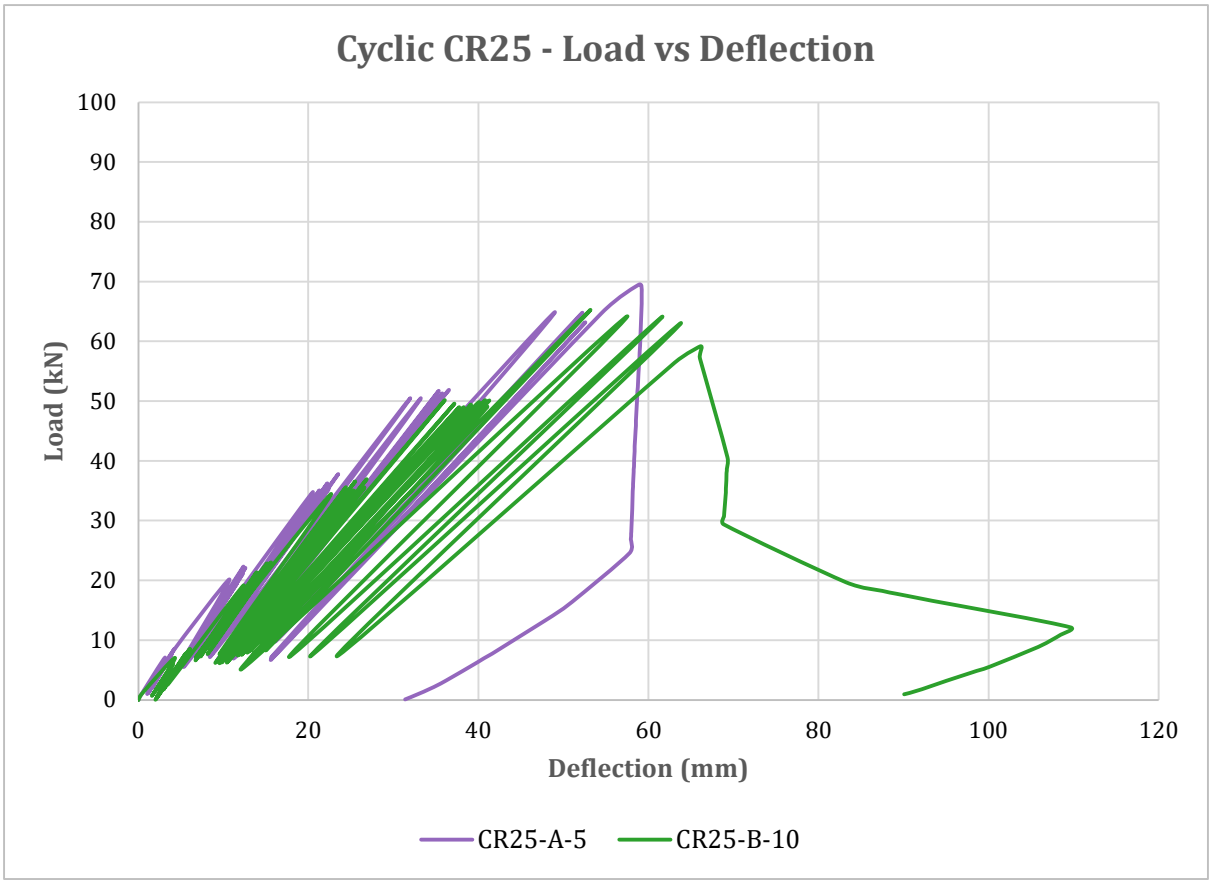

Figure A4.33: Cyclic CR25 Deflection Curves

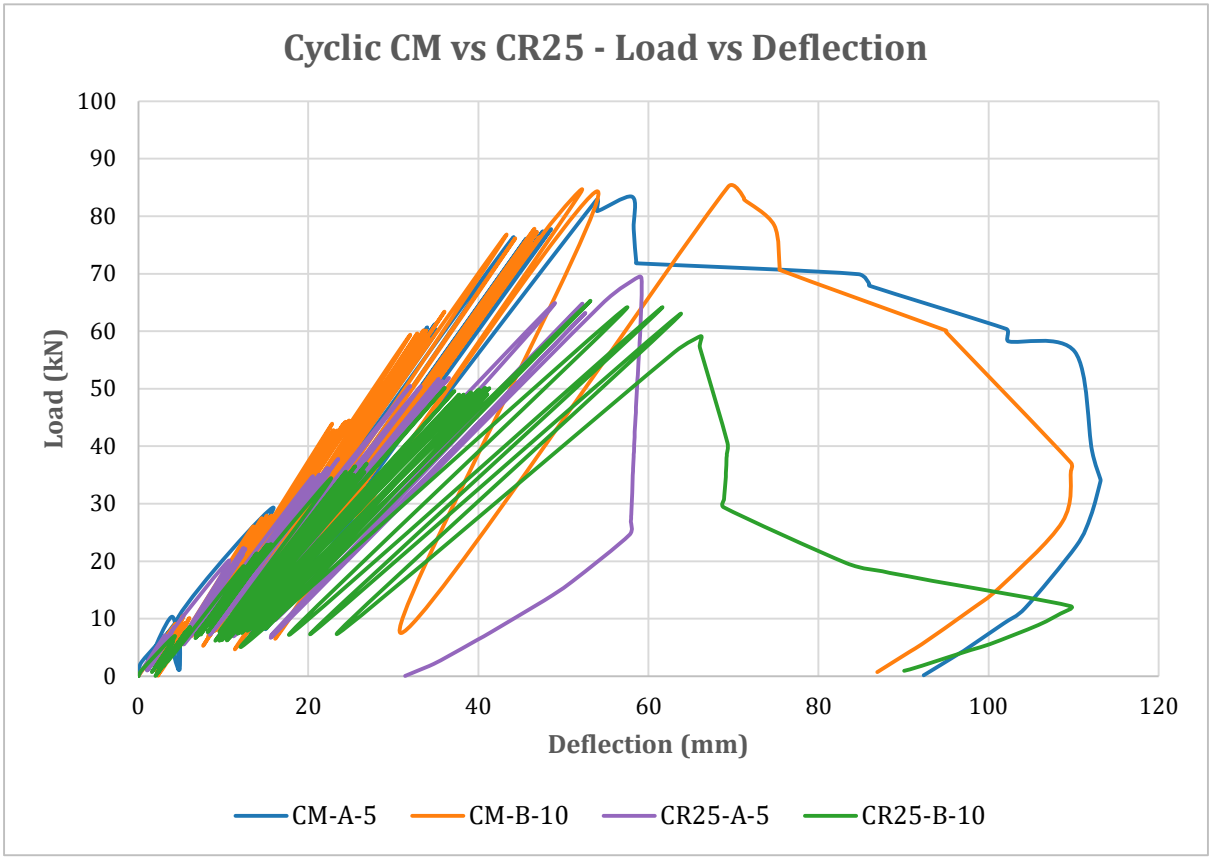

Figure A4.34: Cyclic CM vs CR25 Deflection Curves

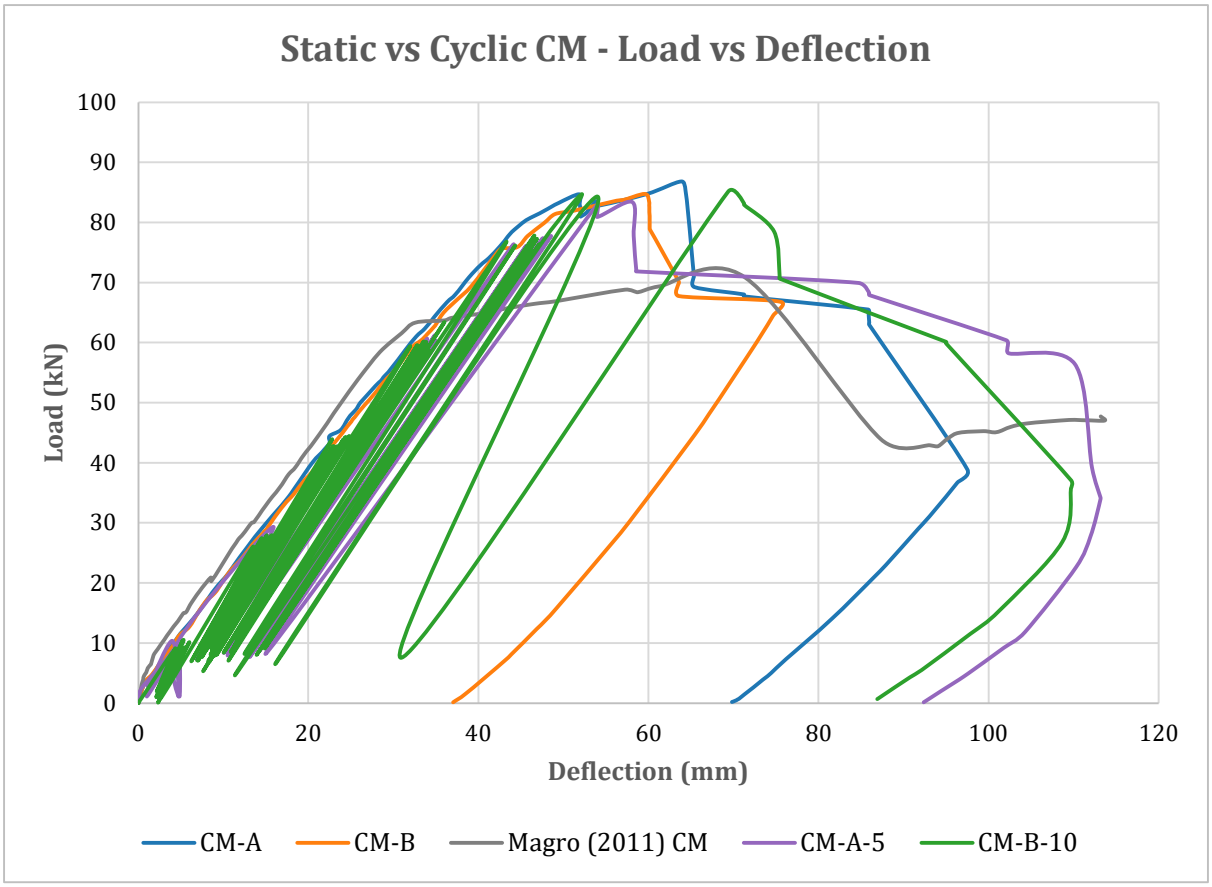

Figure A4.35: Static vs Cyclic CM Deflection Curves

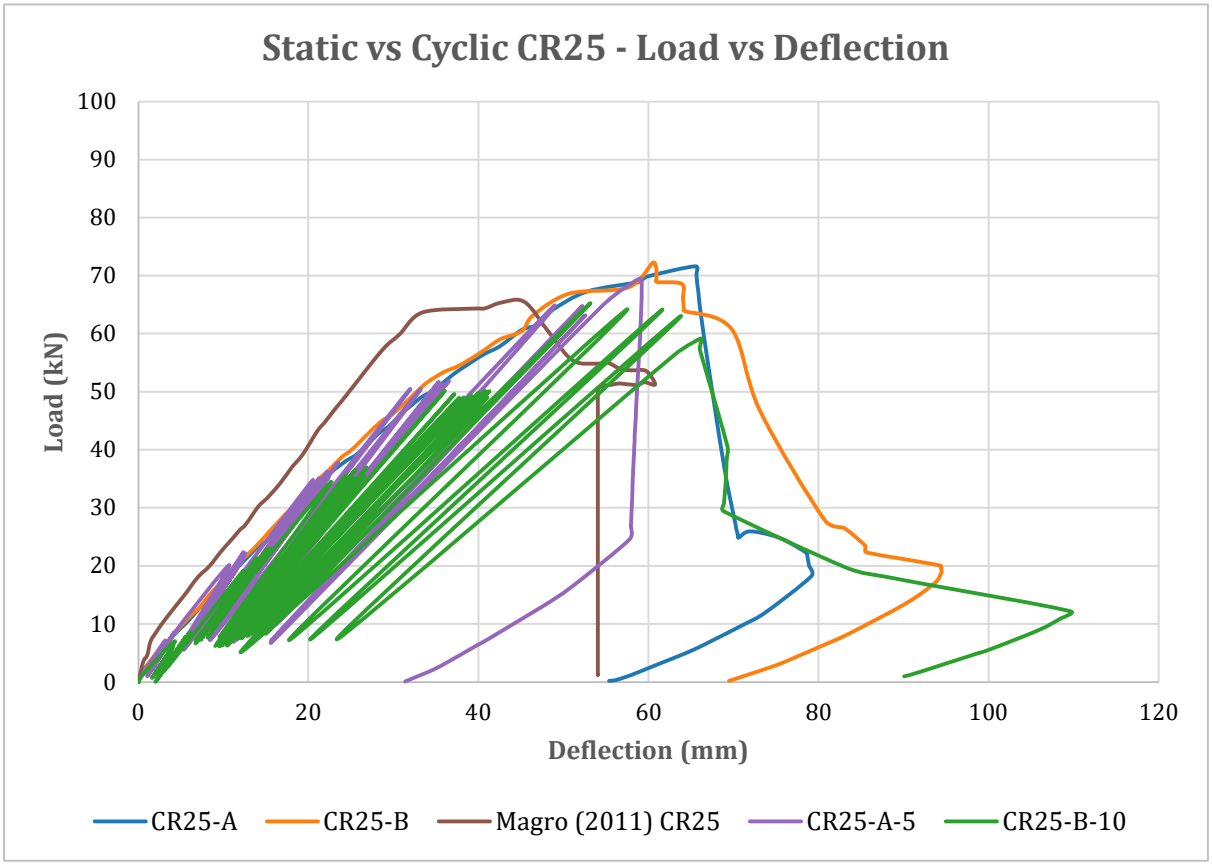

Figure A4.36: Static vs Cyclic CR25 Deflection Curves

Appendix 5: Short Column Compressive Strength Test Results

Table A5.1: Static and Cyclic Column Compressive Strength Test Results

Sample Type	Sample Tested	Time (s)	LVDT 1 (mm)	Compressive Steel Strain (μm/m)	Compressive Concrete Strain (μm/m)	Load (kN)	Mean Ultimate Load (W_{ULT})
Control Column	CM-A	214.80	2.47	-1136.00	-2689.70	1079.10	1020.95
Control Column	CM-B	187.20	2.92	-656.20	-387.50	962.80	
Rubberised Column	CR25-A	94.90	2.70	-677.60	-577.60	478.20	445.20
Rubberised Column	CR25-B	81.30	1.92	-	-424.40	412.20	

Sample Type	Sample Tested	Time (s)	LVDT 1 (mm)	Compressive Steel Strain (μm/m)	Compressive Concrete Strain (μm/m)	Load (kN)	Mean Ultimate Load (W_{ULT})
Control Column	CM-A-5	7924.20	2.12	-1465.90	-719.20	1153.90	926.20
Control Column	CM-B-10	5346.20	2.31	-1030.50	-73.00	698.50	
Rubberised Column	CR25-A-5	2616.40	2.14	-786.10	-833.60	400.60	355.80
Rubberised Column	CR25-B-10	4665.00	2.20	-604.40	-943.70	311.00	

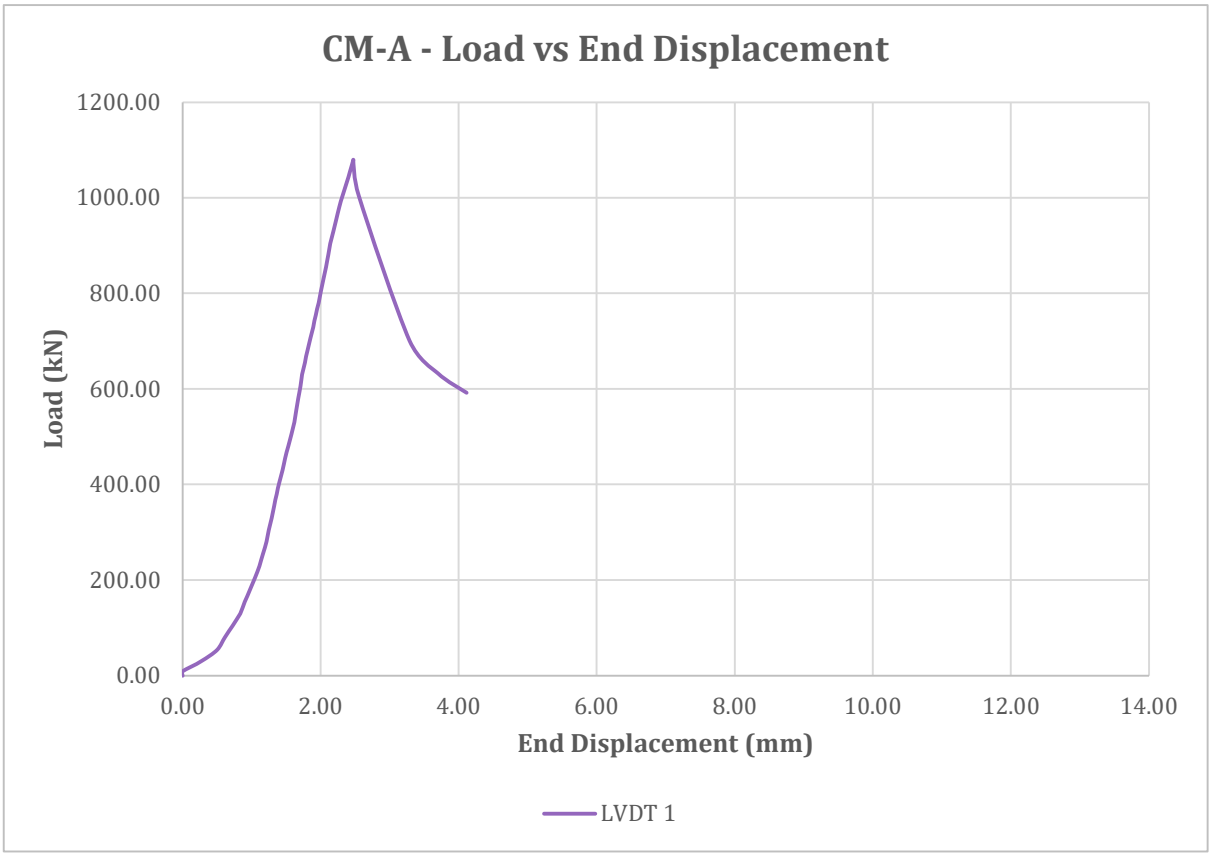

Figure A5.1: CM-A End Displacement Curve - Average

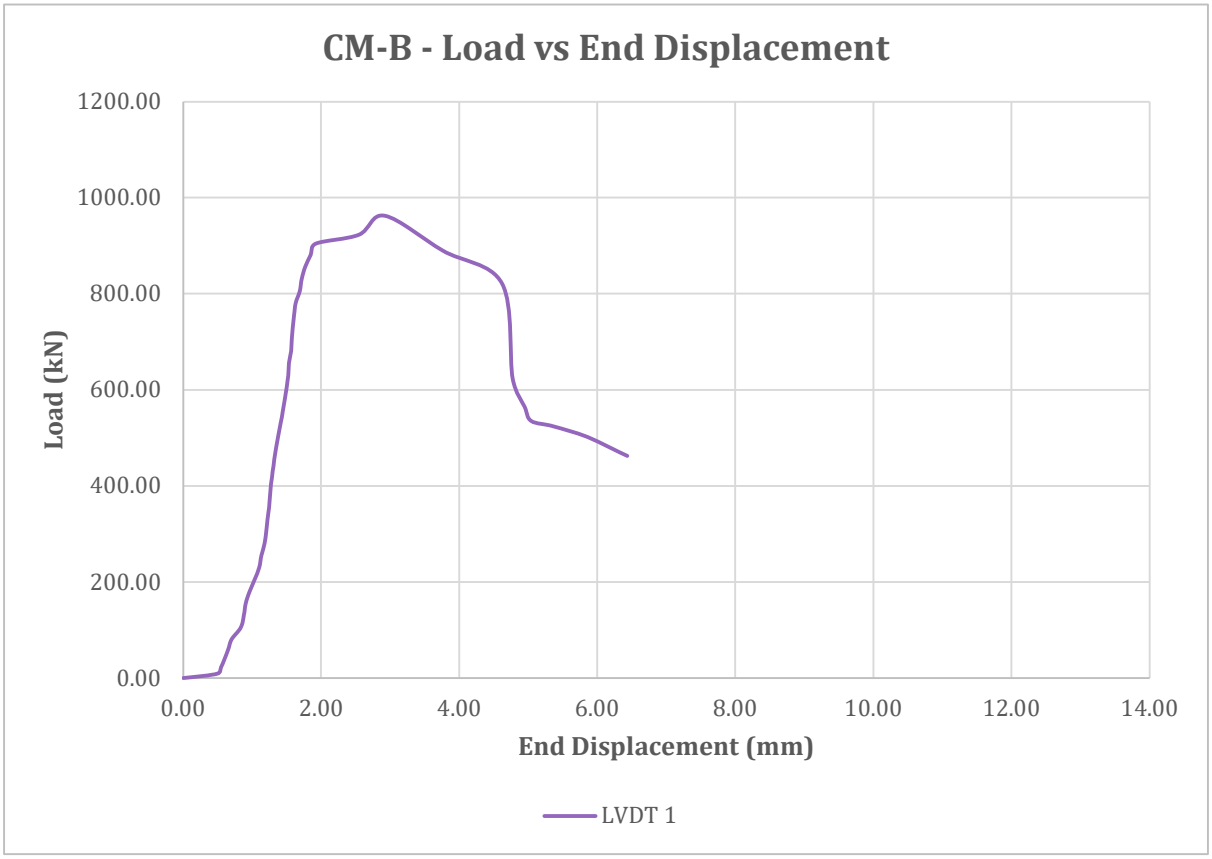

Figure A5.2: CM-B End Displacement Curve - Average

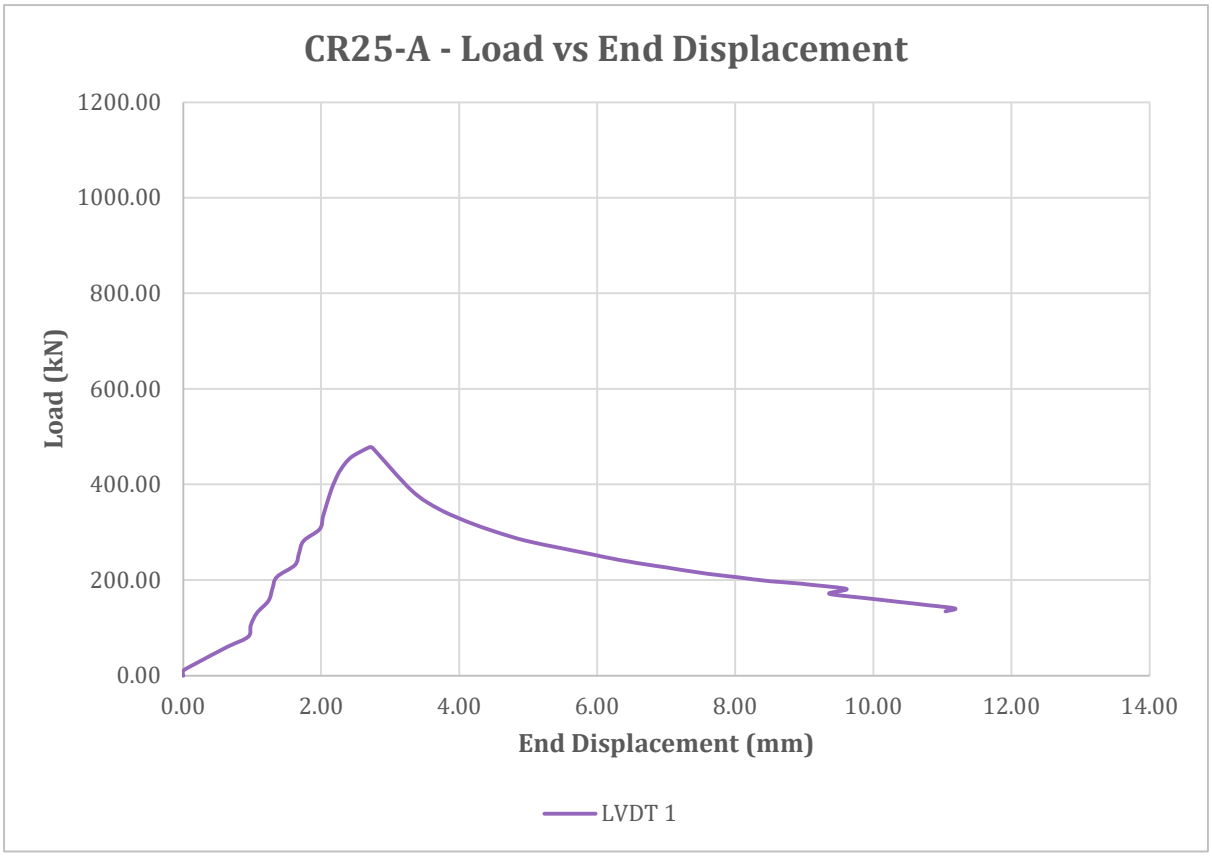

Figure A5.3: CR25-A End Displacement Curve - Average

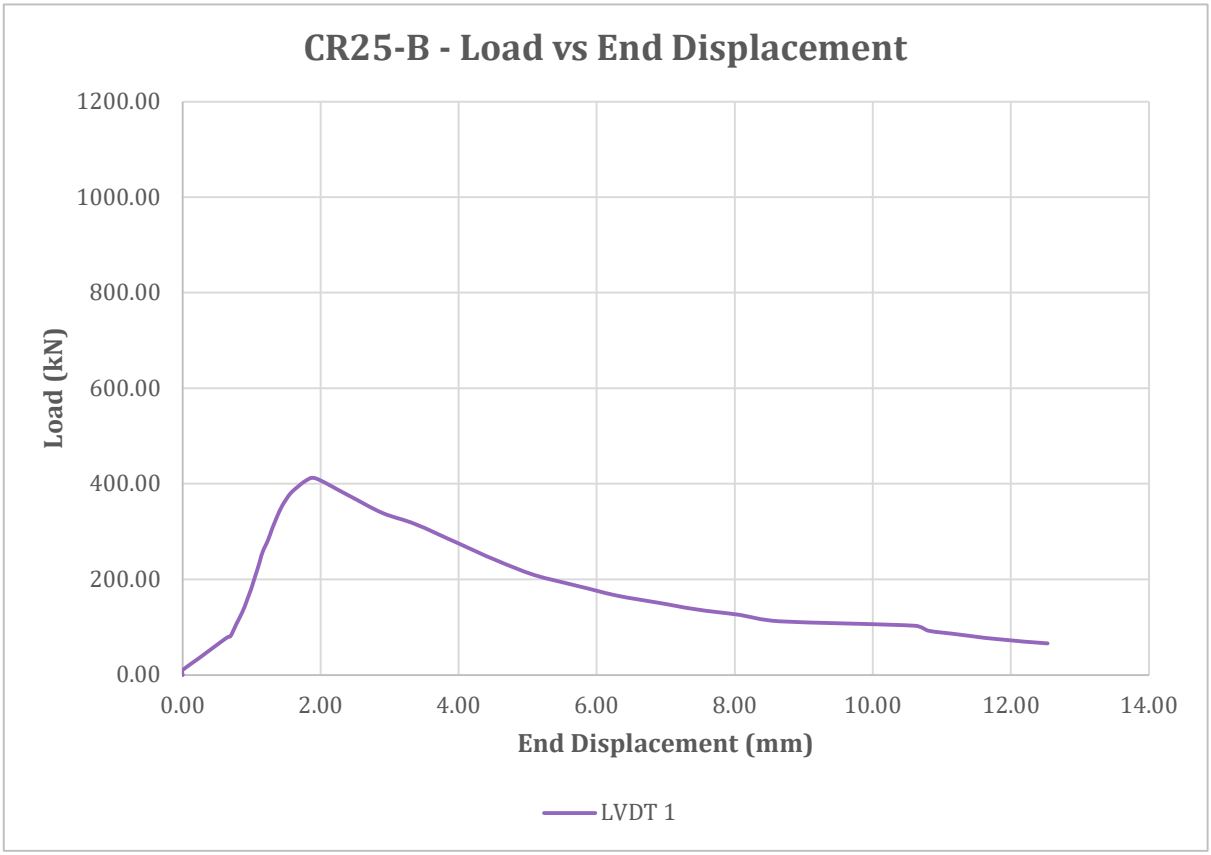

Figure A5.4: CR25-B End Displacement Curve - Average

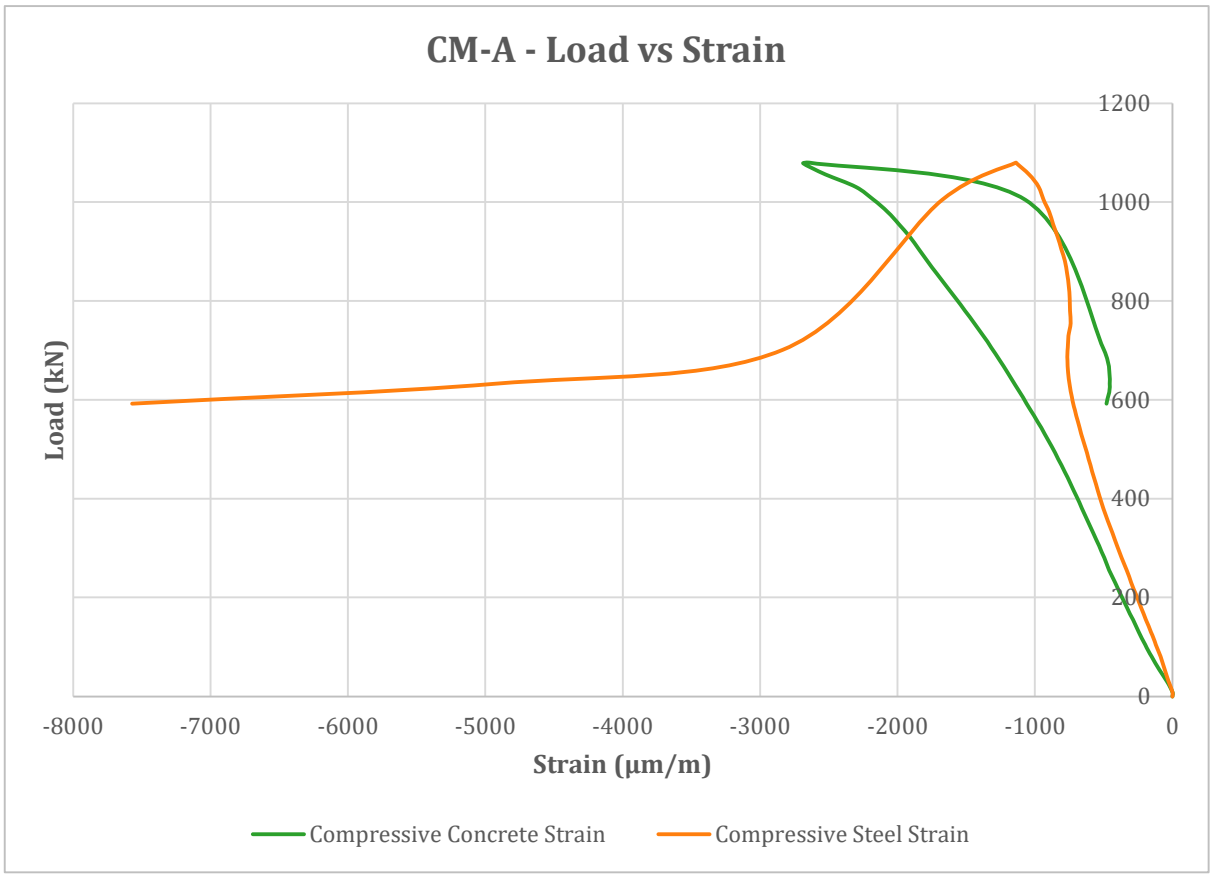

Figure A5.5: Compressive Strains for CM-A

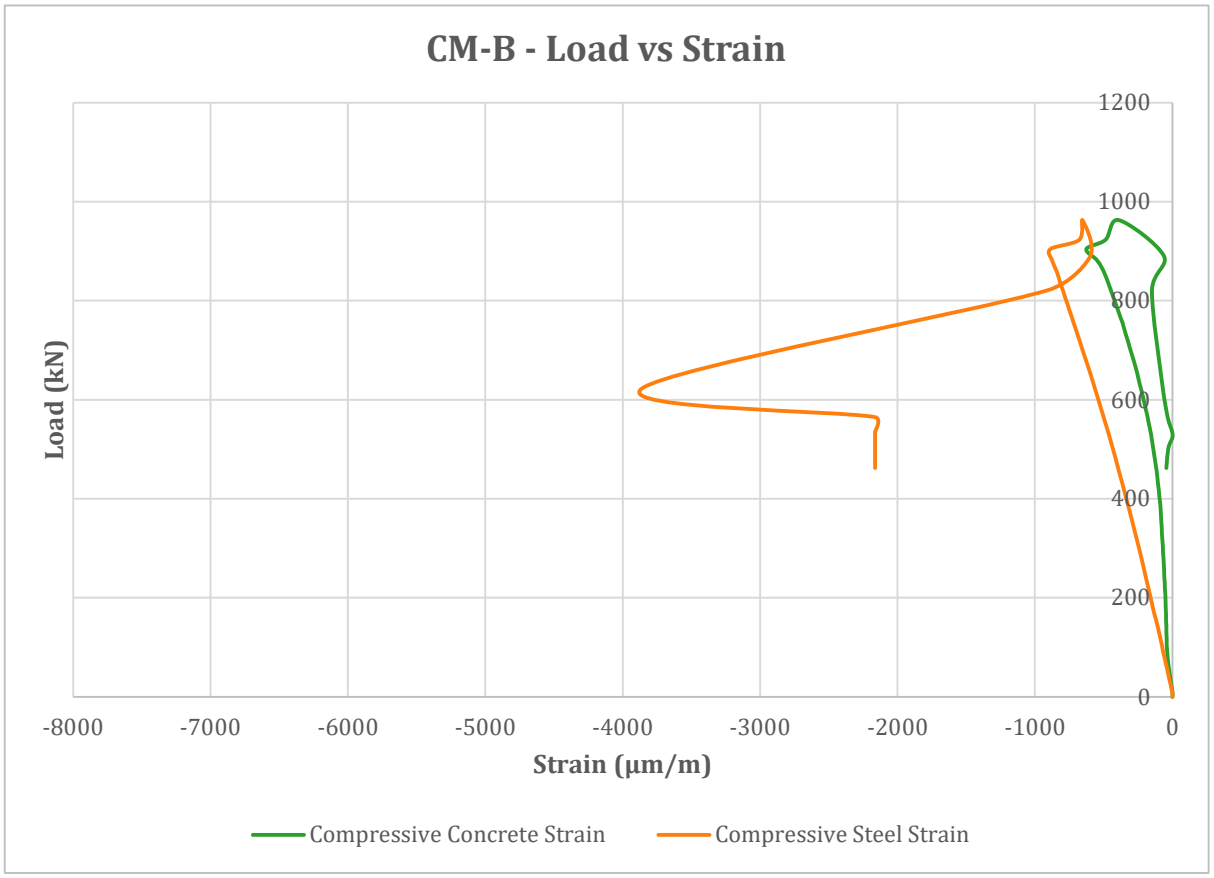

Figure A5.6: Compressive Strains for CM-B

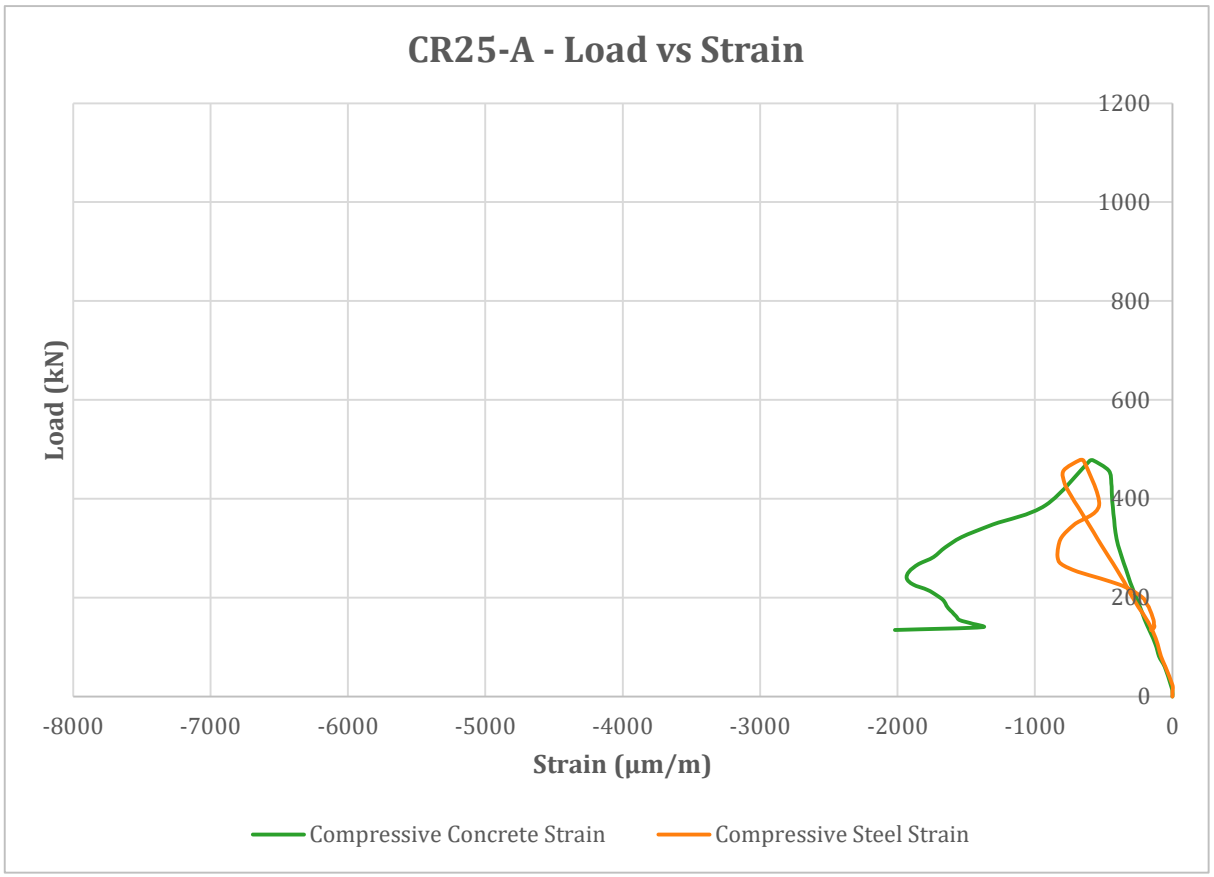

Figure A5.7: Compressive Strains for CR25-A

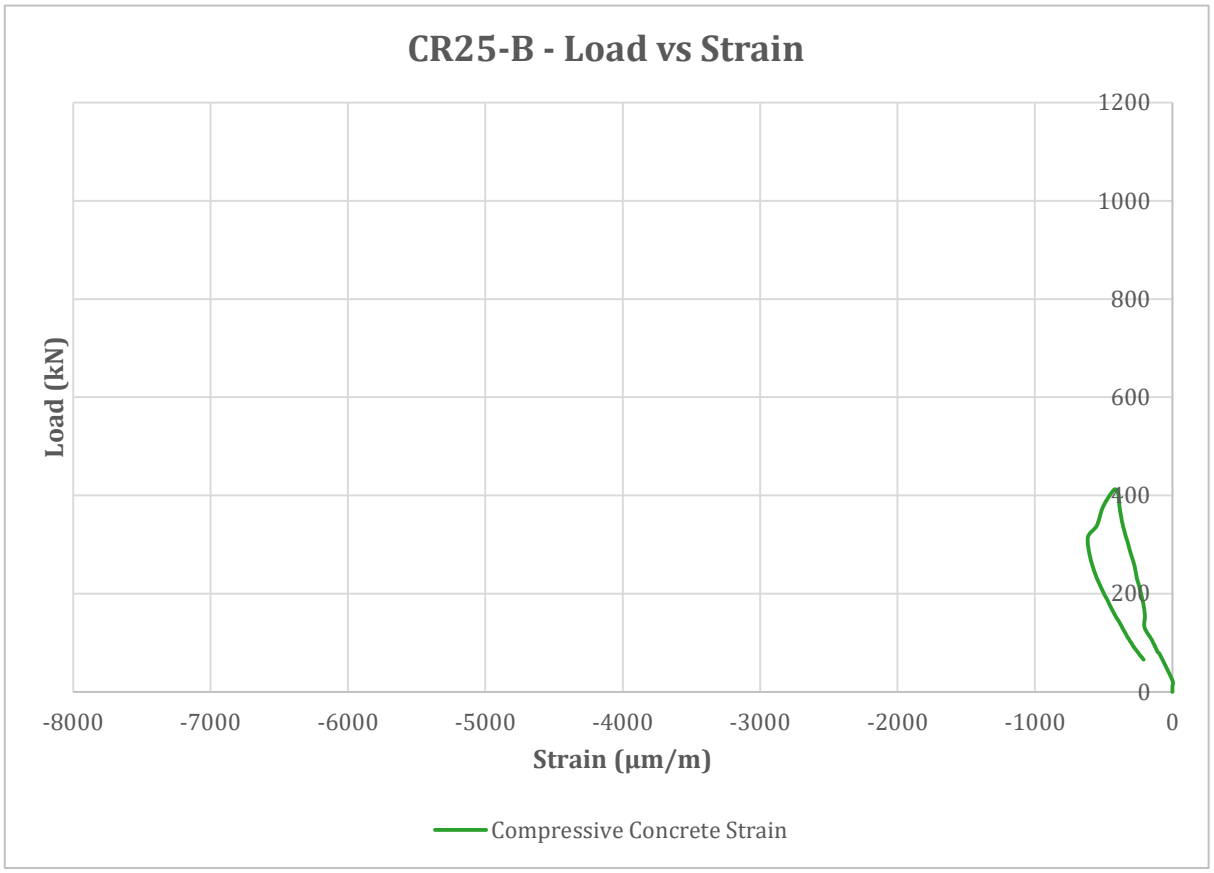

Figure A5.8: Concrete Compressive Strain for CR25-B

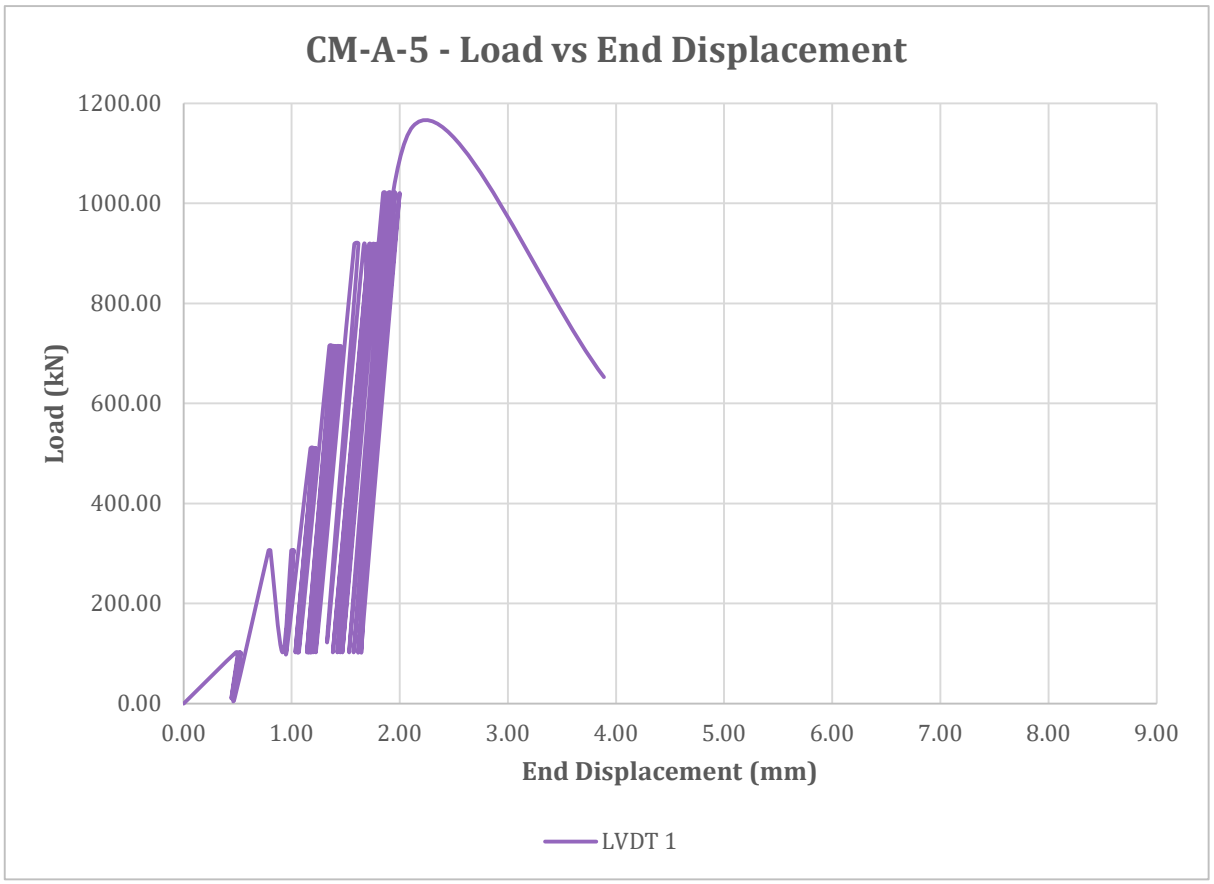

Figure A5.9: End Displacement Curve for CM-A-5

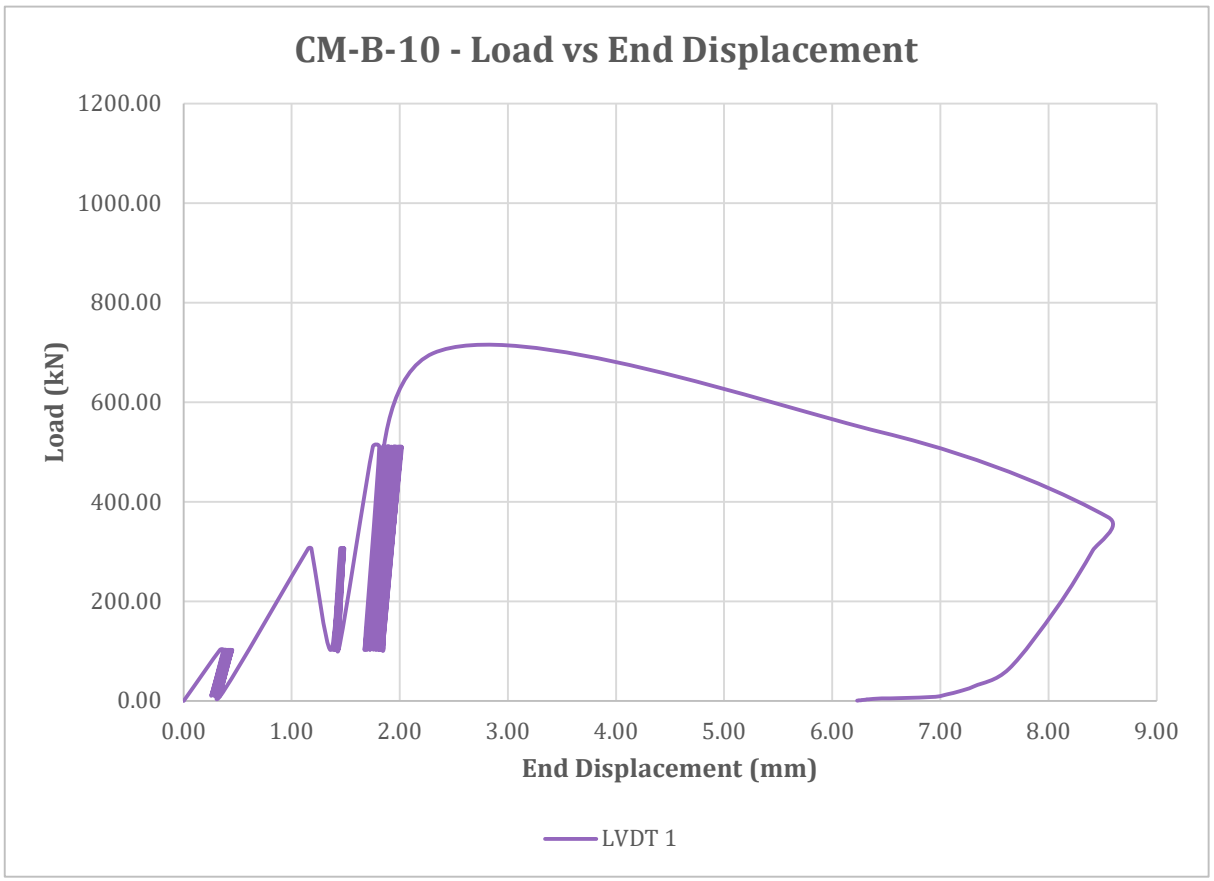

Figure A5.10: End Displacement Curve for CM-B-10

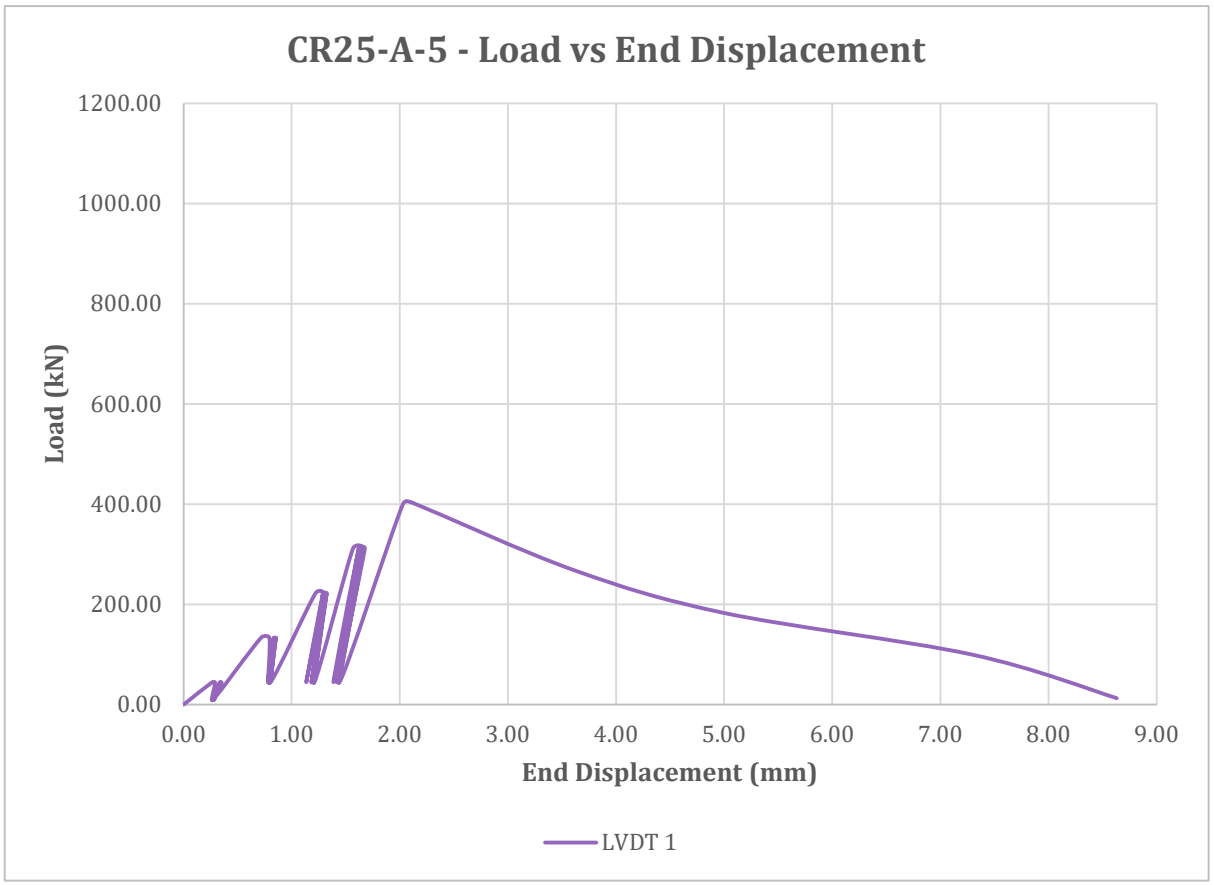

Figure A5.11: End Displacement Curve for CR25-A-5

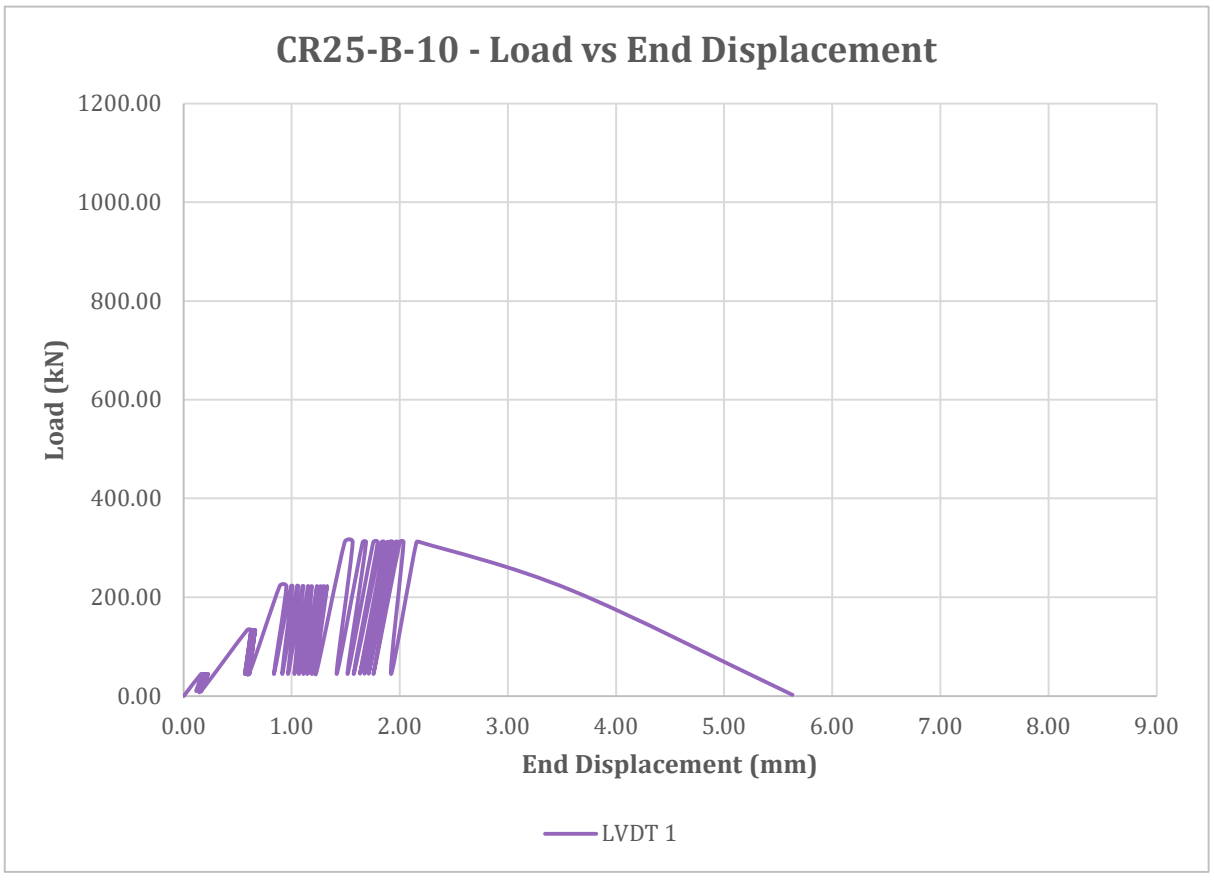

Figure A5.12: End Displacement Curve for CR25-B-10

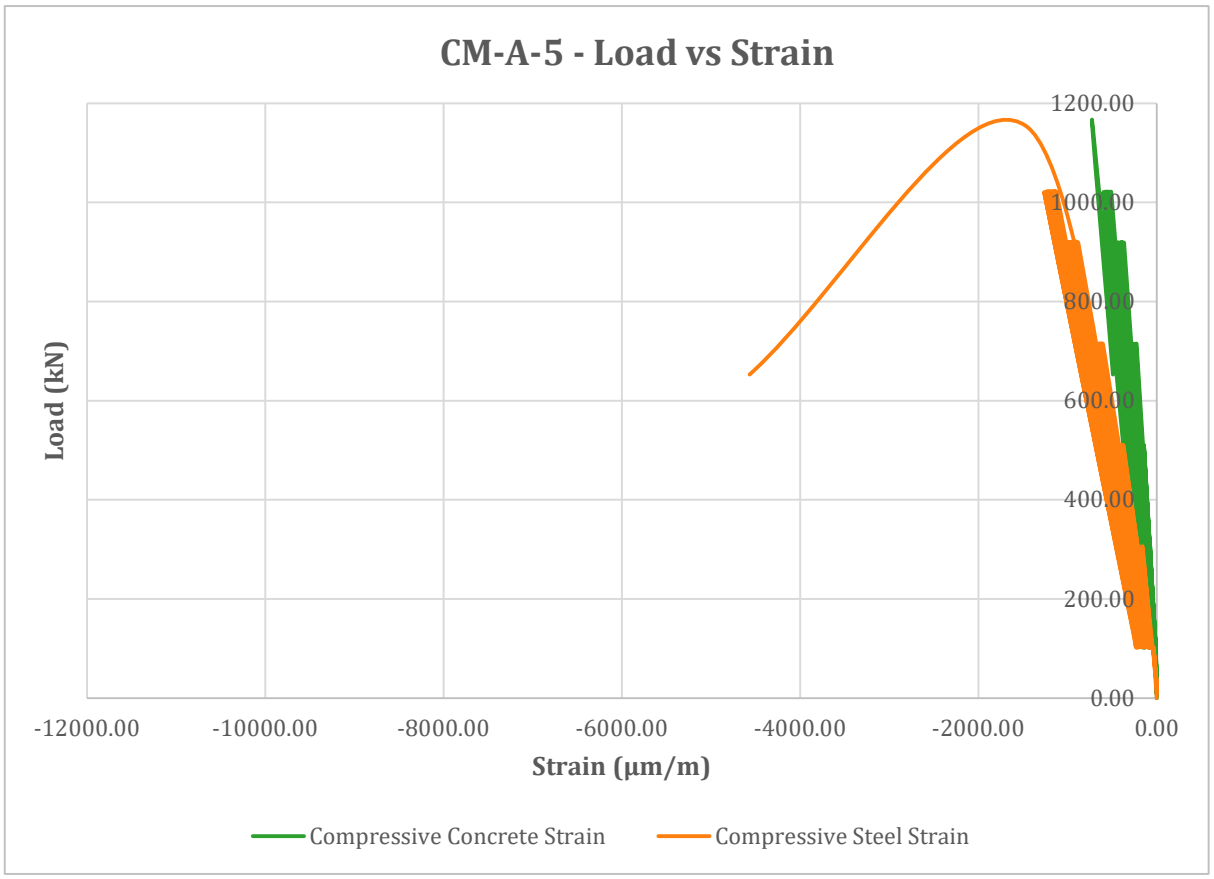

Figure A5.13: Compressive Strains for CM-A-5

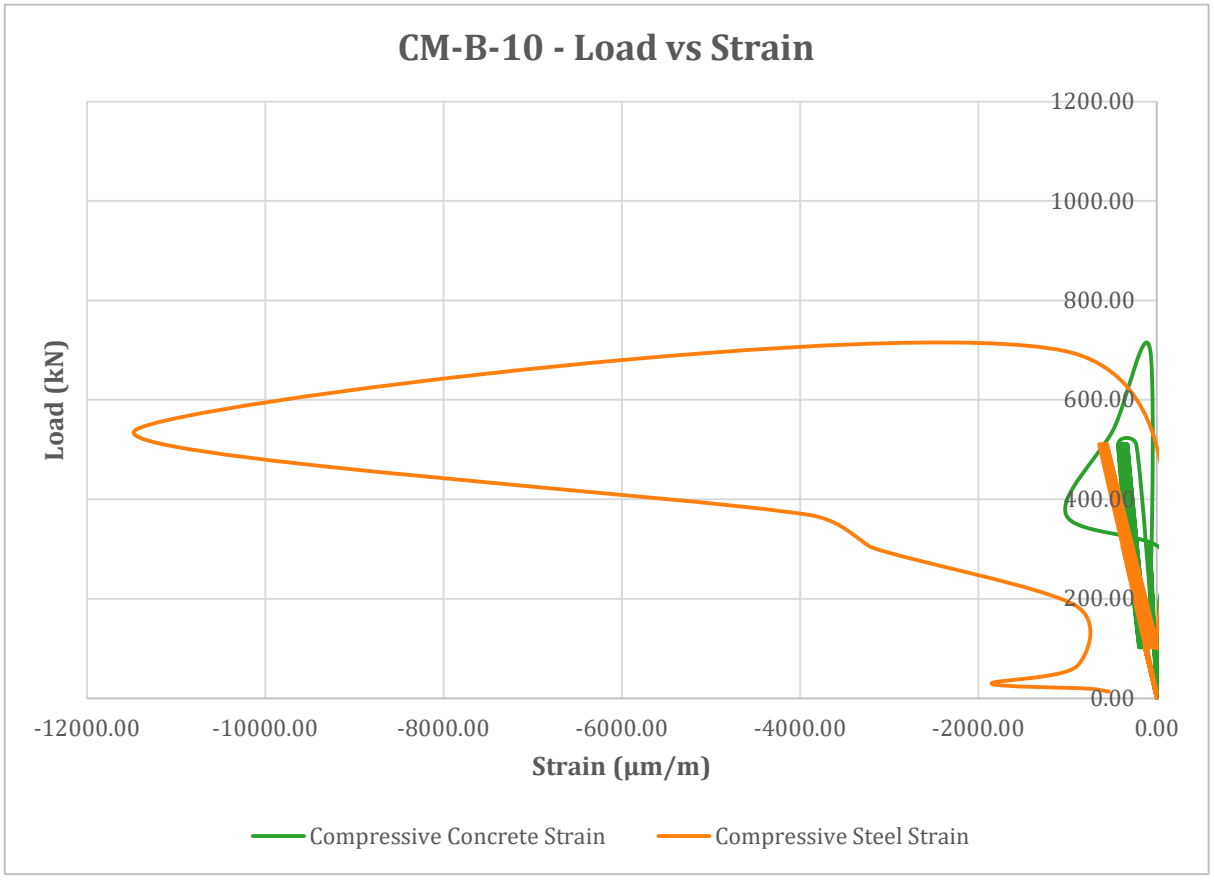

Figure A5.14: Compressive Strains for CM-B-10

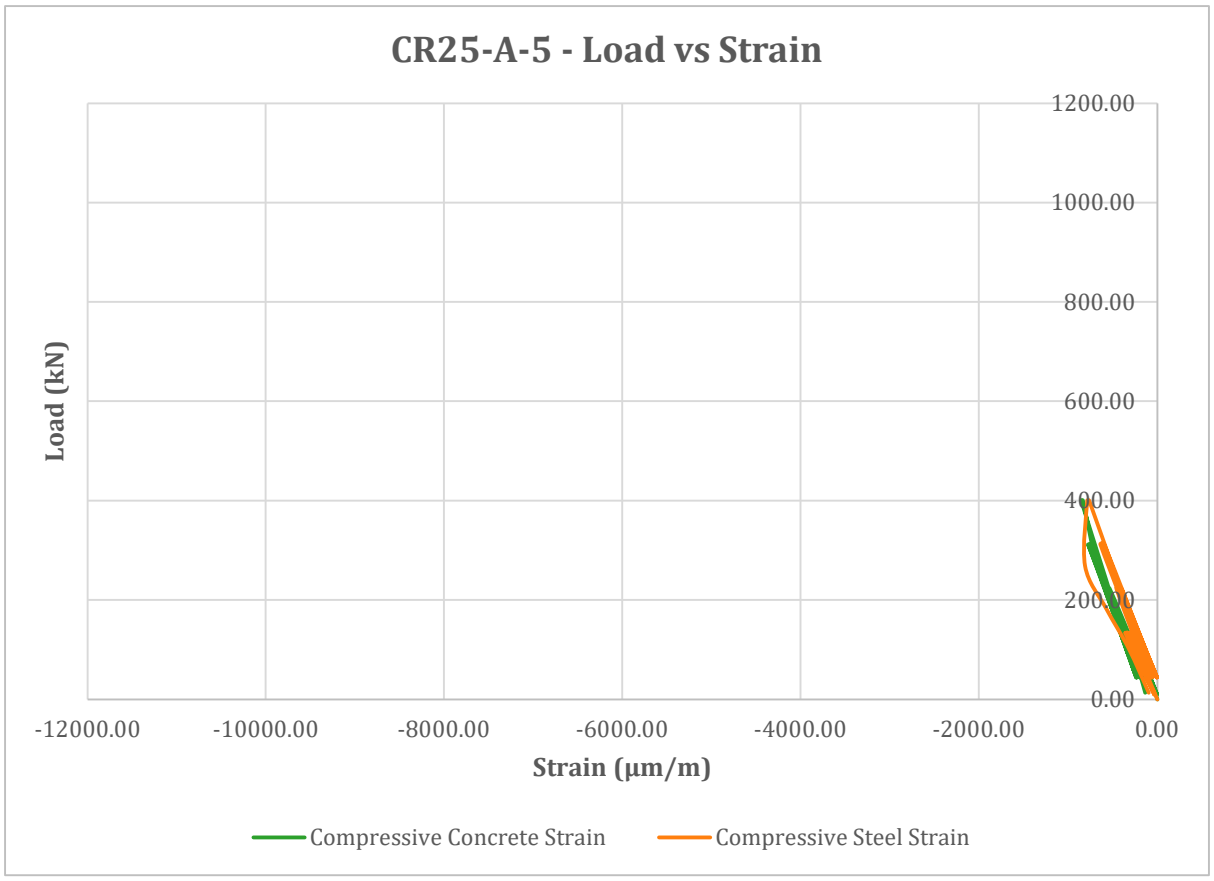

Figure A5.15: Compressive Strains for CR25-A-5

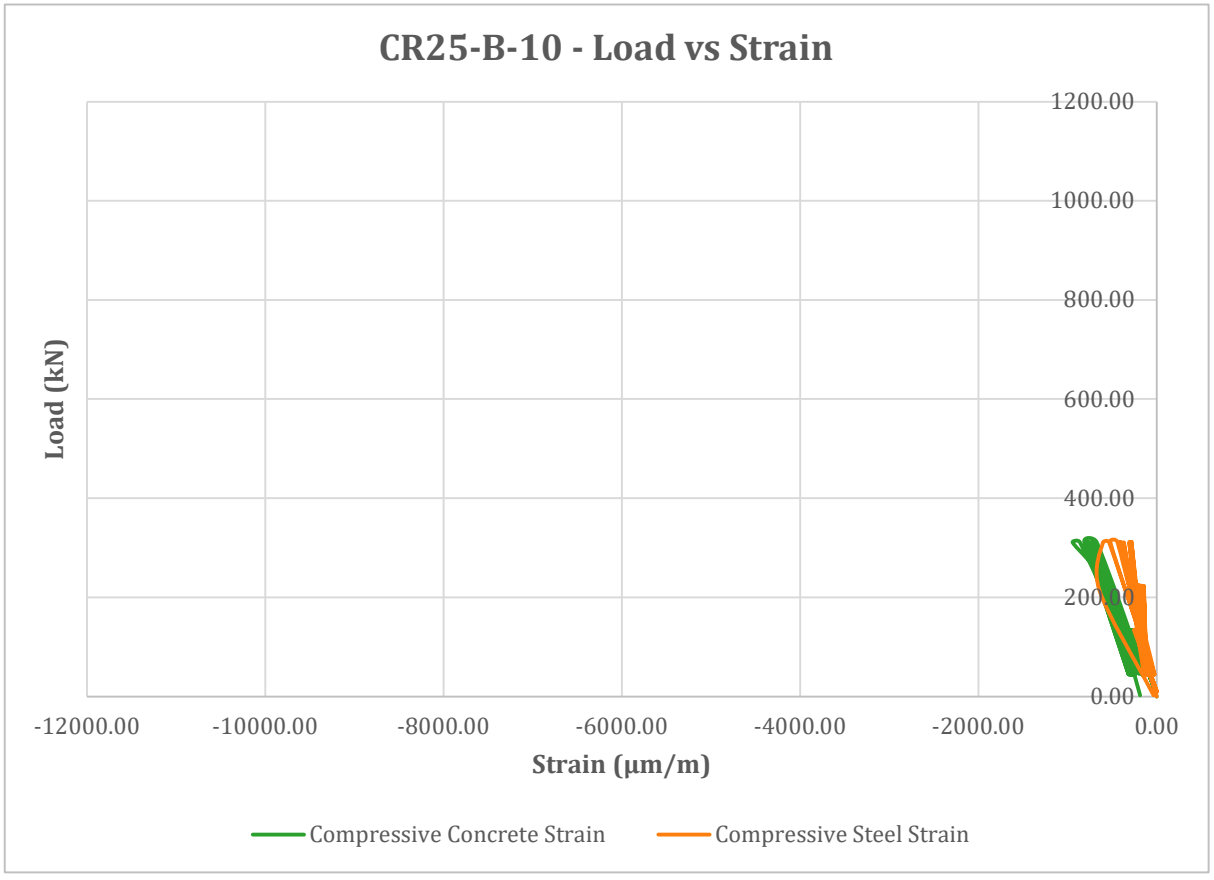

Figure A5.16: Compressive Strains for CR25-B-10

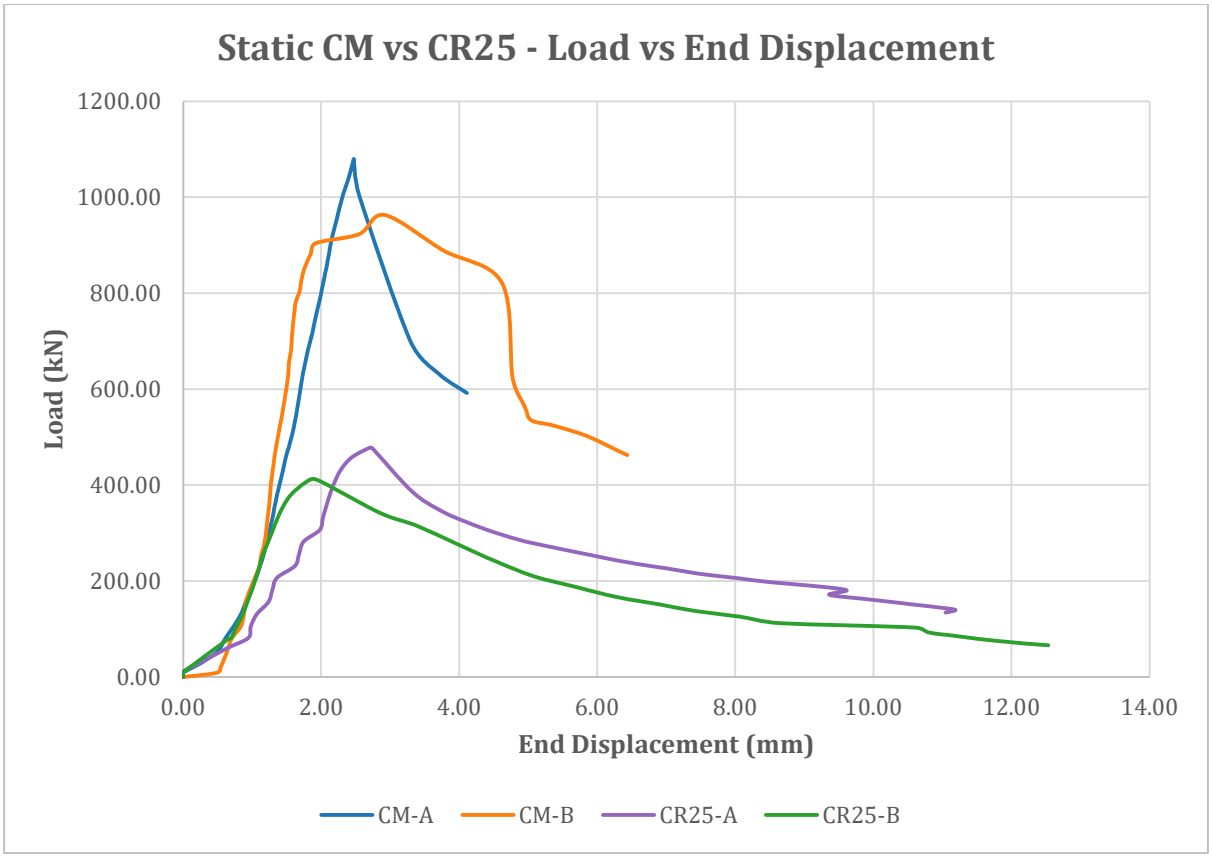

Figure A5.17: End Displacement Comparison Static CM vs CR25

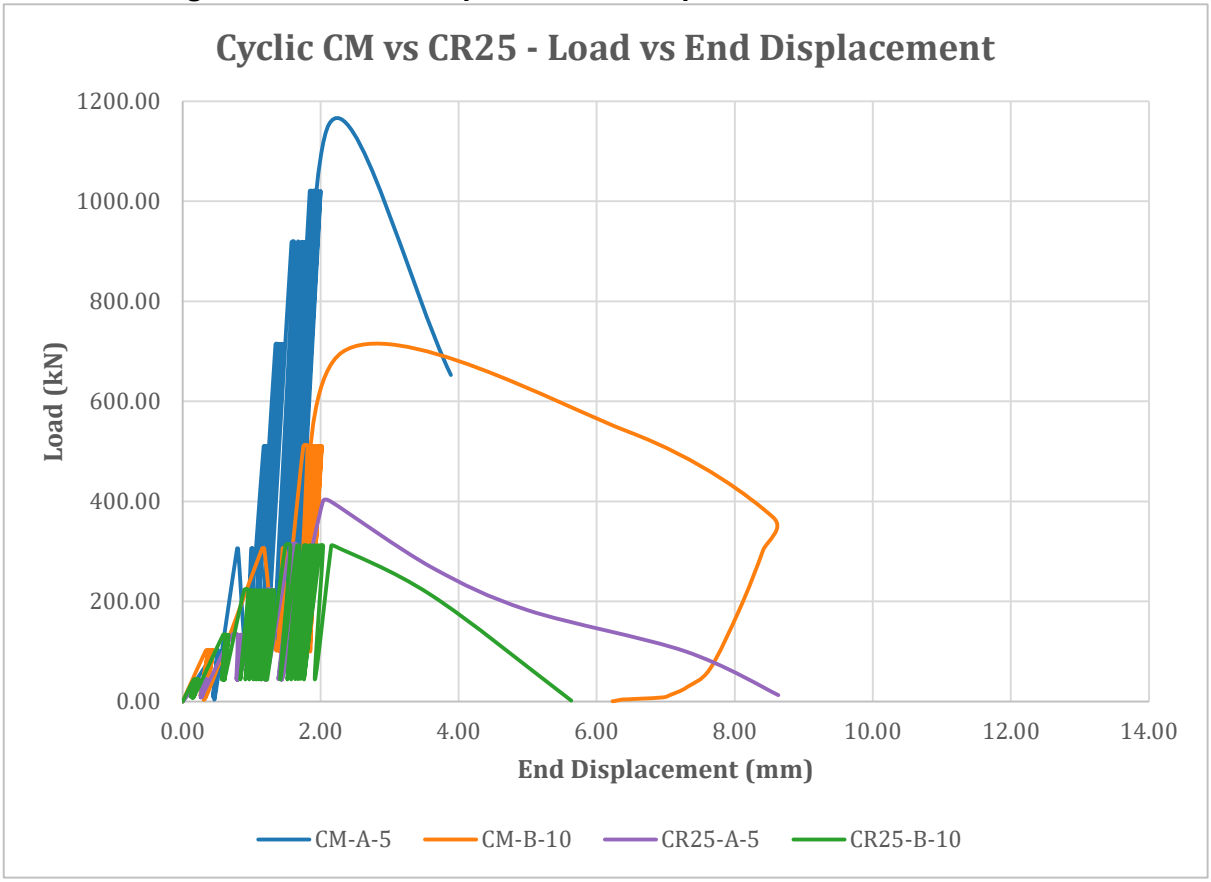

Figure A5.18: End Displacement Comparison Cyclic - CM vs CR25

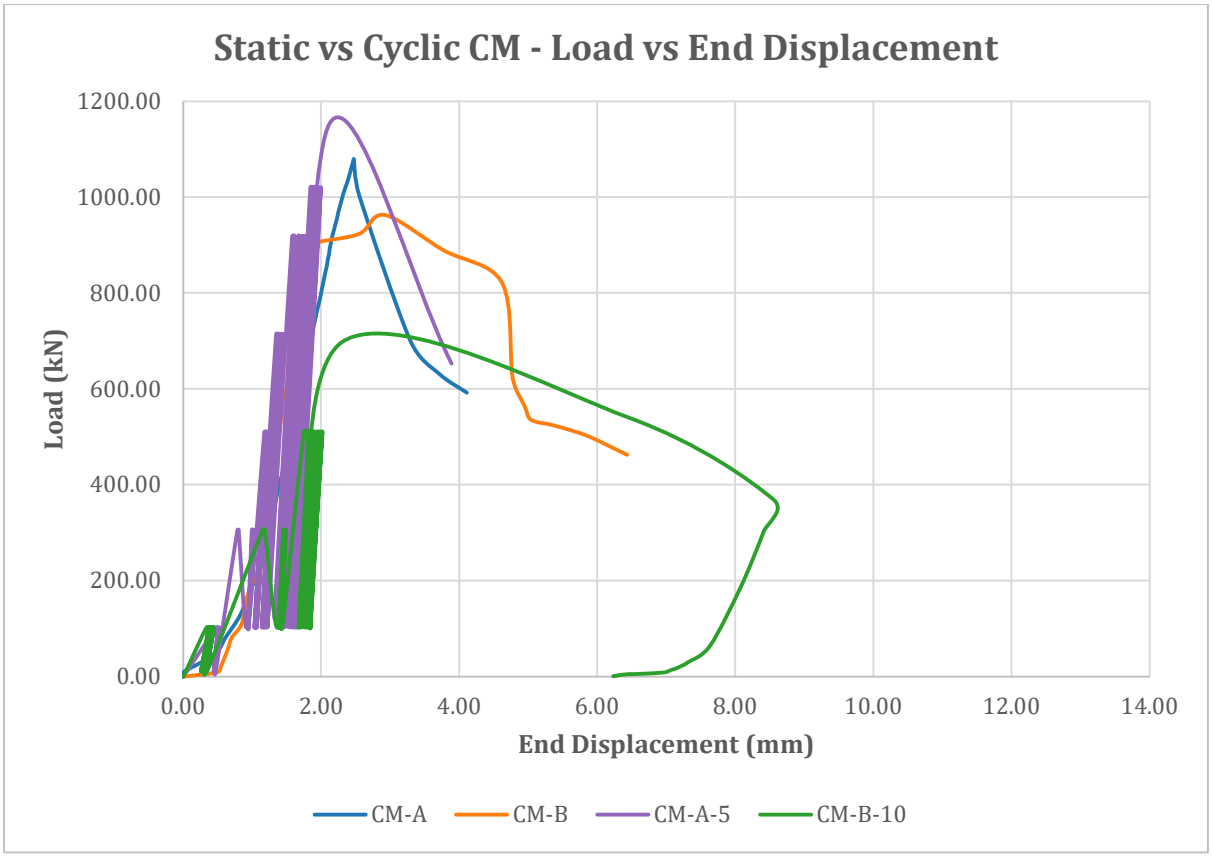

Figure A5.19: End Displacement Comparison CM - Static vs Cyclic

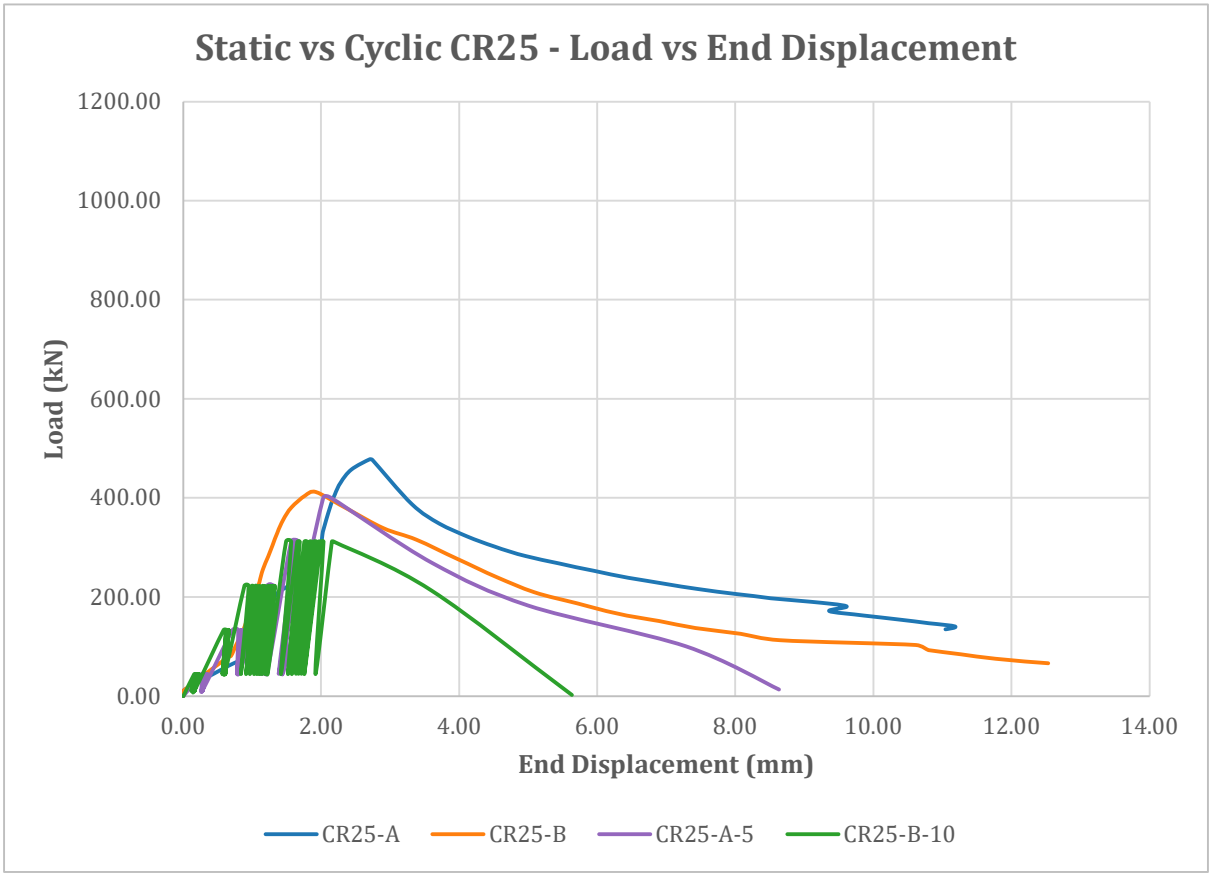

Figure A5.20: End Displacement Comparison CR25 - Static vs Cyclic

Appendix 6: Beam Calculations

Rubberised Concrete Beam - CR-25 (25% Crumb Rubber)
The first set of calculations are carried out with the compressive strengths obtained by Magro (2011) during her study.
This was done to find the amount of reinforcement required in the beams.

Finding Coefficient of Variation of the Control Mix @ 28 day strength:

$f_{cu}{}^* = \mu_{fcu} - K\sigma_{fcu}$

The Coefficient of Variation, C.o.V. is given by:

C.o.V. = σ/μ
σ = C.o.V. x μ
σ_{fcu} = C.o.V. x μ_{fcu}

$f_{cu}{}^* = \mu_{fcu} - K \times [C.o.V.]_{fcu} \times \mu_{fcu}$
$f_{cu}{}^* = \mu_{fcu}[1 - K \times [C.o.V.]_{fcu}]$

Where;	K	1.65	for normal deviation and 5% fractile
	μ_{fcu}	33.26	compressive strength @ 28 days

If	$f_{cu}{}^*$	35	N/mm^2
	μ_{fcu}	33.26	N/mm^2

$35 = 33.26[1-1.65 \times [C.o.V.]_{fcu}]$

	$[C.o.V.]_{fcu}$	-0.031706117
∴	$[C.o.V.]_{fcu}$	-3.17%

To find the amount of steel required for all the beams, first the beam with the lowest compressive strength was worked out.
This was done by limiting the neutral axis to 0.617d, so that the steel would reach its yield point.

Specimen CR-25-28-B : CR-25 mix (using assumed material properties with partial safety factors)

$f_{cu}{}^* = \mu_{fcu}[1 - K \times [C.o.V.]_{fcu}]$

Where;	K	1.65	for normal deviation and 5% fractile
	μ_{fcu}	26.59	compressive strength @ 28 days
	$[C.o.V.]_{fcu}$	-0.031706117	coefficient of variation

$f_{cu}{}^* = 26.59[1 - 1.65 \times -0.031706117]$

∴	$f_{cu}{}^*$	27.98	N/mm^2

Bending of the section will induce a resultant tensile force F_{st} in the reinforcing steel, and a resultant compressive force in the concrete Fcc which acts through the centroid of the effective area of concrete in compression.

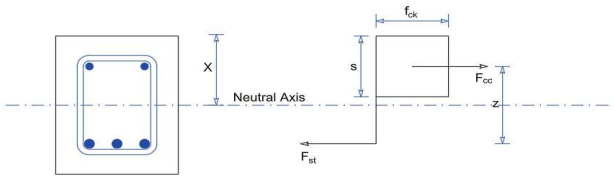

For equilibrium of the compressive and tensile forces on the section,

$F_{cc} = F_{st}$
$0.567 \times f_{ck} \times b \times s = 0.87 \times f_{yk} \times A_s$

Where;	f_{ck}	characteristic compressive strength of concrete
	b	the width of the concrete beam
	s	the depth of the stress block
	f_{yk}	the steel design strength
	A_s	the area of steel provided

s = 0.8x, and x should be limited to 0.617d

Assuming ;	L	4000	mm
	h	250	mm
	b	200	mm
	Diameter bars, ⌀	16	mm
	Cover, c	35	mm

d = h - ⌀/2 - c

∴	d	207	mm

x = 0.617d

∴	x	127.719	mm

s = 0.8x

∴	s	102.1752	mm

For equilibrium of the compressive and tensile forces on the section,

$F_{cc} = F_{st}$
$0.567 \times f_{ck} \times b \times s = 0.87 \times f_{yk} \times A_s$
$0.567 \times 27.98 \times 200 \times 101.88 = 0.87 \times 500 \times A_s$

∴	A_s	745.30	mm^2

This is the maximum amount of reinforcement required to have yielding of the steel, when the neutral axis is limited to 0. 617d.

$n = A_{req} / A_{bar}$

where;	n	number of bars provided
	A_{req}	area of steel required
	A_{bar}	area of chosen bar section

	n	3.7	bars
∴	n	3	bars
where;	A_s	603.3	mm^2
	Diameter bars, ⌀	16	mm

Working beam calculation with the amount of steel provided

For equilibrium of the compressive and tensile forces on the section,

$F_{cc} = F_{st}$

$0.567 \times f_{ck} \times b \times s = 0.87 \times f_{yk} \times A_s$

$0.567 \times 27.98 \times 200 \times s = 0.87 \times 500 \times 603.3$

∴	s	82.71	mm

To find neutral axis (N.A.):

$x = s/0.8$

∴	x	103.38	mm

The equation $F_{st} = 0.87 \times f_{yk} \times A_s$, assumes that the tension reinforcement has yielded, which will be the case if $x < 0.617d$.

$0.617d = 0.617 \times 207mm$

∴	0.617d	127.719	mm
		>x	∴ OK

Moment of resistance, M_{Rd}:

$M_{Rd} = F_{st} \times z$

Where; $z = d - s/2$

$F_{st} = 0.87 \times f_{yk} \times A_s$

∴	M_{Rd}	43.47	kNm

Maximum applied moment, M_{Ed}:

$M_{Ed} = WL/6$

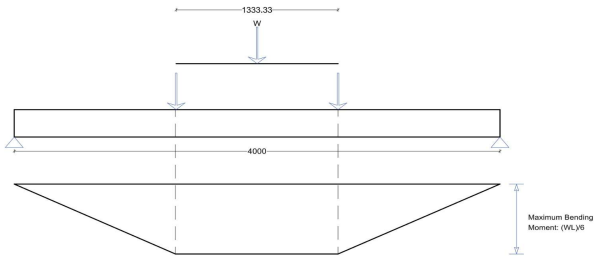

To find load at which beam fails in bending:

$M_{Ed} = M_{Rd}$

$43.47 \times 10^6 = (W \times 4000)/6$

∴	$W_{bending}$	65.21	kN

Applied Shear, V_{Ed}:

$V_{ed} = W/2$

∴	V_{ed}	32.60	kN

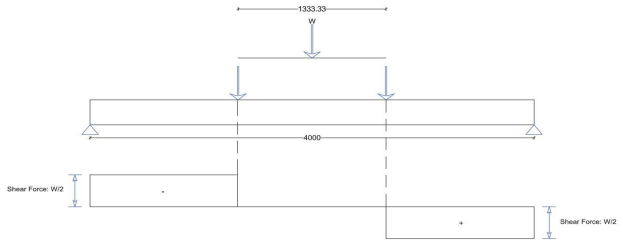

Shear Capacity of concrete, $V_{Rd,c}$ is given by:

$V_{Rd,c} = [C_{rd,c} \times k \times (100\rho_1 f_{ck})^{1/3} + k_1\sigma_{cp}]b_w d$

$> [v_{min} + k_1\sigma_{cp}] \times b_w \times d$

Where; $C_{rd,c} = 0.12$

$k = 1 + \sqrt{200/d}$

$\rho_1 = (A_{s1}/B_w d)$

A_{s1} = the area of tensile reinforcement that extends beyond the section being considered by at least a full anchorage length plus one effective depth (d)

b_w = the smallest width of the section in the tensile area (mm)

∴	$C_{rd,c}$	0.12
	k	1.98
	ρ_1	0.0146

A_{s1} 6 03.3mm^2

bw 200mm

$V_{Rd,c} = [C_{rd,c} \times k \times (100\rho^{1/3} + k1\sigma cp]bwd\ 1fck)$

∴ $V_{Rd,c}$ 33.91kN

$V_{Rd,c,min} = vmin \times bw \times d$

Where; $vmin = 0.035 \times k3/2 \times_{ck} f\ 1/2$

$V_{Rd,c,min} = 0.035xk^{3/2} xfck^{1/2} \times bw \times d$

∴ $V_{Rd,c,min}$ 21.40kN

$V_{Rd,c,min} < V_{Rd,c} > VEd$ ∴ OK

∴ No shear reinforcement is required

∴ Provide minimum amount of shear reinforcement

Compression Strut Capacity, $V_{Rd,max}$ is given by:

$V_{Rd,max} = (bw \times z \times v1 \times fcd)/(\cot\theta + \tan\theta)$

$\theta = 0.5\sin\text{-}1[(V_{Rd,max}/bwd)/0.153fck(1-(fck/250))]$

Where; $V_{Rd,max} = VEd$

∴ θ 0.104o

Since this value < θ = 22o, use θ = 22o

$V_{Rd,max} = (bw \times z \times v1 \times fcd)/(\cot\theta + \tan\theta)$

Where; z = 0.9 d

z = 0.9 x 207 = 186.3mm

v1 = 0.6*(1-fck/250)

v1 = 0.6*(1-(27.98/250)

v1 = 0.53284546

fcd = α cc x fck / γc

=0.85 x 27.98 / 1.5 15.85593305N/mm2

$V_{Rd,max} = (200 \times 186.3 \times 0.5328 \times 15.8559) / (2.5+0.4)$

$V_{Rd,max}$ = 108.5520241kN

$V_{Rd,max} > Ved$ **OK**

Minimum area of steel, pw,min is given by:

$p_{w,min} = 0.08 \times \sqrt{fck} / fyk$

$p_{w,min} = 0.08 \times \sqrt{27.98} / 500$

$p_{w,min} = 0.000846354$

$p_{w,min} = Asw /s \times bw \times \sin\alpha$

$Asw / s = p_{w,min} \times bw \times \sin\alpha$

$Asw/s = 8.47x10 \times 200 \times 1$

Asw / s =0.1692708

Minimum spacing of shear links, smax is given by:

smax =0.75d

smax =0.75 x 207

smax =155.25 mm

Provide: 10mm bars with spacing of 150mm cc [Asw/s = 1.047] in all beams.

Shear resistance of the member governed by 'failure' of the stirrups, $V_{Rd,s}$ is given by:

$V_{Rd,s} = 0.78 \times d \times fyk \times \cot\theta \times Asw/s$

W here;

fyk is the characteristic strength of the link reinforcement.

Asw is the cross-sectional area of the two legs of the link.

s is the spacing of the links

Asw/s = 1.047, which is equal to 10mm bars @ 150mm cc spacing

$V_{Rd,s} = 0.78 \times 207 \times 500 \times 2.5 \times 1.047$

$V_{Rd,s}$ = 211.310775kN

Load for beam to fail in shear:

$W_{shear} = VEd \times 2$ = 422.62155kN

$W_{bending}$, which is equal to 44.51 kN is less than W_{shear} which is equal to 442.6kN, therefore the beam fails in bending.

Rubberised Concrete Beam - CR-25 (25% Crumb Rubber)
The second set of calculations is worked out with the compressive strengths achieved during this programme.
The calculations are worked out considering partial safety factors as per MSA-EN-1992-1-1:2004.

The characteristic design strength, f_{cu}* is given by:

$$f_{cu}^* = \mu_{fcu} - K \times [C.o.V.]_{fcu} \times \mu_{fcu}$$
$$f_{cu}^* = \mu_{fcu}[1 - K \times [C.o.V.]_{fcu}]$$

Where;	K	1.65	for normal deviation and 5% fractile
	μ_{fcu}	8.71	compressive strength @ 28 days
	$[C.o.V.]_{fcu}$	-0.031706117	(found in previous calcualtions)

Area if steel reinforcement provided: 603 mm^2

Bending of the section will induce a resultant tensile force F_{st} in the reinforcing steel, and a resultant compressive force in the concrete Fcc which acts through the centroid of the effective area of concrete in compression.

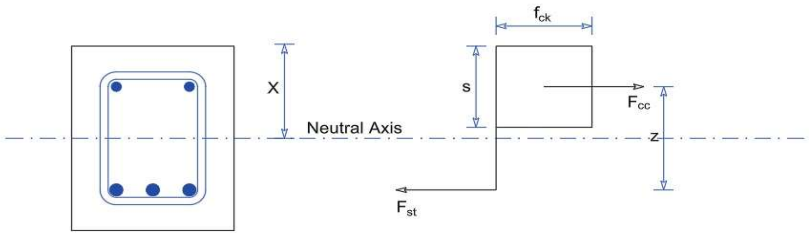

For equilibrium of the compressive and tensile forces on the section,

$$F_{cc} = F_{st}$$
$$0.567 \times f_{ck} \times b \times s = 0.87 \times f_{yk} \times A_s$$
$$0.567 \times 8.71 \times 200 \times s = 0.87 \times 500 \times 603$$
$$1742.567s = 262305$$
$$s = 150.5279281 \text{ mm}$$

Where;	f_{ck}	characteristic compressive strength of concrete
	b	the width of the concrete beam
	s	the depth of the stress block
	f_{yk}	the steel design strength
	A_s	the area of steel provided

To find neutral axis:

$x = s/0.8 =$ 188.1599101 mm

The equation $F_{st} = 0.87 \times f_{yk} \times A_s$, assumes that the tension reinforcement has yielded , which will be the case if x<0.617d.

Assuming ;	L	4000	mm
	h	250	mm
	b	200	mm
	Diameter bars, ⌀	16	mm
	Cover, c	35	mm
	$d = h - ⌀/2 - c$		
∴	d	197	mm
	$x = 0.617d$		
∴	x	121.549	mm

This is less than x(188.16), therefore the assumption made above was correct.

Moment of resistance, M_{Rd}:

$$M_{Rd} = F_{st} \times z$$

Where; $z = d - s/2$

$$F_{st} = 0.87 \times f_{yk} \times A_s$$
$$M_{Rd} = 0.87 \times 500 \times 603 \times (197 - 150.53/2)$$
$$M_{Rd} = 31.93 \text{ kNm}$$

∴

Maximum applied moment, M_{Ed}:

$M_{Ed} = WL/6$

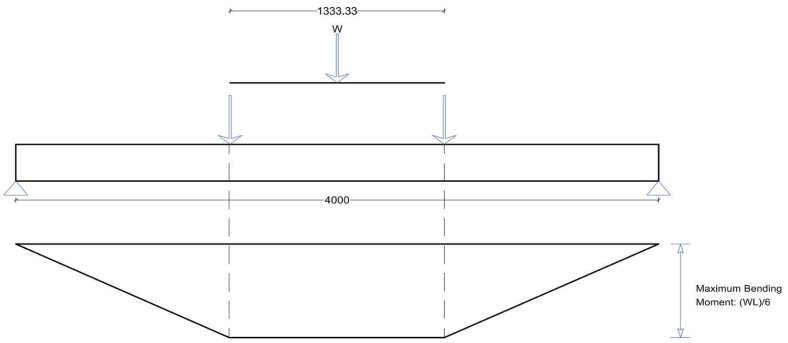

To find load at which beam fails in bending:

$M_{Ed} = M_{Rd}$

$34.56 \times 10^6 = (W \times 4000)/6$

∴ $W_{bending}$ 47.90 kN

Model uncertainty parameter, x_m

Load at which beam failed: 71.95 kN (from testing)

x_m = Actual Failure Load / Predicted Failure Load = 1.502151771

Applied Shear, V_{Ed}:

$V_{ed} = W/2$

∴ V_{ed} 23.95 kN

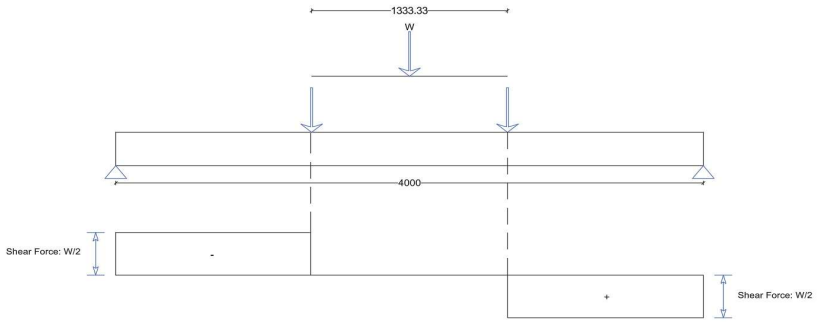

Shear Capacity of concrete, $V_{Rd,c}$ is given by:

$V_{Rd,c} = [C_{rd,c} \times k \times (100\rho_1 f_{ck})^{1/3} + k_1\sigma_{cp}]b_w d$

$> [v_{min} + k_1\sigma_{cp}] \times b_w \times d$

Where; $C_{rd,c} = 0.12$

$k = 1 + \sqrt{200/d}$

$\rho_1 = (A_{s1}/B_w d)$

A_{s1} = the area of tensile reinforcement that extends beyond the section being considered by at leas t a full anchorage length plus one effective depth (d)

b_w = the smallest width of the section in the tensile area (mm)

∴

$C_{rd,c}$	0.12	
k	2.00	
ρ_1	0.0150	
A_{s1}	603	mm^2
b_w	200	mm

$V_{Rd,c} = [C_{rd,c} \times k \times (100\rho_1 f_{ck})^{1/3} + k_1\sigma_{cp}]b_w d$

∴ $V_{Rd,c}$ = 24.50 kN

$V_{Rd,c,min} = v_{min} \times b_w \times d$

Where; $v_{min} = 0.035 \times k^{3/2} \times f_{ck}^{1/2}$

$V_{Rd,c,min} = 0.035 \times k^{3/2} \times f_{ck}^{1/2} \times b_w \times d$

∴ $V_{Rd,c,min}$ 11.51 kN

$V_{Rd,c,min} < V_{Rd,c} > V_{Ed}$ ∴ OK

∴ No shear reinforcement is required

∴ Minimum amount of shear reinforcement provided being 10 mm bars @ 150 c-c

Compression Strut Capacity, $V_{Rd,max}$ is given by:

$V_{Rd,max} = (b_w \times z \times v_1 \times f_{cd})/(\cot\theta + \tan\theta)$

$\theta = 0.5\sin^{-1}[(V_{Rd,max}/b_w d)/0.153 f_{ck}(1-(f_{ck}/250))]$

Where; $V_{Rd,max} = V_{Ed}$

∴ θ 0.245 °

Since this value < θ = 22°, use θ = 22°

$V_{Rd,max} = (b_w \times z \times v_1 \times f_{cd})/(\cot\theta + \tan\theta)$

Where; $z = 0.9\ d$

$z = 0.9 \times 197 =$ 177.3 mm

$v_1 = 0.6*(1-f_{ck}/250)$

$v_1 = 0.6*(1-(8.71/250)$

$v_1 =$ 0.579096

$f_{cd} = \alpha_{cc} \times f_{ck} / \gamma_c$

$= 0.85 \times 8.71 / 1.5$ 4.935666667 N/mm²

$V_{Rd,max} = (200 \times 186.3 \times 0.579096 \times 3.935) / (2.5+0.4)$

$V_{Rd,max} =$ 34.94919043 kN

$V_{Rd,max} > V_{ed}$ **OK**

Shear resistance of the member governed by 'failure' of the stirrups, $V_{Rd,s}$ is given by:

$V_{Rd,s} = 0.78 \times d \times f_{yk} \times \cot\theta \times A_{sw}/s$

Where;

f_{yk} is the characteristic strength of the link reinforcement.
A_{sw} is the cross-sectional area of the two legs of the link.
s is the spacing of the links
A_{sw}/s = 1.047, which is equal to 10mm bars @ 150mm cc spacing

$V_{Rd,s} = 0.78 \times 197 \times 500 \times 2.5 \times 1.047$

$V_{Rd,s} =$ 201.102525 kN

Load for beam to fail in shear:

$W_{shear} = V_{Ed} \times 2 =$ 402.20505 kN

$W_{bending}$, which is equal to 47.90 kN is less than W_{shear}, which is equal to 402.205kN, therefore the beam fails in bending.

Rubberised Concrete Beam - CR-25 (25% Crumb Rubber)
The second set of calculations is worked out with the compressive strengths achieved during this programme.
The calculations are worked out considering partial safety factors as per MSA-EN-1992-1-1:2004.

The characteristic design strength, f_{cu}* is given by:

$$f_{cu}^* = \mu_{fcu} - K \times [C.o.V.]_{fcu} \times \mu_{fcu}$$
$$f_{cu}^* = \mu_{fcu}[1 - K \times [C.o.V.]_{fcu}]$$

Where;	K	1.65	for normal deviation and 5% fractile
	μ_{fcu}	8.71	compressive strength @ 28 days
	$[C.o.V.]_{fcu}$	-0.031706117	(found in previous calcualtions)

Area if steel reinforcement provided: 603 mm^2

Bending of the section will induce a resultant tensile force F_{st} in the reinforcing steel, and a resultant compressive force in the concrete Fcc which acts through the centroid of the effective area of concrete in compression.

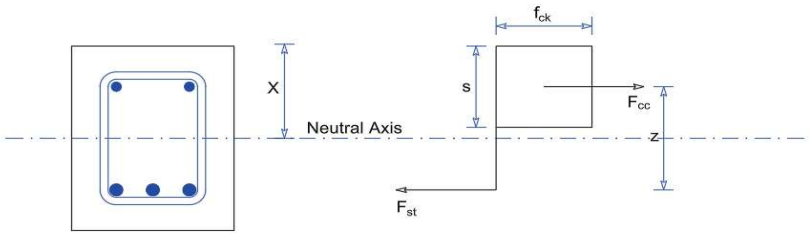

For equilibrium of the compressive and tensile forces on the section,

$$F_{cc} = F_{st}$$
$$0.567 \times f_{ck} \times b \times s = 0.87 \times f_{yk} \times A_s$$
$$0.567 \times 8.71 \times 200 \times s = 0.87 \times 500 \times 603$$
$$1742.567s = 262305$$
$$s = 150.5279281 \text{ mm}$$

Where;	f_{ck}	characteristic compressive strength of concrete
	b	the width of the concrete beam
	s	the depth of the stress block
	f_{yk}	the steel design strength
	A_s	the area of steel provided

To find neutral axis:

$x = s/0.8 =$ 188.1599101 mm

The equation $F_{st} = 0.87 \times f_{yk} \times A_s$, assumes that the tension reinforcement has yielded , which will be the case if x<0.617d.

Assuming ;	L	4000	mm
	h	250	mm
	b	200	mm
	Diameter bars, ⌀	16	mm
	Cover, c	35	mm
	$d = h - ⌀/2 - c$		
∴	d	197	mm
	$x = 0.617d$		
∴	x	121.549	mm

This is less than x(188.16), therefore the assumption made above was correct.

Moment of resistance, M_{Rd}:

$$M_{Rd} = F_{st} \times z$$

Where; $z = d - s/2$

$$F_{st} = 0.87 \times f_{yk} \times A_s$$
$$M_{Rd} = 0.87 \times 500 \times 603 \times (197 - 150.53/2)$$
$$M_{Rd} = 31.93 \text{ kNm}$$

∴

Maximum applied moment, M_{Ed}:

$M_{Ed} = WL/6$

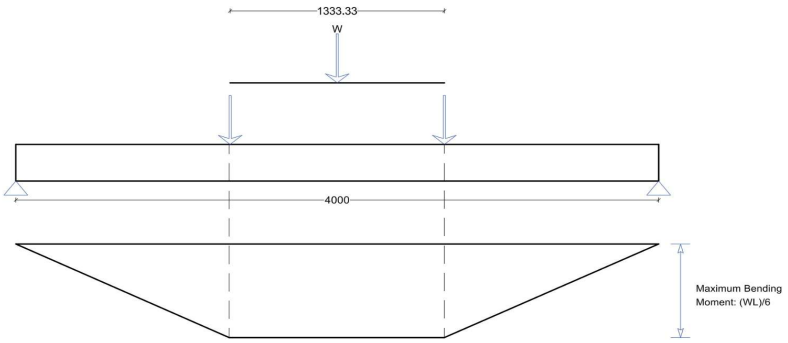

To find load at which beam fails in bending:

$M_{Ed} = M_{Rd}$

$34.56 \times 10^6 = (W \times 4000)/6$

∴ $W_{bending}$ 47.90 kN

Model uncertainty parameter, x_m

Load at which beam failed: 71.95 kN (from testing)

x_m = Actual Failure Load / Predicted Failure Load = 1.502151771

Applied Shear, V_{Ed}:

$V_{ed} = W/2$

∴ V_{ed} 23.95 kN

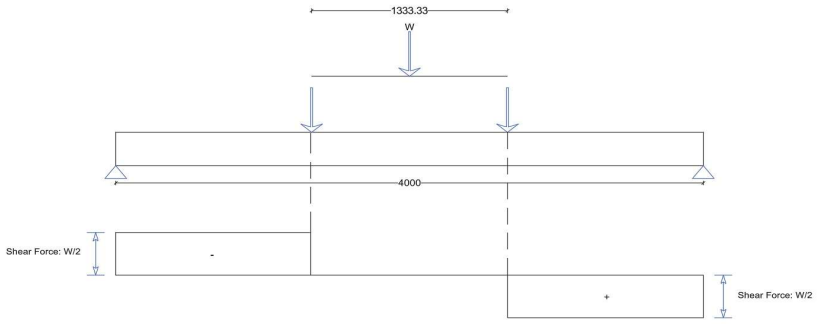

Shear Capacity of concrete, $V_{Rd,c}$ is given by:

$V_{Rd,c} = [C_{rd,c} \times k \times (100\rho_1 f_{ck})^{1/3} + k_1\sigma_{cp}]b_w d$

$> [v_{min} + k_1\sigma_{cp}] \times b_w \times d$

Where; $C_{rd,c} = 0.12$

$k = 1 + \sqrt{200/d}$

$\rho_1 = (A_{s1}/B_w d)$

A_{s1} = the area of tensile reinforcement that extends beyond the section being considered by at leas t a full anchorage length plus one effective depth (d)

b_w = the smallest width of the section in the tensile area (mm)

∴

$C_{rd,c}$	0.12	
k	2.00	
ρ_1	0.0150	
A_{s1}	603	mm^2
b_w	200	mm

$V_{Rd,c} = [C_{rd,c} \times k \times (100\rho_1 f_{ck})^{1/3} + k_1\sigma_{cp}]b_w d$

∴ $V_{Rd,c} =$ 24.50 kN

$V_{Rd,c,min} = v_{min} \times b_w \times d$

Where; $v_{min} = 0.035 \times k^{3/2} \times f_{ck}^{1/2}$

$V_{Rd,c,min} = 0.035 \times k^{3/2} \times f_{ck}^{1/2} \times b_w \times d$

∴ $V_{Rd,c,min}$ 11.51 kN

$V_{Rd,c,min} < V_{Rd,c} > V_{Ed}$ ∴ OK

∴ No shear reinforcement is required

∴ Minimum amount of shear reinforcement provided being 10 mm bars @ 150 c-c

Compression Strut Capacity, $V_{Rd,max}$ is given by:

$V_{Rd,max} = (b_w \times z \times v_1 \times f_{cd})/(\cot\theta + \tan\theta)$

$\theta = 0.5\sin^{-1}[(V_{Rd,max}/b_w d)/0.153 f_{ck}(1-(f_{ck}/250))]$

Where; $V_{Rd,max} = V_{Ed}$

∴ θ 0.245 °

Since this value < θ = 22°, use θ = 22°

$V_{Rd,max} = (b_w \times z \times v_1 \times f_{cd})/(\cot\theta + \tan\theta)$

Where; $z = 0.9\ d$

$z = 0.9 \times 197 =$ 177.3 mm

$v_1 = 0.6*(1-f_{ck}/250)$

$v_1 = 0.6*(1-(8.71/250)$

$v_1 =$ 0.579096

$f_{cd} = \alpha_{cc} \times f_{ck} / \gamma_c$

$= 0.85 \times 8.71 / 1.5$ 4.935666667 N/mm²

$V_{Rd,max} = (200 \times 186.3 \times 0.579096 \times 3.935) / (2.5+0.4)$

$V_{Rd,max} =$ 34.94919043 kN

$V_{Rd,max} > V_{ed}$ **OK**

Shear resistance of the member governed by 'failure' of the stirrups, $V_{Rd,s}$ is given by:

$V_{Rd,s} = 0.78 \times d \times f_{yk} \times \cot\theta \times A_{sw}/s$

Where;

f_{yk} is the characteristic strength of the link reinforcement.
A_{sw} is the cross-sectional area of the two legs of the link.
s is the spacing of the links
$A_{sw}/s = 1.047$, which is equal to 10mm bars @ 150mm cc spacing

$V_{Rd,s} = 0.78 \times 197 \times 500 \times 2.5 \times 1.047$

$V_{Rd,s} =$ 201.102525 kN

Load for beam to fail in shear:

$W_{shear} = V_{Ed} \times 2 =$ 402.20505 kN

$W_{bending}$, which is equal to 47.90 kN is less than W_{shear}, which is equal to 402.205kN, therefore the beam fails in bending.